Driven quantum tunneling

Milena Grifoni, Peter Hänggi*

Institut für Physik Universität Augsburg, Universitätstraße 1, D-86135 Augsburg, Germany

Contents

* Corresponding author.

DRIVEN QUANTUM TUNNELING

Milena GRIFONI, Peter HÄNGGI

Institut für Physik, Universität Augsburg, Universitätstraße 1, D-86135 Augsburg, Germany

1. Introduction

During the last few decades we could bear witness to an immense research activity, both in experimental and theoretical physics, as well as in chemistry, aimed at understanding the detailed dynamics of quantum systems that are exposed to strong time-dependent external fields. The quantum mechanics of explicitly time-dependent Hamiltonians generates a variety of novel phenomena that are not accessible within ordinary stationary quantum mechanics. In particular, the development of laser and maser systems opened the doorway for creation of novel effects in nonlinear quantum systems which interact with strong electromagnetic fields [1–7]. For example, an atom exposed indefinitely to an oscillating field eventually ionizes, whatever the values of the (angular) frequency and the intensity of the field. The rate at which the atom ionizes depends on both, the driving frequency and the intensity. Interestingly enough, in a pioneering paper by H. R. Reiss in 1970 [8], the seemingly paradoxical result was established that extremely strong field intensities lead to smaller transition probabilities than more modest intensities, i.e., one observes a declining yield with increasing intensity. This phenomenon of stabilization that is typical for above threshold ionization (ATI) is still actively discussed, both in experimental and theoretical groups [9,10]. Other activities that are in the limelight of current topical research relate to the active control of quantum processes; e.g. the selective control of reaction yields of products in chemical reactions by use of a sequence of properly designed coherent light pulses [11–13].

Our prime concern here will focus on the tunneling dynamics of time-dependently driven nonlinear quantum systems. Such systems exhibit an interplay of three characteristic components, (i) nonlinearity, (ii) nonequilibrium behavior (as a result of the time-dependent driving), and (iii) quantum tunneling, with the latter providing a paradigm for quantum coherence phenomena.

By now, the physics of *driven quantum tunneling* has generated widespread interest in many scientific communities [1–7] and, moreover, gave rise to a variety of novel phenomena and effects. As such, the field of driven tunneling has nucleated into a whole new discipline.

Historically, first precursors of *driven barrier tunneling* date back to the experimentally observed photon-assisted-tunneling (PAT) events in 1962 in the Al–Al_2O_3–In superconductor–insulator–superconductor hybrid structure by Dayem and Martin [14]. A clear-cut, simple theoretical explanation for the step-like structure in the averaged voltage–tunneling current characteristics was put forward soon afterwards by Tien and Gordon [15] in 1963, who introduced the physics of driving-induced sidechannels for tunneling across a uniformly, periodically modulated barrier. The phenomenon that the quantum transmission can be quenched in arrays of periodically arranged barriers, e.g. semiconductor superlattices, leading to such effects as *dynamic localization* or *absolute negative conductance* have theoretically been described over twenty years ago [16–18]; but these have been verified experimentally only recently [19–22].

The role of time-dependent driving on the *coherent tunneling* between two locally stable wells [23] has only recently been elaborated [24]. As an intriguing result one finds that an appropriately designed coherent cw-drive can bring coherent tunneling to an almost complete standstill, now known as *coherent destruction of tunneling* (CDT) [24–26]. This driving induced phenomenon in turn yields several other new quantum effects such as low frequency radiation and/or intense, nonperturbative even harmonic generation in symmetric metastable systems that possess an inversion symmetry [27–29].

We shall approach this complexity of driven quantum tunneling with a sequence of sections. In the first half of seven sections we elucidate the physics of various novel tunneling phenomena in quantum tunneling systems that are exposed to strong time-varying fields. These systems are described by an explicitly time-dependent Hamiltonian. Thus, solving the time-dependent Schrödinger equation necessitates the development of novel analytic and computational schemes which account for the breaking of time translation invariance of the quantum dynamics in a nonperturbative manner. Beginning with Section 8 we elaborate on the effect of weak, or even strong dissipation, on the coherent tunneling dynamics of driven systems. This extension of quantum dissipation [30–35] to driven quantum systems constitutes a nontrivial task: Now, the bath modes couple resonantly to differences of quasienergies rather than to unperturbed energy differences. The influence of quantum dissipation to driven tunneling is developed theoretically in Sections 8–11, and applied to various phenomena in the remaining Sections 12–14.

The authors made an attempt to comprise in this review many, although necessarily not all important developments and applications of driven tunneling. In doing so, this review became rather comprehensive.

As an inevitable consequence, the authors realize that not all readers will wish to digest the present review in its entirety. We trust, however, that a reader is able to choose from the many methods and applications covered in the numerous sections which he is interested in.

There is the consistent underlying theme of driven quantum tunneling that runs through all sections, but nevertheless, each section can be considered to some extent as self-contained. In this spirit, we hope that the readers will be able to enjoy reading from the selected fascinating developments that characterize driven tunneling, and moreover will become invigorated doing own research in this field.

2. Floquet approach

2.1. Floquet theory

In presence of intense fields interacting with the system it is well known [37–39] that the semiclassical theory (i.e., treating the field as a classical field) provides results that are equivalent to those obtained from a fully quantized theory, whenever fluctuations in the photon number (which, for example, are of importance for spontaneous radiation processes) can safely be neglected. We shall be interested primarily in the investigation of quantum systems with their Hamiltonian being a periodic function in time, i.e.,

$$H(t) = H(t + \mathscr{T}), \tag{1}$$

with $\mathscr{T}$ being the period of the perturbation. The symmetry of the Hamiltonian under discrete time translations, $t \to t + \mathscr{T}$, enables the use of the Floquet formalism [36]. This formalism is the appropriate vehicle to study strongly driven periodic quantum systems: Not only does it respect the periodicity of the perturbation at all levels of approximation, but its use intrinsically avoids also the occurrence of so-called secular terms (i.e., terms that are linear or not periodic in the time variable). The latter characteristically occur in the application of conventional Rayleigh–Schrödinger time-dependent perturbation theory. The Schrödinger equation for the quantum system with coordinate

q may be written as

$$(H(q,t) - \mathrm{i}\hbar\,\partial/\partial t)\Psi(q,t) = 0\,. \tag{2}$$

For the sake of simplicity only, we restrict ourselves here to the one-dimensional case. With

$$H(q,t) = H_0(q) + H_{\mathrm{ext}}(q,t), \qquad H_{\mathrm{ext}}(q,t) = H_{\mathrm{ext}}(q, t + \mathscr{T})\,, \tag{3}$$

the unperturbed Hamiltonian $H_0(q)$ is assumed to possess a complete orthonormal set of eigenfunctions $\{\varphi_n(q)\}$ with corresponding eigenvalues $\{E_n\}$. According to the Floquet theorem, there exist solutions to Eq. (2) that have the form (so-called Floquet-state solution) [36]

$$\Psi_\alpha(q,t) = \exp(-\mathrm{i}\varepsilon_\alpha t/\hbar)\Phi_\alpha(q,t)\,, \tag{4}$$

where $\Phi_\alpha(q,t)$ is periodic in time, i.e., it is a *Floquet mode* obeying

$$\Phi_\alpha(q,t) = \Phi_\alpha(q, t + \mathscr{T})\,. \tag{5}$$

Here, ε_α is a real-valued energy function, being unique up to multiples of $\hbar\Omega$, $\Omega = 2\pi/\mathscr{T}$. It is termed the Floquet characteristic exponent, or the *quasienergy* [37–39]. The term quasienergy reflects the formal analogy with the quasimomentum $\boldsymbol{k}$, characterizing the Bloch eigenstates in a periodic solid. Upon substituting Eq. (4) into Eq. (2) one obtains the eigenvalue equation for the quasienergy ε_α, i.e., with the Hermitian operator

$$\mathscr{H}(q,t) \equiv H(q,t) - \mathrm{i}\hbar\,\partial/\partial t\,, \tag{6}$$

one finds that

$$\mathscr{H}(q,t)\Phi_\alpha(q,t) = \varepsilon_\alpha\Phi_\alpha(q,t)\,. \tag{7}$$

We immediately notice that the Floquet modes

$$\Phi_{\alpha'}(q,t) = \Phi_\alpha(q,t)\exp(\mathrm{i}n\Omega t) \equiv \Phi_{\alpha n}(q,t) \tag{8}$$

with n being an integer number $n = 0, \pm 1, \pm 2, \ldots$ yield the identical solution to that in Eq. (4), but with the shifted quasienergy

$$\varepsilon_\alpha \to \varepsilon_{\alpha'} = \varepsilon_\alpha + n\hbar\Omega \equiv \varepsilon_{\alpha n}\,. \tag{9}$$

Hence, the index α corresponds to a whole class of solutions indexed by $\alpha' = (\alpha, n)$, $n = 0, \pm 1, \pm 2, \ldots$ The eigenvalues $\{\varepsilon_\alpha\}$ therefore can be mapped into a first Brillouin zone, obeying $-\hbar\Omega/2 \le \varepsilon < \hbar\Omega/2$. For the Hermitian operator $\mathscr{H}(q,t)$ it is convenient to introduce the composite Hilbert space $\mathscr{R}\otimes\mathscr{T}$ made up of the Hilbert space $\mathscr{R}$ of square integrable functions on configuration space and the space $\mathscr{T}$ of functions which are periodic in t with period $\mathscr{T} = 2\pi/\Omega$ [40]. For the spatial part the inner product for two square integrable functions $f(q)$ and $g(q)$ is defined by

$$\langle f|g\rangle := \int \mathrm{d}q\, f^*(q)g(q)\,, \tag{10}$$

yielding with $f(q) = \varphi_n(q)$ and $g(q) = \varphi_m(q)$

$$\langle \varphi_n | \varphi_m \rangle = \delta_{n,m} \,. \tag{11}$$

The temporal part is spanned by the orthonormal set of Fourier vectors $\langle t|n\rangle = \exp(in\Omega t)$, $n = 0, \pm 1, \pm 2, \ldots$, and the inner product in $\mathscr{T}$ reads

$$(m,n) := \frac{1}{\mathscr{T}} \int_0^{\mathscr{T}} \mathrm{d}t (\mathrm{e}^{im\Omega t})^* \mathrm{e}^{in\Omega t} = \delta_{n,m} \,. \tag{12}$$

Thus, the eigenvectors of $\mathscr{H}$ obey the orthonormality condition in the composite Hilbert space $\mathscr{R} \otimes \mathscr{T}$, i.e.,

$$\langle\!\langle \Phi_{\alpha'} | \Phi_{\beta'} \rangle\!\rangle := \frac{1}{\mathscr{T}} \int_0^{\mathscr{T}} \mathrm{d}t \int_{-\infty}^{\infty} \mathrm{d}q \, \Phi^*_{\alpha'}(q,t) \Phi_{\beta'}(q,t) = \delta_{\alpha',\beta'} = \delta_{\alpha,\beta} \delta_{n,m} \,, \tag{13}$$

and form a complete set in $\mathscr{R} \otimes \mathscr{T}$,

$$\sum_{\alpha} \sum_{n} \Phi^*_{\alpha n}(q,t) \Phi_{\alpha n}(q',t') = \delta(q - q') \delta(t - t') \,. \tag{14}$$

Note that in Eq. (14) we must extend the sum over all Brillouin zones, i.e., over all the representatives n in a class, cf. Eq. (9). For fixed equal time $t = t'$, the Floquet modes of the first Brillouin zone $\Phi_{\alpha 0}(q,t)$ form a complete set in $\mathscr{R}$, i.e.,

$$\sum_{\alpha} \Phi^*_{\alpha}(q,t) \Phi_{\alpha}(q',t) = \delta(q - q') \,. \tag{15}$$

Clearly, with $t' \neq t + m\mathscr{T} = t \,(\mathrm{mod}\, \mathscr{T})$, the functions $\{\Phi^*_{\alpha}(q,t),\ \Phi_{\alpha}(q',t')\}$ do not form an orthonormal set in $\mathscr{R}$.

2.2. General properties, spectral representations

With a monochromatic perturbation

$$H_{\mathrm{ext}}(q,t) = -Sq \sin(\Omega t + \phi) \,, \tag{16}$$

the quasienergy ε_α is a function of the parameters S and Ω, but does not depend on the arbitrary, but fixed phase ϕ. This is so because a shift of the time origin $t_0 = 0 \to t_0 = -\phi/\Omega$ will lift a dependence of ε_α on ϕ in the quasienergy eigenvalue equation in Eq. (7). In contrast, the time-dependent Floquet function $\Psi_\alpha(q,t)$ depends, at fixed time t, on the phase. The quasienergy eigenvalue equation in Eq. (7) has the form of the time-independent Schrödinger equation in the composite Hilbert space $\mathscr{R} \otimes \mathscr{T}$. This feature reveals the great advantage of the Floquet formalism: It is now straightforward to use all theorems characteristic for time-independent Schrödinger theory for the periodically driven quantum dynamics, such as the Rayleigh–Ritz variation principle for stationary perturbation theory, the von-Neumann-Wigner degeneracy theorem, or the Hellmann–Feynman theorem, etc.

With $H(t)$ being a time-dependent function, the energy E is no longer conserved. Instead, let us consider the averaged energy in a Floquet state $\Psi_\alpha(q,t)$. This quantity reads

$$\bar{H}_\alpha \equiv \frac{1}{\mathscr{T}}\int_0^{\mathscr{T}} \mathrm{d}t\langle \Psi_\alpha(t)|H(t)|\Psi_\alpha(t)\rangle = \varepsilon_\alpha + \left\langle\!\!\left\langle \Phi_\alpha\left|\mathrm{i}\hbar\frac{\partial}{\partial t}\right|\Phi_\alpha\right\rangle\!\!\right\rangle . \tag{17}$$

If we invoke a Fourier expansion of the time-periodic Floquet function $\Phi_\alpha(q,t) = \sum_k c_k(q)\exp(-\mathrm{i}k\Omega t)$, $\sum_k \int \mathrm{d}q|c_k(q)|^2 = 1 = \sum_k \langle c_k|c_k\rangle$, Eq. (17) can be recast as a sum over k, i.e.,

$$\bar{H}_\alpha = \varepsilon_\alpha + \sum_{k=-\infty}^{\infty} \hbar k\Omega\langle c_k|c_k\rangle = \sum_{k=-\infty}^{\infty} (\varepsilon_\alpha + \hbar k\Omega)\langle c_k|c_k\rangle . \tag{18}$$

Hence, $\bar{H}_\alpha$ can be looked upon as the energy accumulated in each harmonic mode of $\Psi_\alpha(q,t) = \exp(-\mathrm{i}\varepsilon_\alpha t/\hbar)\Phi_\alpha(q,t)$, and averaged with respect to the weight of each of these harmonics. Moreover, one can apply the Hellmann–Feynman theorem, i.e.,

$$\frac{\mathrm{d}\varepsilon_\alpha(\Omega)}{\mathrm{d}\Omega} = \left\langle\!\!\left\langle \Phi_\alpha(\Omega)\left|\frac{\partial\mathscr{H}(\Omega)}{\partial\Omega}\right|\Phi_\alpha(\Omega)\right\rangle\!\!\right\rangle . \tag{19}$$

Setting $\tau = \Omega t$ and $\mathscr{H}(q,\tau) = H(q,\tau) - \mathrm{i}\hbar\Omega\partial/\partial\tau$, one finds

$$\left(\frac{\partial\mathscr{H}}{\partial\Omega}\right)_\tau = -\mathrm{i}\hbar\frac{\partial}{\partial\tau} = -\mathrm{i}\hbar\frac{1}{\Omega}\frac{\partial}{\partial t}, \tag{20}$$

and consequently for Eq. (17) [42]

$$\bar{H}_\alpha = \varepsilon_\alpha(S,\Omega) - \Omega\frac{\partial\varepsilon_\alpha(S,\Omega)}{\partial\Omega} . \tag{21}$$

This connection between the averaged energy $\bar{H}_\alpha$ and the quasienergy ε_α in addition provides a relationship between the *dynamical phase* χ_{D}^α of a Floquet state Ψ_α, i.e., [41]

$$\chi_{\mathrm{D}}^\alpha = -\frac{1}{\hbar}\int_0^{\mathscr{T}} \mathrm{d}t\langle \Psi_\alpha|H(t)|\Psi_\alpha\rangle = -\frac{1}{\hbar}\mathscr{T}\bar{H}_\alpha , \tag{22}$$

and a nonadiabatic (i.e. generalized) Berry phase χ_{B}^α, where

$$\chi = \chi_{\mathrm{D}}^\alpha + \chi_{\mathrm{B}}^\alpha = -\varepsilon_\alpha\mathscr{T}/\hbar ; \tag{23}$$

thus yielding

$$\chi_{\mathrm{B}}^\alpha = \mathrm{i}\mathscr{T}\left\langle\!\!\left\langle \Psi_\alpha\left|\frac{\partial}{\partial t}\right|\Psi_\alpha\right\rangle\!\!\right\rangle = -\frac{2\pi}{\hbar}\frac{\partial\varepsilon_\alpha(S,\Omega)}{\partial\Omega} . \tag{24}$$

The part χ_{B}^α of the overall phase χ describes an intrinsic property of a cyclic change of parameters in the periodic Hamiltonian $H(t) = H(t+\mathscr{T})$ that explicitly does *not* depend on the dynamical time interval of cyclic propagation $\mathscr{T}$.

Next we discuss general features of quasienergies and Floquet modes with respect to their frequency and field dependence. As mentioned before, if $\varepsilon_\alpha = \varepsilon_{\alpha 0}$ possesses the Floquet mode $\Phi_{\alpha 0}(q,t)$, the modes

$$\Phi_{\alpha 0} \to \Phi_{\alpha k} = \Phi_{\alpha 0}(q,t)\exp(\mathrm{i}\Omega k t), \quad k = 0, \pm 1, 2, \dots , \tag{25}$$

are also solutions with quasienergies

$$\varepsilon_{\alpha k} = \varepsilon_{\alpha 0} + \hbar k \Omega , \tag{26}$$

yielding identical physical states,

$$\Psi_{\alpha 0}(q,t) = \exp(-\mathrm{i}\varepsilon_{\alpha 0} t/\hbar)\Phi_{\alpha 0}(q,t) = \Psi_{\alpha k}(q,t) . \tag{27}$$

For an interaction $S \to 0$ that is switched off adiabatically, the Floquet modes and the quasienergies obey

$$\Phi_{\alpha k}(q,t) \overset{S\to 0}{\to} \Phi^0_{\alpha k}(q,t) = \varphi_\alpha(q)\exp(\mathrm{i}\Omega k t) \tag{28}$$

and

$$\varepsilon_{\alpha k}(S,\Omega) \overset{S\to 0}{\to} \varepsilon^0_{\alpha k} = E_\alpha + k\hbar\Omega , \tag{29}$$

with $\{\varphi_\alpha, E_\alpha\}$ denoting the eigenfunctions and eigenvalues of the time-independent part H_0 of the Hamiltonian in Eq. (3). Thus, when $S = 0$, the quasienergies depend linearly on frequency so that at some frequency values different levels $\varepsilon^0_{\alpha k}$ intersect. When $S \neq 0$, the interaction operator mixes these levels, depending on the symmetry properties of the Hamiltonian. Given a symmetry for $H(q,t)$, the Floquet eigenvalues $\varepsilon_{\alpha k}$ can be separated into *symmetry classes*: Levels in each class mix with each other, but do not interact with levels of other classes. Let us consider levels $\varepsilon^0_{\alpha n}$ and $\varepsilon^0_{\beta k}$ of the same group at resonances, i.e.,

$$E_\alpha + n\hbar\Omega_{\mathrm{res}} = E_\beta + k\hbar\Omega_{\mathrm{res}} , \tag{30}$$

with Ω_{res} being the frequency of an (unperturbed) resonance. According to the von-Neumann–Wigner theorem [43], these levels of the same class will no longer intersect for finite $S \neq 0$. In other words, these levels develop into avoided crossings, cf. Fig. 1a. If the levels obeying Eq. (30) belong to a different class, for example to different generalized parity states, the quasienergies at finite $S \neq 0$ exhibit exact crossings; cf. Fig. 1b.

These considerations, conducted without any approximation, leading to avoided vs. exact crossings, determine many interesting and novel features of driven quantum systems. Some interesting consequences follow immediately from the structure in Fig. 1: Starting out from a stationary state $\Psi(q,t) = \varphi_1(q)\exp(-\mathrm{i}E_1 t/\hbar)$ the smooth adiabatic switch-on of the interaction with $\Omega < \Omega_{\mathrm{res}}$ ($\Omega > \Omega_{\mathrm{res}}$) will transfer the system into a quasienergy state Ψ_{10} [44–48]. Upon increasing (decreasing) adiabatically the frequency to a value $\Omega > \Omega_{\mathrm{res}}$ ($\Omega < \Omega_{\mathrm{res}}$) and again smoothly switching off the perturbation, the system generally jumps to a different state

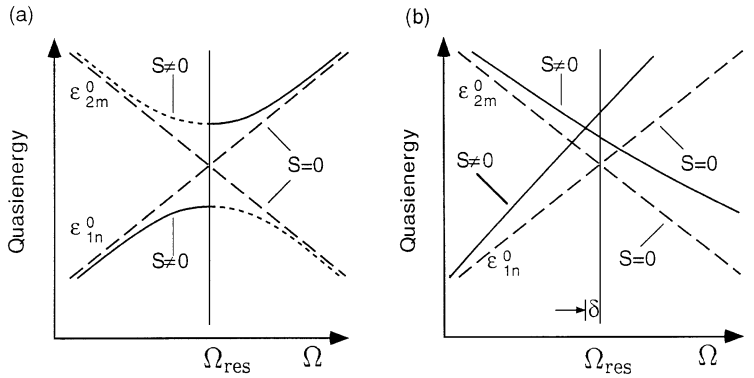

Fig. 1. Quasienergy dependence on the frequency Ω of a monochromatic electric-dipole perturbation near the unperturbed resonance Ω_{res} between two levels. The dashed lines correspond to quasienergies for $S \to 0$. In panel (a), we depict an avoided crossing for two levels belonging to the same symmetry related class. Note that with finite S the dotted parts belong to the Floquet mode Φ_{2m}, while the solid parts belong to the state Φ_{1n}. In panel (b), we depict an exact crossing between two members of quasienergies belonging to different symmetry-related classes. With $S \neq 0$, the location of the resonance generally undergoes a shift $\delta = \Omega_{res}(S \neq 0) - \Omega_{res}(S = 0)$ (so-called Bloch–Siegert shift [66]) that depends on the intensity S. Only for $S \to 0$ does the resonance frequency coincide with the unperturbed resonance Ω_{res}.

$\Psi(q,t) = \varphi_2(q)\exp(-\mathrm{i}E_2 t/\hbar)$. For example, this phenomenon is known in NMR as spin exchange; it relates to a rapid (as compared to relaxation processes) adiabatic crossing of the resonance. Moreover, as seen in Fig. 1a, the quasienergy ε_{2k} and Floquet mode Φ_{2k} as a function of frequency exhibit jump discontinuities at the frequencies of the unperturbed resonance, i.e., the change of energy between the two parts of the solid lines (or dashed lines, respectively).

2.3. Time-evolution operators for Floquet Hamiltonians

The time propagator $U(t,t_0)$, defined by

$$|\Psi(t)\rangle = U(t,t_0)|\Psi(t_0)\rangle, \quad U(t_0,t_0) = 1\,, \tag{31}$$

assumes special properties when $H(t) = H(t+\mathscr{T})$ is periodic. In particular, the propagator over a full period $U(\mathscr{T},0)$ can be used to construct a discrete quantum map, propagating an initial state over long multiples of the fundamental period by observing that

$$U(n\mathscr{T},0) = [U(\mathscr{T},0)]^n\,. \tag{32}$$

This important relation follows readily from the periodicity of $H(t)$ and its definition. Namely, we find with $t_0 = 0$ ($\top$ denotes time ordering of operators)

$$\mathrm{U}(n\mathscr{T},0) = \top \exp\left[-\frac{\mathrm{i}}{\hbar}\int_0^{n\mathscr{T}} \mathrm{d}t\, H(t)\right] = \top \exp\left[-\frac{\mathrm{i}}{\hbar}\sum_{k=1}^{n}\int_{(k-1)\mathscr{T}}^{k\mathscr{T}} \mathrm{d}t\, H(t)\right],$$

which with $H(t) = H(t+\mathscr{T})$ simplifies to

$$U(n\mathscr{T},0) = \top \exp\left[-\frac{\mathrm{i}}{\hbar}\sum_{k=1}^{n}\int_0^{\mathscr{T}} \mathrm{d}t\, H(t)\right] = \top \prod_{k=1}^{n} \exp\left[-\frac{\mathrm{i}}{\hbar}\int_0^{\mathscr{T}} \mathrm{d}t\, H(t)\right]. \tag{33}$$

Because the terms over a full period are equal, they do commute. Hence, the time-ordering operator can be moved in front of a single term, yielding

$$U(n\mathscr{T},0)=\prod_{k=1}^{n}\top\exp\left[-\frac{\mathrm{i}}{\hbar}\int_0^{\mathscr{T}}\mathrm{d}t\,H(t)\right]=[U(\mathscr{T},0)]^n\,. \tag{34}$$

Likewise, one can show that with $t_0=0$ the following relation holds:

$$U(t+\mathscr{T},\mathscr{T})=U(t,0)\,, \tag{35}$$

which implies that

$$U(t+\mathscr{T},0)=U(t,0)U(\mathscr{T},0)\,. \tag{36}$$

Note that $U(t,0)$ does not commute with $U(\mathscr{T},0)$, except at times $t=n\mathscr{T}$, so that Eq. (36) with the right-hand-side product *reversed* does not hold. A most important feature of Eqs. (30)–(36) is that the knowledge of the propagator over a fundamental period $\mathscr{T}=2\pi/\Omega$ provides all the information needed to study the long-time dynamics of periodically driven quantum systems. That is, upon a diagonalization with an unitary transformation S,

$$\mathsf{S}^\dagger U(\mathscr{T},0)\mathsf{S}=\exp(-\mathrm{i}\mathsf{D})\,, \tag{37}$$

with D a diagonal matrix, composed of the eigenphases $\{\varepsilon_\alpha\mathscr{T}\}$, one obtains

$$U(n\mathscr{T},0)=[U(\mathscr{T},0)]^n=\mathsf{S}\exp(-\mathrm{i}n\mathsf{D})\mathsf{S}^\dagger\,. \tag{38}$$

This relation can be used to propagate any initial state

$$|\Psi(0)\rangle=\sum_\alpha c_\alpha|\Phi_\alpha(0)\rangle,\quad c_\alpha=\langle\Phi_\alpha(0)|\Psi(0)\rangle\,, \tag{39}$$

in a stroboscopic manner. This procedure generates a discrete *quantum map*. With $\Psi_\alpha(q,t=0)=\Phi_\alpha(q,t=0)$, its time evolution follows from Eq. (4) as

$$\Psi(q,t)=\sum_\alpha c_\alpha\exp(-\mathrm{i}\varepsilon_\alpha t/\hbar)\Phi_\alpha(q,t)\,. \tag{40}$$

With $\Psi(q,t)=\langle q|U(t,0)|\Psi(0)\rangle$, a spectral representation for the propagator, i.e.,

$$K(q,t;q_0,0):=\langle q|U(t,0)|q_0\rangle\,, \tag{41}$$

follows from Eq. (41) with $\Psi(q,0)=\delta(q-q_0)$ as

$$K(q,t;q_0,0)=\sum_\alpha\exp(-\mathrm{i}\varepsilon_\alpha t/\hbar)\Phi_\alpha(q,t)\Phi_\alpha^*(q_0,0)\,. \tag{42}$$

This relation is readily generalized to arbitrary propagation times $t>t'$, yielding

$$K(q,t;q',t')=\sum_\alpha\exp(-\mathrm{i}\varepsilon_\alpha(t-t')/\hbar)\Phi_\alpha(q,t)\Phi_\alpha^*(q',t')\,. \tag{43}$$

This intriguing result generalizes the familiar form of time-independent propagators to *time-periodic* ones. Note again, however, that the role of the stationary eigenfunction $\varphi_\alpha(q)$ is taken over by the Floquet mode $\Phi_\alpha(q,t)$, being orthonormal only at equal times $t = t' \bmod \mathscr{T}$.

2.4. Generalized Floquet methods for nonperiodic driving

In the previous subsections we have restricted ourselves to pure harmonic interactions. In many physical applications, e.g. see in [7,11–13], however, the time-dependent perturbation has an arbitrary, for example, pulse-like form that acts over a limited time regime only. Clearly, in these cases the Floquet theorem cannot readily be applied. This feature forces one to look for a generalization of the quasienergy concept. Before we start doing so, we note that the Floquet eigenvalues $\varepsilon_{\alpha n}$ in Eq. (9) can also be obtained as the ordinary Schrödinger eigenvalues within a two-dimensional formulation of the time-periodic Hamiltonian in Eq. (3). Setting $\Omega t = \theta$, Eq. (3) is recast as

$$H(t) = H_0(q,p) + H_{\text{ext}}(q,\theta(t))\,. \tag{44}$$

With $\dot{\theta} = \Omega$, one constructs the enlarged Hamiltonian $\tilde{H}(q,p;\theta,p_\theta) = H_0(q,p) + H_{\text{ext}}(q,\theta) + \Omega p_\theta$, where p_θ is the canonically conjugate momentum, obeying

$$\dot{\theta} = \partial\tilde{H}/\partial p_\theta = \Omega\,. \tag{45}$$

The quantum mechanics of $\tilde{H}$ acts on the Hilbert space of square-integrable functions on the extended space of the q-variable and the square-integrable periodic functions on the compact space of the unit circle $\theta = \theta_0 + \Omega t$ (periodic boundary conditions for θ). With $H_{\text{ext}}(q,t)$ given by Eq. (16), the Floquet modes $\Phi_{\alpha k}(q,\theta)$ and the quasienergies $\varepsilon_{\alpha k}$ are the eigenfunctions and eigenvalues of the two-dimensional stationary Schrödinger equation, i.e., with $[\theta, p_\theta] = \mathrm{i}\hbar$,

$$\left\{\frac{-\hbar^2}{2m}\frac{\partial^2}{\partial q^2} + V_0(q) - Sq\sin(\theta+\phi) - \mathrm{i}\hbar\Omega\frac{\partial}{\partial\theta}\right\}\Phi_{\alpha k}(q,\theta) = \varepsilon_{\alpha k}\Phi_{\alpha k}(q,\theta)\,. \tag{46}$$

This procedure opens a door to treat more general, polychromatic perturbations composed of generally incommensurate frequencies. For example, a quasiperiodic perturbation with two incommensurate frequencies Ω_1 and Ω_2, e.g.

$$H_{\text{ext}}(q,t) = -qS\sin(\Omega_1 t) - qF\sin(\Omega_2 t)\,, \tag{47}$$

can be enlarged into a six-dimensional phase space $(q,p_q;\theta_1,p_{\theta_1};\theta_2,p_{\theta_2})$, with $\{\theta_1 = \Omega_1 t;\theta_2 = \Omega_2 t\}$ defined on a torus. The quantization of the corresponding momentum terms yield a stationary Schrödinger equation in the three variables (x,θ_1,θ_2) with a corresponding Hamiltonian operator $\tilde{H}$ given by

$$\tilde{H} = H(q,\theta_1,\theta_2) - \mathrm{i}\hbar\Omega_1(\partial/\partial\theta_1) - \mathrm{i}\hbar\Omega_2(\partial/\partial\theta_2) \tag{48}$$

with eigenvalues $\{\varepsilon_{\alpha,k_1,k_2}\}$ and generalized stationary wavefunctions given by the generalized Floquet modes $\Phi_{\alpha,k_1,k_2}(q,\theta_1,\theta_2) = \Phi_{\alpha,k_1,k_2}(q;\theta_1+2\pi;\theta_2+2\pi)$. An application of this extended two-frequency Floquet theory could be invoked to study the problem of bichromatic field control of tunneling in a double well [49].

There are important qualitative differences between the periodic and the quasi-periodic forcing cases. Let us consider a Hilbert space of finite dimension, such as e.g., a spin $\frac{1}{2}$ system or a N-level system in a radiation field. For a periodic time-dependent driving force the corresponding Floquet operator is a finite-dimensional unitary matrix. Thus, the corresponding quasienergy spectrum is always *pure point*. This, however, is no longer the case for quasi-periodic forcing [50]. We note that a point spectrum implies stable quasiperiodic dynamics (i.e., almost-periodic evolution); in contrast, a continuous spectrum signals an instability (leading to an unstable chaotic behavior) with typically decaying asymptotic correlations. With two incommensurate driving frequencies Ω_1 and Ω_2 the spectrum of the generalized Floquet operator in Eq. (48) can be pure point, absolutely continuous or also purely singular continuous [51–53].

A general perturbation, such as a time-dependent laser-pulse interaction, consists (via Fourier-integral representation) of an infinite number of frequencies, so that the above embedding ceases to be of practical use. The general time-dependent Schrödinger equation

$$\mathrm{i}\hbar(\partial/\partial t)\Psi(q,t) = H(q,t)\Psi(q,t)\,, \tag{49}$$

with the initial state given by $\Psi(q,t_0) = \Psi_0(q)$, can be solved by numerical means, by a great variety of methods [25,54–56]. All these methods must involve efficient numerical algorithms to calculate the time-ordered propagation operator $U(t,t')$. Generalizing the idea of Shirley [37] and Sambe [40] for time-periodic Hamiltonians, it is possible to introduce a Hilbert space for general time-dependent Hamiltonians in which the Schrödinger equation becomes time independent. Following the reasoning by Howland [57], we introduce the reader to the so-called (t,t')-formalism [58].

2.5. *The* (t,t')*-formalism*

The time-dependent solution

$$\Psi(q,t) = U(t,t_0)\Psi(q,t_0) \tag{50}$$

for the explicitly time-dependent Schrödinger equation in Eq. (49) can be obtained as

$$\Psi(q,t) = \Psi(q,t',t)|_{t'=t}\,, \tag{51}$$

where

$$\Psi(q,t',t) = \exp[(-\mathrm{i}/\hbar)\mathscr{H}(q,t')(t-t_0)]\Psi(q,t',t_0)\,. \tag{52}$$

$\mathscr{H}(q,t')$ is the generalized Floquet operator

$$\mathscr{H}(q,t') = H(q,t') - \mathrm{i}\hbar\,\partial/\partial t'\,. \tag{53}$$

The time t' acts as a time coordinate in the generalized Hilbert space of square-integrable functions of q and t', where a box normalization of length $\mathscr{T}$ is used for t' $(0 < t' < \mathscr{T})$. For two functions $\phi_\alpha(q,t), \phi_\beta(q,t)$ the inner, or scalar product reads

$$\langle\!\langle \phi_\alpha|\phi_\beta\rangle\!\rangle = \frac{1}{\mathscr{T}}\int_0^{\mathscr{T}} \mathrm{d}t' \int_{-\infty}^{\infty} \mathrm{d}q\, \phi_\alpha^*(q,t')\phi_\beta(q,t')\,. \tag{54}$$

The proof for Eq. (51) can readily be given as follows [58]: Note that from Eq. (52)

$$i\hbar\frac{\partial}{\partial t}\Psi(q,t',t) = \mathscr{H}(q,t')\exp[-i\mathscr{H}(q,t')(t-t_0)/\hbar]\Psi(q,t',t_0)$$

$$= -i\hbar\frac{\partial}{\partial t'}\Psi(q,t',t) + H(q,t')\Psi(q,t',t)\,. \tag{55}$$

Hence,

$$i\hbar\left(\frac{\partial}{\partial t}+\frac{\partial}{\partial t'}\right)\Psi(q,t',t) = H(q,t')\Psi(q,t',t)\,. \tag{56}$$

Since we are interested in t' only on the contour $t'=t$, where $\partial t'/\partial t = 1$, one therefore finds that

$$\left.\frac{\partial\Psi(q,t',t)}{\partial t'}\right|_{t'=t} + \left.\frac{\partial\Psi(q,t',t)}{\partial t}\right|_{t'=t} = \frac{\partial\Psi(q,t)}{\partial t}\,, \tag{57}$$

which with Eq. (56) for $t=t'$ consequently proves the assertion in Eq. (51).

Note that a long time propagation now requires the use of a large box, i.e., $\mathscr{T}$ must be chosen sufficiently large. If we are not interested in the very-long-time propagation, the perturbation of finite duration can be embedded into a box of finite length $\mathscr{T}$, and periodically continued. This so constructed perturbation now implies a time-periodic Hamiltonian, so that we require time-periodic boundary conditions

$$\Psi(q,t',t) = \Psi(q,t'+\mathscr{T},t)\,, \tag{58}$$

with $0 \le t' \le \mathscr{T}$, and the physical solution is obtained when

$$t' = t \bmod \mathscr{T}\,. \tag{59}$$

Stationary solutions of Eq. (55) thus reduce to the Floquet states, as found before, namely

$$\Psi_\alpha(q,t',t) = \exp(-i\varepsilon_\alpha t/\hbar)\Phi_\alpha(q,t')\,, \tag{60}$$

with $\Phi_\alpha(q,t') = \Phi_\alpha(q,t'+\mathscr{T})$, and $t' = t \bmod \mathscr{T}$. We remark that although $\Psi(q,t',t)$, $\Psi_\alpha(q,t',t)$ are periodic in t', the solution $\Psi(q,t) = \Psi(q,t'=t,t)$ is generally not time periodic.

The (t,t')-method hence avoids the need to introduce the generally nasty time-ordering procedure. Expressed differently, the step-by-step integration that characterizes the time-dependent approaches is not necessary when formulated in the above generalized Hilbert space where $\mathscr{H}(q,t')$ effectively becomes time-independent, with t' acting as coordinate. Formally, the result in Eq. (55) can be looked upon as quantizing the new Hamiltonian $\hat{H}$, defined by

$$\hat{H}(q,p;E,t') = H(q,p,t') - E\,, \tag{61}$$

using for the operator $E \to \hat{E}$ the canonical quantization rule $\hat{E} = i\hbar\,\partial/\partial t$; with $[\hat{E},\hat{t}] = i\hbar$ and $\hat{t}\phi(t) = t\phi(t)$. This formulation of the time-dependent problem in Eq. (49) within the auxiliary t' coordinate is particularly useful for evaluating the state-to-state transition probabilities in pulse-sequence-driven quantum systems [11,13,58].

We conclude this section by commenting on *exactly solvable* driven quantum systems. In contrast to time-independent quantum theory, such exactly solvable quantum systems with time-dependent potentials are extremely rare. One such class of systems are (multidimensional) systems with at most quadratic interactions between momentum and coordinate operators, e.g. the driven free particle [59,60], the parametrically driven harmonic oscillator [61,62], including generalizations that account for quantum dissipation via bilinear coupling to a harmonic bath [63]. Another class entails driven systems operating in a finite or countable Hilbert space, such as some spin system, cf. Sections 3.4 and 7.4, or some tight-binding models, cf. Section 4.

3. Driven two-level systems

3.1. Two-state approximation to driven tunneling

In this section we shall investigate the dynamics of driven two-level-systems (TLS), i.e., of quantum systems whose Hilbert space can be effectively restricted to a two-dimensional space.

The most natural example is that of a particle of total angular momentum $J = \hbar/2$, as for example a silver atom in the ground state. The magnetic moment of the particle is $\boldsymbol{\mu} = \frac{1}{2}\hbar\gamma\boldsymbol{\sigma}$, where γ is the gyromagnetic ratio and $\boldsymbol{\sigma} = (\sigma_x, \sigma_y, \sigma_z)$ are the Pauli spin matrices.[1] When the particle is placed in a time-dependent magnetic field $\boldsymbol{B}(t)$ the time-dependent magnetic Hamiltonian H_{M} thus reads

$$H_{\mathrm{M}}(t) = -\boldsymbol{\mu}\cdot\boldsymbol{B} = -\tfrac{1}{2}\hbar\gamma(\sigma_z B_z(t) + \sigma_x B_x(t) + \sigma_y B_z(t))\,. \tag{62}$$

For a generic quantum system one considers the case in which only a *finite* number of quantum levels strongly interact under the influence of the time-dependent interaction. This means that a truncation to a multi-level quantum system in which only a finite number of quantum states strongly interact is adequate. In particular, the truncation to two relevant levels only is of enormous practical importance in nuclear magnetic resonance, quantum optics, or in low temperature glassy systems, to name only a few. Setting $\hbar\Delta_0 = E_2 - E_1$, this truncation in the energy representation of the ground state $|1\rangle$ and excited state $|2\rangle$ is in terms of the Pauli spin matrices σ_z, σ_x and σ_y given by

$$H_{\mathrm{E}} = -\tfrac{1}{2}\hbar\Delta_0\sigma_z\,, \tag{63}$$

where the subscript "E" indicates that this is the energy representation.

Very frequently in the chemical literature the effects of a *static* electric field $\mathscr{E}_0$ coupling to the transition dipole moment μ between the two levels of a molecule are investigated. Setting

[1] We use for the Pauli matrices the representation

$$\sigma_x = \begin{pmatrix} 0 & 1 \\ 1 & 0 \end{pmatrix}, \quad \sigma_y = \begin{pmatrix} 0 & -i \\ i & 0 \end{pmatrix}, \quad \sigma_z = \begin{pmatrix} 1 & 0 \\ 0 & -1 \end{pmatrix}.$$

That is, σ_z is chosen to be diagonal.

$-\hbar\varepsilon_0/2 = \mathscr{E}_0\mu$, we end up with the TLS Hamiltonian

$$H_{\text{opt}} = -\tfrac{1}{2}\hbar(\Delta_0\sigma_z - \varepsilon_0\sigma_x)\,, \tag{64}$$

which is widely used to investigate *optical* properties.

Diverse physical or chemical systems can be described by the Hamiltonian (63). In particular, a very important class concerns those systems moving in an effective double well potential in the case in which only the lowest energy doublet is occupied. These systems are the simplest one exhibiting quantum interference effects: a system which is initially localized in one well will oscillate clockwise between the eigenstates in the left and right well due to quantum mechanical tunneling. A well-known example is the ammonia molecule NH_3: The nitrogen atom, much heavier than its partners is motionless; the hydrogen atoms form a rigid equilateral triangle whose axis passes through the nitrogen atom. The potential energy is thus only a function of the distance q between the nitrogen atom and the plane defined by the hydrogen atoms. Hence, the potential energy of the system has two equivalent configurations of stable equilibrium, which are symmetric respect to the $q = 0$ plane. Quantum mechanically the hydrogens can tunnel back and forth between the two potential minima [23].

To be more explicit, we characterize the double well by the barrier height E_B, by the separation $\hbar\omega_0 \ll E_B$ of the first excited state from the ground state in either well, and by an intrinsic asymmetry energy $\hbar\varepsilon_0 \ll \hbar\omega_0$ between the ground states in the two wells. At zero temperature, the system will be effectively restricted to the two-dimensional Hilbert space spanned by the two ground states. Taking into account the possibility of tunneling between the two wells, the TLS is then governed by the pseudospin Hamiltonian (*tunneling* or *localized* representation)

$$H_{\text{TLS}} = -\tfrac{1}{2}\hbar(\Delta_0\sigma_x + \varepsilon_0\sigma_z)\,. \tag{65}$$

This is the representation which is convenient to investigate tunneling problems. Here the basis is chosen such that the states $|R\rangle$ (right) and $|L\rangle$ (left) are eigenstates of σ_z with eigenvalues 1 and -1, respectively. Hence, σ_z is related to the position operator q in this discretized representation by $q = \sigma_z d/2$, with d being the spatial distance between the two localized states. The interaction energy $\hbar\Delta_0$ is the energy splitting of a symmetric (i.e., $\varepsilon_0 = 0$) TLS due to tunneling.

We observe now that the unitary transformation

$$R(\theta) = \exp(-\mathrm{i}\theta\sigma_y/2), \quad -\tan\theta = \Delta_0/\varepsilon_0\,, \tag{66}$$

tranforms H_{TLS} as

$$RH_{\text{TLS}}R^{-1} = -\tfrac{1}{2}E\sigma_z, \quad E = \hbar\sqrt{\Delta_0^2 + \varepsilon_0^2}\,, \tag{67}$$

which is of the same form of Eq. (63) with energy splitting E. Note that if the static asymmetry ε_0 originates from an *externally* applied dc-field it may be convenient to apply the transformation $\tilde{R} = \exp(\mathrm{i}\pi\sigma_y/4)$ to the Hamiltonian H_{TLS}. Such a procedure yields

$$\tilde{R}H_{\text{TLS}}\tilde{R}^{-1} = -\tfrac{1}{2}\hbar(\Delta_0\sigma_z - \varepsilon_0\sigma_x) = H_{\text{opt}}\,. \tag{68}$$

Hence, the two transformations R and $\tilde{R}$ coincide when $\varepsilon_0 = 0$.

At this point it is indeed interesting to recall that for the two-level problem, the corresponding density matrix ρ is a 2×2 matrix with matrix elements $\rho_{\sigma,\sigma'}$ (where $\sigma, \sigma' = \pm 1$ are the eigenvalues

of σ_z), whose knowledge enables the evaluation of the expectation value of *any* observable related to the TLS. In particular, because any 2×2 matrix can be written as a linear combination of the Pauli matrices and of the unit matrix I, one has $\rho(t) = I/2 + \sum_{i=x,y,z} \langle \sigma_i \rangle_t \sigma_i/2$, where $\langle \sigma_i \rangle_t := \mathrm{Tr}\{\rho(t)\sigma_i\}$ (with Tr denoting the trace). This yields

$$\langle \sigma_z \rangle_t = \rho_{1,1}(t) - \rho_{-1,-1}(t), \qquad \langle \sigma_x \rangle_t = \rho_{1,-1}(t) + \rho_{-1,1}(t),$$
$$\langle \sigma_y \rangle_t = \mathrm{i}[\rho_{1,-1}(t) - \rho_{-1,1}(t)] , \tag{69}$$

where we denoted by $\rho_{-1,-1}$, and $\rho_{1,1}$ the diagonal matrix elements of the density matrix, and by $\rho_{-1,1}$, $\rho_{1,-1}$ the off-diagonal elements (so-called coherences). We have then for the expectation values $P(t)$ of the position operator

$$P(t) := \mathrm{Tr}\{\rho_{\mathrm{TLS}}(t)\sigma_z\} = \cos\theta \, \mathrm{Tr}\{\rho_{\mathrm{E}}(t)\sigma_z\} + \sin\theta \, \mathrm{Tr}\{\rho_{\mathrm{E}}(t)\sigma_x\} , \tag{70}$$

where $\rho_{\cdots}$ is the density matrix in the corresponding representation. Hence, in the *localized* basis $\langle \sigma_z \rangle_t$ describes the population difference of the localized states. It provides direct informations on the dynamics of the TLS. In the same way, one obtains for the difference $N(t)$ in the population of the energy levels

$$N(t) := \mathrm{Tr}\{\rho_{\mathrm{E}}(t)\sigma_z\} = \cos\theta \, \mathrm{Tr}\{\rho_{\mathrm{TLS}}(t)\sigma_z\} - \sin\theta \, \mathrm{Tr}\{\rho_{\mathrm{TLS}}(t)\sigma_x\} . \tag{71}$$

In particular, $N(t)$ coincides with $\mathrm{Tr}\{\rho_{\mathrm{TLS}}(t)\sigma_x\}$ for the case of a symmetric ($\varepsilon_0 = 0$), undriven TLS. In the absence of driving, the density matrix can be evaluated straightforwardly. A TLS prepared in a localized state at an initial time $t = t_0$ will exhibit an oscillatory, undamped, behavior due to quantum interference effects. One finds in the *localized* basis

$$\langle \sigma_z \rangle_t = \frac{\hbar^2 \varepsilon_0^2}{E^2} + \frac{\hbar^2 \Delta_0^2}{E^2} \cos[E(t - t_0)/\hbar] , \tag{72}$$

$$\langle \sigma_x \rangle_t = \hbar^2 \frac{\varepsilon_0 \Delta_0}{E^2} \{1 - \cos[E(t - t_0)/\hbar]\} , \tag{73}$$

$$\langle \sigma_y \rangle_t = \frac{\hbar \Delta_0}{E} \sin[E(t - t_0)/\hbar] . \tag{74}$$

Hence, a TLS prepared in a localized state at an initial time t_0 will undergo quantum coherent oscillations between its localized states with frequency $E = \hbar(\Delta_0^2 + \varepsilon_0^2)^{1/2}$, corresponding to the energy splitting of the isolated TLS. Correspondingly, as follows from Eq. (71), the difference population of the energy levels is constant for an initially localized state, and given by $N(t) = \hbar\varepsilon_0/E$.

In the following, we shall investigate the evolution of some observables related to the driven TLS in the presence of different kinds of driving forces.

3.2. Linearly polarized radiation fields

Let us next consider, for example, the interaction of the TLS with a classical electric field $\mathscr{E}(t)$. We end up with the time-dependent Hamiltonian

$$H_{\mathrm{E}}(t) = -\tfrac{1}{2}\hbar\Delta_0\sigma_z - \mu\mathscr{E} \sin(\Omega t + \phi)\sigma_x , \tag{75}$$

with $\mu \equiv \langle 2|q|1\rangle$ being the transition dipole moment, and $|1\rangle$, $|2\rangle$ the energy eigenstates. Here we have used a scalar approximation of the electric field $\mathscr{E}$ along the q-direction. The linearly polarized field in Eq. (75) can, with $\hbar\hat{\varepsilon}/2 \equiv \mu\mathscr{E}$, be regarded as a superposition of left- and right-circularly polarized radiation. Namely, setting $\phi = \pi/2$, we have

$$\hat{\varepsilon}\cos\Omega t = \hat{\varepsilon}[\exp(-\mathrm{i}\Omega t) + \exp(\mathrm{i}\Omega t)]/2\,. \tag{76}$$

The effects of the two contributions $\exp(\pm \mathrm{i}\Omega t)$ can be better understood if one considers the quantized version, cf. Eq. (103) below, of the time-dependent Hamiltonian (75). Let us next introduce the product states $|i, n\rangle := |i\rangle|n\rangle$, with $(i = 1, 2)$ and with $|n\rangle$ being a Fock state of the quantized electric field with occupation number n. For the absorption process $|1, n\rangle \to |2, n-1\rangle$, the term $\hat{\varepsilon}\exp(-\mathrm{i}\Omega t)$ supplies the energy $\hbar\Omega$ to the system. It corresponds to the *rotating-wave* (RW) term, while the term $\hat{\varepsilon}\exp(\mathrm{i}\Omega t)$ is called the *anti-rotating-wave* term. This anti-RW term removes the energy $\hbar\Omega$ from the system, i.e., $|1, n\rangle \to |2, n+1\rangle$, and is thus energy nonconserving. Likewise, the term $\exp(\mathrm{i}\Omega t)$ governs the process of emission $|2, n\rangle \to |1, n+1\rangle$, i.e., it is a RW term, while the second-order process $|2, n\rangle \to |1, n-1\rangle$ is again an energy-nonconserving anti-RW term.

Another example of a driven TLS can be obtained in the context of electron-spin resonance (ESR), nuclear magnetic-spin resonance (NMR) or atomic-beam spectroscopy. In this case the TLS is a particle of total angular momentum $J = \hbar/2$ placed in both a static magnetic field B_0 in the z-direction, and a time-dependent oscillating magnetic field $2B_1\cos(\Omega t)$ in x-direction. The magnetic moment of the particle is $\mu = \gamma J$, where γ is the gyromagnetic ratio. The Hamiltonian H_{NMR} for the particle in the time-dependent magnetic field thus reads, cf. Eq. (62),

$$H_{\mathrm{NMR}}(t) = -\boldsymbol{\mu}\cdot\boldsymbol{B} = -\tfrac{1}{2}\hbar\gamma\sigma_z B_0 - \hbar\gamma\sigma_x B_1\cos(\Omega t)\,. \tag{77}$$

With

$$\Delta_0 = \gamma B_0, \qquad \mu\mathscr{E} = \hbar\hat{\varepsilon}/2 = \hbar\gamma B_1\,, \tag{78}$$

this Hamiltonian coincides with the laser-driven TLS in Eq. (75) with $\phi = \pi/2$.

Finally, if one considers the effects of an ac electric field which is modulating the asymmetry energy of the underlying bistable potential, one ends up, in the tunneling representation, with

$$H_{\mathrm{TLS}}(t) = -\tfrac{1}{2}\hbar(\varepsilon_0 + \hat{\varepsilon}\cos\Omega t)\sigma_z - \tfrac{1}{2}\hbar\Delta_0\sigma_x\,. \tag{79}$$

Note that the same form of the Hamiltonian (79) is obtained if one considers the combined effect of a dc–ac electric field on a *symmetric* TLS.

3.2.1. Time evolution of the population of the energy levels

The driven two-level system has a long history, with recent reviews being available [64]. A pioneering piece of work must be attributed to Rabi [65], who considered the two-level system in a circularly polarized magnetic field, a problem that he could solve exactly, see below in Section 3.4. He thereby elucidated how to measure simultaneously both the *sign* as well as the *magnitude* of magnetic moments. However, as Bloch and Siegert experienced soon after [66], this problem is no longer exactly solvable in analytical closed form when the field is linearly polarized,

rather than circularly. Let us start with the linearly polarized case as given by the driven Hamiltonian (75), (76). We set for the wave function in the energy basis $|1\rangle$, $|2\rangle$,

$$\Psi(t) = c_1(t)\exp(\mathrm{i}\Delta_0 t/2)\begin{pmatrix}1\\0\end{pmatrix} + c_2(t)\exp(-\mathrm{i}\Delta_0 t/2)\begin{pmatrix}0\\1\end{pmatrix}, \tag{80}$$

where $|c_1(t)|^2 + |c_2(t)|^2 = 1$. The Schrödinger equation thus has the form

$$\mathrm{i}\hbar\frac{\mathrm{d}}{\mathrm{d}t}\begin{pmatrix}c_1(t)\exp(\mathrm{i}\Delta_0 t/2)\\ c_2(t)\exp(-\mathrm{i}\Delta_0 t/2)\end{pmatrix} = -\frac{\hbar}{2}\begin{pmatrix}\Delta_0 & \hat{\varepsilon}\cos\Omega t\\ \hat{\varepsilon}\cos\Omega t & -\Delta_0\end{pmatrix}\begin{pmatrix}c_1(t)\exp(\mathrm{i}\Delta_0 t/2)\\ c_2(t)\exp(-\mathrm{i}\Delta_0 t/2)\end{pmatrix}, \tag{81}$$

and provides two coupled first-order equations for the amplitudes,

$$\begin{aligned}\mathrm{d}c_1/\mathrm{d}t &= \tfrac{1}{4}\mathrm{i}\hat{\varepsilon}[\exp[\mathrm{i}(\Omega-\Delta_0)t] + \exp[-\mathrm{i}(\Omega+\Delta_0)t]]c_2\,,\\ \mathrm{d}c_2/\mathrm{d}t &= \tfrac{1}{4}\mathrm{i}\hat{\varepsilon}[\exp[-\mathrm{i}(\Omega-\Delta_0)t] + \exp[\mathrm{i}(\Omega+\Delta_0)t]]c_1\,.\end{aligned} \tag{82}$$

With an additional differentiation with respect to time, and substituting $\dot{c}_2$ from the second equation, we readily find that $c_1(t)$ obeys a linear second order ordinary differential equation with time periodic ($\mathscr{T} = 2\pi/\Omega$) coefficients (so termed Hill equation). Clearly, such equations are generally not solvable in analytical closed form. Hence, although the problem is simple, the job of finding an analytical solution presents a hard task! To make progress, one usually invokes, at this stage, the so-called rotating-wave approximation (RWA), assuming that Ω is close to Δ_0 (near resonance), and $\hat{\varepsilon}$ not very large. Then the anti-rotating-wave term $\exp[\mathrm{i}(\Omega+\Delta_0)t]$ is rapidly varying, as compared to the slowly varying rotating-wave term $\exp[-\mathrm{i}(\Omega-\Delta_0)t]$. It thus cannot transfer much population from state $|1\rangle$ to state $|2\rangle$. Neglecting this anti-rotating contribution one finds in terms of the detuning parameter $\delta \equiv \Omega - \Delta_0$ (*rotating-wave approximation*),

$$\frac{\mathrm{d}c_1}{\mathrm{d}t} = \mathrm{i}\frac{\hat{\varepsilon}}{4}\exp(\mathrm{i}\delta t)c_2, \qquad \frac{\mathrm{d}c_2}{\mathrm{d}t} = \mathrm{i}\frac{\hat{\varepsilon}}{4}\exp(-\mathrm{i}\delta t)c_1\,. \tag{83}$$

From Eq. (83) one finds for $c_1(t)$ a linear second-order differential equation with constant coefficients – which can be solved readily for arbitrary initial conditions. For example, setting $c_1(0) = 1$, $c_2(0) = 0$, we arrive at

$$\begin{aligned}c_1(t) &= \exp(\mathrm{i}\delta t)[\cos(\tfrac{1}{2}\Omega_{\mathrm{R}}t) - \mathrm{i}(\delta/\Omega_{\mathrm{R}})\sin(\tfrac{1}{2}\Omega_{\mathrm{R}}t)]\,,\\ c_2(t) &= \exp(-\mathrm{i}\delta t)(\mathrm{i}\hat{\varepsilon}/2\Omega_{\mathrm{R}})\sin(\tfrac{1}{2}\Omega_{\mathrm{R}}t)\,,\end{aligned} \tag{84}$$

where Ω_{R} denotes the celebrated *Rabi frequency*

$$\Omega_{\mathrm{R}} = (\delta^2 + \hat{\varepsilon}^2/4)^{1/2}\,. \tag{85}$$

The populations as a function of time are then given by

$$|c_1(t)|^2 = (\delta/\Omega_{\mathrm{R}})^2 + (\hat{\varepsilon}/2\Omega_{\mathrm{R}})^2\cos^2(\tfrac{1}{2}\Omega_{\mathrm{R}}t)\,, \tag{86}$$

$$|c_2(t)|^2 = (\hat{\varepsilon}/2\Omega_{\mathrm{R}})^2\sin^2(\tfrac{1}{2}\Omega_{\mathrm{R}}t)\,. \tag{87}$$

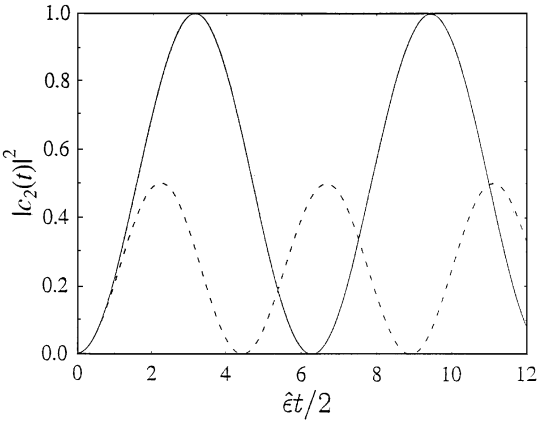

Fig. 2. The population probability of the upper state $|c_2(t)|^2$ as a function of time t at resonance, i.e., $\delta = 0$ (solid line), versus the non-resonant excitation dynamics (dashed line) at $\delta = \hat{\varepsilon}/2 \neq 0$.

Note that at short times t, the excitation in the upper state is independent of the detuning, i.e., $|c_2(t)|^{2\Omega_R t \ll 1}_{\rightarrow} \hat{\varepsilon}^2 t^2/16$. This behavior is in accordance with perturbation theory, valid at small times. Moreover, the population at resonance $\Omega = \Delta_0$ completely cycles the population between the two states, while with $\delta \neq 0$, the lower state is never completely depopulated, see Fig. 2.

Up to now, we have discussed approximate RWA solutions. Explicit results for the time-periodic Schrödinger equation require numerical methods, i.e., one must solve for the quasienergies $\varepsilon_{\alpha n}$ and the Floquet modes $\Psi_{\alpha n}(q,t)$. Without proof we state here some results that are of importance in discussing driven tunneling in the deep quantum regime. For example, Shirley [37] already showed that in the high-frequency regime $\Delta_0 \ll \max[\Omega, (\hat{\varepsilon}\Omega)^{1/2}]$ the quasienergies obey the difference

$$\varepsilon_{2,-1} - \varepsilon_{1,1} = \hbar \Delta_0 J_0(\hat{\varepsilon}/\Omega)\,, \tag{88}$$

where J_0 denotes the zeroth-order Bessel function of the first kind. The sum of the two quasienergies obeys the rigorous relation [37]

$$\varepsilon_{2n} + \varepsilon_{1k} = E_1 + E_2 = 0 \pmod{\hbar\Omega}\,. \tag{89}$$

For weak fields, one can evaluate the quasienergies by use of the stationary perturbation theory in the composite Hilbert space $\mathscr{R} \otimes \mathscr{T}$. In this way one finds:

1. Exact crossings at the parity-forbidden transitions where $\Delta_0 = 2n\Omega$, $n = 1, 2, \ldots$, so that

$$\varepsilon_{2,1} = 0 \pmod{\hbar\Omega}\,. \tag{90}$$

2. At resonance $\Omega = \Delta_0$:

$$\varepsilon_{2,1} = \pm \frac{1}{2}\hbar\Delta_0 (1 + (\hat{\varepsilon}/2\Delta_0)\sqrt{1 - \hat{\varepsilon}^2/64\Delta_0^2}) \pmod{\hbar\Omega}\,. \tag{91}$$

3. Near resonance, one finds from the RWA approximation

$$\varepsilon_{2,1} = \pm \tfrac{1}{2}\hbar\Omega(1 + \Omega_R/\Omega) \pmod{\hbar\Omega}\,, \tag{92}$$

where Ω_R denotes the Rabi frequency in Eq. (85). Correcting this result for counterrotating terms, an improved result, up to order $O(\hat{\varepsilon}^6)$, reads [64]

$$\varepsilon_{2,1} = \pm \tfrac{1}{2}\hbar\Omega(1 + \bar{\Omega}/\Omega) \pmod{\hbar\Omega}, \tag{93}$$

with the effective Rabi frequency $\bar{\Omega}$ given by

$$\bar{\Omega}^2 = \delta^2 + \frac{\Delta_0\hat{\varepsilon}^2}{2(\Omega + \Delta_0)} - \frac{\Delta_0\hat{\varepsilon}^4}{32(\Omega + \Delta_0)^3}. \tag{94}$$

Notice that the maximum of the time-averaged transition probability in Eq. (87) occurs within RWA precisely at $\Omega = \Delta_0$. This result no longer holds with Eq. (94) where the maximum with $\Omega_R \to \bar{\Omega}_R$ in Eq. (86) undergoes a shift, termed the *Bloch–Siegert shift*, i.e., $\Omega_{res} \neq \Delta_0$[64,66]. From $(\partial\bar{\Omega}^2/\partial\Delta_0)_{\hat{\varepsilon}} = 0$ this shift is evaluated as [64,66]

$$\Omega_{res} = \Delta_0 + \frac{\hat{\varepsilon}^2}{16\Delta_0} + \frac{(\hat{\varepsilon}/4)^4}{4\Delta_0^3}. \tag{95}$$

This Bloch–Siegert shift presents a characteristic measure of the deviation beyond the RWA-approximation, as a result of the nonzero anti-rotating-wave terms in Eq. (82).

3.2.2. *Coherent destruction of tunneling (CDT)*

Let us now consider the influence of a monochromatic perturbation on the quantum coherent motion of a tunneling particle between the localized states $|L\rangle$ and $|R\rangle$. This problem is conveniently addressed within the localized basis for the TLS Hamiltonian, cf. Eq. (79). We consider for simplicity only the case of a symmetric TLS, i.e., $\varepsilon_0 = 0$ in Eq. (79). In this case we have $|L\rangle = 2^{-1/2}(|1\rangle - |2\rangle)$, and $|R\rangle = 2^{-1/2}(|1\rangle + |2\rangle)$, with $|1\rangle$ and $|2\rangle$ being the unperturbed energy eigenstates. For the state vector in this localized basis $|L\rangle$ and $|R\rangle$, we set

$$|\Psi(t)\rangle = c_L(t)\exp[-i(\hat{\varepsilon}/2\Omega)\sin(\Omega t)]|L\rangle + c_R(t)\exp[+i(\hat{\varepsilon}/2\Omega)\sin(\Omega t)]|R\rangle. \tag{96}$$

Given the $\cos(\Omega t)$ perturbation (i.e., $\phi = \pi/2$), we consequently obtain from the Schrödinger equation for the amplitudes $\{c_{R,L}(t)\}$ the equation

$$i(d/dt)c_{L,R}(t) = -\tfrac{1}{2}\Delta_0\exp[\pm i(\hat{\varepsilon}/\Omega)\sin(\Omega t)]c_{R,L}(t). \tag{97}$$

For large frequencies $\Omega \gg \Delta_0$, we average Eq. (97) over a complete cycle to obtain the high-frequency approximation

$$i(d/dt)c_{L,R}(t) = -\tfrac{1}{2}\Delta_0 J_0(\hat{\varepsilon}/\Omega)c_{R,L}(t), \tag{98}$$

where $J_0(x) = (\Omega/2\pi)\int_0^{\gg} ds\exp[ix\sin(\Omega s)]$, is the zeroth-order Bessel function of the first kind. This yields equations of motion that mimick those of a static TLS – which are different from the RWA in Eq. (83) – with a frequency-renormalized splitting, cf. also Eq. (88), i.e.,

$$\Delta_0 \to J_0(\hat{\varepsilon}/\Omega)\Delta_0 := \Delta_{eff}. \tag{99}$$

The static TLS is easily solved to give with the initial preparation $c_L(t=0)=1$ for the return probability $P_L(t)$ the approximate result

$$P_L(t) = |c_L(t)|^2 = \cos^2(J_0(\hat{\varepsilon}/\Omega)\Delta_0 t/2)\,. \tag{100}$$

Thus, at the first zero $j_{0,1}$ of $J_0(x)$, i.e. when $\hat{\varepsilon}/\Omega = 2.40482\ldots$, $P_L(t)$ in Eq. (100) precisely equals unity, i.e., the effective tunnel splitting vanishes, in agreement with the result in Eq. (88). Thus, one finds a complete coherent destruction of tunneling (CDT) [24,25,67–72].

This high-frequency TLS approximation for the localization manifold $M^1_{\rm loc}(\hat{\varepsilon},\Omega)$, as determined by the first root of $J_0(\hat{\varepsilon}/\Omega)$, is depicted in Fig. 10a in Section 6.3 by a solid line, and is compared with the result for CDT in a continuous bistable system, cf. Section 6. Higher roots $j_{0,n}$ yield an approximation for the localization manifold $M^n_{\rm loc}(\hat{\varepsilon},\Omega)$ with $n>1$. Moreover, we note that $J_0(x)\sim x^{-1/2}$ as $x\to\infty$. This implies, within the TLS-approximation to driven tunneling, that tunneling is always suppressed for $\Omega>\Delta_0$ for appropriate values of the ratio $\hat{\varepsilon}/\Omega$. An improved formula for $P_L(t)$ in Eq. (100) that contains also higher odd harmonics of the fundamental driving frequency Ω has recently been given in [71].

This driven TLS is closely connected with the problem of periodic, *nonadiabatic* level crossing. In the diabatic limit $\delta\equiv\Delta_0^2/(\hat{\varepsilon}\Omega)\to 0$, corresponding to a large amplitude driving, the return probability has been evaluated by Kayanuma [72]. In our notation and with $\hat{\varepsilon}>\max(\Omega,\Delta_0)$ this result reads

$$P_L(t)\sim \cos^2\left\{(2\Omega/\hat{\varepsilon}\pi)^{1/2}\left[\sin\left(\frac{\hat{\varepsilon}}{\Omega}+\frac{\pi}{4}\right)\right]\frac{\Delta_0 t}{2}\right\}. \tag{101}$$

With $J_0(x)\sim\sqrt{2/\pi x}\sin(x+\pi/4)$, for $x\gg 1$, Eq. (101) reduces for $\hat{\varepsilon}/\Omega\gg 1$ to Eq. (100). Here, the phase factor of $\pi/4$ corresponds to the Stokes phase known from diabatic level crossing [72,73], and $\hat{\varepsilon}/\Omega$ is the phase acquired during a single crossing of duration $\mathscr{T}/2$. The mechanism of coherent destruction of tunneling in this limit $\hat{\varepsilon}>\max(\Omega,\Delta_0)$ is related, therefore, to a destructive interference between transition paths with $\hat{\varepsilon}/\Omega = n\pi + 3\pi/4$.

Additional insight into CDT has been provided by Wang and Shao [69]: They discussed the phenomenon by mapping the driven quantum dynamics to the classical movement of a charged particle moving in a two-dimensional harmonic oscillator potential under a periodically acting, perpendicular magnetic field. The motion of the particle is constrained to the interior of a unit circle in the plane. The behavior of tunneling and localization is described by the radial trajectory of the classical particle. In doing so, the authors have demonstrated that for a particle that starts at the edge of the unit circle localization happens only if the radial trajectory is periodic and essentially runs in a narrow concentric ring within the unit circle.

Finally, for the case of an asymmetric TLS ($\varepsilon_0\neq 0$), one finds for the resonant case, i.e., $\varepsilon_0/\Omega = n$ ($n=1,2,\ldots$), that tunneling is still coherently suppressed at high driving frequencies $\Omega\gg\Delta_0$ whenever the condition

$$J_n(\hat{\varepsilon}/\Omega)=0 \tag{102}$$

is fulfilled. Here, J_n denotes the Bessel function of order n [74,75]. Other forms of quasi-localized tunneling dynamics, such as motion with period $q\mathscr{T}>\mathscr{T}$, with q being a prime number, or quasi-periodic motion have been reported for driven tunneling in the presence of asymmetry [75].

3.3. Tunneling in a cavity

The phenomenon of coherent destruction of tunneling also persists if we use a full quantum treatment for the semiclassical description of the field: For an electric field operator defined as $\hat{\mathscr{E}} = (\hbar g/\mu)(a^\dagger + a)$, where μ is the dipole matrix element between the TLS eigenstates $|1\rangle$ and $|2\rangle$, the quantized version of Eq. (75) reads, see e.g. in [76],

$$H = -\tfrac{1}{2}\hbar\Delta_0\sigma_z + \hbar\Omega a^\dagger a - \hbar g(a^\dagger + a)\sigma_x\,, \tag{103}$$

where $a, a^\dagger$ are the bosonic creation and annihilation operators for the field mode with frequency Ω. With $\langle n\rangle = \langle a^\dagger a\rangle$ being the average value of the occupation number n for a coherent state $|n\rangle$ of the field, the coupling constant g is related to the semiclassical field strength $\hat{\varepsilon}$ by

$$4g\sqrt{\langle n\rangle} = \hat{\varepsilon}\,. \tag{104}$$

The vanishing of the quasienergy difference $\Delta_{\rm eff}$ is then controlled by the roots of the Laguerre polynomial L_n of the order of the photon number n [77–79], i.e.,

$$\Delta_{\rm eff} = \Delta_0 \exp(-2a) L_n(4a)\,, \tag{105}$$

where $a = (g/\Omega)^2$. Note that the semiclassical limit is approached with $g \to 0$, $n \simeq \langle n\rangle \to \infty$, such that $4g\sqrt{n} = \hat{\varepsilon} = \text{const}$, with L_n converging to the zeroth order Bessel function. Hence, we recover the effective tunneling splitting inherent in Eq. (99), i.e., $\Delta_{\rm eff} = \Delta_0 J_0(\hat{\varepsilon}/\Omega)$.

The mechanism of CDT has been investigated in [79] from the viewpoint of quantum optics by studying the photon statistics of the single-mode cavity field in terms of the product states $|i\rangle|n\rangle := |i, n\rangle$, with $i = L, R$. Given the initial preparation $|\Psi(t=0)\rangle = |L\rangle|n\rangle$, the transition probability $P_{n\to m}(t)$ to find the system in the product state $|i, m\rangle$ for any $i = L,R$ after the interaction time t is given by

$$P_{n\to m}(t) = \sum_{i=L,R} |\langle i, m| \exp(-iHt/\hbar)|L, n\rangle|^2\,. \tag{106}$$

For fixed t this quantity yields the photon number distribution with $P_{n\to m}(t=0) = \delta_{n,m}$. For *fixed* m, this transition probability describes the cavity mode-TLS interaction. The tunneling dynamics is then characterized by an amplitude modulation of the (fast) cavity oscillations. The authors in [79] have demonstrated that CDT manifests itself in the limit of large n in a characteristic *slowing down* of the amplitude modulation of the quantity $P_{n\to n}(t)$ monitored versus interaction time t.

The dynamics of the Hamiltonian in Eq. (103) is very rich: As a function of its parameters is able to depict quantum revivals, regular and irregular behavior of occupation probabilities of the TLS, non-integrable semiclassical dynamics, etc. [80]. As such, this simple model constitutes an archetype for studying different aspects of quantum chaos.

3.4. Circularly polarized radiation fields

Here, we explicitly consider the case pioneered by Rabi [65], i.e., a TLS driven in a spatially homogeneous, circularly polarized external radiation field. This represents, for example, the case of

a spin $\frac{1}{2}$ subject to a static magnetic field B_0 along the z direction, and to a time-dependent magnetic field in the x and y directions, i.e., cf. Eq. (77),

$$H(t) = -\boldsymbol{\mu}\cdot\boldsymbol{B} = -\tfrac{1}{2}\hbar\gamma\sigma_z B_0 - \hbar\gamma B_1[\sigma_x\cos(\Omega t) - \sigma_y\sin(\Omega t)]\,. \tag{107}$$

With

$$\Delta_0 = \gamma B_0, \qquad \hat{\varepsilon}/2 = \gamma B_1\,, \tag{108}$$

this leads, in the energy representation, to the Hamiltonian

$$\begin{aligned} H(t) &= -\frac{1}{2}\hbar\Delta_0\sigma_z - \frac{1}{2}\hbar\hat{\varepsilon}[\sigma_x\cos(\Omega t) - \sigma_y\sin(\Omega t)] \\ &= -\frac{1}{2}\hbar\begin{pmatrix}\Delta_0 & \hat{\varepsilon}\exp(\mathrm{i}\Omega t)\\ \hat{\varepsilon}\exp(-\mathrm{i}\Omega t) & -\Delta_0\end{pmatrix}. \end{aligned} \tag{109}$$

Absorbing the phase $\exp(\pm\mathrm{i}\Delta_0 t)$ into the time dependence of the coefficients, i.e., setting $a_{1,2}(t) = c_{1,2}(t)\exp(\pm\mathrm{i}\Delta_0 t)$, we rotate the states around the z-axis by the amount Ωt. With $S_z = \frac{1}{2}\hbar\sigma_z$, one has

$$\begin{pmatrix}b_1(t)\\ b_2(t)\end{pmatrix} = \exp\left(-\frac{\mathrm{i}}{\hbar}S_z\Omega t\right)\begin{pmatrix}a_1(t)\\ a_2(t)\end{pmatrix} = \begin{pmatrix}a_1(t)\exp(-\mathrm{i}\Omega t/2)\\ a_2(t)\exp(+\mathrm{i}\Omega t/2)\end{pmatrix}. \tag{110}$$

Upon a substitution of Eqs. (109) and (110) into the time-dependent Schrödinger equation, and collecting all the terms, results in a time-independent Schrödinger equation for the states $(b_1(t), b_2(t))$, which reads

$$\begin{aligned} -\mathrm{i}\dot{b}_1 &= -\tfrac{1}{2}(\Omega - \Delta_0)b_1 + \tfrac{1}{4}\hat{\varepsilon}b_2\,, \\ -\mathrm{i}\dot{b}_2 &= \tfrac{1}{4}\hat{\varepsilon}b_1 + \tfrac{1}{2}(\Omega - \Delta_0)b_2\,. \end{aligned} \tag{111}$$

Thus, one obtains a harmonic oscillator equation for $b_1(t)$ (and similarly for $b_2(t)$), i.e.,

$$\ddot{b}_1 + \left(\frac{\hat{\varepsilon}^2}{16} + \frac{\delta^2}{4}\right)b_1 = 0\,. \tag{112}$$

It describes an oscillation with frequency $\Omega_{\mathrm{R}} = \sqrt{\hat{\varepsilon}^2/4 + \delta^2}$, where Ω_{R} coincides precisely with the previously found Rabi frequency in Eq. (85). With $c_1(0) = a_1(0) = b_1(0) = 1$, and $c_2(0) = a_2(0) = b_2(0) = 0$ the populations are given by the corresponding relations in Eq. (86), which in this case are *exact*. In particular, the transition probability $W_{1\to 2}(t) = |\langle 2|\Psi(t)\rangle|^2 = |a_2(t)|^2 = |b_2(t)|^2 = |c_2(t)|^2$ obeys

$$W_{1\to 2}(t) = (\hat{\varepsilon}^2/4\Omega_{\mathrm{R}}^2)\sin^2(\tfrac{1}{2}\Omega_{\mathrm{R}}t)\,. \tag{113}$$

At resonance, $\delta = 0$, $\Omega = \Delta_0$, it assumes with $\Omega_{\mathrm{R}}^2 = \hat{\varepsilon}^2/4$ its maximal value $W_{1\to 2}(\hat{t}) = 1$ at times $\hat{t}$ obeying $\hat{\varepsilon}\hat{t}/2 = \pi\,(\mathrm{mod}\,2\pi)$.

We point here to the importance of initial preparation: The coherence effects of a circularly polarized radiation field for an initially *localized* TLS has been investigated in [81]: Interestingly enough, one again finds the phenomenon of CDT if, for sufficiently strong driving strength $\hat{\varepsilon}$, the driving frequency Ω matches precisely the Rabi frequency Ω_{R}.

3.5. *Curve crossing tunneling*

In this subsection we shall investigate the problem proposed by Landau [82], Zener [83] and Stückelberg [84], known as the Landau–Zener–Stückelberg problem of nonadiabatic crossing of energy levels. Put differently, we consider the explicit time-dependent situation in which the (parametric) energy levels of a quantum mechanical Hamiltonian are brought together in the course of time by means of an external perturbation. The original work by Zener concentrates on the electronic states of a bi-atomic molecule, while in that by Landau and Stückelberg one considers two atoms which undergo a scattering process. Because Zener, Landau and Stückelberg restrict themselves to the Hilbert space generated by two electronic functions only, we have to deal with a two-level system. Quantitatively, for a two-level crossing, the problem is described by the time-dependent Hamiltonian

$$H_{\mathrm{LZS}}(t) = -\tfrac{1}{2}\hbar(vt\sigma_z + \Delta_0\sigma_x)\,, \tag{114}$$

where Δ_0 is the coupling between the two levels, and $\hbar v$ is the rate of change of the energy of the *uncoupled* levels due to an external driving bias. In this representation the eigenstates of σ_z are the *diabatic* states $|L\rangle$, $|R\rangle$ which satisfy $\sigma_z|L\rangle = -|L\rangle$ ($\sigma_z|R\rangle = |R\rangle$), while the eigenstates of $H_{\mathrm{LZS}}(t)$, at fixed time t are the *adiabatic* states $|\pm\rangle$ with adiabatic energies $E_\pm(t) = \pm\hbar(\Delta_0^2 + v^2t^2)^{1/2}/2$, cf. Fig. 3. Note that in the infinite past and future the diabatic and adiabatic representations coincide. We assume that at an initial time far away in the past the system is in the lower state. We then ask for the transition probability

$$W_{-\to+}(t\to\infty) = |\langle + |U(\infty,-\infty)|-\rangle|^2 = |\langle L|U(\infty,-\infty)|L\rangle|^2 := P_{\mathrm{LZS}} \tag{115}$$

of finding the system in the excited level in the far future, cf. Fig. 3. $U(t_2,t_1) = \top\exp\{(\mathrm{i}/\hbar)\int_{t_1}^{t_2}H_{\mathrm{LZS}}(t)\,\mathrm{d}t\}$ denotes the time evolution operator. To obtain this transition probability, we follow here closely the approach by Kayanuma [85]. To start, it is convenient to split the Hamiltonian (114) as $H_{\mathrm{LZS}}(t) = H_{\mathrm{d}}(t) + H_\Delta$, where $H_{\mathrm{d}}(t)$ is the time-dependent diagonal part. Hence, the propagator can be expressed by use of Feynman's disentangling theorem [86] as

$$\begin{aligned} U(\infty,-\infty) &= U_{\mathrm{d}}(\infty,-\infty)U_\Delta(\infty,-\infty) \\ &= \exp\left(-\frac{\mathrm{i}}{\hbar}\int_{-\infty}^{\infty}H_{\mathrm{d}}(t)\,\mathrm{d}t\right)\top\exp\left(-\frac{\mathrm{i}}{\hbar}\int_{-\infty}^{\infty}\tilde{H}_\Delta(t)\,\mathrm{d}t\right), \end{aligned} \tag{116}$$

where

$$\tilde{H}_\Delta(t) = \exp\left(\frac{\mathrm{i}}{\hbar}\int_{-\infty}^{t}H_{\mathrm{d}}(t')\,\mathrm{d}t'\right)H_\Delta\exp\left(-\frac{\mathrm{i}}{\hbar}\int_{-\infty}^{t}H_{\mathrm{d}}(t')\,\mathrm{d}t'\right). \tag{117}$$

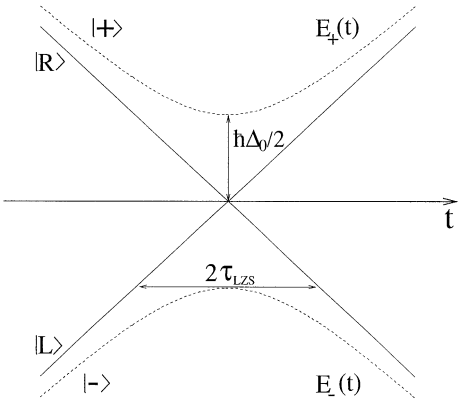

Fig. 3. Crossing of the diabatic energy levels (solid lines) in the Landau–Zener–Stückelberg problem in the course of time. Δ_0 is the coupling between the levels, while the time τ_{LZS} characterizes the time spent in the crossover region. The dashed lines represent the adiabatic energy levels $E_{\pm}(t)$.

Expanding the time-ordered exponent in Eq. (116) one obtains

$$\langle L|U_{\mathrm{d}}(\infty,-\infty)U_{\Delta}(\infty,-\infty)|L\rangle = \sum_{n=0}^{\infty}\left(-\frac{\mathrm{i}}{\hbar}\right)^{n} \times \int_{-\infty}^{+\infty}\mathrm{d}t_n\int_{-\infty}^{t_n}\mathrm{d}t_{n-1}\ldots\int_{-\infty}^{t_2}\mathrm{d}t_1\langle L|U_{\mathrm{d}}(\infty,-\infty)\tilde{H}_{\Delta}(t_n)\tilde{H}_{\Delta}(t_{n-1})\ldots\tilde{H}_{\Delta}(t_1)|L\rangle\,. \tag{118}$$

We observe that the operator U_{d} is diagonal, i.e.,

$$\langle U_{\mathrm{d}}(t_j,t_{j-1})|L\rangle = \exp\left(-\frac{\mathrm{i}v}{4}(t_j^2-t_{j-1}^2)\right)|L\rangle\,,$$

$$\langle U_{\mathrm{d}}(t_j,t_{j-1})|R\rangle = \exp\left(+\frac{\mathrm{i}v}{4}(t_j^2-t_{j-1}^2)\right)|R\rangle\,, \tag{119}$$

while the operator H_{Δ} is non-diagonal and generates spin flips, i.e., $H_{\Delta}|L\rangle = (\hbar\Delta_0/2)|R\rangle$, $H_{\Delta}|R\rangle = (\hbar\Delta_0/2)|L\rangle$. Thus, only an even number of spin flips contribute to the matrix element (118). One finds

$$\langle L|U_{\mathrm{d}}(\infty,-\infty)U_{\Delta}(\infty,-\infty)|L\rangle = \sum_{n=0}^{\infty}\left(-\frac{\Delta_0^2}{4}\right)^{n} \times \int_{-\infty}^{+\infty}\mathrm{d}t_{2n}\int_{-\infty}^{t_{2n}}\mathrm{d}t_{2n-1}\ldots\int_{-\infty}^{t_2}\mathrm{d}t_1\exp\left[-\frac{\mathrm{i}v}{2}\sum_{j=1}^{2n}(-1)^j t_j^2\right]. \tag{120}$$

By making the variable transformation

$$x_1 = t_1,\quad x_p = t_1 + \sum_{j=1}^{p-1}(t_{2j+1}-t_{2j}),\quad y_p = t_{2p}-t_{2p-1}\,, \tag{121}$$

and upon noting that the resulting integrand is symmetric under exchange of the integration variables x_p, one can perform the integrations to obtain

$$\langle L|U_{\mathrm{d}}(\infty,-\infty)U_{\Delta}(\infty,-\infty)|L\rangle = \sum_{n=0}^{\infty}\frac{1}{n!}\left(\frac{\pi\Delta_0^2}{2|v|}\right)^n . \tag{122}$$

This result is recast as

$$P_{\mathrm{LZS}} = \exp(-2\pi\gamma)\,, \tag{123}$$

where $\gamma = \Delta_0^2/(2|v|)$. Note that this result is *exact*. The transition probability P_{LZS} depends only on the ratio between the time $\tau_{\mathrm{LZS}} = \Delta_0/|v|$ spent in the crossover region and the coherent tunneling time $\tau_{\mathrm{coh}} = 2\Delta_0^{-1}$, i.e., $\gamma = \tau_{\mathrm{LZS}}/\tau_{\mathrm{coh}}$.

3.6. Pulse-shaping strategy for control of quantum dynamics

The phenomenon of coherent destruction of tunneling discussed previously in Section 3.2.2 is an example of a dynamical quantum interference effect by which the quantum dynamics can be manipulated by an observer. More generally, the dependence of quasienergies on field strength and frequency can be used to control the emission spectrum by either generating or by selectively eliminating specific spectral lines. For example, the near crossing of quasienergies in a symmetric double well generates anomalous low-frequency lines and – at exact crossing – doublets of intense even-harmonic generation (EHG) [27], see Section 7.3.

This control by a periodic continuous-wave driving can be generalized by recourse to more complex perturbations. The goal by which a pre-assigned task for the output of a quantum dynamics is imposed from the outside by applying a sequence of properly designed (in phase and/or shape) pulse perturbations is known as quantum control [11,13]. For example, a primary goal in chemical physics is to produce desired product yields or to manipulate the atomic and molecular properties of matter [11,13,87,88]. As an archetype situation, we present the control of the quantum dynamics of two coupled electronic surfaces – assuming throughout validity within a rotating wave approximation – i.e.,

$$\mathrm{i}\hbar\frac{\partial}{\partial t}\begin{pmatrix}\Psi_1\\ \Psi_2\end{pmatrix} = \begin{bmatrix} H_1(R) & -\mu(R)\mathscr{E}(t)\\ -\mu(R)\mathscr{E}^*(t) & H_2(R)\end{bmatrix}\begin{pmatrix}\Psi_1\\ \Psi_2\end{pmatrix}, \tag{124}$$

where R denotes the nuclear coordinates and H_1, H_2 are the Born–Oppenheimer Hamiltonians for the ground and excited field free surfaces, respectively. The surfaces are coupled within the dipole approximation by the transition dipole operator $\mu(R)$ and the radiation field $\mathscr{E}(t)$. Notice that the structure in Eq. (124) is identical to that obtained in the driven TLS. Following Kosloff et al. [88], the rate of change to the ground state population $n_1(t) = \langle\Psi_1(t)|\Psi_1(t)\rangle$ is readily evaluated to read

$$\mathrm{d}n_1/\mathrm{d}t = 2\mathrm{Re}\langle\Psi_1|\dot{\Psi}_1\rangle = -(2/\hbar)\mathrm{Im}(\langle\Psi_1(t)|\mu(R)|\Psi_2(t)\rangle\mathscr{E}(t))\,. \tag{125}$$

If we now choose $\mathscr{E}(t)$ as a control, i.e.,

$$\mathscr{E}(t) \to \mathscr{E}_{\mathrm{c}}(t) = \langle\Psi_2(t)|\mu(R)|\Psi_1(t)\rangle C(t)\,, \tag{126}$$

with $C(t)$ a real-valued function, we can freeze the population transfer (null-population transfer), i.e., with Eq. (126),

$$\mathrm{d}n_1/\mathrm{d}t = 0\,, \tag{127}$$

for all times t. In other words, the population in the ground electronic surface, and necessarily also the population of the excited surface, remains fixed. If we were to choose $\mathscr{E}(t) \to \mathrm{i}\mathscr{E}_c(t)$, it would cause population to be transferred to the upper state, while $\mathscr{E}(t) \to -\mathrm{i}\mathscr{E}_c(t)$ would dump population down to the ground state. Hence, by controlling the phase of a laser, we can control the population transfer at will. This phenomenon applies equally well to driven tunneling in a TLS. What can we achieve if we manipulate the amplitude $C(t)$? The change in the energy of the ground state surface, which can be varied by exciting specific ground-state vibrational modes, is obtained as

$$\frac{\mathrm{d}E_1}{\mathrm{d}t} = \frac{\mathrm{d}}{\mathrm{d}t}\frac{\langle \Psi_1(t)|H_1|\Psi_1(t)\rangle}{\langle \Psi_1(t)|\Psi_1(t)\rangle}\,. \tag{128}$$

Under the null-population-transfer condition in Eq. (126), this simplifies to [88]

$$\frac{\mathrm{d}E_1}{\mathrm{d}t} = -\frac{2C(t)}{\hbar n_1}\mathrm{Im}\langle \Psi_1(t)|H_1\mu(R)|\Psi_2(t)\rangle\langle \Psi_2(t)|\mu(R)|\Psi_2(t)\rangle\,. \tag{129}$$

It follows that the sign of $C(t)$ can be used to "heat" or "cool" the ground-state wavepacket; the magnitude of $C(t)$ in turn controls the rate of heating (or cooling). With this scheme of phase and amplitude control of a laser pulse it is possible to excite vibrationally the lower state surface while minimizing radiation damage either by ionizing or by dissociating the corresponding quantum system.

4. Driven tight-binding models

In the previous section we have considered driven two-state systems. Here we shall consider the driven, infinite tight-binding (TB) system. Similar to the case of a two-state system, the infinite TB system can result from the reduction of the tunneling dynamics of a particle moving in an infinite periodic potential $V_0(q) = V_0(q + d)$ within its lowest energy band. To be definite, if one fixes the potential depth such that the Wannier states $|n\rangle$ building up the lowest band have appreciable overlap only with their nearest neighbors $|n \pm 1\rangle$, one obtains the Hamiltonian H_{TB} of the bare multistate system, i.e.,

$$H_{\mathrm{TB}} = -\frac{\hbar\Delta_0}{2}\sum_{n=-\infty}^{\infty}(|n\rangle\langle n+1| + |n+1\rangle\langle n|)\,, \tag{130}$$

where $2\hbar\Delta_0$ is the width of the lowest energy band. The influence of the driving force is described by the perturbation

$$H_{\mathrm{ext}}(t) = -q\hbar[\varepsilon_0 + \hat{\varepsilon}\cos(\Omega t)]/d, \quad q = d\sum_n n|n\rangle\langle n|\,, \tag{131}$$

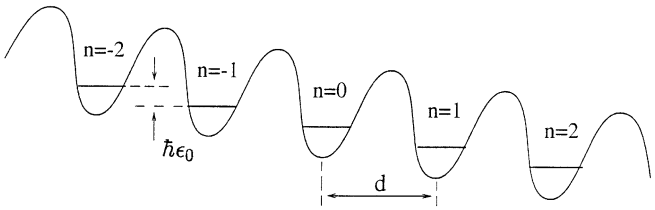

Fig. 4. A periodic potential with lattice constant d and potential drop $\hbar\varepsilon_0$ per period. Within the miniband, tight-binding approximation, the Wannier state $|n\rangle$ localized at the site nd has appreciable overlap only with its nearest neighbors $|n \pm 1\rangle$.

where the operator q measures the position of the particle on the lattice, while $\hbar\varepsilon(t)/d = \hbar(\varepsilon_0 + \hat{\varepsilon}\cos\Omega t)$ measures the potential drop per lattice period d due to externally applied dc- and ac-fields, cf. Fig. 4. In order for the single band approximation to be still consistent, the driving frequency Ω, as well as the ac and dc-bias strengths ε_0 and $\hat{\varepsilon}$, respectively should be chosen much smaller than the gap between the lowest two bands. The problem described by $H(t) = H_{\mathrm{TB}} + H_{\mathrm{ext}}(t)$ has a great variety of applications as, for example, in the investigation of the dynamics of ultracold atoms in standing light waves [89,90], where lattice defects are absent, in high-quality superlattices [16,19–22,91–98], or in thin crystals [99].

Suppose now that the particle has been prepared at time $t_0 = 0$ at the origin $|n = 0\rangle$. Then, the dynamical quantity of interest is the probability $P_n(t)$ for finding the particle at site n at time $t > 0$. In turn, the knowledge of $P_n(t)$ enables the evaluation of all the dynamical quantities of interest in the problem as, for example, the position's expectation value $P(t)$, as well as the diffusive variance $S(t)$, i.e.,

$$\begin{aligned} P(t) &:= \langle q\rangle_t = d\sum_{n=-\infty}^{\infty} nP_n(t)\,, \\ S(t) &:= \langle q^2\rangle_t - \langle q\rangle_t^2 = d^2\sum_{n=-\infty}^{\infty} n^2P_n(t) - P^2(t)\,. \end{aligned} \tag{132}$$

The expectation value $P(t)$ represents the generalization of the quantity $P(t) = \langle\sigma_z\rangle_t$, cf. Eq. (70), introduced in the study of the dynamics of a two-state system.

If there is no external ac–dc field, then the Bloch waves [100]

$$\chi_k = \sum_n \exp(-\mathrm{i}knd)|n\rangle \tag{133}$$

solve the stationary Schrödinger equation $H_{\mathrm{TB}}\chi_k = E(k)\chi_k$ with $E(k)$ an absolutely continuous spectrum, i.e., $E(k) = -\hbar\Delta_0\cos(kd)$. Thus, $2\hbar\Delta_0$ is the width of the resulting energy band. For this problem the propagator $U^0_{l,l'}(t,t')$ from state $|l\rangle$ to state $|l'\rangle$ is explicitly evaluated to read

$$U^0_{l,l'}(t,t') = J_{l-l'}(\Delta_0(t-t'))\mathrm{e}^{(\mathrm{i}\pi/2)(l-l')}\,, \tag{134}$$

where $J_l(x)$ is the lth-order Bessel function. Given the initial condition $P_n(t=0) = \delta_{n,0}$, one then finds $P(t) = 0$ and

$$S(t) = d^2\Delta_0^2t^2/2\,, \tag{135}$$

i.e., the variance of an initially localized wave packet spreads *ballistically* in time (superdiffusion).

In presence of a dc-field $\hbar\varepsilon_0/d$, the Wannier–Stark states [101,102]

$$\phi_m = \sum_n J_{n-m}(\Delta_0/\varepsilon_0)|n\rangle \tag{136}$$

constitute a complete set of energy eigenstates with corresponding – now discrete – eigenvalues $E_m = m\hbar\varepsilon_0$ forming the Wannier–Stark ladder [101–103]. A particular Wannier–Stark state ϕ_m is localized around the mth site with a localization length of the order of $2\Delta_0/\varepsilon_0$ lattice periods. In this case the propagator takes the form

$$U^{\mathrm{DC}}_{l,l'}(t't') = J_{l-l'}\left(\frac{2\Delta_0}{\varepsilon_0}\sin\left(\frac{\varepsilon_0(t-t')}{2}\right)\right)\exp\left\{\mathrm{i}(l-l')\left[\frac{\pi-\varepsilon_0(t-t')}{2}\right] - \mathrm{i}l'\varepsilon_0(t-t')\right\}, \tag{137}$$

which, with the initial condition $P_n(t=0) = \delta_{n,0}$, leads to

$$P_n(t) = J_n^2((2\Delta_0/\varepsilon_0)\sin(\varepsilon_0 t/2))\,. \tag{138}$$

Because Eq. (138) is symmetric in n, one obtains $P(t) = 0$ and

$$S(t) = 2d^2(\Delta_0/\varepsilon_0)^2\sin^2(\varepsilon_0 t/2)\,. \tag{139}$$

Hence, a wavepacket which is initially localized on one site spreads in space and returns back to its initial shape after the Bloch period $\mathscr{T}_{\mathrm{B}} = 2\pi/\varepsilon_0$. The center of the wavepacket, though, remains fixed. On the contrary, if one considers a wavepacket which initially is not sharply localized, one finds that the center of the wavepacket oscillates in space with an amplitude which is inversely proportional to the dc-field strength ε_0, and with temporal period $\mathscr{T}_{\mathrm{B}}$. The shape of the wavepacket remains almost invariant. This is the famous Bloch oscillation that was first discussed by Zener [104]. It has been observed only recently in semiconductor superlattices through the emission of THz radiation by the electrons [91], as well as in optical lattices [89,90].

If only an ac-field is applied, the Floquet states $\Psi_k(t)$ solve the time-dependent Schrödinger equation. They read

$$\Psi_k(t) = \sum_n |n\rangle \exp\left(- \mathrm{i}q_k(t)nd - (\mathrm{i}/\hbar)\int_0^t \mathrm{d}\tau E(q_k(\tau))\right), \tag{140}$$

with $q_k(t) = k + (\hat{\varepsilon}/\Omega)\sin(\Omega t)/d$. Setting $\Psi_k(t) = \Phi_k(t)\exp(-\mathrm{i}\varepsilon(k)t/\hbar)$ with $\Phi_k(t+\mathscr{T}) = \Phi_k(t)$, the quasienergies form again an absolutely continuous spectrum which reads

$$\varepsilon(k) = J_0(\hat{\varepsilon}/\Omega)E(k), \quad \mathrm{mod}\,\hbar\Omega\,. \tag{141}$$

Given the initial condition $P_n(t=0) = \delta_{n,0}$, one finds for the two transport quantities in Eq. (132) [105]

$$P(t) = 0, \qquad S(t) = d^2(\Delta_0^2/2)[u^2(t) + v^2(t)]\,, \tag{142}$$

where

$$\begin{aligned} u(t) &= \int_0^t \mathrm{d}t' \sin[\hat{\varepsilon}/\Omega \sin(\Omega t')]\,, \\ v(t) &= \int_0^t \mathrm{d}t' \cos[\hat{\varepsilon}/\Omega \sin(\Omega t')]\,. \end{aligned} \tag{143}$$

The above equations, Eqs. (142) and (143), can be simplified at long times $t \gg 2\pi/\Omega$ to yield

$$S(t) = d^2 \Delta_{\text{eff}}^2 t^2/2, \quad \Delta_{\text{eff}} = J_0(\hat{\varepsilon}/\Omega)\Delta_0 \,, \tag{144}$$

i.e., the problem of diffusion reduces effectively to that of an undriven particle, cf. Eq. (135), with a renormalized energy bandwidth $2\hbar\Delta_{\text{eff}} \leq 2\hbar\Delta_0$. In particular, when $\hat{\varepsilon}/\Omega$ coincides with a kth zero $j_{0,k}$ of the Bessel function J_0, the wavepacket reassembles itself after a period, as it can be verified from the exact result (142). Hence, on a long time average, it neither moves nor spreads. This phenomenon, termed *dynamic localization* (DL) [16,92,105,109,110], resembles the phenomenon of coherent destruction of tunneling (CDT) discussed for the two-state system in Section 3.2.2. Note, however, that the two phenomena are *very distinct*: The DL is based on a collapse of a band, cf. Eq. (141), while CDT necessitates the crossing of two tunneling related discrete quasienergies. More importantly, the probability of an initially localized preparation $P_n(t=0) = \delta_{n,0}$ does not stay localized. To be definite, with the probability to stay at site $n = 0$ given by [105]

$$P_0(t) = J_0^2(\Delta_0\sqrt{u^2(t) + v^2(t)}) \,, \tag{145}$$

$P_0(t)$ at band collapse becomes an oscillating function with period $2\pi/\Omega$ varying between zero and one. It exhibits stroboscopic localization only at multiples of the driving period, i.e., at $t_n = n2\pi/\Omega$, $n = 0, 1, \ldots$; cf. also Fig. 3a in Ref. [105]. Further, we remark that, while for the two-state system the renormalization (89) of the intersite coupling leading to CDT is a *perturbative* result in the ratio (Δ_0/Ω) between the intersite coupling and the external frequency, the corresponding equation (141) for the quasienergy band is an *exact* result. This is due to exact translational symmetry of an infinite tight-binding lattice with nearest-neighbor intersite interactions.

Finally, in the presence of both ac- and dc-fields the Houston states [106] solve the time-dependent Schrödinger equation. They have the same form as the Floquet states in Eq. (140) solving the Schrödinger equation in the absence of a dc-field, but with $q_k(t)$ in Eq. (140) substituted by

$$q_k(t) = k + [\varepsilon_0 t + (\hat{\varepsilon}/\Omega)\sin(\Omega t)]/d \,. \tag{146}$$

However, it must be recognized that the problem now contains two frequencies, the ac-frequency Ω and the Bloch frequency $\Omega_B = \varepsilon_0$. As a consequence, it turns out that the Houston states coincide with the Floquet states of $H_{TB} + H_{ext}(t)$ only at resonance, when multiples of the driving frequency match the rungs of the Wannier–Stark ladder, i.e., $\varepsilon_0 = n\Omega$ [96,107], see Fig. 5. In this case $\Psi_k(t) = \Phi_k(t)\exp(-\mathrm{i}\varepsilon(k)t/\hbar)$ assumes the Floquet form with $\Phi_k(t+\mathscr{T}) = \Phi_k(t)$ and corresponding quasienergies given by

$$\varepsilon(k) = \frac{1}{\mathscr{T}}\int_0^{\mathscr{T}} \mathrm{d}t E(q_k(t)) = (-1)^n J_n\left(\frac{\hat{\varepsilon}}{\Omega}\right)E(k), \quad \mathrm{mod}\,\hbar\Omega \,. \tag{147}$$

The quasimomentum k then remains a good quantum number for the eigenfunctions $\Phi_k(t)$ despite the presence of the dc-field. Whereas the Wannier–Stark states are localized, an additional resonant ac-field leads again to *extended* quasienergies states that form quasienergy bands of finite width. Therefore, a resonant ac-field can destroy Wannier–Stark localization even if its amplitude is infinitesimally small [111].

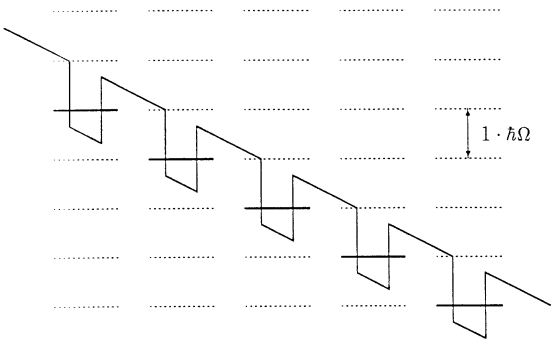

Fig. 5. A tight-binding lattice driven by dc- and ac-fields exhibits quasi-energy bands if the energy $n\hbar\Omega$ of n photons precisely matches the energy difference $\hbar\varepsilon_0$ between adjacent rungs of the Wannier–Stark ladder. The emergence of the quasi-energy band occurs because, as depicted schematically in this figure for $n = 1$, at resonance, the energies of the atomic states "dressed" by the ac-field are exactly aligned with the rungs of the Wannier–Stark ladder.

In presence of random static disorder these delocalized states tend to localize again [95,96,108], and it is even possible to control the degree of localization, i.e., the localization length, by appropriately varying the ac-field amplitude [95–97].

An arbitrary, initially localized wavepacket $\Psi(t = 0)$ can be represented as a superposition of Floquet states with a certain momentum distribution $\hat{f}(k, 0)$, and the time evolution of each component is given by $\hat{f}(k, \mathscr{T}) = \hat{f}(k, 0)\exp(-i\varepsilon(k)\mathscr{T}/\hbar)$. Assuming that the initial momentum distribution is sharply peaked around k_0, the time-averaged group velocity of the wavepacket is

$$\bar{v} = \left|\frac{d\varepsilon(k)}{dk}\right|_{k_0} = (-1)^n \frac{\Delta_0 d}{2} J_n\left(\frac{\hat{\varepsilon}}{\Omega}\right)\sin(k_0 d)\,. \tag{148}$$

Hence, the wavepacket generally moves along the whole lattice, and simultaneously is spreading. When $\hat{\varepsilon}/\Omega$ coincides with a kth zero $j_{n,k}$ of the Bessel function J_n the wavepacket reassembles itself after a period. Hence, on average, it neither moves nor spreads and the dynamic localization phenomenon occurs.

We observe that interesting new features occur when coupling to higher bands start to play a role. As pointed out in [112], in the presence of a static electric field the spectrum consists of two interpenetrating Wannier–Stark ladders. In the presence of ac-fields, quasienergy bands occur [103,113,114] whose bandwidth can be controlled by appropriately tuning of the ac-field parameters.

Finally, a nonperturbative investigation of the influence of a strong laser field on the band structure of a one-dimensional Kronig–Penney periodic delta potential has been investigated in [115].

5. Driven quantum wells

With the recent advent of powerful radiation sources, which are able to deliver extremely strong and coherent electric driving fields, the quantum transport in solid state devices, such as in

superconductors and semiconductor heterojunctions, has been revolutionalized. The latter, by now, can even be nanostructured. Of particular interest is the role of photon-assisted tunneling (PAT) in single, double-barrier and periodic superlattice-like structures. The mechanism of PAT has originally been observed in the experiments by Dayem and Martin [14] in the stationary dc-current–voltage characteristics of a superconductor (Al)–insulator (Al_2O_3)–superconductor (In) (SIS)–structure. Motivated by this very experiment, Tien and Gordon [15] put forward a simple theory, which continues to enjoy great popularity up to these days.

5.1. Driven tunneling current within Tien–Gordon theory

Following Tien and Gordon [15] one considers two (superconducting) films A and B with a time-dependent electric field acting normal to their surface. In doing so, one neglects the intermediate insulating regime where the wave functions drop off sharply. Neglecting electron–field interactions in this region one can use the potential of film A as a reference, and the main effect of the electromagnetic field is accounted for by adding a time-dependent, but spatially constant, potential that is being built up across the insulator in regions with coordinates q in film B. Hence, neglecting the interface, the total Hamiltonian reads, see Fig. 6,

$$H(t) = \begin{cases} H_0(q) + \hat{V}\cos\Omega t, & q \text{ in } B\,, \\ H_0(q), & q \text{ in } A\,. \end{cases} \tag{149}$$

Note that this Hamiltonian describes driven quantum transport that does not involve the spatial dependence. Hence, within the region of the film B, the wave function simply assumes an overall phase factor given by

$$\exp\{-\mathrm{i}\eta(t)/\hbar\} = \exp\left\{(-\mathrm{i}/\hbar)\int_0^t \mathrm{d}s\,\hat{V}\cos(\Omega s)\right\}, \tag{150}$$

meaning that the wave function with coordinates q in part of film B is given exactly by

$$\Psi(q,t) = \varphi(q)\exp\{-\mathrm{i}Et/\hbar\}\exp\{-\mathrm{i}\eta(t)/\hbar\}\,. \tag{151}$$

Put differently, the interaction in Eq. (149) does clearly not change the spatial dependence of the unperturbed Hamiltonian H_0, whose wave function is given by the first two contributions in Eq. (151). Note however, that the solution in Eq. (151) is *not* an exact wave function $\Psi(q,t)$ in *all* space of film A (where $H(t)$ equals H_0) and film B, because no wave function matching at the interface has been accounted for. The phase can be readily written as $\exp\{-\mathrm{i}\eta(t)/\hbar\} = \exp\{-\mathrm{i}(\hat{V}/\hbar\Omega)\sin(\Omega t)\}$, which, by use of the generating function of ordinary Bessel functions, is recast as

$$\exp\{-\mathrm{i}\eta(t)/\hbar\} = \sum_{n=-\infty}^{\infty} J_n(\hat{V}/\hbar\Omega)\exp(-\mathrm{i}n\Omega t)\,. \tag{152}$$

This form allows for a simple interpretation for PAT: In this theory, photon absorption ($n > 0$) or emission ($n < 0$) is viewed as creating a new set of (electron) eigenstates of energy $E + n\hbar\Omega$, where

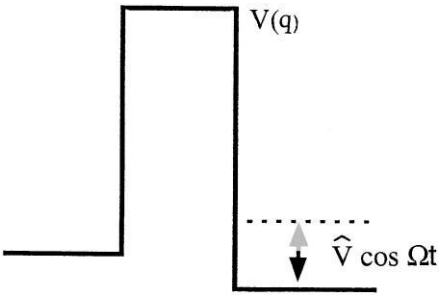

Fig. 6. The Tien–Gordon model: a time-dependent uniform electric field acting normal to the surfaces A and B of two superconducting films builds up a potential modulation across the tunneling barrier separating the two films. The potential of film A is taken as a reference. The electric field then sets up a potential difference $\hat{V}\cos(\Omega t)$ in film B.

E denotes the eigenenergy of the original state with $H(t) = H_0$ throughout A and B. The probability of absorbing (or emitting) n photons *equals each other*, and is given by the weight $J_n^2(a)$, with a being the dimensionless radiation quantity

$$a := \hat{V}/\hbar\Omega\,. \tag{153}$$

We remark that this argument is inversely proportional to the *first power* in Ω. The theory allows for a straightforward evaluation of the *average* dc-current $I_0(V_0,\hat{V},\Omega)$ in presence of an additional applied dc-bias V_0. In terms of the dc-tunneling-current, i.e.,

$$I_{AB}^{\mathrm{dc}}(V_0) = C\int_{-\infty}^{\infty} \mathrm{d}E[f(E - V_0) - f(E)]\varrho_A(E - V_0)\varrho_B(E)\,, \tag{154}$$

where C is a proportionality constant, the f's are the Fermi factors, and $\varrho_{A,B}$ are the densities of states in A and B, respectively, the effect of an ac-modulating voltage drop in film B results in a nonzero, average tunneling current. It explicitly reads [15]

$$I_0(V_0,\hat{V},\Omega) = \sum_{n=-\infty}^{\infty} J_n^2(\hat{V}/\hbar\Omega)I_{AB}^{\mathrm{dc}}(V_0 + n\hbar\Omega)\,. \tag{155}$$

We note that such SIS-structures are commonly used for high-frequency detection [116]. The Tien–Gordon theory – for additional insight into this approach see also [116,117] – has recently been successfully applied in explaining qualitatively the experimental findings of PAT through quantum dots [118–120], in quantum point contacts [121], for stimulated emission and absorption in THz-irradiated resonant tunneling diodes [122]. Interestingly enough, the simple theory in Eq. (154) for the average dc-current also qualitatively describes the experimentally observed PAT-phenomena in superlattices, particularly the emergence of "absolute negative conductance" near zero bias voltage V_0. In other words, it might occur that $I_0(V_0,\hat{V},\Omega) < 0$ for small but positive applied dc-bias V_0 [16–22,98]; see also in Section 13. In recent years, more realistic theoretical descriptions beyond the Tien–Gordon level have been developed by various groups [123–138].

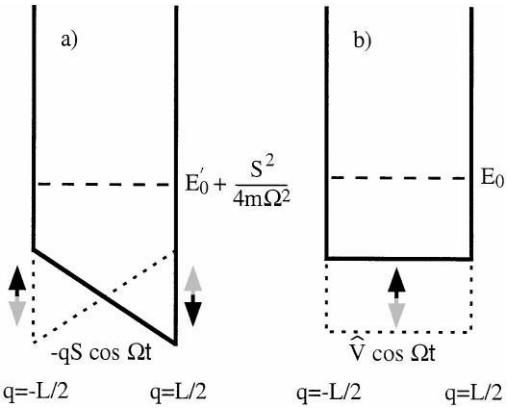

Fig. 7. Driven quantum wells: An infinite high square well sandwiched between two walls at $q = \pm L/2$, and driven by (a) an external field $-qS\cos(\Omega t)$, or (b) driven by a uniform in space, time-dependent potential $\hat{V}(t) = \hat{V}\cos(\Omega t)$. The situation in (b) is generally referred to as "Tien–Gordon" case. The location of the lowest quasienergy ε_0 is indicated by the dashed line. For case (a) one has $\varepsilon_0 = E_0' + S^2/(4m\Omega^2)$, and $\varepsilon_0(S,\Omega) \overset{S\to 0}{\to} E_0 = \hbar^2\pi^2/2mL^2$, being the ground state energy of an undriven square well. For case (b) one has $\varepsilon_0 = E_0$.

In principle, the exact description of strong ac-field interactions necessitates a full treatment in terms of Floquet theory for the total Schrödinger equation of system – leads – ac-field interactions, which generally constitutes a difficult task. In the following we address in some detail such analysis for a strongly driven quantum well.

5.2. Floquet treatment for a strongly driven quantum well

In the previous subsection we considered the effects of a – spatially constant – time-dependent modulation across a tunneling barrier. In cases where the coherence length of the wave function is smaller than the region of uniform modulation, boundary conditions at the interfaces must be taken into account. The case of a quantum well of width L and finite height V_0, where only the quantum well but not the neighboring regions is subject to a uniform bias modulation has been considered in [127,128,133,134], see Fig. 7b for the case of a quantum well with infinte high walls. This situation is of interest, for example, to investigate transmission probabilities through a double-barrier resonant tunneling diode [122], or driven tunneling through a quantum dot [118–120]. The Hamiltonian *inside* the quantum well reads

$$H(t) = -\frac{\hbar^2}{2m}\frac{\partial^2}{\partial q^2} + \hat{V}\cos(\Omega t), \qquad -\frac{L}{2} \le q \le \frac{L}{2}, \tag{156}$$

with m denoting the effective mass. At the interfaces, $q = \pm L/2$, the wave function and its flux must be continuous. To satisfy these requirements, one needs to superimpose many wave functions of the general form (151) inside the quantum well. This yields for the wave function inside the

quantum well the solution

$$\Psi_E(q,t) = \sum_{n=-\infty}^{\infty} \exp[-\mathrm{i}(E + n\hbar\Omega)t/\hbar][A_n \exp(\mathrm{i}k_n q) + B_n \exp(-\mathrm{i}k_n q)] \times \exp\left(-\mathrm{i}\frac{\hat{V}}{\hbar\Omega}\sin(\Omega t)\right), \tag{157}$$

where E denotes a bound state energy in the undriven quantum well. Hence, the wave function $\Psi_E(q,t)$ is of the Floquet form

$$\Psi_E(q,t) = \exp(-\mathrm{i}\varepsilon t/\hbar)\Phi_E(q,t)\,, \tag{158}$$

with $\Phi_E(q,t)$ periodic in $\mathscr{T} = 2\pi/\Omega$, and with quasienergy $\varepsilon = E \bmod \hbar\Omega$. In the form given by Eq. (157) the full wave function is built up by an infinite sum over *transport* sidebands, where the nth transport sideband is characterized by the quasiwavevector k_n, defined as

$$\hbar k_n = \sqrt{2m(E + n\hbar\Omega)}\,. \tag{159}$$

The coefficients A_n and B_n are determined by the matching conditions for the wave function and its flux at the interfaces $q = \pm L/2$. Hence, when time-dependent transport through a barrier is investigated, transport sidebands with a definite quasiwavevector k_n must be considered. It is important to notice that because of the residual periodic time dependence carried by each transport sidebands, these transport sidebands are *not* obtained by a Fourier decomposition of the periodic Floquet mode, in contrast to the Tien–Gordon case discussed in the preceding subsection. For this problem the probability S_n to find the particle in a particular transport sideband n has been evaluated in [133,134] under the assumption that $n\hbar\Omega \ll E$ and $n\hbar\Omega \ll V_0 - E$, for all sufficiently populated sidebands. To lowest order in the quantities $n\hbar\Omega/E$ and $n\hbar\Omega/(V_0 - E)$, one obtains

$$S_n = J_n^2(\gamma\hat{V}/\hbar\Omega)\,, \tag{160}$$

where the coefficient $\gamma \leq 1$ depends on the characteristics of the quantum well. In the limit $L \to \infty$ the Tien–Gordon problem discussed in the previous section is recovered. Correspondingly, $\gamma \to 1$.

One can directly apply these results to the problem of evaluating the transmission probability of an electron traversing a double-barrier structure with a central oscillating quantum well. Assuming that the incoming electron enters the quantum well in the channel n_{in} and exits via the channel n_{out}, the total transmission probability $T_{n_{\mathrm{in}},n_{\mathrm{out}}}$ from channel n_{in} to channel n_{out} is

$$T_{n_{\mathrm{in}},n_{\mathrm{out}}} = T_0 S_{n_{\mathrm{in}}} S_{n_{\mathrm{out}}}\,, \tag{161}$$

where $T_0(E)$ denotes the transmission probability $n_{\mathrm{in}} = 0 \to n_{\mathrm{out}} = 0$ for a static double barrier structure at a corresponding energy E. With incoming energy E of the scattering particle taken at resonance, the transmission probability $T_0(E)$ in a symmetric double barrier equals one. Hence, for an incoming electron in the sideband n_{in} quenching of the transmission probability $T_{n_{\mathrm{in}}n_{\mathrm{out}}}$ occurs at the zeros of $J_{n_{\mathrm{in}}}(\gamma\hat{V}/\hbar\Omega)$ and/or $J_{n_{\mathrm{out}}}(\gamma\hat{V}/\hbar\Omega)$.

Qualitative new results are obtained when the assumption of a uniform spatial modulation of the quantum well is abandoned. In the following we consider the problem of a strongly driven quantum well of width L, sandwiched between two *infinitely* high walls at $q = \pm L/2$, as depicted in Fig. 7a, being harmonically driven by an electric field $-Sq\cos(\Omega t)$, i.e., its Hamiltonian reads

$$H(t) = -\frac{\hbar^2}{2m}\frac{\partial^2}{\partial q^2} + Sq\cos(\Omega t), \qquad -\frac{L}{2} \le q \le \frac{L}{2}. \tag{162}$$

The Hamiltonian in Eq. (162) appears very simple. Nevertheless, in contrast to the familiar time-independent case with $S = 0$, *no exact* solutions are known when $S \neq 0$ [139–142]. Usually, only perturbative solutions valid to first order in the driving strength S, i.e., a linear response treatment, is deduced [144,145]. As mentioned earlier, with continuous coordinates q and corresponding continuous momenta p, the total time-dependent Hamiltonian must contain interactions that are constant, linear, or at most quadratic in q and/or p for it to be exactly solvable, see Refs. [59–63]. The Hamiltonian in Eq. (162) possesses a generalized parity symmetry P, where $P: q \to -q;\ t \to t + \pi/\Omega$. The lowest discrete quasienergy ε_0 associated to the Floquet state $\Psi_0(q,t) = \exp(-\mathrm{i}\varepsilon_0 t/\hbar)\Phi_0(q,t)$, with $\Phi_0(q,t)$ periodic in $\mathscr{T} = 2\pi/\Omega$, can be expressed in the form [142]

$$\varepsilon_0 = E_0'(S,\Omega) + S^2/4m\Omega^2, \quad \mathrm{mod}\,\hbar\Omega, \tag{163}$$

where $E_0'(S \to 0, \Omega)$ approaches the lowest unperturbed bound state $E_0 = \hbar^2\pi^2/2mL^2$. The periodic Floquet mode Φ_0 of even parity reads

$$\begin{aligned}\Phi_0(q,t) = \sum_{n=-\infty}^{\infty} A_n\{&\exp[-\mathrm{i}k_n(q - S\cos(\Omega t)/m\Omega^2)] \\ &+ (-1)^n \exp[-\mathrm{i}k_n(q - S\cos(\Omega t)/m\Omega^2)]\}\exp(-\mathrm{i}n\Omega t) \\ &\times \exp(-\mathrm{i}Sq\sin(\Omega t)/\hbar\Omega)\exp(\mathrm{i}S^2\sin(2\Omega t)/8\hbar m\Omega^3),\end{aligned} \tag{164}$$

where

$$\hbar^2 k_n^2(S,\Omega) = 2m[E_0'(S,\Omega) + n\hbar\Omega]. \tag{165}$$

In the form given by Eq. (164) the wave function is built up by an infinite sum over sidebands which, due to the residual q-dependence and periodic t-dependence of the phase, cf. last line in Eq. (165), can neither be interpreted as energy sidebands as in the Tien–Gordon case, nor as transport sidebands as for the spatially uniform driven quantum well. The set of coefficients $\{A_n(S,\Omega)\}$ and the energy $E_0'(S,\Omega)$ must be obtained from the boundary condition that a Floquet mode of even parity (odd parity) $\Phi_{\mathrm{even}}(q,t)(\Phi_{\mathrm{odd}}(q,t))$ obeys $\Phi_{\mathrm{even}}(\pm L/2, t) = \Phi_{\mathrm{even}}(\mp L/2, t + \pi/\Omega) = 0$, ($\Phi_{\mathrm{odd}}(\pm L/2, t) = -\Phi_{\mathrm{odd}}(\mp L/2, t + \pi/\Omega) = 0$), at *all* times t. This set $\{A_n(S,\Omega)\}$ is conveniently obtained by using again the generating function of Bessel functions J_n occurring implicitly in Eq. (164), cf. Eq. (152); however, the resulting system of equations is far too complicated to be solved exactly in analytical terms, see Ref. [142] where an explicit approximation valid to order v^2 of the relative spacing $v = \hbar\Omega/E_0'$ is presented. In terms of the quantities

$$v = \hbar\Omega/E_0'(S,\Omega), \qquad u = k_0(S,\Omega)S/m\Omega^2, \tag{166}$$

and observing that $k_n = k_0(1 + nv)^{1/2}$, see Eq. (165), one finds from this approximative solution to leading order

$$E'_0(S,\Omega) = E_0\left(1 - \frac{u^2v^2}{8}\right), \qquad k_0(S,\Omega) = \frac{\pi}{L}\left(1 - \frac{u^2v^2}{16}\right). \tag{167}$$

In the same way, the coefficients A_n can be evaluated to second order in v [142]. Finally, much information on the transmission probability can be gained from an investigation of the side-bands weights S_n, where S_n is the probability of the nth sideband, i.e.,

$$S_n = w_n|A_n|^2/\sum_n w_n|A_n|^2\,, \tag{168}$$

where $w_n = |1 + (-1)^n J_0(2k_nS/m\Omega^2)\sin(k_nL)/k_nL|$. With $v \ll 1$, the weights S_n go to zero at the roots of $J_n(k_0S/m\Omega^2)$. The weights S_n of these sidebands are depicted in Fig. 8. These weights strongly vary as a function of the driving strength S. In particular, we observe that channels with $n < 0$ are generally stronger than those with $n > 0$. This is in contrast to the case of a spatially uniform driven quantum well. The latter predicts from Eq. (160) *equal* weights for the side-channels. Most importantly, the transport side-band amplitudes are a nonmonotonic function of the driving strength S, see Fig. 8, and these sidebands *scale* with $Sk_0/m\Omega^2 \propto \Omega^{-2}$ rather than with $a = \hat{V}/\hbar\Omega \propto \Omega^{-1}$, being typical for a situation which is ruled by a uniform potential modulation as in the Tien–Gordon theory, see in this context also the corollary in Ref. [131].

This reasoning can be extended to include Floquet states originating from higher levels. In this case the original spectrum of bound states $E_n = \hbar^2(n+1)^2\pi^2/2mL^2$ evolves into a discrete quasienergy spectrum

$$\varepsilon_n(S,\Omega) = E'_n(S,\Omega) + S^2/4m\Omega^2, \quad \mathrm{mod}\,\hbar\Omega\,, \tag{169}$$

with $E'_n(S,\Omega) := (\hbar k_0^{(n)}(S,\Omega))^2/2m$, i.e., with vanishing field $\varepsilon_n(S,\Omega) \overset{S\to 0}{\to} E_n$ and $k_0^{(n)}(S,\Omega)L \overset{S\to 0}{\to} (n+1)\pi$, and corresponding Floquet modes of even and odd generalized parity symmetry. For a numerical study of $E'_n(S,\Omega)$ vs. S see Ref. [141]. Next, we note that in the case of a uniform potential modulation, and infinite height walls at $q = \pm L/2$, cf. part b in Fig. 7, the Tien–Gordon theory becomes *exact*, yielding the quasienergies

$$\varepsilon_n(S,\Omega) = E_n, \quad \mathrm{mod}\,\hbar\Omega\,, \tag{170}$$

with corresponding Floquet modes, which simply acquire a time-dependent phase, i.e.,

$$\Phi_n(q,t) = \varphi_n(q)\exp\{-\mathrm{i}\hat{V}\sin(\Omega t)/\hbar\Omega\}\,. \tag{171}$$

Here, $\varphi_n(q)$ are again the unperturbed wave functions of an infinitely high square well. Clearly, due to the q-independent, uniform interaction $\hat{V}\cos(\Omega t)$ the spatial dependence of the Floquet modes $\Phi_n(q,t)$ cannot be affected, nor is the value of the quasienergy, i.e., $\varepsilon_n = E_n$.

We end this section by addressing the relevance of these results for PAT in realistic situations with a single quantum well of finite barrier height, as it occurs with a double-barrier structure. As shown in Ref. [142], the analytical prediction for quenching the PAT-assisted tunneling current,

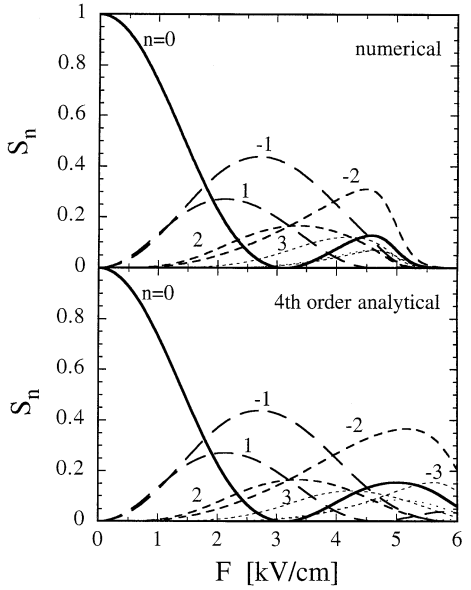

Fig. 8. Weights of the sidebands, see Eq. (168), of a driven single electron square quantum well. The weights S_n are evaluated for a well of width $L = 16\,\text{nm}$ (yielding for the static ground state energy $E_0 = 21\,923\,\text{meV}$) vs. driving laser field strength $F := S/e$ and with photon energy $\hbar\Omega = 5.38\,\text{meV}$. The top panel depicts the numerical exact solution; the lower panel shows the analytic prediction valid up to fourth order in $v = \hbar\Omega/E_0' \sim \frac{1}{4}$. Note that the weights are different for $\pm n$.

implying that $S_n \to 0$, are in good agreement whenever the photon energy $\hbar\Omega$ *exceeds* the tunneling linewidth Δ_0 of a static resonance. Note that the case with an infinitely high quantum well implicitly assumes that $\Delta_0 = 0$. The theory outlined in this section also applies to multiple quantum wells as they occur in PAT in superlattices: There, quantum ac-transport predominantly proceeds via sequential resonant tunneling. Hence, here too, it is sufficient to consider the physics in a single driven quantum well to describe the main features of PAT.

6. Tunneling in driven bistable systems

In this section we address the physics of coherent transport in bistable systems. These systems are abundant in the chemical and physical sciences. On a quantum mechanical level of description bistable, or double-well potentials, are associated with a paradigmatic coherence effect, namely quantum tunneling. Here we shall investigate the influence of a spatially homogeneous monochromatic driving on the quantal dynamics in a symmetric, quartic double well. This archetype system is particularly promising for studying the interplay between classical nonlinearity – its classical dynamics exhibits chaotic solutions – and quantum coherence. Its Hamiltonian reads [24,25]

$$H(q,p;t) = (p^2/2m) + V_0(q) + qS\sin(\Omega t + \phi)\,, \tag{172}$$

with the quartic double-well potential

$$V_0(q) = -(m\omega_0^2/4)q^2 + (m^2\omega_0^4/64E_B)q^4 . \tag{173}$$

Here, m denotes the mass of the particle, ω_0 is the classical frequency at the bottom of each well, E_B the barrier height, and S, Ω and ϕ are the amplitude, angular frequency and phase of the driving. The number of doublets with energies below the barrier top is approximately given by $D = E_B/\hbar\omega_0$. The classical limit hence amounts to $D \to \infty$.

For ease of notation, we introduce the dimensionless variables

$$\bar{q} = \frac{\sqrt{m\omega_0\hbar}}{q}, \qquad \bar{p} = \frac{p}{\sqrt{m\omega_0\hbar}} \tag{174}$$

and

$$\bar{t} = \omega_0 t, \qquad \bar{\omega} = \frac{\Omega}{\omega_0}, \qquad \bar{S} = \frac{S}{\sqrt{m\omega_0^3\hbar}}, \tag{175}$$

where the overbar is omitted in the following. This is equivalent to setting in Eq. (173) formally $m = \hbar = \omega_0 = 1$.

As discussed in Section 2, the symmetry of $H(t)$ reflects a discrete translation symmetry in multiples of the external driving period $\mathscr{T} = 2\pi/\Omega$, i.e., $t \to t + n\mathscr{T}$. Hence, the Floquet operator describes the stroboscopic quantum propagation

$$U(n\mathscr{T}, 0) = [U(\mathscr{T}, 0)]^n . \tag{176}$$

Besides the invariance under discrete time translations, this periodically driven symmetric system exhibits a generalized parity symmetry P, i.e.,

$$P : q \to -q; \qquad t \to t + \mathscr{T}/2 . \tag{177}$$

This generalized parity is a symmetry in the composite Hilbert space $\mathscr{R} \otimes \mathscr{T}$. Denoting the reflection at the origin, i.e., $q \to -q$ by the ordinary operator $\mathscr{P}$, Eq. (177) implies

$$H(t + \mathscr{T}/2) = \mathscr{P}H(t)\mathscr{P} . \tag{178}$$

From this identity it follows that the *second* half of a full period $\mathscr{T}$ can be expressed by the propagator over the first half, i.e., $U(\mathscr{T}, \mathscr{T}/2) = \mathscr{P}U(\mathscr{T}/2, 0)\mathscr{P}$, yielding

$$\begin{aligned} U(\mathscr{T}, 0) &= U(\mathscr{T}, \mathscr{T}/2)U(\mathscr{T}/2, 0) \\ &= (\mathscr{P}U(\mathscr{T}/2, 0)\mathscr{P})U(\mathscr{T}/2, 0) = (\mathscr{P}U(\mathscr{T}/2, 0))^2 . \end{aligned} \tag{179}$$

Just as in the unperturbed case with $S = 0$, this allows the classification of the corresponding quasienergies $\varepsilon_{\alpha n}$ into an even and an odd subset. For very weak fields $S \to 0$, the quasienergies $\varepsilon_{\alpha k}$ follow from Eq. (29) as

$$\varepsilon_{\alpha k}^0(S, \Omega) = E_\alpha + k\Omega, \quad k = 0, \pm 1, \pm 2, \ldots , \tag{180}$$

with $\{E_\alpha\}$ being the unperturbed eigenvalues in the symmetric double well. As pointed out in Eq. (9), this infinite multiplicity is a consequence of the fact that there are infinitely many possibilities to construct equivalent Floquet modes, cf. Eq. (8): The multiplicity is lifted if we

consider the cyclic quasienergies mod Ω. Given a pair of quasienergies $\varepsilon_{\alpha,k}$, $\varepsilon_{\alpha',k'}$, $\alpha \neq \alpha'$, a physical significance can be attributed to the difference $\Delta k = k' - k$. For example, a crossing $\varepsilon_{\alpha,k} = \varepsilon_{\alpha',k+\Delta k}$ can be interpreted as a (Δk)-photon transition. With $S > 0$, the equality in Eq. (180) no longer provides a satisfactory approximation. Nevertheless, the driving field is still most strongly felt near the resonances $\varepsilon_{\alpha,k} \approx \varepsilon_{\alpha',k'}$. The physics of periodically driven tunneling can be qualified by the following two properties:

(i) First we observe, by an argument going back to von Neumann and Wigner [43], that, in absence of any asymmetry, two parameters must be varied independently to locate an accidental degeneracy. In other words, exact quasienergy crossings are found at most at isolated points in the parameter plane (S, Ω), i.e., the quasienergies exhibit typically avoided crossings. In presence of the generalized parity symmetry in Eq. (177) in the extended space $\mathscr{R} \otimes \mathscr{T}$, however, this is true only among states belonging to the same parity class, or for cases of driven tunneling in presence of an asymmetry (then Eq. (177) no longer holds). With the symmetry in Eq. (177) present, however, quasienergies associated with eigenstates of opposite parity do exhibit exact crossings and form a one-dimensional manifold in the (S, Ω)-plane, i.e., $\{\varepsilon(S, \Omega)\}$ exhibit an exact crossing along lines. With $S \to -S$, implying $\varepsilon(S, \Omega) = \varepsilon(-S, \Omega)$, these lines are symmetric around the Ω-axis.

(ii) Second, the effective coupling due to the finite driving between two unperturbed levels at the crossing $E_\alpha = E_{\alpha'} - \Delta k\Omega$, as reflected in the degree of splitting of that crossing at $S \neq 0$, rapidly decreases with increasing Δk, proportional to the power law $S^{\Delta k}$. This suggests the interpretation as a (Δk)-photon transition. Indeed, this fact can readily be substantiated by applying the usual (Δk)th-order perturbation theory. As a consequence, for small driving S only transitions with Δk a small whole number do exhibit a significant splitting.

6.1. Limits of slow and fast driving

In the limits of both slow (adiabatic) and fast driving, we have a clearcut separation of time scales between the inherent tunneling dynamics and the external periodic driving. Hence, the two processes effectively uncouple. As a consequence, driven tunneling results in a mere renormalization of the bare, lowest order, tunnel splitting Δ_0, and likewise for higher-order tunnel splittings $\Delta_n = E_{n+2} - E_{n+1}$. This result can be substantiated by explicit analytical calculations [25]. Let us briefly address the adiabatic limit, i.e., the driving frequency Ω satisfies $\Omega \ll \Delta_0$. Setting $\tilde{\phi} \equiv (\Omega t + \phi)$, the tunneling proceeds in the adiabatic potential

$$V(q, \tilde{\phi}) = V_0(q) + qS \sin \tilde{\phi} \,. \tag{181}$$

The use of the quantum adiabatic theorem predicts that $\Psi(q, t)$ will cling to the same instantaneous eigenstates. Thus, the evaluation of the periodic-driving renormalized tunnel splitting follows the reasoning used for studying the bare tunnel splitting in presence of an asymmetry ε_0,

$$\varepsilon_0 = V(q_-, \tilde{\phi}) - V(q_+, \tilde{\phi}) \,, \tag{182}$$

with $q_\pm$ denoting the two minima of the symmetric unperturbed metastable states. With the instantaneous splitting determined by $\Delta(S, \phi) = (\Delta_0^2 + \varepsilon_0^2)^{1/2}$, the averaging over the phase ϕ between $[0, 2\pi]$ yields for the renormalized tunnel splitting $\Delta_{\mathrm{ad}}(S)$, the result [25]

$$\Delta_{\mathrm{ad}}(S) = (2\Delta_0/\pi)(1 + u)^{1/2} E[\sqrt{u/(1 + u)}] \geq \Delta_0 \,, \tag{183}$$

with $u = 32S^2D/\Delta^2$, and $E[x]$ denoting the complete elliptical integral. This shows that $\Delta_{\rm ad}$ increases proportional to S^2 as $u \ll 1$, and is increasing proportional to S for $u \gg 1$. Hence, a particle localized in one of the two metastable states will not stay localized there (this would be the prediction based on the classical adiabatic theorem) but rather will tunnel forth and back with an increased tunneling frequency $\Delta_{\rm ad} > \Delta_0$. Obviously, with the slowly changing quantum system passing a near degeneracy (tunnel splitting) the limits $\hbar \to 0$, Ω fixed and small (classical adiabatic theorem) and $\Omega \to 0$, $\hbar$ fixed (quantum adiabatic theorem) are not equivalent.

The limit of high-frequency driving can be treated analytically as well. The unitary transformation

$$\Psi(q,t) = \exp(-{\rm i}(S/\Omega)\cos(\Omega t + \phi)q)g(q,t) \tag{184}$$

describes the quantum dynamics within the familiar momentum coupling in terms of an electromagnetic potential $A(t) = -(S/\Omega)\cos(\Omega t + \phi)$, i.e., the transformed Hamiltonian reads

$$\tilde{H}(q,t) = H_0(q,p) - A(t)p\,, \tag{185}$$

with H_0 the Hamiltonian in the absence of the driving field. We drop all time-dependent contributions that do not depend on q and p. Next we remove this $A(t)p$-term by a Kramers–Henneberger transformation [143], i.e.,

$$g(q,t) = \exp\left(-{\rm i}\int^t {\rm d}t' A(t')p\right) f(q,t) \tag{186}$$

to yield

$$\hat{H}(q,t) = \tfrac{1}{2}p^2 + V_0(q - (S/\Omega^2)\sin(\Omega t + \phi))\,, \tag{187}$$

resulting in a removal of the $A(t)p$-term, and the time dependence shifted into the potential $V(q,t)$. After averaging over a cycle of the periodic perturbation we obtain an effective Hamiltonian

$$H_{\rm H} = \frac{1}{2}p^2 - \frac{1}{4}q^2\left[1 - \frac{3}{16D}\left(\frac{S}{\Omega^2}\right)^2\right] + \frac{1}{64D}q^4\,, \tag{188}$$

with a frequency-dependent curvature. This large-frequency approximation results in a high-frequency renormalized tunnel splitting [25],

$$\Delta_{\rm H} = \Delta_0\left(1 - \frac{3}{16D}\left(\frac{S}{\Omega^2}\right)^2\right)\exp(2S^2/\Omega^4) \geq \Delta_0\,. \tag{189}$$

Hence, fast driving results in an effective reduction of barrier height, thereby increasing the net tunneling rate. Note here the different behavior of the effective tunnel splitting on the angular frequency of periodic driving: In the two-state model (99), the argument in the function yielding the driving induced, effective tunnel splitting for fast fields $\Omega > \Delta_0$ exhibits a scaling proportional to Ω^{-1}; in contrast, here, with a spatially extended coordinate q for a bistable potential, the scaling becomes proportional to Ω^{-2} in the regime $\Omega \gg \omega_0$.

In conclusion, the regime of adiabatic slow driving and very-high-frequency driving (away from high-order resonances) can be modeled via a driving-induced enhancement of the tunnel splitting.

6.2. *Driven tunneling near a resonance*

Qualitative changes of the tunneling behavior are expected as soon as the driving frequency becomes comparable to internal resonance frequencies of the unperturbed double well with energy eigenstates $E_1, E_2, \ldots$ with corresponding eigenfunctions $\varphi_1(x), \varphi_2(x), \ldots$ Thus, such resonances occur at $\Omega = E_3 - E_2, E_4 - E_1, E_5 - E_2, \ldots$ etc. A spectral decomposition of the dynamics resolves the temporal complexity which is related to the landscape of quasienergies planes $\varepsilon_{\alpha,k}(S, \Omega)$ in parameter space. Most important are the features near close encounters among the quasienergies. In particular, two quasienergies can cross one another if they belong to different parity classes, or otherwise, they form an avoided crossing. The situation for a single-photon transition-induced tunneling is depicted in Fig. 9 at the fundamental resonance $\Omega = E_3 - E_2$. For $S > 0$, the corresponding quasienergies $\varepsilon_{2,k}$ and $\varepsilon_{3,k-1}$ form avoided crossings, because they possess equal parity quantum numbers. Starting from a state localized in the left well, we depict in Fig. 9a the probability to return $P_{\mathrm{L}}(t_n) = |\langle \Psi(0) | \Psi(t_n) \rangle|^2$, $t_n = n\mathscr{T}$. Instead of a monochromatic oscillation, which characterizes the unperturbed tunneling we observe in the driven case a complex beat pattern. Its Fourier transform reveals that it is mainly composed of two groups of three frequencies each (Fig. 9b). These beat frequencies can be associated with transitions among Floquet states at the avoided crossing pertaining to the two lowest doublets. The lower triplet is made up of the differences of the quasienergies $\varepsilon_{3,-1}$, $\varepsilon_{2,0}$, and $\varepsilon_{1,0}$; the higher triplet is composed of the differences $\varepsilon_{4,-1} - \varepsilon_{3,-1}$, $\varepsilon_{4,-1} - \varepsilon_{2,0}$, $\varepsilon_{4,-1} - \varepsilon_{1,0}$ [25]. An analytical, weak-field and weak-coupling treatment of a resonantly driven two-doublet system has been presented with Refs. [146,147]. The use of a nonlinear resonance for controlling tunneling has been studied for the case of a driven double-square well system in [148].

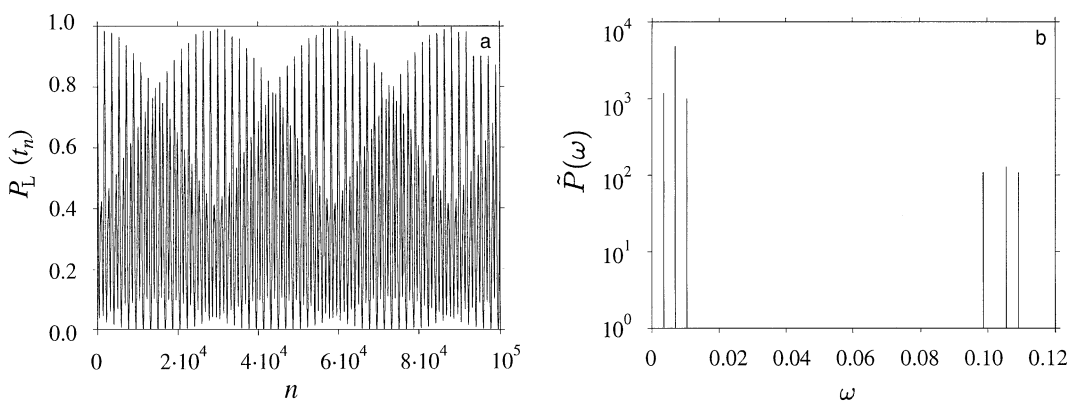

Fig. 9. Tunneling in a double well driven at the fundamental resonance $\Omega = E_3 - E_2$. (a) Time evolution of the return probability $P_{\mathrm{L}}(t_n)$, $t_n = n\mathscr{T}$ for a state initially localized in the left well over the first 10^5 time steps; (b) corresponding local spectral two-point correlations $\tilde{P}(\omega)$ [25]. The dimensionless parameter values are $D = 2$, $S = 2 \times 10^{-3}$, and $\Omega = 0.876$.

6.3. Coherent destruction of tunneling in bistable systems

A particularly interesting phenomenon occurs if we focus on nearly degenerate states that are tunnel splitted. For example, let us consider in the deep quantum regime the two quasienergies $\varepsilon_{1,k}(S,\Omega)$ and $\varepsilon_{2,k}(S,\Omega)$. The subsets $\{\varepsilon_1(S,\Omega)\}$ and $\{\varepsilon_2(S,\Omega)\}$ belong to different parity classes so that they can form exact crossings on one-dimensional manifolds, see below Eq. (180); put differently, at the crossing the corresponding two-photon transition that bridges the unperturbed tunnel splitting Δ_0 is parity-forbidden. To give an impression of driven tunneling in the deep quantum regime, we study how a state, prepared as a localized state centered in the left well, evolves in time under the external force. Since this state is approximately given by a superposition of the two lowest unperturbed eigenstates, $|\Psi(0)\rangle \approx (|\Psi_1\rangle + |\Psi_2\rangle)/\sqrt{2}$, its time evolution is dominated by the Floquet-state doublet originating from $|\Psi_1\rangle$ and $|\Psi_2\rangle$, and the splitting $\varepsilon_2 - \varepsilon_1$ of its quasienergies. Then a vanishing of the difference $\varepsilon_{2,-1} - \varepsilon_{1,1}$ might have an intriguing consequence: For an initial state prepared exactly as a superposition of the corresponding two Floquet states $\Psi_1(q,t)$ and $\Psi_2(q,t)$, cf. Eqs. (4) and (8), the probability to return $P_L(t_n)$, probed at multiples of the fundamental driving period $\mathcal{T} = 2\pi/\Omega$, becomes time independent. This gives us the possibility that tunneling can be brought to a complete standstill [24,25]. For this to happen, it is necessary that the particle neither spreads and/nor tunnels back and forth during a full cycle of the external period $\mathcal{T}$ after which the two Floquet modes assemble again [67]. Hence, this condition [24,67], together with the *necessary* condition of *exact crossing* between the tunneling related quasienergies $\varepsilon_{2n,k-1} = \varepsilon_{2n-1,k+1}$ (n is number of tunnel-splitted doublet) guarantees that tunneling can be brought to a complete standstill in a dynamically coherent manner. In Fig. 10a we depict the corresponding one-dimensional manifold of the jth crossing between the quasienergies that relate to the lowest tunnel doublet, i.e., $M_{\mathrm{loc}}^{j=1}(S,\Omega)$, which is a closed curve that is reflection symmetric with respect to the line $S = 0$. There a localization of the wave function $\Psi(q,t)$ can occur. A typical time evolution of $P_L(t_n)$ for a point on the linear part of that manifold is depicted in Fig. 10b.

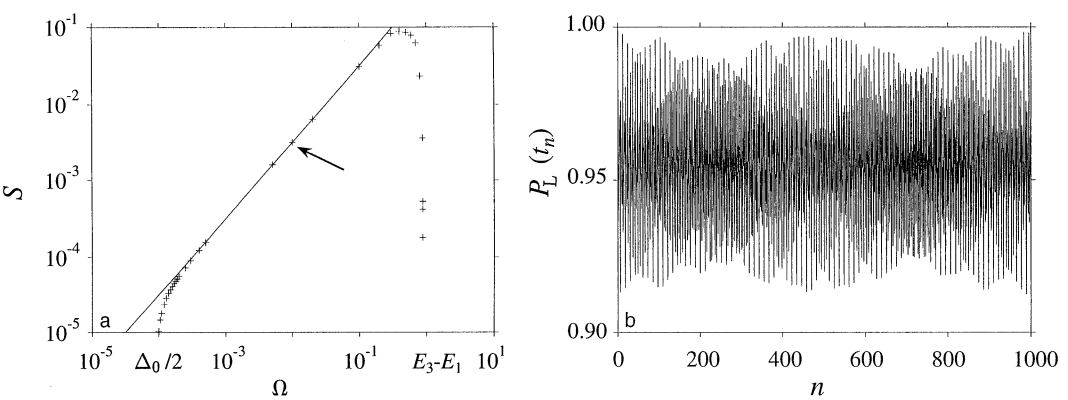

Fig. 10. Suppression of tunneling in a driven double well at an exact quasienergy crossing, $\varepsilon_{2,-1} = \varepsilon_{1,1}$. (a) One of the manifolds in the (S,Ω)-plane where this crossing occurs (data obtained by diagonalization of the full Floquet operator for the driven double well are indicated by crosses, the full line has been derived from a two-state approximation, the arrow indicates the parameter pair for which part (b) of this figure has been obtained); (b) time evolution of the return probability $P_L(t_n)$ over the first 1000 time steps starting from an initial state prepared as a coherent state in the left well. Dimensionless parameters are $D = 2$ (i.e., $\Delta_0 = 1.895\ldots10^{-4}$), $S = 3.171$, $\Omega = 0.01$.

Moreover, a time-resolved study over a full cycle (not depicted) does indeed show that the particle stays localized also at times $t \neq t_n$. Almost complete destruction of tunneling is found to occur on M^1_{loc} for $\Delta_0 < \Omega < E_3 - E_2$. For $\Omega \to E_3 - E_2$, the strong participation of a third quasienergy mixes nonzero frequencies into the time dependence so that coherent destruction of tunneling at all times ceases to exist. For small frequencies, $\Delta_0/2 \leq \Omega \leq \Delta_0$, and corresponding small driving strengths S, as implied by $M^1_{\mathrm{loc}}(S, \Omega)$, the driven quantum mechanics approaches the unperturbed quantum dynamics. In particular, it follows from (28) and (29) for $\Omega \to \Delta_0/2$ and $S \to 0$, i.e., $\Phi_{1,1}(q,t) = \varphi_1(q)\exp(\mathrm{i}\Omega t)$, $\Phi_{2,-1}(q,t) = \varphi_2(q)\exp(-\mathrm{i}\Omega t)$, that

$$P_{\mathrm{L}}(t) = |\langle \Psi(0)|\Psi(t)\rangle|^2 = \cos^2(\Delta_0 t/2), \quad \Omega = \Delta_0/2\,. \tag{190}$$

For $\Omega \approx \Delta_0$, $\varepsilon_{1,1}$ and $\varepsilon_{2,-1}$ exhibit an exact crossing. With corresponding Floquet modes determined from perturbation theory as

$$\begin{aligned} \Phi_{1,1}(q,t) &\approx \frac{1}{\sqrt{2}}[\varphi_1(q)\exp(\mathrm{i}\Omega t) + \mathrm{i}\varphi_2(q)]\,, \\ \Phi_{2,-1}(q,t) &\approx \frac{1}{\sqrt{2}}[\varphi_2(q)\exp(-\mathrm{i}\Omega t) + \mathrm{i}\varphi_1(q)]\,, \end{aligned} \tag{191}$$

the result for $P_{\mathrm{L}}(t)$, with $\Psi(q,0) = [\varphi_1(q) + \varphi_2(q)]/\sqrt{2}$, localized in the left well, becomes

$$P_{\mathrm{L}}(t) \approx \tfrac{1}{4}[3 + \cos(2\Delta_0 t)], \quad \Omega \approx \Delta_0\,. \tag{192}$$

For larger frequencies obeying $\Delta_0 < \Omega < E_3 - E_2$, the Floquet modes can be approximated by [67]

$$\begin{aligned} \Phi_{1,1}(q,t) &\approx \varphi_2(q)|\sin(\Omega t)| - \mathrm{i}\varphi_1(q)\cos(\Omega t)\,, \\ \Phi_{2,-1}(q,t) &\approx \varphi_1(q)|\sin(\Omega t)| - \mathrm{i}\varphi_2(q)\cos(\Omega t)\,. \end{aligned} \tag{193}$$

This results in a complete localization, i.e.,

$$P_{\mathrm{L}}(t) = 1, \qquad \Delta_0 < \Omega < E_3 - E_2\,. \tag{194}$$

Throughout Eqs. (190)–(194), we set the initial phase in Eq. (172) equal to zero.

Starting from a coherent state localized in the left well, taken as the ground state of the harmonic approximation, we depict in Fig. 11 the spatially resolved tunneling dynamics for $|\Psi(q,t)|^2$ at time $t = 0$ and at time $t = 458\,\mathscr{T}$ for $\Omega = 0.01 = 52.77\Delta_0$, and $S = 3.17 \times 10^{-3}$, yielding an exact crossing between $\varepsilon_{1,1}$ and $\varepsilon_{2,-1}$. For this value of $n = 458$, the deviation which originates from small admixtures of higher-lying quasienergy states to the initial coherent state, is exceptionally large. For other times the localization is even better. It is hence truly remarkable that the coherent destruction of tunneling on $M^1_{\mathrm{loc}}(S, \Omega)$, with $\Delta_0 < \Omega < E_3 - E_2$, is essentially not affected by the intrinsic time dependence of the corresponding Floquet modes, nor by the presence of other quasienergy states $\varepsilon_{\alpha,k}$, $\alpha = 3,4,\ldots$

Hence, as discussed in Section 3.2.2, additional insight into the mechanism of coherent destruction of tunneling can be obtained if one simplifies the situation by neglecting all of the spatial

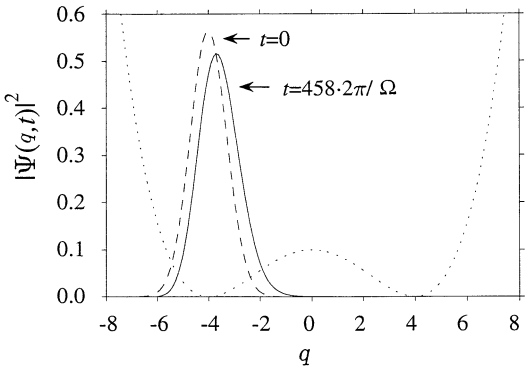

Fig. 11. Coherent destruction of tunneling in a double well. The probability $|\Psi(q,t)|^2$ at $t = 458\,\mathscr{T}$ (full line) is compared with the initial state (dashed line, the dotted line depicts the unperturbed symmetric bistable potential). The parameters are $D = 2$, $S = 3.171 \times 10^{-3}$ and $\Omega = 0.01$, i.e., Ω equals 52.77 times the unperturbed tunneling splitting.

information contained in the Floquet modes $\Phi_\alpha(q,t)$ and restricting the influence of all quasienergies to the lowest doublet only [67–72]. Such a two-state approximation cannot reproduce those sections of the localization manifolds that are affected by resonances, e.g. the part in Fig. 10a that bends back to $S = 0$ for $\Omega < E_3 - E_2$, nor can it reproduce the correct dynamics for $\Omega > E_3 - E_2$. Nevertheless, it provides a simple explanation of the CDT phenomenon for frequencies $E_3 - E_2 > \Omega > \Delta_0$. Then, the average over a complete cycle of the external perturbation yields a static approximation with a frequency-renormalized splitting $\Delta_0 \to \Delta_{\text{eff}}$, where

$$\Delta_{\text{eff}} = J_0(\hat{\varepsilon}/\Omega)\Delta_0\,, \tag{195}$$

with $S\langle\varphi_1|q|\varphi_2\rangle = \hat{\varepsilon}/2$, and J_0 the zeroth-order Bessel function of the first kind. This gives for the return probability $P_{\text{L}}(t)$ the approximate result of Eq. (100), i.e., $P_{\text{L}}(t) = \cos^2(J_0(\hat{\varepsilon}/\Omega)\Delta_0 t/2)$. On the localization manifold $M^1_{\text{loc}}(\hat{\varepsilon},\Omega)$, we find localization at the first zero $j_{0,1}$ of $J_0(\hat{\varepsilon}/\Omega)$, i.e., $\hat{\varepsilon}/\Omega = 2.40482\ldots$, in agreement with the result in Eq. (88). On this manifold, $P_{\text{L}}(t)$ precisely equals unity, i.e., the effective tunnel splitting vanishes. Thus one finds a complete coherent destruction of tunneling. This high-frequency TLS approximation, as determined by the first root of $J_0(\hat{\varepsilon}/\Omega)$, is depicted in Fig. 10a by a solid line. Note that, within the TLS-approximation to driven tunneling, tunneling is always suppressed when $\Omega > \Delta_0$. With $\Omega > E_2 - E_1$, this two-level prediction thus fails to describe the numerically established enhancement of tunneling in the full double well away from resonant transitions [24,25].

7. Sundry topics

The physics of driven tunneling, as demonstrated with the foregoing sections, exhibits a rich structure and carries a potential for various prominent applications. In the following, we shall report on some special applications that provide the seed for interesting new physics. Our selection is by no means complete but has been determined mainly by our knowledge and prejudices only. For example, we do not discuss here in detail the role of nonadiabatic CDT that controls the

experimentally observed anomalous enhancement of ionization rates of laser-driven diatomic molecules [149], or the vibrational mode-specific CDT-induced quenching of proton tunneling in jet-cooled tropolene molecules [150]. Yet another application of CDT in nuclear physics is the tunneling control in the periodically driven Lipkin N-body fermion system with SU(2) symmetry: At CDT conditions a coherent suppression of tunneling between Hartree–Fock minima in the N-fermion quantum system occurs [151].

7.1. Pulse-shaped controlled tunneling

Some important aspects involve the *shaping* of the driving field that itself can influence the driven tunneling dynamics. For example, Bavli and Metiu [152] have demonstrated that a semi-infinite laser pulse of appropriate shape can be used to conveniently localize a particle in a double-well potential, hence creating a localized initial state as a superposition of energy eigenstates. This very initial condition plays a key role for most of our discussion on driven tunneling throughout this report. Pulse-shaping can be used also to directly influence the dynamics of the tunneling process.

Following the reasoning of Holthaus [153] we show that an appropriate shaping of the laser pulse opens a pathway of controlling in situ the tunneling process. As a result, one finds that population transfer in a bistable potential can be achieved on time scales which can be orders of magnitude *shorter* than the bare tunneling time scale of the undriven system. Hence, this process is opposite to the localization that characterizes CDT; it rather describes an acceleration effect for the tunneling process. Within a pragmatic approach we use the bistable model discussed in Section 6, i.e., a driven tunneling dynamics expressed in the dimensionless units, see Eqs. (174) and (175) by the Hamiltonian

$$H(q,p;t) = \frac{p^2}{2} - \frac{q^2}{4} + \frac{q^4}{64D} + q\lambda(t)\sin(\Omega t + \phi)\,, \tag{196}$$

where $\lambda(t)$ describes the pulse shape. If E_1 and $E_2 > E_1$ denote the lowest eigenenergies of the unperturbed double well with corresponding wave function $\varphi_1(q)$ and $\varphi_2(q)$, the tunneling dynamics of the undriven system evolves in time as

$$\Psi(q,t) = 2^{-1/2}\mathrm{e}^{-\mathrm{i}E_1 t}[\varphi_1(q) + \varphi_2(q)\mathrm{e}^{-\mathrm{i}(E_2-E_1)t}]\,, \tag{197}$$

for which, after the "tunneling time"

$$\tau_0 = \pi/(E_2 - E_1) = \pi/\Delta_0\,, \tag{198}$$

the relative phase of the two wave functions has acquired the value of π. This implies that an initially localized particle in one of the wells has tunneled after a time τ_0 into the neighboring well. For a fixed strength $\lambda(t) = \lambda$, the Floquet modes $\Phi_\alpha(q,t;\lambda) = \Phi_\alpha(q,t+\mathscr{T};\lambda)$, see Eq. (7), with $\mathscr{T} = 2\pi/\Omega$, are solutions of a generalized Schrödinger equation with the eigenvalues becoming the quasienergies $\varepsilon_\alpha^\lambda$. Let us next invoke the adiabatic principle for Floquet states: If the system is prepared in a Floquet state and if the parameter $\lambda(t)$ is varied sufficiently slowly, the system remains in the Floquet state connected to the initial one. This adiabatic Floquet principle [44–48] is not obvious: Note that the quasienergies are dense in the first Brillouin zone $-\Omega/2 \le \varepsilon < \Omega/2$, and

that the usual gap condition of the standard adiabatic theorem must be replaced by a condition on the ineffectiveness of resonances [47,48]. Let the pulse $\lambda(t)$ now be switched on slowly from zero, i.e., the pulse duration $\mathscr{T}_{\mathrm{p}}$ is much longer than the driving period $\mathscr{T}$. The Floquet state $\Psi(q,t)$, starting from

$$\Psi(q,t=0) := \varphi_{\mathrm{L}}, \tag{199}$$

see Eq. (197), evolves then adiabatically into

$$\Psi(q,t) = 2^{-1/2}\left\{\Psi_1(q,t;\lambda(t))\exp\left[-\mathrm{i}\int_0^t \mathrm{d}s\,\varepsilon_1^{\lambda(s)}\right] + \Psi_2(q,t;\lambda(t))\exp\left[-\mathrm{i}\int_0^t \mathrm{d}s\,\varepsilon_2^{\lambda(s)}\right]\right\}, \tag{200}$$

with the relative phase acquiring after a complete duration $\mathscr{T}_{\mathrm{p}}$ of a pulse the value

$$\Delta_{\mathrm{T}}(\mathscr{T}_{\mathrm{p}}) = \int_0^{\mathscr{T}_{\mathrm{p}}} \mathrm{d}s(\varepsilon_2^{\lambda(s)} - \varepsilon_1^{\lambda(s)})\,. \tag{201}$$

If the conditions are such that

$$\Delta_{\mathrm{T}}(\mathscr{T}_{\mathrm{p}}) = (2n+1)\pi, \quad n = 0, \pm 1, \pm 2, \ldots \tag{202}$$

the initial localized wave function has, up to an irrelevant overall phase factor, evolved into a localized wave function in the neighboring well. Thus, the pulse has forced the particle to tunnel in time $\mathscr{T}_{\mathrm{p}}$ through the barrier. The advantageous feature of strong laser-pulse driving is now that the quasienergy difference $\varepsilon_2^{\lambda} - \varepsilon_1^{\lambda}$ may become much larger than the original tunnel splitting $\Delta_0 = E_2 - E_1$; thus, the actual tunneling time τ_{T}, which now is defined by $\pi = \Delta_{\mathrm{T}}(\tau_{\mathrm{T}})$, can assume values much *shorter* than the bare tunneling time τ_0 in Eq. (198). The viability of this mechanism has been demonstrated with Ref. [153], wherein the time-dependent Schrödinger equation corresponding to Eq. (196) was solved numerically with $\lambda(t)$ conveniently chosen as

$$\lambda(t) = \lambda_{\max}\sin^2(\pi t/\mathscr{T}_{\mathrm{p}}), \quad 0 \le t \le \mathscr{T}_{\mathrm{p}}\,. \tag{203}$$

The results are depicted in Fig. 12. The manipulation of the relative phase between the two adiabatically moving components of the wave function results in speeding up the tunneling time τ_{T} by orders of magnitude, e.g. $\tau_{\mathrm{T}} \simeq 10^{-2}\tau_0$ in the calculation in Fig. 12. Intuitively, this speed-up effect is rooted in the large differences of quasienergies with the corresponding Floquet states acquiring admixtures from excited states that are located closer to the barrier top and, therefore, these tunnel faster. It surely would be of interest to measure this tunneling acceleration with suitably engineered semiconductor double-quantum well structures, or in laser-assisted tunneling of proton transfer in molecules.

7.2. Chaos-assisted driven tunneling

A periodically driven nonlinear classical dynamics generally exhibits chaos [154,155]. Clearly, the archetype system of a periodically driven, symmetric double well in Eqs. (172)–(175) is an ideal candidate to study the interplay between nonlinear tunneling quantum dynamics and classical Hamiltonian chaos. The parameter that controls the semiclassical limit is the scaled barrier height

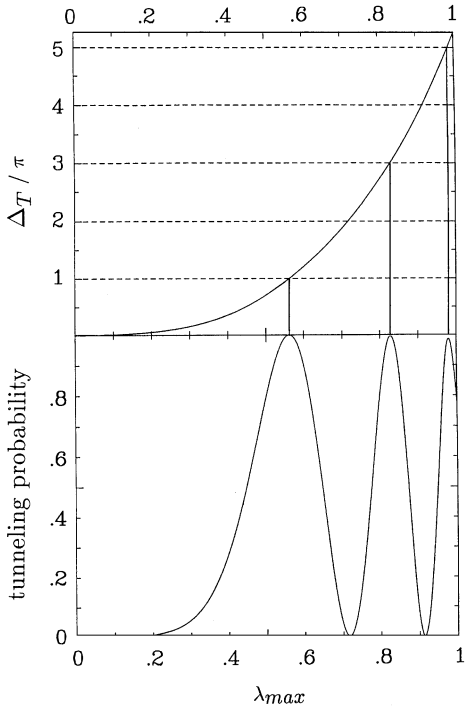

Fig. 12. Pulse-shaped controlled tunneling in the symmetric double well, Eq. (196), with dimensionless parameters $D = 2.5$, $\tau_0 = 49766\ \mathscr{T}$, $\mathscr{T} = 2\pi/\Omega$, and $\Omega = 1.5$, and with $\tau_0 = \pi/(E_2 - E_1)$ the tunneling time. The pulse function $\lambda(t) = \lambda_{\max} \sin^2(\pi t/\mathscr{T}_p)$ with $\mathscr{T}_p = 500\mathscr{T}$ is used. The upper-half depicts the tunneling phase functional $\Delta_T(\mathscr{T}_p)/\pi$ vs. the maximal amplitude $\lambda_{\max}$. For the maximal amplitudes $\lambda_{\max}$ satisfying the condition in Eq. (202), note the vertical lines in the upper panel, a complete transfer of localization from "left" to "right" occurs, i.e., $\Psi(q, t = 0) = \varphi_L \to \Psi(q, t = \mathscr{T}_p) = \varphi_R$. The lower half depicts the tunneling probability, $|\langle \varphi_R | \Psi(\mathscr{T}_p) \rangle|^2$, vs. $\lambda_{\max}$, as calculated numerically from the time-dependent Schrödinger equation for the Hamiltonian (196). The agreement with the prediction from the adiabatic Floquet principle is remarkable.

$D = E_B/\hbar\omega_0$. While the phenomenon of coherent destruction of tunneling in a double well is controlled by the dynamics in the deep quantum regime with D small, the semiclassical limit amounts to letting $D \to \infty$. In the latter case the number of doublets below the barrier becomes very large. The idea that chaotic layers separating symmetry-related regular regions can give rise to quantal tunneling is known as dynamical tunneling [156]. The fingerprints of dynamical tunneling in the spectrum has been discussed by Bohigas et al. [157–160]. These works on chaos-assisted tunneling were based on *time-independent* two-dimensional nonlinear oscillator systems. Moreover, tunneling through dynamical barriers has been studied with forced nonlinear oscillator systems [161–163].

The effect of a chaos-assisted increase of the tunneling rate in a *driven* double well was first pointed out by Lin and Ballentine [164,165], and by Plata and Gomez-Llorente [166]. By monitoring the Husimi distributions [167,168] of the wave functions, these authors showed that for certain values of the driving parameters for the Hamiltonian in Eq. (172) the rate of tunneling can be enhanced by orders of magnitudes. This enhancement phenomenon should not be confused with

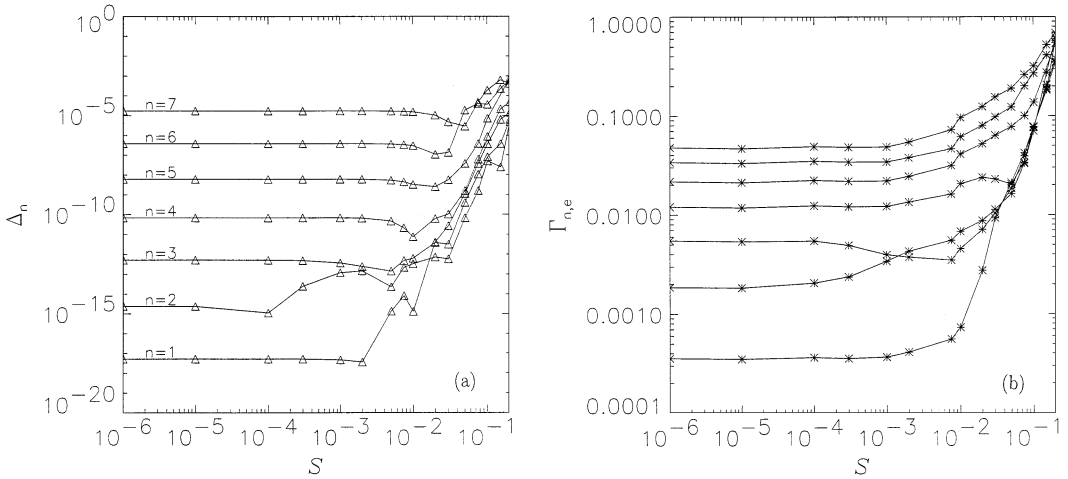

Fig. 13. Chaos-assisted driven tunneling: (a) Tunneling splittings $\Delta_n = |\varepsilon_{n,e} - \varepsilon_{n,0}|$ of associated (even and odd) pairs of quasienergies in a driven, symmetric double well, see Eqs. (172)–(174) vs. driving strength S of the periodic driving $-qS\cos(\Omega t)$. (b) Corresponding overlaps $\Gamma_n = \frac{1}{\mathcal{T}}\int_0^{\mathcal{T}} dt \int_\Lambda dp\, dq\, h_{n,e}(q,p,t)$ of the corresponding Husimi representation $h_{n,e}$ for the Floquet state $\Psi_{n,e}$ with the chaotic layer Λ around the separatrix vs. driving strength S. The dimensionless parameter values are $D = 8$ and $\Omega = 0.95$.

the pulse-shaped enhancement discussed in Section 7.1; the latter is controlled by the (adiabatic) lowest two quasienergy states in the deep quantum regime, the former is related to the interplay between different topologies of phase space in the strongly driven system near the classical limit with $D \gg 1$.

The interplay between regular and chaotic regions in driven tunneling has been investigated in terms of the Floquet spectrum by Utermann et al. [169,170]. The underlying scenario for chaos-assisted driven tunneling is as follows.

For not too strong driving, the classical phase space of this system is characterized by a pair of symmetry-related regular regions near the minima of the unperturbed potential, embedded in a chaotic layer along the unperturbed separatrix. Quantal quasienergy states localized in the regular regions form tunnel doublets with exponentially small splittings. These doublets do break up, and their splittings will reach values of the order of the mean level spacing, as soon as the associated pair of quantizing tori dissolves in the chaotic layer. Therefore, the tunnel splittings depend strongly on the nature of regular vs. chaotic phase space regions to which the corresponding pair of Floquet states predominantly belongs. These ideas have been tested by studying the break-up of tunnel splittings Δ_n versus the driving amplitude S, and comparing the behavior with the measure of overlap $\Gamma_{n,e}$ of the Husimi representation of associated (even) Floquet state with the chaotic region in the vicinity of the separatrix; for further details we refer to [169,170].

Fig. 13, which depicts these measures as a function of driving strength S, shows a striking qualitative agreement between the functional dependences of the splittings Δ_n and the corresponding overlaps Γ_n of its corresponding Husimi representation with the chaotic layer. Both quantities exhibit a transition to steep exponential growth as the chaotic sea (not shown) along the separatrix spreads at the expense of regular regions around the potential minima.

7.3. Even harmonic generation in driven double wells

As Bavli et al. [27–29] have shown, the phenomenon of coherent destruction of tunneling for electrons in a quantum double well implies striking new features when related spectroscopic quantities are investigated. By studying the dipole moment $\mu(t)$ that is *dynamically* induced by the action of the laser driving field, one encounters new phenomena such as anomalous even-harmonic-generation (EHG), and a novel low-frequency radiation generation (LFG). These phenomena are a priori rather surprising: The double well of the type in Eq. (172) in which the electron is moving is *symmetric*, i.e., the undriven Hamiltonian is invariant with respect to a parity transformation of the electron position q. Perturbation theory to all orders consequently implies that such a system *cannot* produce even harmonics. We note, however, that the violation of this selection rule takes place precisely at the same points in the parameter space $\{S, \Omega\}$ where the necessary (but not sufficient) condition for CDT occurs, i.e., exact crossings between associated pairs of quasienergies of opposite generalized parity symmetry P, cf. Eq. (177).

The new phenomena can be best understood in terms of the spectral properties of quasienergies. In terms of the time-dependent wave function $\Psi(q,t)$ of the time-dependent Schrödinger equation, i.e.,[2]

$$\Psi(q,t) = \sum_{\alpha} A_{\alpha} \exp(-\mathrm{i}\varepsilon_{\alpha} t/\hbar) \Phi_{\alpha}(q,t)\,, \tag{204}$$

and expanding the periodic Floquet mode $\Phi_{\alpha}(q,t) = \Phi_{\alpha}(q, t+\mathscr{T})$ into Fourier series, i.e.,

$$\Psi(q,t) = \sum_{\alpha} A_{\alpha} \exp(-\mathrm{i}\varepsilon_{\alpha} t/\hbar) \sum_{n=-\infty}^{\infty} \exp(-\mathrm{i}n\Omega t) c_n(q;\alpha)\,, \tag{205}$$

we find for the time-dependent dipole moment

$$\mu(t) = \langle \Psi(t)|q|\Psi(t)\rangle \tag{206}$$

the spectral Floquet representation

$$\mu(t) = \sum_{\alpha}\sum_{\beta} A_{\alpha}^{*} A_{\beta} \exp[\mathrm{i}(\varepsilon_{\alpha} - \varepsilon_{\beta})t/\hbar] \sum_{n=-\infty}^{\infty} \sum_{m=-\infty}^{\infty} \exp[\mathrm{i}(n-m)\Omega t] \int_{-\infty}^{\infty} \mathrm{d}q\, c_n^{*}(q;\alpha) q c_m(q;\beta)\,. \tag{207}$$

The generalized parity $P: q \to -q; t \to t + \mathscr{T}/2$, cf. Eq. (177), implies even or odd generalized parity $P(\alpha) = \pm 1$ for the Floquet modes $\Phi_{\alpha}(q, t+\mathscr{T}/2) = \pm \Phi_{\alpha}(q,t)$. In particular, one finds that the integral in Eq. (207) vanishes, i.e.,

$$\int_{-\infty}^{\infty} \mathrm{d}q\, c_n^{*}(q;\alpha) q c_m(q;\beta) = 0\,, \tag{208}$$

if $P(\alpha) = P(\beta)$ and $n-m$ is even, or $P(\alpha) \neq P(\beta)$ and $n-m$ is odd.

[2] If the drive has a constant amplitude, i.e., a pure periodic driving field, the coefficients A_{α} are independent of time. If the system is driven by a semi-infinite pulse, the coefficients A_{α} become dependent on time, i.e., $A_{\alpha} \to A_{\alpha}(t)$, but become again independent of time when the transients excited by turning on the pulse quiet down.

These selection rules describe all of the novel spectroscopic features discussed in Ref. [27]. There, Bavli and Metiu have shown that EHG appears and LFG disappears when two quasienergies become degenerate. Moreover, the selection rules explain why one cannot detect pure even harmonics when the quasienergies do not exhibit exact crossings, and that one observes for an initially localized state with $P(\alpha) \neq P(\beta)$ no shifted odd harmonics regardless of angular driving frequency Ω and driving strength S. In somewhat greater detail we observe that the frequencies $\omega(\alpha, \beta; n - m)$ occurring in the spectrum of $\mu(t)$ have the form

$$\hbar\omega(\alpha, \beta; n - m) = \varepsilon_\alpha(\Omega, S) - \varepsilon_\beta(\Omega, S) + (n - m)\hbar\Omega \,. \tag{209}$$

Therefore, we can characterize the spectrum according to four types:

1. The static dipole component corresponds to $\alpha = \beta$ and $n = m$, and is independent of time. For a symmetric system this term is always *zero*, except when $n = m$ and $P(\alpha) \neq P(\beta)$ with $\varepsilon_\alpha(\Omega, s) = \varepsilon_\beta(\Omega, S)$, i.e., at the exact crossing points that rule CDT. The dynamic localization yielding CDT thus generates also a nontrivial dynamically induced static dipole moment!
2. Purely harmonic terms correspond to $\alpha = \beta$ and $n \neq m$. For a symmetric double well *no* terms with $(n - m)$ even appear, hence – away from points of accidental degeneracy – no even harmonics are present in the spectrum.
3. Shifted harmonic terms correspond to $\alpha \neq \beta$ and $n \neq m$, and a progression of doublets occur at $\hbar\omega(\alpha, \beta; n - m) = (n - m)\hbar\Omega \pm [\varepsilon_\alpha(\Omega, S) - \varepsilon_\beta(\Omega, S)]$. If $P(\alpha) = P(\beta)$, then no shifted *even* harmonics occur; if $P(\alpha) \neq P(\beta)$, then no shifted *odd* harmonics occur.
4. Finally, the fourth type occurs for $\alpha \neq \beta$ and $n = m$. They oscillate with frequency $\omega(\alpha, \beta; 0) = [\varepsilon_\alpha(\Omega, S) - \varepsilon_\beta(\Omega, S)]/\hbar$ and are termed "bandhead" terms by Bavli and Metiu.

As already mentioned, the spectrum changes as two Floquet states α and β possessing a *different* generalized parity $P(\alpha) \neq P(\beta)$ approach each other, and become degenerate. Then, the frequency of a "bandhead" term is becoming smaller, and eventually approaches zero. This is the effect of LFG, which in turn provides the generation of a *nonzero static dipole*. Moreover, the two shifted harmonics having the frequencies $\omega(\alpha, \beta; 2n) = 2n\Omega \pm [\varepsilon_\alpha(\Omega, S) - \varepsilon_\beta(\Omega, S)]/\hbar$ *collapse* at the point of degeneracy $\varepsilon_\alpha = \varepsilon_\beta$ with $P(\alpha) \neq P(\beta)$. In this limit, one observes a progression of (doubly degenerate) even harmonics of frequency $2n\Omega$; hence, EHG. The dependence of the spectral weights on the choice of initial condition, i.e., optical $\mu(t = 0) = 0$, versus tunneling initial conditions, i.e., $\mu(t = 0) = 1$, have been investigated in Ref. [28]. As mentioned at the beginning of this section, tunneling initial conditions can be realized with a semi-infinite laser pulse [27,152]. Compared to optical initial conditions, i.e., preparation in the ground state, localized initial conditions are more difficult to realize, but preparation of such coherent states has been recently achieved experimentally [171,172]. As demonstrated by Dakhnovskii and Bavli [28], a considerable amount of LFG, but only weak EHG, can be obtained for excitation from the ground state.

For a discussion of the possibility to observe these effects experimentally we refer to the literature [27]. They are not easy to detect, due to various dephasing effects. Good candidates to observe these phenomena of EHG and LFG are quantum double-well heterostructures and optical systems. Alternatively, generation of strong higher-order harmonics has been predicted for *short* laser pulse driven diatomic molecular ions [173,174].

7.4. General spin systems driven by circularly polarized radiation fields

The fact that the time evolution of a TLS in a circularly polarized field can be factorized in terms of a time-independent Hamiltonian in Eq. (111) is surprising. We note that this factorization involves a rotation around the z-axis, i.e., $|a(t)\rangle \rightarrow |b(t)\rangle = \exp(-\mathrm{i}S_z\Omega t/\hbar)|a(t)\rangle$. This feature can be generalized to any higher-dimensional system, such as a magnetic system or a general quantum system that can be brought into the structure which, in a representation where J_z is diagonal, is of the form

$$H(t) = H_0(J^2) + H_1(J_z) - \hat{\varepsilon}[J_x \cos(\Omega t) - J_y \sin(\Omega t)] \,. \tag{210}$$

Here, $H_0(J^2)$ contains all interactions that are rotationally invariant (Coulomb interactions, spin–spin and spin–orbit interactions). If we now define $R(t) := \exp(-\mathrm{i}J_z\Omega t/\hbar)$ and observe that

$$\begin{aligned} R(t)J_xR(t)^{-1} &= J_x \cos\Omega t + J_y \sin\Omega t \,, \\ R(t)J_yR(t)^{-1} &= -J_x \sin\Omega t + J_y \cos\Omega t \,, \\ R(t)J_zR(t)^{-1} &= J_z \,, \end{aligned} \tag{211}$$

we find upon substituting Eq. (211) into Eq. (210)[3]

$$\tilde{H}(t) \equiv R(t)H(t)R^{-1}(t) = H_0(J^2) + H_1(J_z) - \hat{\varepsilon}J_x \,. \tag{212}$$

Hence, the transformed Hamiltonian becomes independent of time. With the propagator obeying

$$\frac{\partial}{\partial t}U(t,t_0) = -\frac{\mathrm{i}}{\hbar}H(t)U(t,t_0) = -\frac{\mathrm{i}}{\hbar}R^{-1}(t)\tilde{H}R(t)U(t,t_0) \,,$$

we find from

$$\frac{\partial}{\partial t}[R(t)U(t,t_0)R^{-1}(t_0)] = -\frac{\mathrm{i}}{\hbar}\hat{H}[R(t)U(t,t_0)R^{-1}(t_0)] \,, \tag{213}$$

where

$$\hat{H} = \tilde{H} + \Omega J_z = H_0 + H_1(J_z) - \hat{\varepsilon}J_x + \Omega J_z \,, \tag{214}$$

that the propagator factorizes into the form

$$U(t,t_0) = \exp\left(\frac{\mathrm{i}}{\hbar}J_z\Omega t\right)\exp\left(-\frac{\mathrm{i}}{\hbar}\hat{H}(t-t_0)\right)\exp\left(-\frac{\mathrm{i}}{\hbar}J_z\Omega t_0\right). \tag{215}$$

---

[3] Such a factorization method equally well applies to rotationally invariant Hamiltonians H_0 which are subject to externally applied, monochromatic, spatially homogeneous, circularly polarized *electric* fields $\mathscr{E}(t) = -(\mathrm{d}/\mathrm{d}t)\boldsymbol{A}(t)$, with $\boldsymbol{A}(t) = \Omega^{-1}(\mathscr{E}_0 \cos(\Omega t), \mathscr{E}_0 \sin(\Omega t), 0)$. Then the interaction with the field transforms into $R(t)[\boldsymbol{p} - Q\boldsymbol{A}(t)]^2R^{-1}(t) = [\boldsymbol{p} - Q\tilde{\boldsymbol{A}}]^2$, with $\tilde{\boldsymbol{A}} = \Omega^{-1}(\mathscr{E}_0, 0, 0)$, and Q being the charge.

Because $\exp(iJ_z\Omega t/\hbar)$ at times $t = 2\pi/\Omega$ equals 1 for integer values of the angular momentum and -1, for half-integer values, respectively, the propagator in Eq. (215) can be recast into the Floquet form in Eq. (36), i.e.,

$$U(t + n\mathscr{T}, 0) = U(t, 0)[U(\mathscr{T}, 0)]^n . \tag{216}$$

With $J_z = \pm 1, \pm 2, \ldots$, the Floquet form, cf. Eq. (35), is achieved already with Eq. (215). For half-integer spin the corresponding Floquet form is obtained by setting for the propagator

$$U(t, t_0) = \exp\left(\frac{i}{\hbar}\left(J_z + \frac{\hbar}{2}\right)\Omega t\right)\exp\left(-\frac{i}{\hbar}\left(\hat{H} + \frac{\hbar}{2}\Omega\right)(t - t_0)\right)\exp\left(-\frac{i}{\hbar}\left(J_z + \frac{\hbar}{2}\right)\Omega t_0\right), \tag{217}$$

since the first and third contribution are now periodic with period $\mathscr{T}$. Given the eigenvalues $\{\hat{\varepsilon}_\alpha\}$ of $\hat{H}$, the exact quasienergies are given by the relation

$$\varepsilon_\alpha = (\hat{\varepsilon}_\alpha + \hbar\Omega/2) \bmod \hbar\Omega . \tag{218}$$

The general results derived here carry a great potential for applications involving time-dependent tunneling of spin in magnetic systems with anisotropy, and strongly driven molecular and quantum optical systems as well.

7.4.1. Tunneling of giant spins in ac-fields

In recent years, macroscopic tunneling of magnetization has been the subject of intense research [175,176]. More recently, the problem of tunneling of a giant spin with spin quantum number $J \gg 1$ under periodic magnetic field perturbation has attracted interest in connection with the behavior of macroscopic magnetic moments in an anisotropic field [177,178]. Introducing a WKB-analysis for semiclassical-driven quantum systems, these authors assess that, as a rule, tunneling of spin is generally hampered rather than accelerated. One particular driven anisotropic spin system is given by the Hamiltonian

$$H = -\gamma J_z^2 - \hat{\varepsilon}[J_x \cos(\Omega t) + J_y \sin(\Omega t)] , \tag{219}$$

which is of the circularly polarized type considered in Eq. (210). The anisotropy, which produces the "energy barrier", is given by the term $-\gamma J_z^2$. For $\Omega = 0$, the ground-state splitting results as [179]

$$\hbar\Delta_0 = \hat{\varepsilon}\left(\frac{\hat{\varepsilon}}{\hbar\gamma J}\right)^{2J-1}, \quad J \gg 1 . \tag{220}$$

Tunneling of giant spin is shown to occur at frequencies $\Omega = \hbar\gamma, 2\hbar\gamma, \ldots, J\hbar\gamma$, with blocking of tunneling occurring in between. In particular, for Ω obeying [178]

$$(2\hat{\varepsilon}/e\hbar\gamma J)^{4J} \ll 2\Omega/\hbar\gamma \ll 1, \quad J \gg 1 , \tag{221}$$

where e denotes the basis of the natural logarithm, coherent tunneling is hampered. We note that, by expressing (221) in terms of the energy splitting (220), this condition implies high-frequency driving $\Omega \gg \Delta_0$, with no conclusions being made about the behavior in the adiabatic regime.

8. Driven dissipative tunneling

Up to this point in our review we have investigated the effects of driving on a quantum system with few degrees of freedom, under the hypothesis that this system could be considered as isolated from its surroundings. This idealization often fails to describe thermal and dynamical properties of real physical or chemical systems when the quantum system is in mutual contact with a thermal reservoir. In this case, the system has to be considered as an open system. The coupling with a heat bath causes damping of the quantum system and no longer is the dynamics predicted by the Schrödinger equation [30–35]. In the following, we shall be interested in the investigation of the dynamical behavior of a "small" quantum system in contact with a heat bath, and that additionally is subject to an external, generally time-dependent force. We start the discussion of dissipative-driven tunneling by presenting first the basic methodology used to describe quantum dissipation. In the following section we discuss a Floquet–Markov–Born approximation to the dynamics which can be applied to highly nonlinear systems under the assumption of *weak coupling* between the system and the reservoir, and whenever the external driving field is periodic. An application of this method is considered in Section 14.2, where driven tunneling in a dissipative double-well potential is discussed. In Section 10, we shall present the real-time path integral technique, which allows to treat the dissipative influence systematically. In particular, for a harmonic thermal bath, the bath degrees of freedom can be eliminated exactly. We shall apply this method to investigate driven tunneling in dissipative tight-binding systems in Sections 11–13, and the extended double-well system in Section 14.3. A comparison between the path integral results and those of other methods will also be discussed.

8.1. The harmonic thermal reservoir

A great number of methods and techniques have been developed to investigate the thermodynamics and dynamics of open quantum systems in the absence of driving. A basic approach is to regard the system and reservoir as constituting a conservative many-body system. In this picture, dissipation comes into play because of energy transfer between the small system and the large environment. Once the energy is deposited into the environment, it is not returning within any finite time scale of physical relevance (infinite Poincaré recurrence time). If the equations of motion for the closed system are *linear* in the bath coordinates, the latter can be eliminated exactly and one obtains closed equations for the damped system alone. This restriction on linearity assumes that any bath degree of freedom is sufficiently weakly perturbed by the coupling with the small system [30–35]. This is a physically reasonable assumption when the reservoir is macroscopic. It is important to notice that this does not necessarily imply that the dissipative influence of the environment on the small system is weak, because the number of bath degrees of freedom which couple to the small system is very large. For a more detailed and complete description we refer to books, reviews and articles such as, for example, Refs. [32–35]. Here, we generalize these concepts to include the effects of *time-dependent driving*.

A general form of the Hamiltonian of the driven system-plus-reservoir complex which satisfies the requirement of a linear coupling of the bath degrees of freedom to the system degree of freedom is given by

$$H(t) = H_0 + H_B + H_{SB} + H_{ext}(t)\,, \tag{222}$$

where H_0 is the Hamiltonian of the isolated, generally nonlinear system,

$$H_0 = p^2/2m + V_0(q)\,. \tag{223}$$

Here we restrict ourselves to a one-dimensional system coordinate q. A generalization of the formalism to higher-dimensional cases is straightforward. The terms $H_B + H_{SB}$ describe the reservoir as a set of N harmonic oscillators linearly coupled in the bath coordinates x_i to the system via the interaction term H_{SB}. That is,

$$H_B + H_{SB} = \frac{1}{2}\sum_{i=1}^{N}\left[\frac{p_i^2}{m_i} + m_i\omega_i^2\left(x_i - \frac{c_i}{m_i\omega_i^2}F(q)\right)^2\right]. \tag{224}$$

Here, the term $F^2(q)\sum_i c_i^2/2m_i\omega_i^2$ has been introduced to avoid renormalization effects of the potential $V_0(q)$ induced by coupling to the reservoir. The generally nonlinear function $F(q)$ describes a nonlinear system-bath coupling. Finally,

$$H_{ext}(t) = -\mathscr{S}(q)\mathscr{E}(t) \tag{225}$$

describes the interaction of the quantum system with an external force. For the sake of simplicity, we shall further restrict our discussion to the case that the dissipation mechanism is strictly linear in q, that is, $F(q) = q$, which describes a bi-linear system-bath coupling. Defining next $V_1(q,t) = V_0(q) - \mathscr{S}(q)\mathscr{E}(t)$, we find

$$H(t) = \frac{p^2}{2m} + V_1(q,t) + \frac{1}{2}\sum_{i=1}^{N}\left[\frac{p_i^2}{m_i} + m_i\omega_i^2\left(x_i - \frac{c_i}{m_i\omega_i^2}q\right)^2\right]. \tag{226}$$

Without driving, this Hamiltonian has been used to investigate quantum dissipation since the late 1950s [30,33–35,180–184]. In particular, Magalinskij [180] pioneered (see also [182,184]), the so-termed "quantum Langevin equation" for the coordinate *operator* q, by starting from the full system-plus-bath Hamiltonian. Generalized to our time-dependent Hamiltonian this Heisenberg operator equation for the coordinate operator q takes the form

$$m\frac{\mathrm{d}^2q(t)}{\mathrm{d}t^2} + m\int_{t_0}^{t}\mathrm{d}t'\gamma(t-t')\frac{\mathrm{d}q(t')}{\mathrm{d}t'} + \frac{\partial V_1(q,t)}{\partial q} = \zeta(t) - m\gamma(t-t_0)q(t_0)\,, \tag{227}$$

where t_0 denotes the time of initial preparation. Note that in the literature (but not here) the initial term $m\gamma(t-t_0)$ is frequently dropped[4] assuming that with time $t_0 \to -\infty$, $\lim_{t_0\to-\infty}\gamma(t-t_0) = 0$. By doing so, however, one neglects transient effects. Here,

$$\zeta(t) = \sum_i\left[c_ix_i(t_0)\cos\left[\omega_i(t-t_0)\right] + \frac{c_i}{m_i\omega_i}p_i(t_0)\sin\left[\omega_i(t-t_0)\right]\right] \tag{228}$$

[4] For a detailed discussion of the use and abuse of (quantum) Langevin equations using the stochastic force $\xi(t) = \zeta(t) - m\gamma(t-t_0)q(t_0)$ we refer to [185].

is a *random force operator* obeying Gaussian statistics, with zero mean $\langle\zeta(t)\rangle_\beta = 0$, and force–force correlation

$$K(t) = \langle\zeta(t)\zeta(0)\rangle_\beta = \frac{\hbar m}{\pi}\int_0^\infty \mathrm{d}\omega\,\omega\tilde{\gamma}'(\omega)[\coth(\hbar\beta\omega/2)\cos(\omega t) - \mathrm{i}\sin(\omega t)]\,. \tag{229}$$

Here, $\beta = 1/k_\mathrm{B}T$ is the inverse temperature. The bracket $\langle\ \rangle_\beta$ indicates the statistical average with respect to the bath Hamiltonian H_B. Moreover, $\tilde{\gamma}'(\omega)$ is the real part of the Fourier transform $\tilde{\gamma}(\omega)$ of the time-dependent damping coefficient $\gamma(t)$ given by

$$\gamma(t-t') = \frac{1}{m_i}\sum_{i=1}^{N}\frac{c_i^2}{m_i\omega_i^2}\cos[\omega_i(t-t')]\,. \tag{230}$$

It is interesting to observe that the result (229) for the force–force correlation function derived for the oscillator model is a general result of the fluctuation-dissipation theorem, and is therefore independent of the microscopic details of the harmonic bath [180]. In the classical limit $\hbar \to 0$ the quantum Langevin equation reduces to the well-known phenomenological Langevin equation with memory-dependent damping, and where the force–force correlator of the classical force $\zeta_\mathrm{cl}(t)$ satisfies $\langle\zeta_\mathrm{cl}(t)\zeta_\mathrm{cl}(t')\rangle_\beta = 2mk_\mathrm{B}T\gamma(|t-t'|)$.

8.2. The reduced density matrix

Starting from the full system-plus-bath Hamiltonian (222), the aim of the following sections will be to evaluate the reduced dynamics of the system described by the reduced density operator $\rho(t) = \mathrm{Tr}_\mathrm{B}\{W(t)\}$, where Tr_B denotes the trace over the bath degrees of freedom of the Hamiltonian (226), and with $W(t)$ being the density operator of the system-plus-reservoir complex. In terms of the density operator at initial time $W(t_0)$ and of the time evolution operator $U(t,t_0) = \top\exp\{-i\int_{t_0}^t \mathrm{d}t'\,H(t')/\hbar\}$, where $\top$ denotes the time-ordering operator, it reads

$$W(t) = U^\dagger(t,t_0)W(t_0)U(t,t_0)\,. \tag{231}$$

In the following it will be convenient to consider an intial condition on $W(t)$ of the Feynman–Vernon type [186], that is, to assume that at the initial time $t = t_0$ the bath is in thermal equilibrium and uncorrelated to the system. Hence, $W(t_0)$ has the form

$$W(t_0) = \rho_S(t_0)W_\mathrm{B}\,, \tag{232}$$

where $W_\mathrm{B} = \exp(-\beta H_\mathrm{B})/\mathrm{Tr}_\mathrm{B}\{\exp(-\beta H_\mathrm{B})\}$ is the canonical density operator of the heat bath, and ρ_S that of the system described by the Hamiltonian $H_\mathrm{S}(t) = H_0 + H_\mathrm{ext}(t)$. The inclusion of more realistic initial preparations goes beyond the scope of this review. We refer to Refs. [34,187] where this generalization is implemented for open systems without driving. Nevertheless, we observe that while the effects of the initial preparation are crucial in the investigation of the transient dynamics of the system, if the total system is ergodic, initial preparation effects will have decayed when the asymptotic dynamics is considered.

8.3. The environmental spectral density

It is convenient at this point to introduce the spectral function $J(\omega)$ [32] of the environmental coupling, i.e.,

$$J(\omega) = \frac{\pi}{2} \sum_{i=1}^{N} \frac{c_i^2}{m_i \omega_i^2} \delta(\omega - \omega_i) \,. \tag{233}$$

Because we aim at the environment to constitute a proper heat bath, we shall consider $J(\omega)$ to be continuous. Hence, the sum in Eqs. (230) and (233) may be replaced by an integral. In doing so one obtains

$$J(\omega) = \omega m \tilde{\gamma}'(\omega) \,. \tag{234}$$

The model described by the Hamiltonian (226) is thus completely fixed by the mass m, the time-dependent potential $V_1(q,t)$ and by the spectral density $J(\omega)$.[5] Moreover, the latter is completely determined by the frequency-dependent damping coefficient $\tilde{\gamma}'(\omega)$ which already appears in the classical equations of motion. Hence, whenever $J(\omega)$ cannot be extracted from microscopical considerations on the composite system, a conventional molecular dynamics simulation may be used to compute $\tilde{\gamma}'(\omega)$, and in turn $J(\omega)$. When the damping coefficient is frequency-independent, i.e., $\tilde{\gamma}(\omega) = \gamma$, the dynamics is memoryless, and the spectral density assumes the Ohmic form

$$J(\omega) = m\gamma\omega \,. \tag{235}$$

This corresponds in the classical case to a Langevin equation with delta-correlated Gaussian random forces (white noise). In reality, any physical spectral density falls off in the limit $\omega \to \infty$. Hence, a cutoff frequency ω_c on the spectral density has to be introduced, which sets the time scale $\tau_c = 1/\omega_c$ for inertia effects in the reservoir. For example, for the Drude-regularized kernel $\gamma(t) = \gamma\omega_c \exp(-\omega_c t)$ the spectral density reads

$$J(\omega) = \frac{m\gamma\omega}{1 + \omega^2/\omega_c^2} \,. \tag{236}$$

This is of the Ohmic form when $\omega \ll \omega_c$. Very often in the literature the case of Ohmic friction with an exponential cutoff is considered. In this case

$$J(\omega) = m\gamma\omega \mathrm{e}^{-\omega/\omega_c} \,. \tag{237}$$

This reasoning can be extended to consider the case of general frequency-dependent damping. That is, it is assumed that the spectral density has a power-law dependence on the frequency for frequencies less than a characteristic cutoff frequency ω_c. Introducing a cutoff function $f(\omega, \omega_c)$, the spectral density then has the form

$$J(\omega) \propto \gamma_s \omega^s f(\omega, \omega_c), \quad f(\omega, \omega_c) \to 0 \quad \text{if } \omega \gg \omega_c \,, \tag{238}$$

[5] This fact, for example, no longer holds true if one considers a *different* system-bath coupling, such as a coupling to a bath composed of two-level systems.

where $s > 0$. As already discussed, the case $s = 1$ describes Ohmic damping. The cases $0 < s < 1$, and $s > 1$, are known as sub-Ohmic and super-Ohmic, respectively. The case of Ohmic friction is important, e.g., for charged interstitials in metals or in Josephson systems. On the other hand, super-Ohmic dissipation with $s = 3$ or $s = 5$ (depending on the properties of the strain field) describes the low-temperature dynamics of a phonon bath in the bulk [34].

It is clear that the assumption of Eq. (238) may oversimplify the problem for frequencies ω of the order of, or greater than ω_c. Nevertheless, whenever $J(\omega)$ falls off at least as some negative power of ω when $\omega \to \infty$, the effects of the environmental high-frequency modes can be absorbed into a renormalization of the parameters appearing in the Hamiltonian H_S of the system; see [188] for the case of a double-well system.

9. Floquet–Markov approach for weak dissipation

In this section we shall describe the Floquet–Markov–Born approximation to the dynamics, which can be applied to strongly nonlinear systems under the assumption of *weak coupling* between the system and the reservoir, and whenever the external driving field $\mathscr{E}(t)$ is *periodic*, i.e., if

$$\mathscr{E}(t + \mathscr{T}) = \mathscr{E}(t), \quad \mathscr{T} = 2\pi/\Omega\,. \tag{239}$$

This method combines the Markov–Born approach to quantum dissipation (leading to a master equation for the reduced density operator) with the Floquet formalism, cf. Section 2, that allows to treat time-periodic forces of arbitrary frequency and strength. While the Floquet formalism amounts to using an optimal representation and is exact, the simplification brought by the Markov–Born approximation is achieved at the expense of the regime of validity of the method. The Markov–Born approximation, in fact, restricts the application of the master equation for the reduced density operator to weakly damped systems for which the dissipative relaxation times are large compared to the relevant time scales of the isolated system, and also to the thermal time scale $\hbar\beta$. For example, for Ohmic damping, the Markov–Born approximation requires that the conditions $\hbar\gamma \ll k_B T$, and $\gamma \ll \Delta_{\alpha,\nu}$ are satisfied, where $\Delta_{\alpha,\nu}$ are the transition frequencies of the central system, see Eq. (247) below. A subtle point is that the results so obtained depend on whether the Markovian approximation is made with respect to the eigenenergy spectrum of the small quantum system *without* driving, or with respect to the quasienergy Floquet spectrum of the small quantum system in the *presence* of driving [189], that is, the two procedures do not commute. Here we shall report on the results of a Markovian description of the dynamics based on a quasienergy spectrum. This method has recently been applied to the parametrically driven harmonic oscillator [190], and to the dissipative tunneling of a particle in a driven bistable potential [191,192]. The latter case is discussed in Section 14.2.

9.1. Generalized master equation for the reduced density operator

The starting point of this method is the equation of motion for the reduced density operator $\rho(t) = \mathrm{Tr}_B\{W(t)\}$ (where Tr_B denotes the trace over the bath degrees of freedom of the Hamiltonian (222)), as it can be derived from the Liouville–von Neumann equation

$$\dot{W}(t) = -(\mathrm{i}/\hbar)[H(t), W(t)] \tag{240}$$

for the full density operator $W(t)$ of system-plus-reservoir. For simplicity, we assume that at the initial time $t = t_0$ the bath is in thermal equilibrium and is uncorrelated with the system, cf. (232). Under the hypothesis of a *weak* coupling to the reservoir, a transformation into the interaction picture allows a weak coupling expansion with respect to the interaction Hamiltonian H_{SB}. Tracing out the bath degrees of freedom, and by making a Markovian approximation by assuming that the autocorrelations of the bath decay on a time scale $\hbar/k_B T$ much shorter than the time scale $1/\gamma$ of the system correlations, one arrives at equations of motion for the reduced density matrix. They have the form [193–195]

$$\dot{\rho}(t) = -\frac{\mathrm{i}}{\hbar}[H_S(t), \rho(t)] - \frac{1}{\hbar^2}\int_0^\infty \mathrm{d}\tau\{K'(\tau)[q, [\tilde{q}(t-\tau, t), \rho(t)]] - \mathrm{i}K''(\tau)[q, [\tilde{q}(t-\tau, t), \rho(t)]_+]\}\,, \tag{241}$$

where $K'(\tau)$ and $K''(\tau)$ are the real and imaginary parts, respectively, of the force–force correlation function $K(\tau)$ in Eq. (229). Here, $[A, B]_+ = AB + BA$ is the anticommutator, while the tilde denotes the interaction picture defined by

$$\tilde{A}(t, t') = U_0^\dagger(t, t') A U_0(t, t')\,, \tag{242}$$

$$U_0(t, t') = \top \exp\left(-\frac{\mathrm{i}}{\hbar}\int_{t'}^{t} \mathrm{d}t''\,(H_S(t'') + H_B)\right), \tag{243}$$

with $\top$ the time-ordering operator.

9.2. *Floquet representation of the generalized master equation*

In Section 2 we saw that for a time-periodic Hamiltonian $H_S(t)$, the Floquet theorem asserts that there exists a complete set of solutions of the form

$$|\Psi_\alpha(t)\rangle = \mathrm{e}^{-\mathrm{i}\varepsilon_\alpha t/\hbar}|\Phi_\alpha(t)\rangle, \quad |\Phi_\alpha(t + \mathscr{T})\rangle = |\Phi_\alpha(t)\rangle\,. \tag{244}$$

The quasienergy ε_α plays the role of a phase and therefore is only defined mod $\hbar\Omega$. We shall apply the Floquet theorem to the Hamiltonian $H_S(t) = H_0 + H_{ext}(t)$, cf. Eq. (222), and use the basis $\{|\Psi_\alpha(t)\rangle\}$ of the undamped system as an optimal representation to decompose states and operators. In particular, the matrix elements $X_{\alpha\beta}(t)$ of the position operator q with the representation of states $|\Psi_\alpha(t)\rangle$ read

$$X_{\alpha\beta}(t) = \mathrm{e}^{\mathrm{i}(\varepsilon_\alpha - \varepsilon_\beta)t/\hbar}\langle\Phi_\alpha(t)|q|\Phi_\beta(t)\rangle = \sum_k \mathrm{e}^{\mathrm{i}\Delta_{\alpha\beta k}t} X_{\alpha\beta k}\,, \tag{245}$$

where

$$X_{\alpha\beta k} = \frac{1}{\mathscr{T}}\int_0^{\mathscr{T}} \mathrm{d}t\,\mathrm{e}^{-\mathrm{i}k\Omega t}\langle\Phi_\alpha(t)|q|\Phi_\beta(t)\rangle\,, \tag{246}$$

and where the transition energies are given by

$$\hbar \Delta_{\alpha\beta k} = \varepsilon_\alpha - \varepsilon_\beta + k\hbar\Omega \,. \tag{247}$$

The fact that the Floquet states $|\Psi_\alpha(t)\rangle$ solve the Schrödinger equation allows for a formal simplification of the master equation (241). Representing the density operator in this basis, i.e.,

$$\rho_{\alpha\beta}(t) = \langle \Psi_\alpha(t)|\rho(t)|\Psi_\beta(t)\rangle \,, \tag{248}$$

the master equation takes the form

$$\begin{aligned}\dot\rho_{\alpha\beta}(t) = {} & \frac{1}{\pi\hbar}\int_0^\infty \mathrm{d}\omega\, J(\omega) n_{\mathrm{th}}(\omega) \int_0^\infty \mathrm{d}\tau\, \mathrm{e}^{\mathrm{i}\omega\tau} \mathscr{R}_{\alpha\beta}(t-\tau,t) \\ & + \frac{1}{\pi\hbar}\int_0^\infty \mathrm{d}\omega\, J(\omega)[1+n_{\mathrm{th}}(\omega)] \int_0^\infty \mathrm{d}\tau\, \mathrm{e}^{-\mathrm{i}\omega\tau} \mathscr{R}_{\alpha\beta}(t-\tau,t) + \mathrm{h.c.}\,,\end{aligned} \tag{249}$$

where $n_{\mathrm{th}}(\omega) = 1/[\exp(\hbar\omega/k_{\mathrm{B}}T) - 1]$ gives the thermal occupation of the bath oscillator with frequency ω, and

$$\mathscr{R}_{\alpha\beta}(t-\tau,t) = \sum_{\alpha'\beta'} \left(X_{\alpha\alpha'}(t-\tau)\rho_{\alpha'\beta'}(t)X^*_{\beta\beta'}(t) - X^*_{\alpha'\alpha}(t)X_{\alpha'\beta'}(t-\tau)\rho_{\beta'\beta}(t)\right). \tag{250}$$

Inserting next the identity $\int_0^\infty \mathrm{d}\tau\, \mathrm{e}^{\mathrm{i}\omega\tau} = \pi\delta(\omega) + \mathscr{P}(\mathrm{i}/\omega)$, with $\mathscr{P}$ denoting the principal value, and the Fourier expansion (246) of the matrix elements $X_{\alpha\beta}(t)$, the equation of motion (249) for $\dot\rho_{\alpha\beta}$ can be expressed in terms of the time-independent matrix elements $X_{\alpha\beta k}X^*_{\alpha'\beta'k'}$, multiplied by phase factors $\exp[\mathrm{i}(\Delta_{\alpha\beta k} - \Delta_{\alpha'\beta'k'})t]$.

9.3. Rotating-wave approximation

The resulting equation is still rather complicated so that, frequently, the rotating-wave approximation (RWA) is introduced [189]; cf. also Section 3.2.1. In the RWA it is usually assumed that phase factors $\exp[\mathrm{i}(\Delta_{\alpha\beta k} - \Delta_{\alpha'\beta'k'})t]$ oscillate faster than all other time dependences, and hence can be neglected. This argument applies, however, only to quasienergy spectra that do *not* possess systematic degeneracies or quasidegeneracies. For the case of the parametric harmonic oscillator, for example, which has the peculiarity of equidistant quasienergy levels the condition $(\alpha - \beta, k) = (\alpha' - \beta', k')$ is sufficient to ensure $\Delta_{\alpha\beta k} = \Delta_{\alpha'\beta'k'}$; thus, these terms have to be kept in the RWA [190]. For the driven double well, in the vicinity of the manifold where relevant quasienergy crossings occur, cf. Section 6, the conservative time evolution contains very small energy scales, and correspondingly large time scales. In order to obtain an adequate description for the reduced dynamics one can *only* drop terms with $k \neq k'$ [191,192]. Within the simplest RWA one finds [189]

$$\begin{aligned}\dot\rho_{\alpha\alpha}(t) &= \sum_\nu \left[A_{\alpha\nu}\rho_{\nu\nu}(t) - A_{\nu\alpha}\rho_{\alpha\alpha}(t)\right], \\ \dot\rho_{\alpha\beta}(t) &= -\frac{1}{2}\sum_\nu (A_{\nu\alpha} + A_{\nu\beta})\rho_{\alpha\beta}(t), \quad \alpha \neq \beta \,,\end{aligned} \tag{251}$$

where

$$A_{\alpha\beta} = \sum_{k=-\infty}^{\infty} [\gamma_{\alpha\beta k} + n_{\rm th}(|\Delta_{\alpha\beta k}|)(\gamma_{\alpha\beta k} + \gamma_{\beta\alpha - k})] ,$$
$$\gamma_{\alpha\beta k} = 2\pi\theta(\Delta_{\alpha\beta k}) J(\Delta_{\alpha\beta k}) |X_{\alpha\beta k}|^2 . \tag{252}$$

Hence, within the simplest RWA two decoupled subsets of equations are obtained. One subset describes the approach of the diagonal elements towards a steady state (dissipation), while the other is concerned with the decay of the off-diagonal elements (effect of decoherence). The time-independent coefficients $A_{\alpha\beta}$ contain the specifics of the potential and driving through the quasienergy differences $\Delta_{\alpha\beta k}$, and Floquet modes via $X_{\alpha\beta k}$. The equation for the nondiagonal elements is easily integrated, and predicts exponentially vanishing off-diagonal elements at long times. Hence, the reduced density matrix becomes diagonal in the Floquet basis at long times. These features are a consequence of the RWA, they do not hold true if such an approximation is not performed.

We shall discuss the predictions of Eq. (241) for the case of a particle in a driven double-well potential in greater detail in Section 14.2 below.

10. Real-time path integral approach to driven tunneling

10.1. The influence-functional method

A very useful tool to describe non-equilibrium time-dependent dissipative phenomena is the real-time path integral approach. Within the simple phenomenological model described by the Hamiltonian in Eqs. (224) and (226), it enables to evaluate the trace operation involved in the definition of the reduced density matrix $\rho(t) = {\rm Tr}_{\rm B}\{W(t)\}$ of the relevant system exactly. Here, we shall assume the factorized intial condition (232) for the total density matrix $W(t)$, and refer to [34,187] for the case of more general initial conditions.

As proposed by Feynman and Vernon [186], to carry out the reduction it is convenient to express the reduced density matrix (RDM) in the coordinate representation of the full time evolution operator $U(t, t_0)$. Introducing the N-component vector $\boldsymbol{x}(t_k) := \boldsymbol{x}_k = (x_{k,1}, \ldots, x_{k,N})$ for the bath coordinates at time t_k, and setting $\boldsymbol{x}(t) = \boldsymbol{x}_{\rm f}$, the matrix elements of the RDM at time t read

$$\rho(q_{\rm f}, q'_{\rm f}; t) := \int {\rm d}\boldsymbol{x}_{\rm f} \langle q_{\rm f} \boldsymbol{x}_{\rm f} | W(t) | q'_{\rm f} \boldsymbol{x}_{\rm f} \rangle . \tag{253}$$

Using next the path-integral representation of the time evolution operator in the coordinate representation, $\rho(q_{\rm f}, q'_{\rm f}; t)$ may be expressed in terms of the initial density matrix $\rho(q_{\rm i}, q'_{\rm i}; t_0)$ at the time t_0 as [34,187]

$$\rho(q_{\rm f}, q'_{\rm f}; t) = \int {\rm d}q_{\rm i} \int {\rm d}q'_{\rm i} \mathscr{J}(q_{\rm f}, q'_{\rm f}, t | q_{\rm i}, q'_{\rm i}, t_0) \rho(q_{\rm i}, q'_{\rm i}; t_0) . \tag{254}$$

Here $\mathscr{J}$ is the propagating function of the reduced density which can be expressed as the double path-integral

$$\mathscr{J}(q_{\rm f}, q'_{\rm f}, t|q_{\rm i}, q'_{\rm i}, t_0) = \int \mathscr{D}q \int \mathscr{D}q' \mathscr{A}[q]\mathscr{B}[q]\mathscr{A}^*[q']\mathscr{B}^*[q']\mathscr{F}[q, q'] \,, \tag{255}$$

where the sum is over all real-time paths $q(t')$, $q'(t')$ obeying the constraints $q(t_0) = q_{\rm i}$, $q'(t_0) = q'_{\rm i}$, and $q(t) = q_{\rm f}$, $q'(t) = q'_{\rm f}$. The quantity

$$\mathscr{A}[q] = \exp\left\{\frac{\rm i}{\hbar}\int_{t_0}^{t} {\rm d}t' \left[\frac{1}{2}m\dot{q}^2 - V_0(q)\right]\right\} \tag{256}$$

is the probability amplitude of the quantum system to follow the path $q(t')$ in the absence of external driving and fluctuating forces $\zeta(t)$. The factor

$$\mathscr{B}[q] = \exp\left\{\frac{\rm i}{\hbar}\int_{t_0}^{t} {\rm d}t' \mathscr{E}(t')\mathscr{S}(q(t'))\right\} \tag{257}$$

incorporates the effect of the external driving force, cf. (225), and $\mathscr{F}[q, q']$ is the Feynman–Vernon influence functional which describes the influences of the fluctuating force. For a harmonic bath (Gaussian statistics), it takes the form $\mathscr{F}[q, q'] = \exp\{-\Phi[q, q']/\hbar\}$, with

$$\begin{aligned}\Phi[q, q'] &= {\rm i}(m\gamma(t_0)/2)\int_{t_0}^{t} {\rm d}t' \,(q^2(t') - q'^2(t')) \\ &\quad + \frac{1}{\hbar}\int_{t_0}^{t} {\rm d}t' \int_{t_0}^{t'} {\rm d}t''(q(t') - q'(t'))(K(t' - t'')q(t'') - K^*(t' - t'')q'(t'')) \,,\end{aligned} \tag{258}$$

where $K(t)$ is the force autocorrelation function given in Eq. (229). Finally, $\int \mathscr{D}q$ symbolically means summation in function space over all paths with the end-points $(q_{\rm f}, q'_{\rm f})$ held fixed. Hence, the price to be paid for the exact evaluation of the trace over the bath degrees of freedom is the appearance of a term that is nonlocal in time in the influence functional $\mathscr{F}[q, q']$. The latter couples the same path q or q', as well as the two different paths q, q', at different times. To better illustrate the effect of the influence functional $\mathscr{F}[q, q']$, it is useful to introduce center of mass and relative coordinates, i.e.,

$$\eta(t) = q(t) + q'(t), \qquad \xi(t) = q(t) - q'(t) \,. \tag{259}$$

Here $\eta(t)$ describes propagation along the diagonal of the density matrix, while the path $\xi(t)$ is a measure of how far the system gets off-diagonal while propagating. In terms of these new paths one obtains for $\tilde{\Phi}[\eta, \xi] = \Phi[q, q']$ [34,187],

$$\begin{aligned}\tilde{\Phi}[\eta, \xi] &= \frac{1}{\hbar}\int_{t_0}^{t} {\rm d}t' \int_{t_0}^{t'} {\rm d}t''\xi(t')K'(t' - t'')\xi(t'') \\ &\quad + {\rm i}(m/2)\int_{t_0}^{t} {\rm d}t' \int_{t_0}^{t'} {\rm d}t''\xi(t')\gamma(t' - t'')\dot{\eta}(t'') + {\rm i}(m/2)\eta_0 \int_{t_0}^{t} {\rm d}t' \,\gamma(t')\xi(t') \,,\end{aligned} \tag{260}$$

with $\eta_0 = \eta(t_0)$, and where $K'(t)$ is the real part of the kernel $K(t)$, cf. (229). Equivalently, by performing two partial integrations, the influence functional can be recast in the form

$$\tilde{\Phi}[\eta,\xi] = -\frac{1}{\hbar}\int_{t_0}^{t} \mathrm{d}t' \int_{t_0}^{t'} \mathrm{d}t''[\dot{\xi}(t')L'(t'-t'')\dot{\xi}(t'') + \mathrm{i}\dot{\xi}(t')L''(t'-t'')\dot{\eta}(t'')]$$
$$+ \xi(t)\int_{t_0}^{t} \mathrm{d}t''[L'(t-t'')\dot{\xi}(t'') + \mathrm{i}L''(t-t'')\dot{\eta}(t'')] + \mathrm{i}\eta_0\left[\xi(t)L''(t) - \int_{t_0}^{t} \mathrm{d}t'\xi(t')L''(t')\right], \tag{261}$$

with $L'(t)$ and $L''(t)$ being the real and imaginary parts of

$$L(t) = \frac{1}{\hbar\pi}\int_0^\infty \mathrm{d}\omega\, \frac{J(\omega)}{\omega^2}\, \frac{\cosh(\hbar\omega\beta/2) - \cosh[\omega(\hbar\beta/2 - \mathrm{i}t)]}{\sinh(\hbar\omega\beta/2)}, \tag{262}$$

respectively.

Using this method an exact analytical solution has been discussed for the driven, dissipative parametric harmonic oscillator [63]. In Sections 11–13 we shall describe an application to the study of tunneling in driven tight-binding systems. In the remainder of this section, instead, we shall briefly discuss a numerical methodology to discretize the full Feynman propagator. Using this method some results on the driven two-level-system and on the driven double-well system are discussed below in Sections 12 and 14.3, respectively.

10.2. Numerical techniques: The quasiadiabatic propagator method

The quasiadiabatic propagator path-integral method (QUAPI) [196–198] allows efficient real-time path-integral calculations that may even span long time intervals. In the QUAPI, an appropriate partitioning of the propagator leads to a modified path-integral expression which contains the one-dimensional propagator describing the evolution of the uncoupled system along bare paths, and a nonlocal influence functional that includes multidimensional corrections to the bare paths. To achieve this, one divides the total time into M small time intervals $\Delta t = (t - t_0)/M$. Denoting now $H_0 + H_{\mathrm{ext}}(t) = H_{\mathrm{S}}(t)$, and the bath contribution $H_{\mathrm{B}} + H_{\mathrm{SB}}$ of the N harmonic oscillators in Eq. (226) as

$$H_{\mathrm{B}} + H_{\mathrm{SB}} = H_{\mathrm{R}} := \sum_{j=1}^{N} H_{\mathrm{R}}^{(j)}(q), \tag{263}$$

the propagator between time $t_k = k\Delta t$ and $t_{k+1} = t_k + \Delta t$ is split symmetrically as

$$U(t_{k+1}, t_k) = \top \mathrm{e}^{-\mathrm{i}/\hbar\int_{t_k}^{t_{k+1}} \mathrm{d}t' H(t')} = \top \mathrm{e}^{-\mathrm{i}/\hbar[H_{\mathrm{R}}\Delta t + \int_{t_k}^{t_{k+1}} \mathrm{d}t' H_{\mathrm{S}}(t')]}$$
$$\approx \mathrm{e}^{-\mathrm{i}H_{\mathrm{R}}\Delta t/(2\hbar)} U_{\mathrm{S}}(t_{k+1}, t_k) \mathrm{e}^{-\mathrm{i}H_{\mathrm{R}}\Delta t/(2\hbar)}, \tag{264}$$

where

$$U_{\mathrm{S}}(t_{k+1}, t_k) = \top \mathrm{e}^{-\mathrm{i}/\hbar\int_{t_k}^{t_{k+1}} \mathrm{d}t' H_{\mathrm{S}}(t')}. \tag{265}$$

Because the operators H_S and H_R do not commute, the splitting is not exact, and the error is of the order of $[H_R,[H_S,H_R]]\Delta t^3$. The short-time propagator in the position representation between the time t_k and the time t_{k+1} is then given by

$$\langle q_{k+1}\boldsymbol{x}_{k+1}|U(t_{k+1},t_k)|q_k\boldsymbol{x}_k\rangle \approx \langle q_{k+1}|U_S(t_{k+1},t_k)|q_k\rangle \times \prod_{j=1}^{N}\langle x_{k+1,j}|e^{-iH_R^{(j)}(q_{k+1})\Delta t/2\hbar}e^{-iH_R^{(j)}(q_k)\Delta t/2\hbar}|x_{k,j}\rangle ,$$

and is usually termed the quasiadiabatic propagator. It describes the exact dynamics of the relevant system in the limit of vanishing coupling to the bath. Introducing next the *discretized* (with respect to time) paths $q(t)$ and $q'(t)$, i.e., the evolution of the paths q, q' from the time t_0 to the time $t = M\Delta t$ is described by the finite sequences $\{q_0,q_1,\ldots,q_M\}$, $\{q'_0,\ldots,q'_M\}$, and performing the trace over the bath degrees of freedom, the time evolution of the RDM is described by the multidimensional path integral

$$\begin{aligned}\rho(q_f,q'_f,t) = \int dq_0 \ldots \int dq_{M-1}\int dq'_0 \ldots \int dq'_{M-1} \\ \times \langle q_f|U_S(t,t_{M-1})|q_{M-1}\rangle \ldots \langle q_1|U_S(t_1,t_0)|q_0\rangle \\ \times \langle q_0|\rho(t_0)|q'_0\rangle\langle q'_0|U_S^{\dagger}(t_1,t_0)|q'_1\rangle \ldots \langle q'_{M-1}|U_S^{\dagger}(t,t_{M-1})|q'_f\rangle \\ \times \mathscr{F}[\{q_0,q_1,\ldots,q_f\},\{q'_0,q'_1,\ldots,q'_f\}] . \end{aligned} \tag{266}$$

Here, $\mathscr{F}[\{q_0,q_1,\ldots,q_f\},\{q'_0,q'_1,\ldots,q'_f\}]$ is the Feynman–Vernon influence functional evaluated on the discretized paths q, q' where we have set $q_f = q_M, q'_f = q'_M$. In the limit $M\to\infty$ the expression (258) for the influence functional is recovered. To calculate the multidimensional path-integral numerically, one needs to discretize the paths also in space. A conventional trapezoidal calculation would require a fine grid which would lead to very high-dimensional sums. A more convenient method is to use the minimal number of basis functions for which evaluating the matrix elements in Eq. (266) is sufficient to describe the system dynamics. A useful observation is that, in the absence of driving and of coupling to the bath, the propagator for the uncoupled system is diagonal in the basis $\{|\varphi_i\rangle\}$ of the energy eigenstates of the time-independent Hamiltonian H_0. On the other hand, the influence functional is conveniently expressed in the basis $\{|u_i\rangle\}$ in which the operator q is diagonal. Hence, in the absence of driving, a useful choice for the basis functions is the *discrete variable representation* (DVR) [199]. This amounts to choose the first n energy eigenstates $|\varphi_j\rangle$ of the system Hamiltonian H_0, and to perform the unitary transformation

$$|u_i\rangle = \sum_{j=i}^{n} L_{i,j}|\varphi_j\rangle , \tag{267}$$

that selects n position eigenstates $|u_i\rangle$ by means of the orthogonal transformation matrix $L_{i,j}$. This diagonalizes the coupling and gives an appropriate approximation for the requirement of completeness of the discrete basis. The number n of energy eigenstates chosen depends on the problem, and it is usually between 2 and 20. The path integral is then decomposed into sums over matrix

elements in the DVR basis multiplied with the influence functional evaluated at the eigenvalues of the position operator. In the presence of driving, the time-dependent Hamiltonian $H_S(t)$ is not anymore diagonal in the basis of H_0, though the choice of the discrete set $\{|\varphi_i\rangle\}$ continues to be convenient for the numerical calculations. Recently, a novel basis set constructed in terms of appropriate moving basis sets has also been proposed [196]. The practical applicability of the QUAPI method depends critically on the dimension of the multidimensional path-integral. The numerical effort for global evaluation of the path integral grows exponentially with the number of time slices. If one is interested in the long-time dynamics, iterative schemes are therefore necessary. For this to work, the fact that the range of nonlocal interactions in the influence functional described by the correlation function $K(t)$ in Eq. (229) is finite in time, with a maximum at $t = 0$, is crucial. Then, the path integration can be truncated, and the time evolution equation leads to an iterative tensor multiplication scheme [197,198]. The number of time steps after which the path integration is truncated determines the rank of the tensor in the multiplication scheme. Despite the fact that the range of nonlocal interactions is finite in time, it decays only algebraically for Ohmic damping at temperature $T = 0$, and exponentially for $T > 0$ [34]. This has to be taken into account at very low temperatures, when the length of the convergence factor, as given by the bath correlations, diverges. Finally, it is worth remarking that the discrete variable representation of the QUAPI offers a direct way of reducing an extended double-well dynamics to a reduced, finite-level-system dynamics continuously, by decreasing the number of DVR states. More generally, the DVR method should provide an unified approach to investigate the dynamics of continuous or tight-binding models. The QUAPI method has been sucessfully applied to investigate the driven spin–boson system [200–202], and part of the results found will be discussed in Section 12. In Section 14.3 we discuss the results of the QUAPI on dynamical hysteresis in the driven and dissipative double-well potential [203,204].

11. The driven dissipative two-state system (general theory)

11.1. The driven spin-boson model

In this section we shall investigate the driven dynamics of a dissipative two-level system (TLS). As discussed in Section 3, the driven TLS can model the physics of intrinsic two-level systems, such as spin $\frac{1}{2}$ particles in external magnetic fields or, more generally, the motion of a quantum particle at low temperatures in an effective double-well potential in the case that only the lowest energy doublet is occupied. In this latter case, the dissipative TLS can describe, for example, hydrogen tunneling in condensed media [205], tunneling of atoms between an atomic-force microscope tip and a surface [206],[6] or of the magnetic flux in a superconducting quantum interference device (SQUID) [208]. Recent experiments on submicrometer Bi wires have measured transition rates of two-level systems coupled to conduction electrons [209,210]. Moreover, since the seminal works

[6] Here, the quantum dissipation for Xe-atoms tunneling between an atomic-force-microscope tip and a Ni(100) surface is Ohmic-like [207].

by Marcus [211] and Levich [212] this same model has been applied to describe nonadiabatic chemical reactions in the condensed phase, such as electron transfer (ET) [35,213–217] or proton transfer reactions [218,219].

As illustrated in Section 3, to investigate tunneling problems, the two-level system is conveniently described by the pseudospin Hamiltonian (65)

$$H_0 := H_{\mathrm{TLS}} = -\frac{\hbar}{2}(\Delta_0\sigma_x + \varepsilon_0\sigma_z)\,. \tag{268}$$

The basis is chosen such that the states $|R\rangle$ (right) and $|L\rangle$ (left) are eigenstates of σ_z with eigenvalues $+1$ and -1, respectively. The interaction energy $\hbar\Delta_0$ is the energy splitting of a symmetric TLS due to tunneling. Because of its fundamental role in the understanding of the interplay among quantum coherence, dissipation and driving in nonlinear quantum systems, we shall dedicate all of this section to the driven and dissipative two-level system. Moreover, this problem can – to a large extent – be treated in analytical terms.

Quite generally, the stochastic influence of the bath results in a reduction of the coherent tunneling motion by incoherent processes [32–35], and may even lead to a transition to localization at zero temperature [220]. An important question is to which degree the dissipative TLS dynamics is influenced by externally applied time-dependent fields [67,68,191,192, 200–202,221–250]. In particular, as discussed in Section 3.2.2, in the absence of interaction with a bath, a complete destruction of tunneling can be induced by a coherent driving field of appropriate frequency and strength [24,67,68]. This effect persists in the presence of dissipation [191,192,225,226,229,238]. The transition temperature above which quantum coherence is destroyed by a stochastic environment is modified by a driving field [225,226,238]. The possibility to control a priori the proton transfer by an electric field has been first addressed in [223] in the classical limit. This same issue applied to the case of electron transfer rate in a polar solvent was subsequently discussed in [227,228]. Long-time coherent oscillations may arise due to driving induced correlations between tunneling transitions [191,192,200–222,229,246]. Other interesting examples of control of the TLS dynamics are the enhancement of the TLS response to a weak coherent signal [232,233] for optimal values of the temperature, i.e., quantum stochastic resonance (QSR), see Section 12.1.4, or of the periodic asymptotic tunneling amplitude vs. friction strength [200]. The possibility of inversion of the population between the donor and the acceptor in an ET process has been recently investigated in [225,228,236], while a stabilization of the transfer rate by a periodic field has been discussed in [201,202]. Novel effects, such as an exponential enhancement of the transfer rate by an electric field modulating the coupling between the localized states has been addressed recently in [238]. Finally, interesting phenomena arise when a stochastic (e.g. of the dichotomous type) modulation of the intersite coupling [239,240] or of the asymmetry energy between the two-state-system [241] is applied.

We shall apply here the path-integral formalism described in the previous section to investigate the reduced dynamics of the driven and dissipative TLS. As a first step to characterize the driven dissipative TLS, we have to specifiy the Hamiltonian term $H_{\mathrm{ext}}(t)$ introduced in Eq. (222) describing the interaction with external time-dependent fields. Usually, only the effects of a driving field modulating the asymmetry energy between the two wells are considered [200–202,221–236,244,246–250]. Here, following [238,243], we generalize the model to include the

possibility of external (*multiplicative* or *additive*) modulation of the coupling energy between the localized states. This time dependence of the coupling parameter could arise, for example, from an ac-modulation of the barrier height or width of the underlying double-well potential, and could be realized in a superconducting loop with two Josephson junctions [208]. We observe that (see the detailed discussion in Section 12 below), while the effect of asymmetry modulation is additive, a barrier modulation results in a *multiplicative* (exponential) modification of the coupling parameter. Another example of time-dependent tunneling-coupling may arise in long-range bridge-assisted electron-transfer (ET) [239,240]. In this case, the direct coupling between donor and acceptor is negligibly small to cause ET. However, the intervening medium can provide states which serve as a "bridge" in the long-range ET, and hence induce a *stochastically fluctuating* effective electronic coupling between donor and acceptor states. A general Hamiltonian for the driven TLS reads

$$H_{\mathrm{TLS}} + H_{\mathrm{ext}}(t) = -\tfrac{1}{2}\hbar[\Delta(t)\sigma_x + \varepsilon(t)\sigma_z]\,. \tag{269}$$

Here, $\Delta(t)$ and $\varepsilon(t)$ are explicitly time-dependent, but generally are not periodic. The specific form of this time dependence depends on the characteristics of the driving fields.

Finally, like in Eq. (224), we characterize the thermal bath as an ensemble of harmonic oscillators described by the Hamiltonian H_{B}, and we consider bi-linear couplings to the heat bath that are sensitive to the value of the position operator σ_z. For example, a dipole-local-field coupling provides a simple physical model for this type of coupling. In this discretized representation the interaction Hamiltonian H_{SB} assumes the form $H_{\mathrm{SB}} = -(\sigma_z d/2)\sum_i c_i x_i := -\sigma_z X/2$, where x_i is a bath coordinate and d is the tunneling distance. We end up with the time-dependent spin–boson Hamiltonian[7]

$$H(t) = -\tfrac{1}{2}\hbar[\Delta(t)\sigma_x + \varepsilon(t)\sigma_z] - \tfrac{1}{2}\sigma_z X + H_{\mathrm{B}}\,, \tag{270}$$

with

$$H_{\mathrm{B}} = \frac{1}{2}\sum_i \left(\frac{p_i^2}{m_i} + m_i\omega_i^2 x_i^2\right). \tag{271}$$

In the following we derive formally exact solutions for the reduced density matrix and discuss analytical and numerical approximations. Moreover, we illustrate some important examples of control of tunneling by external monochromatic or polychromatic fields and discuss the phenomenon of quantum stochastic resonance.

11.2. The reduced density matrix (RDM) of the driven spin–boson system

We wish to compute the reduced density matrix (RDM) $\rho(t) = \mathrm{Tr}_{\mathrm{B}}\{W(t)\}$ of the driven spin–boson system. We consider a factorized initial state $W(t_0) = \rho_{\mathrm{S}}(t_0)W_{\mathrm{B}}$ for the density matrix $W(t)$ of system-plus-reservoir.

[7] Note that throughout this and the next section the "bare" tunneling splitting Δ_0 in Eq. (268) denotes the tunneling splitting that is already renormalized by high-frequency mode contributions of the bath with frequency $\omega > \omega_{\mathrm{c}}$, with ω_{c} appearing in the spectral density $J(\omega)$ in Eq. (238) [188].

In particular, we suppose that at times $t < t_0$ the particle is held at the site $\sigma_z = 1$ with the bath being in thermal equilibrium. For this problem the RDM is a 2×2 matrix with matrix elements $\rho_{\sigma,\sigma'} := \rho(\sigma, \sigma'; t)$, where $\sigma, \sigma' = \pm 1$, whose knowledge enables the evaluation of the expectation value of *any* observable related to the TLS. In particular, as discussed in Section 3, the knowledge of the RDM is equivalent to knowing the expectation values $\langle \sigma_i \rangle_t := \mathrm{Tr}\{\rho(t)\sigma_i\}$, cf. Eq. (69). In the localized representation we prefer to use, $\langle \sigma_z \rangle_t$ describes the population difference of the two localized states. It provides therefore direct information on the dynamics of the TLS. In order to evaluate other observables related to the TLS, such as e.g. the coherences, one must evaluate the expectations values $\langle \sigma_x \rangle_t$ and $\langle \sigma_y \rangle_t$.

In the presence of driving and dissipation the quantum coherent motion described earlier by Eqs. (72)–(74) will be modified. Let us next investigate these modifications.

11.2.1. Exact path-integral solution for the RDM

For a harmonic bath, the trace over the bath degrees of freedom prescribed in the definition of $\rho(t)$ can be performed exactly by using the Feynman–Vernon path-integral method [186] discussed in Section 10. In particular, the matrix elements $\rho_{\sigma,\sigma'}$ of the reduced density matrix are expressed in terms of the double path integral in Eq. (255) as

$$\rho_{\sigma,\sigma'}(t) = \int \mathscr{D}q \int \mathscr{D}q' \mathscr{A}[q] \mathscr{B}[q] \mathscr{A}^*[q'] \mathscr{B}^*[q'] \mathscr{F}[q, q'] \,, \tag{272}$$

in which the sum is over all real-time paths $q(t')$, $q'(t')$ with the imposed constraints $q(0) = q'(0) = d/2$, $q(t) = \sigma d/2$ and $q'(t) = \sigma' d/2$ ($\sigma = \pm 1, \sigma' = \pm 1$).[8] The quantity $\mathscr{A}[q]$ is the probability amplitude of the TLS to follow the path $q(t')$ in the absence of driving and fluctuating forces. The factor $\mathscr{B}[q]$ incorporates the effect of the driving force, and $\mathscr{F}[q, q']$ is the Feynman–Vernon influence functional, cf. Eq. (258). For the driven TLS it is convenient to slightly modify the definition of the center of mass and relative coordinates in Eq. (259) in order to obtain dimensionless coordinates. We introduce

$$\xi_{\mathrm{TLS}}(t) = [q(t') - q'(t')]/d, \qquad \eta_{\mathrm{TLS}}(t') = [q(t') + q'(t')]/d \,. \tag{273}$$

Now, a two-state system starting out from a diagonal state of the density matrix is again in a diagonal state after any even number of transitions, and in an off-diagonal state after any odd number of transitions. Hence, $\xi_{\mathrm{TLS}}(t) = 0$ and $\eta_{\mathrm{TLS}}(t) = 1$ or -1 depending on whether one is in the state $\rho_{1,1} := \mathrm{RR}$ or $\rho_{-1,-1} := \mathrm{LL}$ of the RDM, respectively. On the other hand, $\eta_{\mathrm{TLS}}(t) = 0$ and $\xi_{\mathrm{TLS}}(t) = 1$, or -1, if one is in the state $\rho_{1,-1} := \mathrm{RL}$, or $\rho_{-1,1} := \mathrm{LR}$. Suppose that we want to evaluate $\langle \sigma_z \rangle_t$. A general path will have $2n$ transitions at flip times t_j, $j = 1, 2, \ldots, 2n$, within the

[8] Note that this implicitly means that we express the double path integral in the discrete variable representation (DVR), see Section 10.2 and Eq. (267), in which the operator q is diagonal. For the case of a TLS the DVR basis and the localized basis formed by the vectors $|L\rangle$, $|R\rangle$ *coincide*. This does not hold anymore true if, for example, the reduction of the double-well potential to the first two doublets is considered, see Section 14.1.

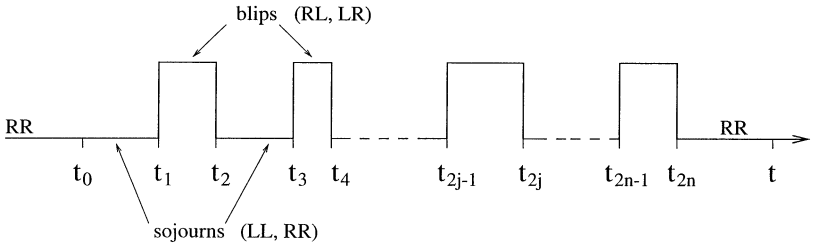

Fig. 14. Generic path with $2n$ transitions at flip times $t_1, t_2, \ldots, t_{2n}$ contributing to the population difference $\langle \sigma_z \rangle_t$ between the localized states of a driven and dissipative two-level-system. The time intervals spent in a diagonal state RR or LL of the reduced density matrix are called sojourns, and the time intervals spent in an off-diagonal state RL or LR are termed blips. The initial and final sojourns are fixed by the condition $\rho_{\sigma,\sigma'}(t_0) = \rho_{\sigma,\sigma'}(t) \equiv RR$ on the reduced density matrix.

interval $t_0 < t' < t$. Such a path can be parametrized by

$$\begin{aligned} \xi^{(2n)}(t') &= \sum_{j=1}^{n} \xi_j [\theta(t' - t_{2j-1}) - \theta(t' - t_{2j})] , \\ \eta^{(2n)}(t') &= \sum_{j=0}^{n} \eta_j [\theta(t' - t_{2j}) - \theta(t' - t_{2j+1})] , \end{aligned} \tag{274}$$

where $t_{2n+1} \equiv t$, $\theta(t)$ is the unit step function, and where the labels $\xi_j = \pm 1$ and $\eta_j = \pm 1$ mark the two off-diagonal LR or RL, and diagonal states RR or LL of the RDM, respectively, cf. Fig. 14. On the other hand, if we want to evaluate $\langle \sigma_x \rangle_t$ or $\langle \sigma_y \rangle_t$ a general path will have $2n + 1$ transitions at corresponding flip times t_j, $j = 1, 2, \ldots, 2n + 1$ within the interval $t_0 < t' < t$. The periods $t_{2j} < t' < t_{2j+1}$ in which the system is in a diagonal state RR or LL are usually referred to as *sojourns*. Likewise, the periods $t_{2j-1} < t' < t_{2j}$ in which the system stays in off-diagonal states RL or LR are termed *blips* [32,34], see Fig. 14. To evaluate now the dissipative influence, it is convenient to consider the influence functional in the form given by Eq. (261), where the *time derivatives* $\dot{\eta}_{\mathrm{TLS}}(t)$ and $\dot{\xi}_{\mathrm{TLS}}(t)$ of the sequences of sojourns, and of blips, respectively, occur. This yields

$$\begin{aligned} \dot{\xi}^{(2n)}(t') &= \sum_{j=1}^{n} \xi_j [\delta(t' - t_{2j-1}) - \delta(t' - t_{2j})] , \\ \dot{\eta}^{(2n)}(t') &= \sum_{j=1}^{n} [\eta_j \delta(t' - t_{2j}) - \eta_{j-1} \delta(t' - t_{2j-1})] . \end{aligned} \tag{275}$$

For later convenience we note that a blip transition acts as an effective *neutral* dipole, where to the jth blip with spin flips at times t_{2j-1} and t_{2j} are associated the charges $\phi_{2j-1} := \xi_j$ and $\phi_{2j} := -\xi_j$, respectively. This does not hold true for the sojourn transitions.

Let us next introduce the functions $Q_{j,k} := Q(t_j - t_k)$, and

$$\begin{aligned} \Lambda_{j,k} &= Q'_{2j,2k-1} + Q'_{2j-1,2k} - Q'_{2j,2k} - Q'_{2j-1,2k-1} , \\ X_{j,k} &= Q''_{2j,2k+1} + Q''_{2j-1,2k} - Q''_{2j,2k} - Q''_{2j-1,2k+1} , \end{aligned} \tag{276}$$

with $Q'(t)$ and $Q''(t)$ being the real and imaginary parts of the bath correlation function $Q(t) := d^2 L(t)$, respectively, with $L(t)$ defined in Eq. (262), i.e.,

$$Q(t) = \frac{d^2}{\hbar\pi}\int_0^\infty \mathrm{d}\omega \frac{J(\omega)}{\omega^2} \frac{\cosh(\hbar\omega\beta/2) - \cosh[\omega(\hbar\beta/2 - \mathrm{i}t)]}{\sinh(\hbar\omega\beta/2)} . \tag{277}$$

The function $\Lambda_{j,k}$ describes the interblip correlations of the dipole pair $\{j,k\}$, while the function $X_{j,k}$ describes the correlations of the blip j with a preceding sojourn k. The influence function $\tilde{\Phi}^{(n)}$, cf. Eq. (261), for a path with n transitions in the off-diagonal states of the RDM then becomes

$$\tilde{\Phi}^{(n)} = \sum_{j=1}^{n} Q'_{2j,2j-1} + \sum_{j=2}^{n}\sum_{k=1}^{j-1} \xi_j \xi_k \Lambda_{jk} - i\sum_{j=1}^{n}\sum_{k=0}^{j-1} \xi_j \eta_k X_{jk} . \tag{278}$$

Finally, we point out that within this parametrization the sum over histories of paths is represented (i) by the sum over any number of flip times, (ii) by the time-ordered integrations over the flip times $\{t_j\}$, and (iii) by the sum over all possible arrangements $\{\xi_j = \pm 1\}$ and $\{\eta_j \pm 1\}$ of the blip and sojourn intervals. Introducing for the time integrals the compact notation

$$\int_{t_0}^{t} \mathscr{D}_n\{t_j\} \cdots := \int_{t_0}^{t} \mathrm{d}t_n \int_{t_0}^{t_n} \mathrm{d}t_{n-1} \cdots \int_{t_0}^{t_2} \mathrm{d}t_1 \cdots , \tag{279}$$

the path summation takes the form

$$\int \mathscr{D}q \int \mathscr{D}q' \cdots \Rightarrow \sum_{n=0}^{\infty} \int_{t_0}^{t} \mathscr{D}_n\{t_j\} \sum_{\{\xi_j\}} \sum_{\{\eta_j\}} \cdots . \tag{280}$$

The double path-integral can now be performed, and the formal solution for $\langle\sigma_x\rangle_t$ and $\langle\sigma_y\rangle_t$ reads [243]

$$\langle\sigma_x\rangle_t = \frac{1}{2}\sum_{n=0}^{\infty}\left(-\frac{1}{2}\right)^n \int_{t_0}^{t} \mathscr{D}_{2n+1}\{t_j\}\delta_{2n+1}\{t_j\} \sum_{\{\xi_j = \pm 1\}} \xi_{n+1}(F^{(+)}_{n+1} C^{-}_{n+1} + F^{(-)}_{n+1} C^{+}_{n+1}) , \tag{281}$$

$$\langle\sigma_y\rangle_t = \frac{1}{2}\sum_{n=0}^{\infty}\left(-\frac{1}{2}\right)^n \int_{t_0}^{t} \mathscr{D}_{2n+1}\{t_j\}\delta_{2n+1}\{t_j\} \sum_{\{\xi_j = \pm 1\}} (F^{(+)}_{n+1} C^{+}_{n+1} - F^{(-)}_{n+1} C^{-}_{n+1}) , \tag{282}$$

where $t_{2n+2} = t$. For $\langle\sigma_z\rangle_t$ one obtains

$$\langle\sigma_z\rangle_t = 1 + \sum_{n=1}^{\infty}\left(-\frac{1}{2}\right)^n \int_{t_0}^{t} \mathscr{D}_{2n}\{t_j\}\delta_{2n}\{t_j\} \sum_{\{\xi_j = \pm 1\}} (F^{(+)}_{n} C^{+}_{n} - F^{(-)}_{n} C^{-}_{n}) . \tag{283}$$

Here, the set $\{\xi_j\}$ labels the two off-diagonal states of the reduced density matrix, while the sum over the diagonal states visited at intermediate times has already been performed. The influence of the driving is contained in the factors

$$\delta_n\{t_j\} = \prod_{j=1}^{n} \Delta(t_j) , \tag{284}$$

and

$$C_n^+ = \cos\phi_n, \qquad C_n^- = \sin\phi_n\ , \tag{285}$$

where

$$\phi_n = \sum_{j=1}^{n}\ \xi_j\zeta(t_{2j}, t_{2j-1}), \qquad \zeta(t,t') = \int_{t'}^{t} \mathrm{d}t''\varepsilon(t'')\ . \tag{286}$$

All the dissipative influences are in the functions $F_n^{(\pm)}$. Combining all intrablip and interblip correlations in the expression

$$G_n = \exp\left(-\sum_{j=1}^{n}\ Q'_{2j,2j-1} - \sum_{j=2}^{n}\sum_{k=1}^{j-1}\ \xi_j\xi_k\Lambda_{j,k}\right), \tag{287}$$

and introducing the phases $\chi_{n,k} = \sum_{j=k+1}^{n}\xi_j X_{j,k}$ which describe the correlations between the kth sojourn and the $n-k$ succeeding blips, the functions $F_n^{(\pm)}$ take the form

$$F_n^{(+)} = G_n\prod_{k=0}^{n-1}\ \cos\chi_{n,k}, \qquad F_n^{(-)} = F_n^{(+)}\tan\chi_{n,0}\ . \tag{288}$$

Up to here the results are exact, though they are far too complex to be handled analytically. Hence, one has to resort to suitable approximation schemes and subsequent numerical computations. Before proceeding along these lines, it is advantageous to cast the expression for $\langle\sigma_z\rangle_t$ into the form of a master equation [222], and the expression for $\langle\sigma_x\rangle_t$ into an integral expression [243]. Interestingly, this can be performed exactly.

11.2.2. Exact master equations and integral expressions for the RDM

To obtain the above-mentioned relations for the expectations $\langle\sigma_i\rangle_t$, we define modified influence functions $\tilde{F}_n^{(\pm)}$ involving suitable subtractions of products of lower-order influence functions, i.e.,

$$\tilde{F}_n^{(\pm)} = F_n^{(\pm)} - \sum_{j=2}^{n}\ (-1)^j \sum_{m_1,\ldots,m_j} F_{m_1}^{(+)}F_{m_2}^{(+)}\cdots F_{m_j}^{(\pm)}\delta_{m_1+\cdots+m_j,n}\ ,$$

where the inner sum is over positive integers m_j. By definition, each subtraction involves again time ordering for the flip times. In the subtracted terms, the bath correlations are only inside of each of the individual factors $F_{m_j}^{(\pm)}$, i.e., there are no correlations between these factors. We next introduce the kernels $Y^{(\pm)}(t,t')$ defined by the series expression

$$Y^{(\pm)}(t,t') = \sum_{n=0}^{\infty}\ (-1)^n\int_{t'}^{t}\mathrm{d}t_{2n+1}\cdots\int_{t'}^{t_3}\mathrm{d}t_2\ \delta_{2n+1}\{t_j\}2^{-(n+1)}\sum_{\{\xi_j=\pm1\}}\ \xi_{n+1}\tilde{F}_{n+1}^{(\mp)}C_{n+1}^{(\pm)}\ . \tag{289}$$

In the same way the kernels $K^{(\pm)}(t,t')$ are defined by the series

$$K^{(\pm)}(t,t') = \Delta(t)\sum_{n=0}^{\infty}\ (-1)^n\int_{t'}^{t}\mathrm{d}t_{2n+1}\cdots\int_{t'}^{t_3}\mathrm{d}t_2\,\delta_{2n+1}\{t_j\}2^{-(n+1)}\sum_{\{\xi_j=\pm1\}}\ \tilde{F}_{n+1}^{(\pm)}C_{n+1}^{(\pm)}\ , \tag{290}$$

where the label + (or −) indicates that the respective kernel is an even (or odd) function of the bias energy $\varepsilon(t)$. The product functions $\tilde{F}_n^{(\mp)}C_n^{(\pm)}$, $\tilde{F}_n^{(\pm)}C_n^{(\pm)}$ depend on flip times, where the first and the last one are identified with t' and t, respectively. All intermediate flip times are integrated over as prescribed by Eqs. (289) and (290). Taking the time derivative of Eqs. (281)–(283), it is found that the formal solution for $\langle\sigma_z\rangle_t$ can be recast in the form of an exact generalized master equation (GME) [222]

$$\frac{\mathrm{d}}{\mathrm{d}t}\langle\sigma_z\rangle_t = \int_{t_0}^{t} \mathrm{d}t'[K^{(-)}(t,t') - K^{(+)}(t,t')\langle\sigma_z\rangle_{t'}] \,, \tag{291}$$

as follows from an iterative solution of Eq. (291) with (290). In contrast, there is no closed master equation for $\langle\sigma_x\rangle_t$ or $\langle\sigma_y\rangle_t$. Instead, the following exact integral relations hold [243]:

$$\langle\sigma_x\rangle_t = \int_{t_0}^{t} \mathrm{d}t'[Y^{(+)}(t,t') + Y^{(-)}(t,t')\langle\sigma_z\rangle_{t'}] \tag{292}$$

$$\langle\sigma_y\rangle_t = -\frac{1}{\Delta(t)}\frac{\mathrm{d}}{\mathrm{d}t}\langle\sigma_z\rangle_t \,. \tag{293}$$

Here, the initial condition $\langle\sigma_z\rangle_{t_0} = 1$ is assumed. These exact results show that, for a localized initial condition, no integro-differential equation exists for the expectation values of $\langle\sigma_x\rangle$ and $\langle\sigma_y\rangle$. This is indeed remarkable.

11.3. The case $\alpha = 1/2$ of Ohmic dissipation

Let us consider the case in which the bath has an Ohmic spectrum with an exponential cutoff as in Eq. (237), i.e.,

$$J(\omega) = (2\pi\hbar/d^2)\alpha\omega \mathrm{e}^{-\omega/\omega_c} \,, \tag{294}$$

where the dimensionless coupling constant $\alpha = m\gamma d^2/2\pi\hbar$ has been introduced. For this particular form, the bath correlation functions $Q'(\tau)$ and $Q''(\tau)$, see Eq. (277), can be evaluated exactly [251,252], yielding

$$\begin{aligned} Q'(\tau) &= \alpha \ln(1 + \omega_c^2\tau^2) + 4\alpha \ln\left|\frac{\Gamma(1 + 1/\hbar\beta\omega_c)}{\Gamma(1 + 1/\hbar\beta\omega_c + \mathrm{i}\tau/\hbar\beta)}\right| \,, \\ Q''(\tau) &= 2\alpha \,\mathrm{atan}(\omega_c\tau) \,, \end{aligned} \tag{295}$$

where $\Gamma(z)$ denotes the gamma function.

In the following we shall discuss a closed-form solution for the special value $\alpha = \frac{1}{2}$ of the Ohmic strength in the limit of a large cutoff ω_c. In fact, in this limit, the case $\alpha = \frac{1}{2}$ represents a sort of "critical point" (in the absence of driving) in the investigation of the destruction of quantum coherence by bath-induced incoherent tunneling transitions. For the case of a symmetric system, $\alpha = \frac{1}{2}$ represents the "critical" dissipative value for which coherent tunneling is destroyed by the

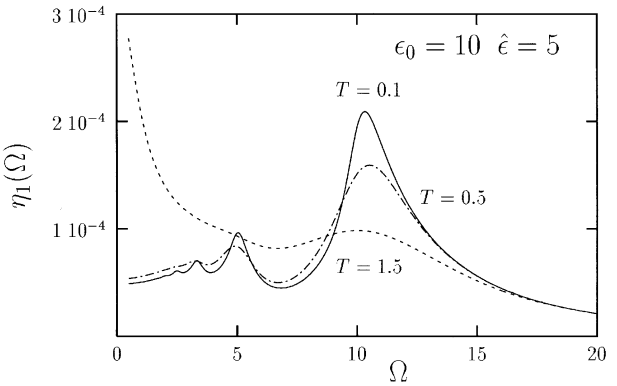

Fig. 15. Fundamental spectral amplitude η_1 vs. driving frequency Ω for different temperatures for the case $\alpha = \frac{1}{2}$ of Ohmic dissipation. At high temperatures only incoherent relaxation occurs (dashed lines). As the temperature is decreased, resonances appear at submultiples $\Omega = \varepsilon_0/n$ ($n = 1, 2, \dots$) of the static bias ε_0 (dot-dashed and full lines). These denote the occurrence of driving-induced coherence. Frequencies are in units of $\Gamma_0 = \pi\Delta_0^2/\omega_c$, temperatures in units of $\hbar\Gamma_0/k_B$.

dissipative environment for any temperature [32,34]. Hence, for $\alpha \geq \frac{1}{2}$, the tunneling dynamics is always incoherent down to $T = 0$. Note also that the critical value of α for the destruction of quantum coherence depends on the specific transport quantity which is investigated [253,254]. In the presence of driving this situation is modified due to driving-induced coherent processes that render the low-temperature dynamics non-Markovian, see Fig. 15.

To be definite, we shall term the "scaling limit" the limit $\omega_c\tau \gg 1$ and $\hbar\omega_c \gg k_B T$, where τ is the argument of the Ohmic functions $Q'(\tau)$ and $Q''(\tau)$ in Eq. (295). In this limit, the functions $Q'(\tau)$ and $Q''(\tau)$ appearing implicitly in Eqs. (291) and (292) assume the form

$$Q'(\tau) = 2\alpha \ln[\hbar\beta\omega_c/\pi \sinh(\pi\tau/\hbar\beta)], \qquad Q''(\tau) = \pi\alpha \,\mathrm{sgn}(\tau) \,. \tag{296}$$

In this limit, the series expression (283) seems ill defined, due to the multiple occurrence of $\cos(\pi\alpha)$-factors which become zero at $\alpha = \frac{1}{2}$. It is though well defined for α-values arbitrarily close to $\frac{1}{2}$. Taking then the limit $\alpha \to \frac{1}{2}$ the calculation can be carried out if one observes that the zeros of $\cos(\pi\alpha)$ are indeed compensated by a corresponding number of divergences in the integrals over the blip and sojourn lengths. If the integration is handled with care in this way, using the technique developed first in [255] for the case of a static bias, and generalized in [221,238] to the driven case, the power series (283) in the tunneling transitions can be summed up *exactly* in closed form. One then finds for $P(t) := \langle\sigma_z\rangle_t$ the result

$$P(t) = P^{(a)}(t) + P^{(s)}(t) \,, \tag{297}$$

where

$$\begin{aligned} P^{(a)}(t) &= \int_0^t \mathrm{d}t_2 \mathrm{e}^{-\int_{t_0}^{t}\mathrm{d}s\Gamma(s)} \int_0^{t_2} \mathrm{d}t_1 \Delta(t_2)\Delta(t_1) \mathrm{e}^{-Q'(t_2-t_1)} \mathrm{e}^{-\int_{t_1}^{t_2}\mathrm{d}s\Gamma(s)/2} \sin[\zeta(t_2,t_1)] \,, \\ P^{(s)}(t) &= \mathrm{e}^{-\int_0^t \mathrm{d}s\Gamma(s)} \,. \end{aligned} \tag{298}$$

The function $\zeta(t,t')$ is defined in Eq. (286), and additionally we have introduced the relaxation rate $\Gamma(t) = \pi\Delta^2(t)/2\omega_c$. Here, $P^{(a)}(t)$ represents the contribution to $P(t)$ that is antisymmetric with respect to an inversion of the bias $\varepsilon \to -\varepsilon$. It determines the long-time dynamics. The investigation of the symmetric contribution $P^{(s)}(t)$ is, on the other hand, of interest to obtain information on the transient dynamics. It decays to zero as $t \to \infty$. As expected, Eq. (298) predicts that in the absence of driving a symmetric TLS undergoes, for *any* temperature, incoherent relaxation with rate $\Gamma_0 := \pi\Delta_0^2/2\omega_c$. Note that for this special case $\alpha = \frac{1}{2}$ the relaxation rate coincides with the tunneling splitting Δ_e, see Eq. (310) below, renormalized by bath modes with $\omega < \omega_c$. Further, $P^{(s)}(t)$ is not sensitive to asymmetry modulation. Along the same line is $\langle\sigma_x\rangle_t \equiv 0$. To conclude, we observe that, as argued in Ref. [32], the error introduced in $P(t)$ by approximating the bath correlation functions $Q'(\tau)$ and $Q''(\tau)$ as in Eq. (296) can in the worst case become comparable to the value assumed by $P(t)$ itself only at long times when the condition $t > \ln(\omega_c/\Delta_0)/\Gamma_0$ is satisfied.

For general forms of dissipation, the exact master equation (291) and the related equations for $\langle\sigma_x\rangle_t$, $\langle\sigma_y\rangle_t$ cannot be solved exactly. In the following, we shall discuss approximations that render the analytical analysis more tractable.

11.4. Approximate treatments

11.4.1. The noninteracting-blip approximation (NIBA)

The noninteracting-blip approximation (NIBA) has been reviewed in [32], and since, successfully applied to investigate the tunneling dynamics in different parameter regimes. An extension of the NIBA to the driven case has been discussed in [221,225,226,229,236,243]. The NIBA is a rather good approximation for sufficiently large temperatures and/or dissipative strength, and/or for strong bias. Moreover, in the absence of driving, it provides a systematic weak damping approximation down to the lowest temperatures for the case of a symmetric system, i.e., $\varepsilon_0 = 0$. This has been confirmed via a direct comparison between the NIBA prediction and its next order correction given by the interacting-blip-chain-approximation (IBCA), cf. Section 11.4.3, real-time Monte-Carlo calculations [252,256], and by calculations via the numerical QUAPI method discussed in Section 10.2 [201].

In the NIBA one formally neglects the blip–blip interactions $\Lambda_{j,k}$. Furthermore, the sojourn–blip interactions $X_{j,k}$ are disregarded except neighboring ones with $k = j-1$, and they are approximated by $X_{j,j-1} = Q''(\tau_j)$. Hence, in the NIBA, the influence functions $\tilde{\Phi}^{(n)}$ in Eq. (278) depend on the blip length alone, i.e.,

$$\tilde{\Phi}^{(n)}_{\mathrm{NIBA}} = \sum_{j=1}^{n} \left[Q'(\tau_j) - \mathrm{i}\xi_j\eta_{j-1}Q''(\tau_j)\right] , \tag{299}$$

with $\tau_j = t_{2j} - t_{2j-1}$ the length of the jth blip interval. Because interblip correlations are disregarded in the NIBA, the modified influence functions $\tilde{F}^{(\pm)}_n$ are zero for all $n \neq 1$, and therefore the series expansions (289) and (290) reduce to the terms of lowest order in $\Delta(t)$. Under these approximations, defining $P(t) := \langle\sigma_z\rangle_t$, we obtain from Eqs. (291)–(293) the explicit form

$$\frac{\mathrm{d}}{\mathrm{d}t}P(t) = \int_{t_0}^{t} \mathrm{d}t' \left[K^{(-)}(t,t') - K^{(+)}(t,t')P(t')\right] \tag{300}$$

and

$$\langle \sigma_x \rangle_t = \int_{t_0}^{t} \mathrm{d}t' [\, Y^{(+)}(t,t') + Y^{(-)}(t,t') P(t')] \tag{301}$$

$$\langle \sigma_y \rangle_t = -\frac{1}{\Delta(t)} \frac{\mathrm{d}}{\mathrm{d}t} P(t) \,, \tag{302}$$

with the NIBA kernels

$$\begin{aligned} K^{(+)}(t,t') &= \Delta(t)\Delta(t') \mathrm{e}^{-Q'(t-t')} \cos[Q''(t-t')] \cos[\zeta(t,t')] \,, \\ K^{(-)}(t,t') &= \Delta(t)\Delta(t') \mathrm{e}^{-Q'(t-t')} \sin[Q''(t-t')] \sin[\zeta(t,t')] \end{aligned} \tag{303}$$

and

$$\begin{aligned} Y^{(+)}(t,t') &= \Delta(t') \mathrm{e}^{-Q'(t-t')} \sin[Q''(t-t')] \cos[\zeta(t,t')] \,, \\ Y^{(-)}(t,t') &= \Delta(t') \mathrm{e}^{-Q'(t-t')} \cos[Q''(t-t')] \sin[\zeta(t,t')] \,. \end{aligned} \tag{304}$$

Evaluation of the GME (300) and of Eqs. (301) and (302) gives the dynamics of the spin–boson model within the NIBA. We observe that, as shown in [257,258] for the undriven case, and generalized to the driven case in [225,226,236], the polaron transformation approach used in the small polaron model [259] leads, to lowest-order perturbation theory in the bath renormalized tunneling splitting, to a master equation analogous to Eq. (300), and possessing identical kernels (303).

Thus far, the NIBA has been discussed on a purely formal level only. The key idea that underpins the NIBA is that a blip transition acts like an effective dipole, cf. Eq. (275), which interacts only weakly with a neighboring dipole. Let us consider a spectral density of the form, cf. Eq. (238),

$$J(\omega) = (2\pi\hbar/d^2)\alpha_s \tilde{\omega}^{1-s} \omega^s \exp(-\omega/\omega_c) \,, \tag{305}$$

where α_s is the dimensionless coupling constant, and where $\alpha_1 := \alpha$ is the Ohmic coupling constant already introduced in Section 11.3; cf. Eq. (294). Let us first consider the undriven case. Then, we can distinguish between three different regimes in which the NIBA is justified:

(i) The first regime is encountered when the average blip length is so small compared to the average sojourn length, that the blip–blip interactions $\Lambda_{j,k}$ and the sojourn–blip interactions may be neglected. The suppression of the blip length against the sojourn length is favoured by the particular form $\propto \exp(-Q'(t))$ of the intrablip interactions appearing in the interaction function G_n in Eq. (287), which tend to suppress the blip length. On the contrary, the average blip-plus-sojourn length is constant and of the order of t/n for a path with $2n$ transitions up to time t. We observe then that the function $Q'(t)$ behaves at long times as t^{1-s} at zero temperature, and as t^{2-s} at finite temperatures. Hence, long blips τ are exponentially suppressed by the intrablip interactions $\propto \exp(-Q'(\tau))$ for any temperature in the sub-Ohmic case $0 < s < 1$, and in the case $1 \leq s < 2$ at finite temperatures. In turn, because it is the *difference* of the Q' that enters the interblip correlation factor $\propto \exp(-\Lambda_{j,k})$, cf. Eq. (276), this factor can be set equal to unity with negligible error. In particular, if the function Q' increases linearly with t, then the interblip interactions $\Lambda_{j,k}$ cancel out exactly.

It then turns out that the NIBA is justified always in the sub-Ohmic case $s < 1$, in the Ohmic case $s = 1$ for high enough temperatures and/or dissipative strength, and in the case $1 < s < 2$ for high enough temperatures. To be precise, for Ohmic dissipation it is always justified when $\alpha > 1$, or when $k_B T \geq \hbar \Delta_0$, with α arbitrary.

(ii) For super-Ohmic dissipation with $s > 2$ the intrablip interactions are not effective in suppressing the blip lengths. Though, the NIBA can be justified for arbitrary dissipation as long as the system exhibits overdamped dynamics, as it is, for example, for a strong static bias $\varepsilon_0 > \Delta_0$.

(iii) In addition, the NIBA is a systematic weak damping approximation down to zero temperature for the case of a *symmetric* system ($\varepsilon_0 = 0$). In fact, the effect of the interblip correlations $\Lambda_{j,k}$ is of the order of the square of the coupling constant α_s, whereas that of the intrablip correlations considered in the NIBA is of linear order.

In the *presence of driving*, the parameter regime in which conditions (i)–(iii) are valid become modified.

Let us, for example, consider the case of a driving field which modulates the asymmetry energy of the TLS (i.e., $\Delta(t) = \Delta_0$ in Eq. (269)). For a very slow driving field the overall effect is an adiabatic modulation of the asymmetry energy of the TLS [221]. In general, condition (i) still holds true. Condition (ii) gets modified because the system will show an overdamped dynamics when $|\varepsilon(t)| > \Delta_0$. On the contrary, a fast oscillating driving field tends to suppress long blips [229]. Hence, NIBA should be justified even better in the presence of a fast oscillating field, if it is already justified in the undriven case. For example, denoting by $\Delta_{\rm eff} \leq \Delta_0$ the tunneling splitting renormalized by a fast ac-field, cf. Eq. (359) below, the NIBA condition in (i) for the case of an Ohmic bath becomes $\alpha > 1$ or $k_B T > \hbar \Delta_{\rm eff}$.

We observe, on the contrary, that a fast ac-field which is modulating the coupling energy of the TLS, cf. Eq. (383) below, tends to enhance quantum coherence. In this case the validity range of NIBA is diminished. For example, denoting by $\Delta_{{\rm eff},\delta} \geq \Delta_0$ the field renormalized tunneling splitting, cf. Eq. (386) below, the NIBA condition in (i) for the case of an Ohmic bath becomes $\alpha > 1$, or $k_B T > \hbar \Delta_{{\rm eff},\delta}$.

In the absence of driving, Eq. (326) below is conveniently solved by Laplace transformation [32,34]. The study of the resulting pole equation for the Laplace transform of $P(t) := \langle \sigma_z \rangle_t$ gives information on the transient dynamics. In particular, for Ohmic dissipation and weak Ohmic coupling $\alpha \ll 1$, cf. Eqs. (238) and (294), the NIBA predicts a destruction of the damped coherent motion described by Eq. (72) above a crossover temperature $T^*(\alpha) \simeq \hbar \Delta_0 / k_B \alpha$ [32,34]. For $\alpha \geq \frac{1}{2}$ the dynamics is incoherent down to $T = 0$, cf. also [254]. For super-Ohmic dissipation with $s > 2$, the NIBA predicts underdamped motion up to high temperatures T_s^*. For the case $s = 3$ we have $T_3^* \simeq (\hbar \tilde{\omega} / k_B \sqrt{\alpha_3})$ [260]. These predictions have been confirmed by Monte-Carlo calculations [252,256]. Finally, the NIBA predicts that the TLS dynamics approaches incoherently a stationary equilibrium value $P_{\rm st} = \langle \sigma_z \rangle_\infty = \tanh(\hbar \varepsilon_0 / 2 k_B T)$ with relaxation rate Γ_0 given by

$$\Gamma_0 = \Delta_0^2 \int_0^\infty {\rm d}\tau \, h^{(+)}(\tau) \cos(\varepsilon_0 \tau) \,, \tag{306}$$

and with $P_{\rm st} = \rho_0 / \Gamma_0$, where

$$\rho_0 = \Delta_0^2 \int_0^\infty {\rm d}\tau \, h^{(-)}(\tau) \sin(\varepsilon_0 \tau) \,. \tag{307}$$

For later convenience we have introduced here the kernels

$$h^{(+)}(\tau) = \mathrm{e}^{-Q'(\tau)}\cos[Q''(\tau)]\,,$$
$$h^{(-)}(\tau) = \mathrm{e}^{-Q'(\tau)}\sin[Q''(\tau)]\,. \tag{308}$$

Inserting the expressions (296) for the Ohmic kernels $Q'(\tau)$ and $Q''(\tau)$ valid in the scaling approximation $\omega_c\tau \gg 1$, $\hbar\omega_c \gg k_B T$, one finds for the undriven, Ohmic NIBA rate [34,32]

$$\Gamma_0 = \frac{\Delta_0^2}{2\omega_c}\left(\frac{\hbar\beta\omega_c}{2\pi}\right)^{1-2\alpha}\frac{|\Gamma(\alpha + \mathrm{i}\hbar\beta\varepsilon_0/2\pi)|^2}{\Gamma(2\alpha)}\cosh(\hbar\beta\varepsilon_0/2)\,, \tag{309}$$

where $\Gamma(z)$ denotes the Gamma function. The above expression (309) is defined for any value of the coupling constant α. To investigate the tunneling dynamics for weak coupling $\alpha \ll 1$ it is convenient to introduce

$$\Delta_e = \Delta_0(\Delta_0/\omega_c)^{\alpha/(1-\alpha)}[\cos(\pi\alpha)\Gamma(1-2\alpha)]^{1/(2-2\alpha)}\,, \tag{310}$$

which is the bath-renormalized tunneling splitting when $\alpha < 1$. In terms of Δ_e the static rate, when $\alpha < 1$, has then the form

$$\Gamma_0 = \sin(\pi\alpha)\frac{\Delta_e}{2\pi}\left(\frac{\hbar\beta\Delta_e}{2\pi}\right)^{1-2\alpha}|\Gamma(\alpha + \mathrm{i}\hbar\beta\varepsilon_0/2\pi)|^2\cosh(\hbar\beta\varepsilon_0/2)\,. \tag{311}$$

On the contrary, for nonzero bias $\varepsilon_0 \neq 0$, NIBA breaks down for weak damping and low temperatures. In fact, because $|P_{st}| \to 1$ when $T \to 0$, the NIBA predicts an incorrect symmetry breaking at low temperatures, weak coupling and arbitrary small bias energies ε_0. In the same way, the NIBA predicts for $\langle\sigma_x\rangle_t$ a stationary equilibrium value $\langle\sigma_x\rangle_\infty = (\Delta_0/\varepsilon_0)\tanh(\hbar\varepsilon_0/2k_B T)$. That is, it occurs an unphysical divergence $\langle\sigma_x\rangle_\infty \to \infty$ when $T \to 0$ and for arbitrary small bias.

For a discussion of the predictions of the NIBA resulting from the above equations in the presence of driving we refer the reader to the next section. In the following subsections, by taking into account subsequent terms of the series expansions (289) and (290), which thereby account for interblip correlations, we calculate corrections to the NIBA systematically.

11.4.2. Systematic weak damping approximation

For weak damping, nonzero bias and low temperatures the NIBA breaks down because the bath correlations $\Lambda_{j,k}$ and $X_{j,k}$ contribute to effects which depend linearly on $J(\omega)$. The kernels $K^{(\pm)}(t,t')$ in Eq. (290) have been discussed for weak-damping in Ref. [222]. They have the form

$$\mathrm{K}^{(+)}(t,t') = \Delta(t)\Delta(t')\cos[\zeta(t,t')][1 - Q'(t-t')]$$
$$+ \int_{t'}^{t}\mathrm{d}t_2\int_{t'}^{t_2}\mathrm{d}t_1\delta_4\{t_j\}\sin[\zeta(t,t_2)]P_0(t_2,t_1)\sin[\zeta(t_1,t')]$$
$$\times[Q'(t-t') + Q'(t_2-t_1) - Q'(t_2-t') - Q'(t-t_1)]$$

and

$$K^{(-)}(t,t') = \Delta(t)\Delta(t')\sin[\zeta(t,t')]Q''(t-t') - \int_{t'}^{t} \mathrm{d}t_2 \int_{t'}^{t_2} \mathrm{d}t_1\, \delta_4\{t_j\}\sin[\zeta(t,t_2)]P_0(t_2,t_1)\cos[\zeta(t_1,t')][Q''(t-t') - Q''(t_2-t')]\,. \tag{312}$$

In these weak-coupling expressions, the first part represents the NIBA. The residual contributions have been written in such a way that the term $P_0(t_2,t_1)$ is sandwiched between two blip-like contributions occurring in the time intervals $t_1 - t'$ and $t - t_2$. The term $P_0(t_2,t_1)$ takes into account all the tunneling transitions of the *undamped* system during the interblip interval $t_2 - t_1$. It reads

$$P_0(t,t_0) = 1 + \sum_{n=1}^{\infty} (-1)^n \int_{t_0}^{t} \mathscr{D}_{2n}\{t_j\}\delta_{2n}\{t_j\}\prod_{j=1}^{n} \cos[\zeta(t_{2j},t_{2j-1})]\,, \tag{313}$$

and it reduces to Eq. (72) in the absence of driving. Note that, accordingly, $P_0(t,t_0)$ satisfies a master equation as in Eq. (291) with kernels $K^{(+)}(t,t') = \Delta(t)\Delta(t')\cos[\zeta(t,t')]$ and $K^{(-)}(t,t') = \Delta(t)\Delta(t')\sin[\zeta(t,t')]$.

The weak-damping form of $\langle\sigma_z\rangle_t$ is obtained from the solution of the GME (291) with the kernels (312) substituted. Again, $\langle\sigma_y\rangle_t$ results by differentiation according to Eq. (293). On the other hand, the weak-damping form of $\langle\sigma_x\rangle_t$ results from the integral relation

$$\langle\sigma_x\rangle_t = \int_{t_0}^{t} \mathrm{d}t'\, \Delta(t')\sin[\zeta(t,t')]\langle\sigma_z\rangle_{t'}\,. \tag{314}$$

The coupled set of Eq. (291) can be investigated by Laplace transformation methodology thereby generalizing the method developed in Refs. [34,32,261] for the static case, and in [222,229] for the driven case.

The case of ac-monochromatic driving modulating the asymmetry energy will be discussed in Section 12.

11.4.3. The interacting-blip chain approximation

In this subsection we briefly describe an approximation beyond the NIBA, which has been introduced only recently [244]. We set $t_0 = 0$. In addition to the NIBA-interactions in Eq. (299), this improved approximation accounts also for the interactions of all nearest-neighbor blip pairs $\Lambda_{j,j-1}$ and the full interactions of the nearest-neighbor sojourn–blip pairs $X_{j,j-1}$ as well. Diagramatically, we then have a chain of blips with nearest-neighbor interactions. Therefore, this approximation has been called the interacting-blip chain approximation (IBCA) [244]. A pictorial description illustrating the chain of interacting blips as considered in the IBCA is sketched in Fig. 16 for the three-blip contribution to $\langle\sigma_z\rangle_t$. In the IBCA, the influence function $\tilde{\Phi}^{(n)}$, cf. Eq. (278), is given by,

$$\tilde{\Phi}^{(n)}_{\mathrm{IBCA}} = \sum_{j=1}^{n} Q'_{2j,2j-1} + \sum_{j=2}^{n} \xi_j\xi_{j-1}\Lambda_{j,j-1} - \mathrm{i}\sum_{j=1}^{n} \xi_j\eta_{j-1}X_{j,j-1} \tag{315}$$

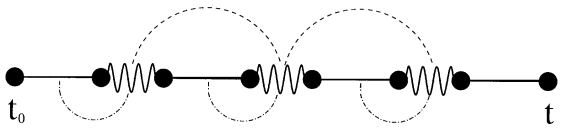

Fig. 16. Three-blip contribution in the IBCA. The solid line represents a sojourn, and the curly line a blip interval. The blip–blip correlations $\Lambda_{j,j-1}$ are sketched by a dashed curve, and the sojourn–blip correlations $X_{j,j-1}$ by a dotted curve. The intrablip interactions as well as the individual contributions in $\Lambda_{j,j-1}$ are not depicted.

with the full nearest-neighbor sojourn–blip interaction reading

$$X_{j,j-1} = Q''_{2j,2j-1} + Q''_{2j-1,2j-2} - Q''_{2j,2j-2} \,. \tag{316}$$

To investigate the dynamics of $\langle \sigma_i \rangle_t$ in the IBCA, one introduces the conditional probabilities $R_+(t;\tau)$ and $R_-(t;\tau)$ for the particle with initial diagonal state $\eta_0 = +1$ to hop at time $t-\tau$ into the final off-diagonal state $\xi_f = +1$ and $\xi_f = -1$, respectively, and afterwards staying there until time t. After that, the period τ left until time t is spent in this off-diagonal state. Upon integrating the conditional probabilities $R_\pm(t;\tau)$ over the period τ, one obtains the off-diagonal elements of the reduced density matrix at time t as

$$\langle \sigma_x \rangle_t = \int_0^t \mathrm{d}\tau [R_+(t;\tau) + R_-(t;\tau)] \,, \tag{317}$$

$$\langle \sigma_y \rangle_t = \mathrm{i} \int_0^t \mathrm{d}\tau [R_+(t;\tau) - R_-(t;\tau)] \,. \tag{318}$$

The quantity $\langle \sigma_z \rangle_t$ is obtained by integrating $\langle \sigma_y \rangle_t$, i.e., from Eq. (293)

$$\langle \sigma_z \rangle_t = 1 - \int_0^t \mathrm{d}t' \, \Delta(t') \langle \sigma_y \rangle_{t'} \,. \tag{319}$$

According to Eqs. (317)–(319), the dynamical problem is solved up to quadratures once the quantities $R_\pm(t';\tau)$ are known in the interval $0 \le t' \le t$. As discussed in [244], the quantities $R_\pm(t';\tau)$ obey inhomogenous coupled integral equations which can be solved numerically by an iteration scheme.

The predictions of the IBCA for both $\langle \sigma_z \rangle_t$ and $\langle \sigma_x \rangle_t$ are compared with those of the NIBA in Fig. 17. Note that, even though low temperatures and moderate damping are assumed, the NIBA provides a fairly good approximation for $\langle \sigma_z \rangle_t$. This holds no longer necessarily true for $\langle \sigma_x \rangle_t$.

11.5. Adiabatic perturbations and weak dissipation

In this section we discuss how to tackle the time-dependent problem for the case of a perturbation which is varying slowly as compared to the time scales of the unperturbed system. Let us consider the Hamiltonian (269) of the form

$$H_{\mathrm{TLS}}(t) = -\tfrac{1}{2}\hbar [\Delta_0 \sigma_x + \varepsilon(t) \sigma_z] \,, \tag{320}$$

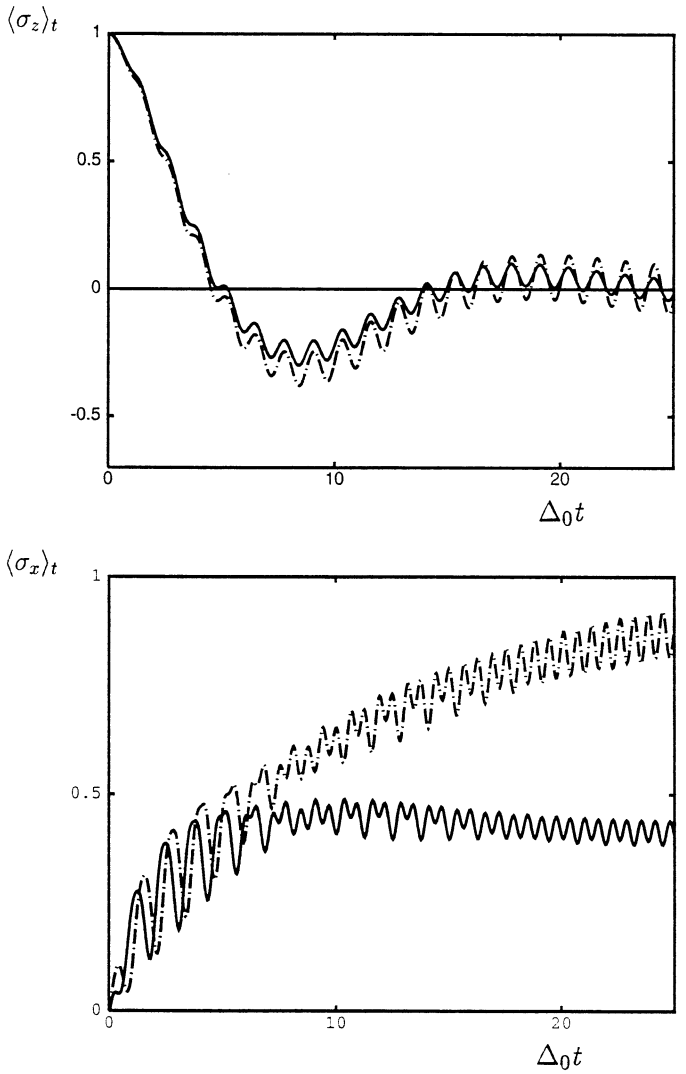

Fig. 17. The population difference $\langle\sigma_z\rangle_t$ between the localized states of a two-level-system and the coherence $\langle\sigma_x\rangle_t$ are depicted for the case of a symmetric TLS ($\varepsilon_0 = 0$) driven by an ac-field $\hat{\varepsilon}\cos(\Omega t)$ and Ohmic dissipation. The field parameters are $\hat{\varepsilon} = 2.5\Delta_0$, $\Omega = 5\Delta_0$, and the dissipation parameters are $\alpha = 0.25$, $k_B T = 0.05\hbar\Delta_0$, i.e., moderate damping and low temperatures. The full-line curve depicts the IBCA prediction and the dash–dotted the NIBA. Minor deviations of the IBCA from the NIBA curve occur for $\langle\sigma_z\rangle_t$ while the differences are drastic for $\langle\sigma_x\rangle_t$. At long times only *odd* harmonics contribute to $\langle\sigma_z\rangle_t$, and only *even* ones to $\langle\sigma_x\rangle_t$.

where

$$|\mathrm{d}\varepsilon(t)/\mathrm{d}t| \ll \Delta_0^2 \,. \tag{321}$$

In this case it is convenient to perform a time-dependent unitary transformation

$$R(t) = \exp\{-\mathrm{i}\theta(t)\sigma_y/2\}, \quad \theta(t) = -\arccot[\varepsilon(t)/\Delta_0] \,, \tag{322}$$

which, at any instant, diagonalizes the time-dependent TLS Hamiltonian in Eq. (320). Taking also into account the TLS interaction term with the bath, the Hamiltonian $H(t)$ in Eq. (270) is transformed into

$$H_{\rm ad}(t) = R(t)H(t)R^{-1}(t) = -\frac{1}{2}E(t)\sigma_z + \frac{\hbar\Delta_0}{E(t)}X\sigma_z + \frac{\hbar\varepsilon(t)}{E(t)}X\sigma_x + H_{\rm B}\,, \tag{323}$$

where $E(t) = \hbar(\Delta_0^2 + \varepsilon^2(t))^{1/2}$ is the adiabatic energy splitting. Due to the explicit time dependence of the transformation (322), however, the transformed Hamiltonian $H_{\rm ad}(t)$ *does not commute* with the transformed time-evolution operator $U_{\rm ad}(t_2,t_1) = \top \exp\{-{\rm i}/\hbar\int_{t_1}^{t_2} {\rm d}t\, H_{\rm eff}(t)\}$. Here,

$$H_{\rm eff}(t) = H_{\rm ad}(t) - {\rm i}\hbar R(t)({\rm d}R^{-1}/{\rm d}t)\,. \tag{324}$$

By evaluating $-{\rm i}\hbar R(t)({\rm d}R^{-1}/{\rm d}t) = (\hbar^3\Delta_0/E^3)({\rm d}\varepsilon(t)/{\rm d}t)$, one readily observes that the second term on the r.h.s. of Eq. (324) can be treated as a perturbation only when inequality (321) holds, i.e., for *adiabatic* driving. Moreover, because of the rotation (322), the bath couples both to σ_z and to σ_x. Thus, the transformation turns out to be useful only if, in addition to adiabaticity, the bath is weakly coupled to the TLS, hence allowing a perturbative expansion in the bath–TLS interaction.

This method will be applied in Section 12.1.2 to evaluate the TLS dynamics for weak dissipation and in the presence of a slow monochromatic field, and in Section 12.5 in the context of the dissipative Landau–Zener–Stückelberg problem.

12. The driven dissipative two-state system (applications)

12.1. Tunneling under ac-modulation of the bias energy

To make quantitative predictions the detailed form of the driving field has to be specified. In this section we shall study the effects of a driving field which *periodically* modulates the bias energy of the undriven TLS. To be definite, we consider a time-dependent TLS of the form

$$H_{\rm TLS}(t) = -\tfrac{1}{2}\hbar\{\Delta_0\sigma_x + [\varepsilon_0 + \hat{\varepsilon}\cos(\Omega t)]\sigma_z\}\,. \tag{325}$$

In the following, we shall focus our attention to the investigation of the position expectation value $P(t) := \langle\sigma_z\rangle_t$ which is the relevant quantity in the context of control of tunneling. The same line of reasoning applies to the quantities $\langle\sigma_x\rangle_t$ and $\langle\sigma_y\rangle_t$.

Before we restrict ourselves to parameter regimes for which the approximations on the bath correlation functions discussed in the previous section apply, we outline some general characteristics of the driven dynamics. We observe that the generalized master equation (291) is conveniently solved by Laplace transformation techniques. Introducing the Laplace transform $\hat{P}(\lambda) = \int_0^\infty {\rm d}t\, {\rm e}^{-\lambda t}P(t)$ of $P(t)$, one obtains

$$\lambda\hat{P}(\lambda) = 1 + \int_0^\infty {\rm d}t\, {\rm e}^{-\lambda t}[\hat{K}_\lambda^{(-)}(t) - \hat{K}_\lambda^{(+)}(t)P(t)]\,, \tag{326}$$

where $\hat{K}_\lambda^{(\pm)}(t) = \int_0^\infty {\rm d}t'\, {\rm e}^{-\lambda t'}K^{(\pm)}(t+t',t)$. In the absence of driving, the kernels $\hat{K}_\lambda^{(\pm)}$ do not depend on time, and Eq. (326) reproduces all the known results in the literature [32,34].

For *periodic* driving the kernels $\hat{K}_\lambda^{(\pm)}(t)$ have the periodicity of the external field, and thus can be expanded in a Fourier series, i.e.,

$$\hat{K}_\lambda^{(\pm)}(t) = \sum_{m=-\infty}^{\infty} k_m^{\pm}(\lambda) \mathrm{e}^{-\mathrm{i}m\Omega t} . \tag{327}$$

This allows for a recursive solution of Eq. (326) [229]. In particular, the asymptotic dynamics is determined by the poles of the recursive solution at $\lambda = \pm \mathrm{i}m\Omega$, where m is an integer number. Thus, the asymptotic dynamics is periodic in time with the periodicity $\mathscr{T} = 2\pi/\Omega$ of the driving force, i.e.,

$$\lim_{t\to\infty} P(t) = P^{(\mathrm{as})}(t) = P^{(\mathrm{as})}(t+\mathscr{T}) = \sum_{m=-\infty}^{\infty} p_m \mathrm{e}^{-\mathrm{i}m\Omega t} , \tag{328}$$

with [229]

$$p_0 = \frac{k_0^-(0)}{k_0^+(0)} - \sum_{m\neq 0} \frac{k_m^+(0)}{k_0^+(0)} p_m , \tag{329}$$

and for $m \neq 0$

$$p_m = \frac{\mathrm{i}}{m\Omega}\left(k_m^-(-\mathrm{i}m\Omega) - \sum_n k_{m-n}^+(-\mathrm{i}m\Omega) p_n \right). \tag{330}$$

From Eqs. (329) and (330) it is found that the asymptotic expectation obeys the integro-differential equation

$$\dot{P}^{(\mathrm{as})}(t) = \mathscr{F}(t) - \frac{\Omega}{2\pi}\int_0^{2\pi/\Omega} \mathrm{d}t' \, P^{(\mathrm{as})}(t') \mathscr{L}(t', t-t') , \tag{331}$$

which describes the time evolution within a period $\mathscr{T}$. Here,

$$\begin{aligned} \mathscr{F}(t) &= \sum_n \mathrm{e}^{-\mathrm{i}n\Omega t} k_n^-(-\mathrm{i}n\Omega) , \\ \mathscr{L}(t,t') &= \sum_{m,n} \mathrm{e}^{-\mathrm{i}m\Omega t} \mathrm{e}^{-\mathrm{i}n\Omega t'} k_m^+(-\mathrm{i}n\Omega) . \end{aligned} \tag{332}$$

This result is still *exact*. It explicitly shows that also the asymptotic-driven dynamics is intrinsically *non-Markovian*, and is not invariant under continuous-time translations.

An analysis of the symmetry properties of the kernels $\hat{K}_\lambda^{(\pm)}$ upon inverting the bias $\varepsilon \to -\varepsilon$, depicts selection rules for the harmonics p_m. From Eq. (330) it follows that for a symmetric TLS, i.e., if $\varepsilon_0 = 0$, in the presence of monochromatic driving only the *odd* harmonics of $\langle \sigma_z \rangle_t$ are different from zero [229]. This is known to hold true also in classical systems [262]. In the same way, $\langle \sigma_x \rangle_t$ and $\langle \sigma_y \rangle_t$ obey selection rules. Namely, only the *even* harmonics of $\langle \sigma_x \rangle_t$ and the odd harmonics of $\langle \sigma_y \rangle_t$ are different from zero if $\varepsilon_0 = 0$.

12.1.1. Control of tunneling within the NIBA

Let us next consider the dynamics of $P(t)$ within the NIBA. For the case of monochromatic driving the functions $k_m^{\pm}$ can be explicitly evaluated to yield [229]

$$k_m^{\pm}(\lambda) = \Delta_0^2 \int_0^{\infty} \mathrm{d}\tau \, \mathrm{e}^{-\lambda\tau} h^{(\pm)}(\tau) A_m^{\pm}(\tau) \,, \tag{333}$$

where the functions $h^{(\pm)}(t)$ have been introduced earlier in Eq. (308), and where

$$\begin{aligned} A_{2m}^{-}(\tau) &= (-1)^m \mathrm{e}^{-\mathrm{i}m\Omega\tau} \sin(\varepsilon_0\tau) J_{2m}\left(\frac{\hat{\varepsilon}}{\Omega} \sin\frac{\Omega\tau}{2}\right), \\ A_{2m+1}^{-}(\tau) &= (-1)^m \mathrm{e}^{-\mathrm{i}(m+1/2)\Omega\tau} \cos(\varepsilon_0\tau) J_{2m+1}\left(\frac{2\hat{\varepsilon}}{\Omega} \sin\frac{\Omega\tau}{2}\right). \end{aligned} \tag{334}$$

Here $J_m(z)$ denotes the ordinary Bessel function of order m, and

$$\begin{aligned} A_{2m}^{+}(\tau) &= (-1)^m \mathrm{e}^{-\mathrm{i}m\Omega\tau} \cos(\varepsilon_0\tau) J_{2m}\left(\frac{2\hat{\varepsilon}}{\Omega} \sin\frac{\Omega\tau}{2}\right), \\ A_{2m+1}^{+}(\tau) &= (-1)^{m+1} \mathrm{e}^{-\mathrm{i}(m+1/2)\Omega\tau} \sin(\varepsilon_0\tau) J_{2m+1}\left(\frac{2\hat{\varepsilon}}{\Omega} \sin\frac{\Omega\tau}{2}\right). \end{aligned} \tag{335}$$

Hence, knowledge of the functions $k_m^{\pm}$ allows a spectral investigation of the asymptotic dynamics; cf. the study of nonlinear Quantum Stochastic Resonance as in Section 12.1.4, or the phenomenon of dynamical hysteresis as in Section 14.3.

Some characteristics of the driven dynamics obtained by a numerical integration of the NIBA master equation are shown in Figs. 18 and 19. The bath is assumed to have an Ohmic spectrum with an exponential cutoff as in Eq. (294), i.e.,

$$J(\omega) = (2\pi\hbar/d^2)\alpha\omega \mathrm{e}^{-\omega/\omega_c} \,. \tag{336}$$

In Fig. 18, some general effects of dissipation (dashed curve), and of dissipation-plus-driving (dot-dashed curve) on the undriven and undamped coherent tunneling dynamics (full-line curve) are shown. Dissipation tends to destroy quantum coherence and, at long times, in the absence of driving, the stationary equilibrium value P_{st} is reached. When an additional driving field is acting, the driven and dissipative motion becomes periodic at long time, the resulting dynamics being governed by Eq. (331). In Fig. 19 is depicted that driving-induced correlations may lead, for example, to large amplitude oscillations in the asymptotic dynamics of a strongly biased, $\varepsilon_0 \gg \Delta_0$, TLS: The long-time dynamics being almost localized in the absence of driving becomes strongly delocalized in the presence of driving, i.e., in general is $P_{\mathrm{st}} \neq \langle P^{(\mathrm{as})}(t) \rangle_{\mathscr{T}} = p_0$. Moreover, a fine *resonance* structure may be superimposed onto the oscillatory behavior. For large asymmetries ε_0 the number n of resonances is given by the ratio $n = \varepsilon_0/\Omega$. This phenomenon may be interpreted as a multiphoton absorption or emission process at the proper frequencies of the TLS. As the temperature, or the coupling strength, are increased, this coherent oscillatory behavior is smoothed out by bath-induced incoherent transitions (not shown).

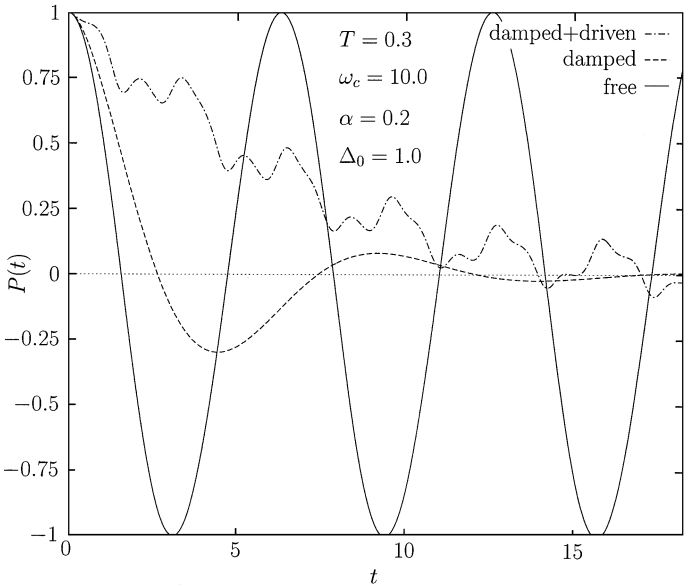

Fig. 18. Influence of dissipation and driving on the tunneling dynamics of a symmetric, $\varepsilon_0 = 0$, two-level-system. Depicted is the population difference $P(t) := \langle \sigma_z \rangle_t$ between the localized states. For comparison, are depicted also the nondissipative, undriven coherent tunneling case (solide line), and the Ohmic damped, undriven case (dashed curve). The influence of dissipation results in a decay of quantum coherence towards equal populations of the localized states. The effect of an additional ac-field $\hat{\varepsilon}\cos(\Omega t)$ results in an oscillatory relaxation towards an asymptotic, periodic long-time dynamics (dot-dashed curve). The chosen driving parameters are $\Omega = 2$ and $\hat{\varepsilon} = 6$. Frequencies are given in units of Δ_0, temperatures in units of $\hbar\Delta_0/k_B$.

As shown by Eq. (300) or Eqs. (326) and (331) the transient dynamics, as well as the long-time dynamics, depend on an intriguing interplay between the stochastic and the external driving forces. In the following we shall first briefly discuss the linear response limit of Eqs. (329) and (330), being valid for *any* angular driving frequency Ω. Subsequently, we release the assumption of weak external fields and we study the nonlinear dynamics in different parameter regimes.

12.1.1.1. Linear response approximation. On the assumption that the driving force is weak, Eqs. (329) and (330) can be evaluated by linearizing them in the amplitude $\hat{\varepsilon}$ of the time-dependent force. To linear order in $\hat{\varepsilon}$, only the coefficients $k_m^{\pm}$ with $m = 0, \pm 1$ contribute. Further, the linearized coefficients $k_0^{\pm(0)}$ are of order zero in $\hat{\varepsilon}$, while the coefficients $k_1^{\pm(1)}$ are of order $\hat{\varepsilon}$. In terms of these linearized coefficients, and of the zeroth-order function

$$v(\Omega, \varepsilon_0) = \Delta_0^2 \int_0^\infty \mathrm{d}\tau \, \mathrm{e}^{\mathrm{i}\Omega\tau} h^{(+)}(\tau) \cos(\varepsilon_0 \tau) \,, \tag{337}$$

one finds for the linear susceptibility $\tilde{\chi}(\Omega)$ to $\langle \sigma_z \rangle_t$, i.e., for

$$\tilde{\chi}(\Omega) = \frac{\mathrm{i}}{4\hbar} \int_{-\infty}^{\infty} \mathrm{d}\tau \, \theta(\tau) \langle [\sigma_z(\tau), \sigma_z(0)] \rangle_\beta \,, \tag{338}$$

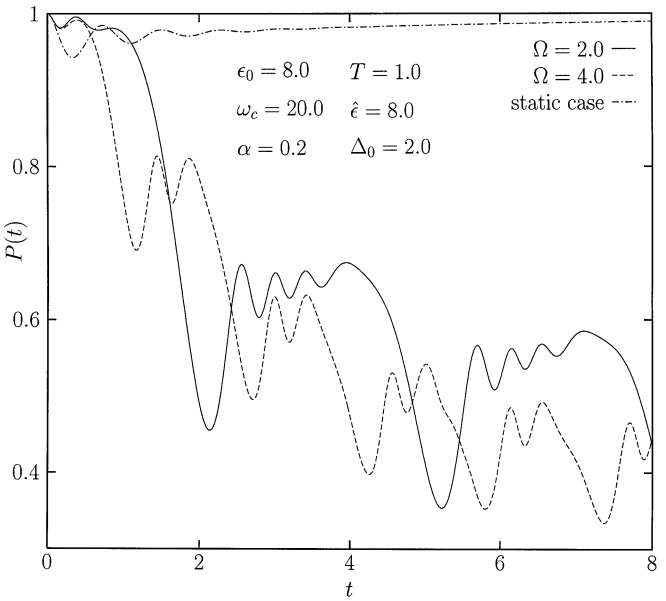

Fig. 19. Driven and damped dynamics of a biased, $\varepsilon_0 \neq 0$, two-level-system. Large amplitude oscillations in the long-time dynamics of the population difference $P(t) := \langle \sigma_z \rangle_t$ are induced by a monochromatic field of intensity $\hat{\varepsilon}$ and intermediate frequency Ω. Ohmic dissipation is considered. For comparison, the dissipative behavior in the absence of driving (static case) is also shown. The fine resonance structure can be interpreted as the result of multiphoton absorption or emission at the proper frequency of the TLS: the number n of resonances observed satisfies the relation $n = \varepsilon_0/\Omega$, where $\hbar\varepsilon_0$ is the static asymmetry energy of the TLS. Frequencies are in units of $\delta = \Delta_0/2$, temperatures in units of $\hbar\delta/k_B$.

the result [229]

$$\tilde{\chi}(\Omega) = \frac{1}{\hbar\hat{\varepsilon}[-\mathrm{i}\Omega + v(\Omega, \varepsilon_0)]}\left(k_1^{-(1)}(-\mathrm{i}\Omega) - k_1^{+(1)}(-\mathrm{i}\Omega)\frac{k_0^{-(0)}(0)}{k_0^{+(0)}(0)}\right). \tag{339}$$

In Eq. (338), $\theta(\tau)$ is the Heaviside function, $[\,,]$ denotes the commutator and $\langle\,\rangle_\beta$ the thermal average of the full system in the absence of the external periodic force ($\hat{\varepsilon} = 0$). This susceptibility leads for the asymptotic expectation to the linear response result

$$P^{(\mathrm{as})}(t) = P_{\mathrm{st}} + \hbar\hat{\varepsilon}[\tilde{\chi}(\Omega)\mathrm{e}^{-\mathrm{i}\Omega t} + \tilde{\chi}(-\Omega)\mathrm{e}^{\mathrm{i}\Omega t}]\,, \tag{340}$$

where $P_{\mathrm{st}} = \tanh(\hbar\varepsilon_0/2k_BT) = k_0^{-(0)}(0)/k_0^{+(0)}(0)$, with $k_0^{+(0)}(0) = \Gamma_0$, cf. Eq. (306). This result, within NIBA, holds for any driving frequency Ω.

It is now interesting to observe that for low enough frequencies $\Omega \to 0$, one can linearize (in Ω) the integrals defining $v(\Omega, \varepsilon_0)$ and the linearized coefficients $k_1^{\pm(1)}(-\mathrm{i}\Omega)$. We obtain $v(\Omega, \varepsilon_0) \simeq v(0, \varepsilon_0) = k_0^{+(0)}(0)$ together with

$$\begin{aligned} k_1^{-(1)}(-\mathrm{i}\Omega) &\simeq k_1^{-(1)}(0) = \frac{\hat{\varepsilon}}{2}\frac{\mathrm{d}}{\mathrm{d}\varepsilon_0}k_0^{-(0)}(0)\,, \\ k_1^{+(1)}(-\mathrm{i}\Omega) &\simeq k_1^{+(1)}(0) = \frac{\hat{\varepsilon}}{2}\frac{\mathrm{d}}{\mathrm{d}\varepsilon_0}k_0^{+(0)}(0)\,. \end{aligned} \tag{341}$$

Hence, within this adiabatic limit the linear susceptibility is readily found to assume a *Lorentzian* form, i.e.,

$$\tilde{\chi}(\Omega) \simeq \tilde{\chi}_{\rm ad}(\Omega) = \frac{1}{4k_{\rm B}T}\,\frac{1}{\cosh^2(\hbar\varepsilon_0/2k_{\rm B}T)}\,\frac{1}{1-{\rm i}\Omega\Gamma_0^{-1}}\,. \tag{342}$$

If the specific form, Eq. (336), of the Ohmic interaction is assumed, in the temperature regime $\hbar\omega_{\rm c} \gg k_{\rm B}T$, the adiabatic condition reads $\hbar\Omega \ll 2\pi\alpha k_{\rm B}T$.

12.1.1.2. Markovian regime. In the following we discuss the Markovian limit $\tau_{\rm K}(\Omega,\hat{\varepsilon}) \ll \{\mathscr{T}, \Gamma_{\rm H}^{-1}, \dots\}$. Here $\tau_{\rm K}$ is the characteristic memory time of the kernels of Eq. (290) which describe the influence of the environment and of the driving. That is, we assume that $\tau_{\rm K}$ is the smallest time scale of the problem. It should be e.g. smaller than the driving period $\mathscr{T}$, or of the average decay time $\Gamma_{\rm H}^{-1}$. We denoted by $\Gamma_{\rm H} := k_0^+(\lambda = 0)$, cf. Eq. (333), the average of the time-dependent relaxation rate $\Gamma_{\rm M}(t)$ governing the transient *long-time* dynamics, cf. Eqs. (344) and (351) below. The restriction on the frequency arises from an analysis of the poles of the exact NIBA equation (326). As discussed above, the long-time dynamics is dominated by the poles of $\hat{P}(\lambda)$ at $\lambda = \pm {\rm i}m\Omega$ (with m an integer number), leading to the integro-differential equation (331) for the asymptotic periodic dynamics. In the regime $\Omega \ll \tau_{\rm K}^{-1}$ the driving field is sufficiently slow that, to leading order, driving-induced non-Markovian correlations do not contribute to the long-time dynamics [221,229].

In the Markovian limit, the long-time behavior, within the NIBA, is intrinsically incoherent and the Markovian approximation $P_{\rm M}(t)$ to $P(t)$ obeys the rate equation

$$\dot{P}_{\rm M}(t) = -\Gamma_{\rm M}(t)[P_{\rm M}(t) - P_{\rm M,ns}(t)]\,, \tag{343}$$

with the time-dependent rate given by

$$\Gamma_{\rm M}(t) = \Delta_0^2 \int_0^\infty {\rm d}\tau\, h^{(+)}(\tau)\cos[\zeta(t,t-\tau)]\,, \tag{344}$$

with $\zeta(t,t') = \int_{t'}^t {\rm d}t''\,\varepsilon(t'')$. The time-dependent, nonstationary quantity $P_{\rm M,ns}(t)$ is given by

$$P_{\rm M,ns}(t) = \rho_{\rm M}(t)/\Gamma_{\rm M}(t)\,, \tag{345}$$

where $\rho_{\rm M}(t)$ reads

$$\rho_{\rm M}(t) = \Delta_0^2 \int_0^\infty {\rm d}\tau\, h^{(-)}(\tau)\sin[\zeta(t,t-\tau)]\,. \tag{346}$$

In the limit $\hat{\varepsilon} \to 0$ the rate $\Gamma_{\rm M}(t)$ reduces to the static rate Γ_0 in Eq. (306). Eq. (343) is readily solved in terms of quadratures [221,229]. Note that, in general, $\Gamma_{\rm M}(t) \neq \lim_{\lambda\to 0}\hat{K}_\lambda^{(+)}(t)$, and $\rho_{\rm M}(t) \neq \lim_{\lambda\to 0}\hat{K}_\lambda^{(-)}(t)$. This holds true *only* in the adiabatic limit $(\Omega\tau_K) \to 0$, for which

$$\zeta(t,t-\tau) \to \tau\varepsilon(t), \quad P_{\rm M,ns}(t) \to \tanh[\hbar\beta\varepsilon(t)/2] := P_{\rm ad,ns}\,. \tag{347}$$

Hence, in this adiabatic limit $\varepsilon(t)$ behaves like a time-dependent asymmetry, and an adiabatic detailed balance condition is fulfilled in analogy with the static case. In general, however, the detailed balance condition *does not* hold in the presence of driving; see also point (v) in the next section for the case of a high-frequency field.

In Fig. 20 the predictions of the Markovian approximation given by Eq. (343) are compared with those of the exact NIBA equation (300) for the case of moderately small Ohmic friction, see Eq. (294). The predictions of the high-frequency non-Markovian approximation (348) discussed in the next subsection are also depicted. In Fig. 20a, a moderate driving frequency $\Omega = \Delta_0 = \varepsilon_0/4$ is considered. For these parameters the Markovian approximation (343) is very good. The frequency is increased to $\Omega = 15\Delta_0$ in Fig. 20b. In this latter parameter regime the Markovian approximation breaks down but the high-frequency approximation (350) discussed in the next section describes well the non-Markovian dynamics.

12.1.1.3. High-frequency regime. In the high-frequency regime $\Omega \gg \{\Gamma_{\rm H}, \varepsilon_0, \Delta_0\}$, the driving field oscillates too fast to account for the details of the dynamics within one period. Hence, a first approximation to the true dynamics described by Eq. (300) amounts to approximate the kernels $K^{\pm}(t,t')$ in Eq. (300) with their average $\langle K^{(\pm)}(t,t')\rangle_{\mathscr{T}} := K_0^{(\pm)}(t-t')$ over a period [or $\hat{K}_\lambda^{(\pm)}(t)$ in Eq. (326) with their corresponding averages $k_0^{\pm}(\lambda)$ given by the term with $m=0$ in Eq. (333)]. Hence, the essential dynamics of $P(t)$ is described by $\langle P(t)\rangle_{\mathscr{T}} := P_{\rm H}(t)$ [222,227–229,236]. Time translation invariance is recovered by such an averaging procedure, and the resulting equation for $P_{\rm H}(t)$ obtained from Eq. (291) is of *convolutive* form. It reads

$$\dot{P}_{\rm H}(t) = -\int_0^t {\rm d}t' K_0^{(+)}(t-t') P_{\rm H}(t') + \int_0^t {\rm d}t' K_0^{(-)}(t-t')\,. \tag{348}$$

From Eq. (326) one obtains (for convenience we explicitly indicate the field dependence of the kernels $k_0^{\pm}(\lambda)$),

$$\hat{P}_{\rm H}(\lambda) = \frac{1 + k_0^{-}(\lambda,\hat{\varepsilon})/\lambda}{\lambda + k_0^{+}(\lambda,\hat{\varepsilon})}\,. \tag{349}$$

From Eqs. (348) and (349) some useful and insightful features of the high-frequency driving dynamics can be discussed.

(i) A high-frequency field suppresses the periodic long-time oscillations, and [as seen by approximating $k_0^{\pm}(\lambda) \simeq k_0^{\pm}(0)$] the driven TLS satisfies at *long times* the rate equation

$$\dot{P}_{\rm H}(t) = -\Gamma_{\rm H}[P_{\rm H}(t) - P_{\rm H,ns}]\,, \tag{350}$$

where $P_{\rm H,ns} = k_0^{-}(0)/k_0^{+}(0)$ is the averaged nonstationary equilibrium value at high frequencies. The high-frequency relaxation rate $k_0^{+}(0) := \Gamma_{\rm H}$ is given by

$$\Gamma_{\rm H} = \Delta_0^2 \int_0^\infty {\rm d}\tau\, h^{(+)}(\tau)\cos(\varepsilon_0\tau) J_0\!\left(\frac{2\hat{\varepsilon}}{\Omega}\sin\frac{\Omega\tau}{2}\right). \tag{351}$$

Note that $\Gamma_{\rm H} = \langle \Gamma_{\rm M}(t)\rangle_{\mathscr{T}}$, with $\Gamma_{\rm M}(t)$ the Markovian rate of Eq. (343). From Eq. (350) we may conclude that for high-frequency monochromatic driving the long-time behavior is governed within a good approximation by a Markovian dynamics.

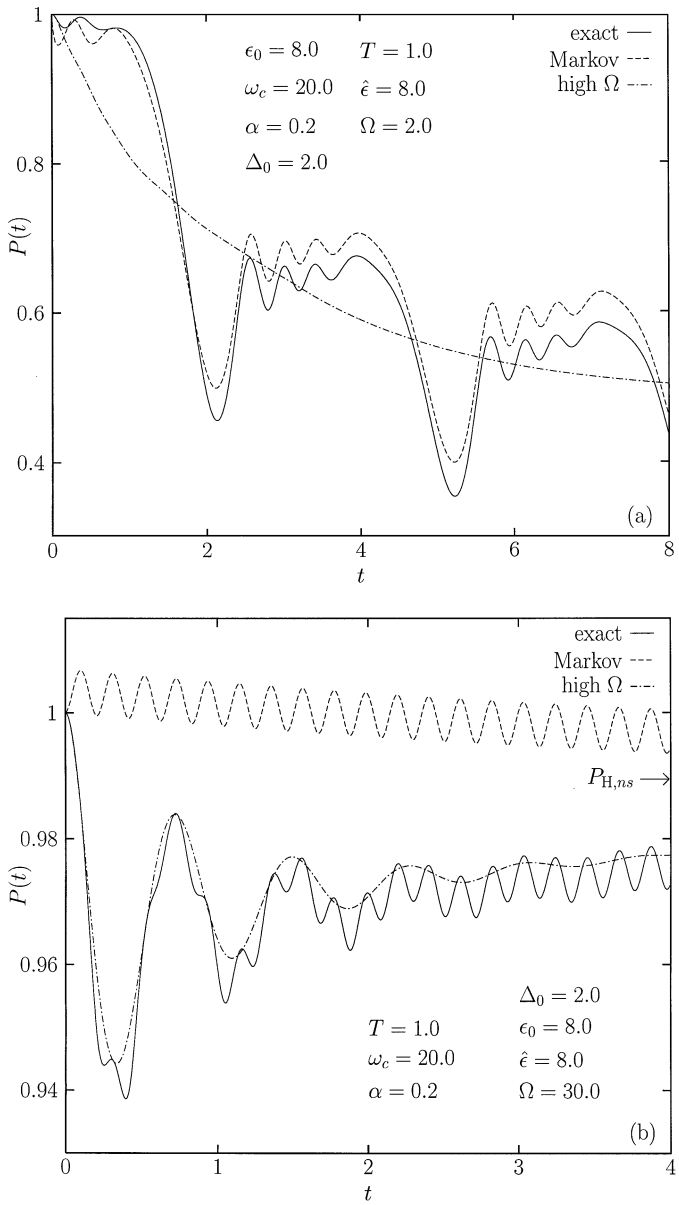

Fig. 20. Comparison between the predictions of the NIBA equations (291) and (303) for the population difference $P(t) := \langle \sigma_z \rangle_t$ and those of the Markovian and high-frequency approximations (343) and (350), respectively. Ohmic dissipation is considered. Frequencies are in units of $\delta = \Delta_0/2$, temperatures in units of $\hbar\delta/k_{\mathrm{B}}$. Panel (a) A monochromatic field of intermediate frequency $\Omega = \Delta_0 = \varepsilon_0/4$ is used. Panel (b) The frequency is increased to be $\Omega = 15\Delta_0$. In this latter case the Markovian approximation breaks down, but the non-Markovian high-frequency approximation (350) describes the dynamics well.

(ii) Note, however, that while Eq. (348) constitutes a valid approximation to investigate the high-frequency, transient dynamics, it misses the periodic oscillations around the asymptotic mean value $P_{\mathrm{H,ns}}$. Going beyond the simple approximation (348), one obtains to leading order in $|k_m^+(\mathrm{i}n\Omega)|/\Omega \ll 1$ the result [229]

$$P^{(\mathrm{as})}(t) = P_{\mathrm{H,ns}} + \sum_{m\neq 0} p_m(\Omega)\,\mathrm{e}^{-\mathrm{i}m\Omega t}\,,$$
$$p_m(\Omega) = \frac{\mathrm{i}}{m\Omega}[k_m^-(-\mathrm{i}m\Omega) - k_m^+(-\mathrm{i}m\Omega)P_{\mathrm{H,ns}}]\,. \tag{352}$$

(iii) Eq. (350) may be used to investigate the modification of the transfer rate Γ_{H} as compared to the static one Γ_0. This issue is prominent in the context of control of chemical reaction. In the case of long-range electron transfer (ET) reactions [227,228,236], for example, Γ_{H} determines the transfer rate between the donor and acceptor states.

Let us consider the case of Ohmic dissipation in Eq. (294). As a first feature, because $|J_0(z)| \leq 1$, it is apparent that for a symmetric TLS the effect of a fast asymmetry modulation results in an overall reduction of the incoherent tunneling rate Γ_{H} as compared to the Ohmic static one Γ_0, cf. Eq. (309), whenever $\alpha < \frac{1}{2}$.

Secondly, the relaxation rate can be controlled by appropriately choosing the external field parameters. To see this, it is convenient to expand the high-frequency rate into Fourier series as

$$\Gamma_{\mathrm{H}} = \sum_{n=-\infty}^{\infty} J_n^2(\hat{\varepsilon}/\Omega)\Gamma_0(\varepsilon_0 + n\Omega)\,, \tag{353}$$

where Γ_0 is the static rate (306). Hence, via photon absorption or emission the ac-field opens new tunneling channels, each weighted by the Bessel function $J_n^2(\hat{\varepsilon}/\Omega)$. As shown in Fig. 21, the rate might be enhanced as compared to the static case when the resonance condition $\varepsilon_0 = n\Omega$ is fulfilled, and when the corresponding channel has a nonzero weight $J_n^2(\hat{\varepsilon}/\Omega)$. Vice versa, as shown in the inset of Fig. 21, Γ_{H} can become strongly suppressed.

(iv) As first discovered in [201,202], a fast monochromatic field can *stabilize* localized states without much fine-tuning of external conditions. Some numerical results obtained in [201,202] by using the tensor propagator method discussed in Section 10.2 are shown in Fig. 22, where the decay rate Γ is depicted as a function of the Ohmic coupling parameter α. In contrast to the undriven case (dashed curve), it is shown that the decay rate Γ is largely independent on the dimensionless Ohmic coupling parameter α and on the driving frequency Ω, depending mainly on the driving strength $\hat{\varepsilon}$. A similar behavior is also demonstrated in [201] for the case of a super-Ohmic bath. Finally note that, as confirmed in [201,202], the high-frequency NIBA rate Γ_{H} represents an extremely good approximation to the exact numerical rate Γ in the parameter regime considered for the numerical calculations.

(v) Eq. (350) also leads to the possibility of *inversion* of asymptotic populations of the localized states of the TLS by a fast ac-field. This feature again entails important applications as, for example, the possible inversion of the direction of long-range electron-transfer chemical reactions [228,236]. This fact relies on the observation that, in the presence of a fast ac-field, the detailed-balance condition between the forward $\Gamma_{\mathrm{f}} = (k_0^+(0) + k_0^-(0))/2$, and backward $\Gamma_{\mathrm{b}} =$

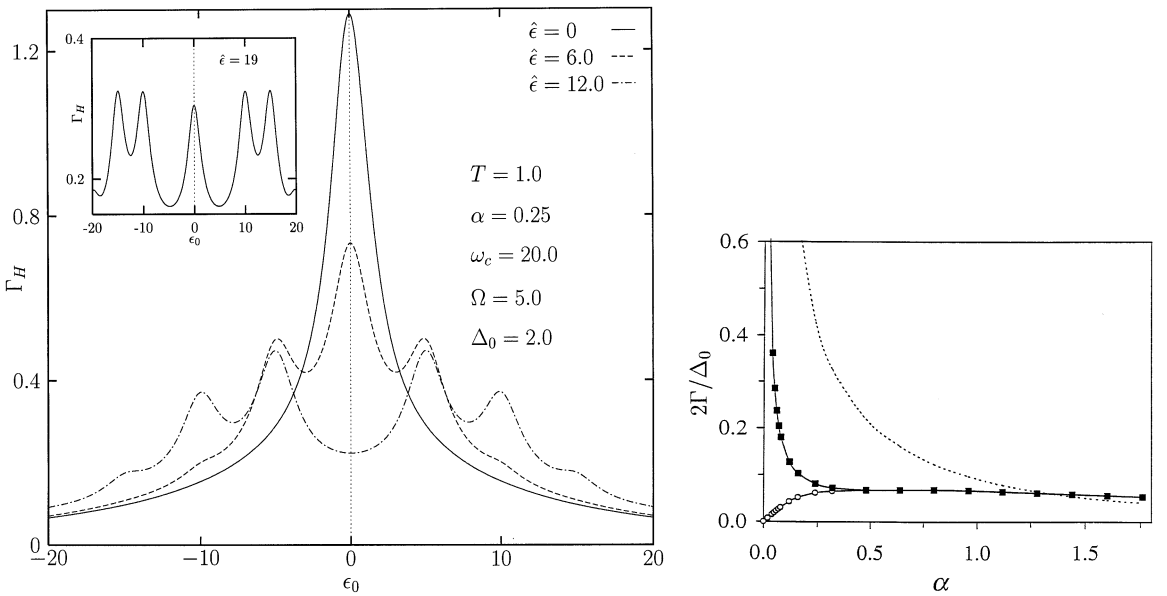

Fig. 21. Dependence of the high-frequency rate $\Gamma_{\rm H}$ of a driven and Ohmically damped TLS vs. the static asymmetry ε_0. The peaks at $\varepsilon_0 = n\Omega$ describe photon absorption or emission processes. In the inset the amplitude $\hat{\varepsilon}$ of the ac-field is chosen such that the Bessel function $J_1(\hat{\varepsilon}/\Omega)$ vanishes; hence, the first resonance peak disappears. Frequencies are in units of $\delta = \Delta_0/2$, temperatures in units of $\hbar\delta/k_{\rm B}$.

Fig. 22. Numerical results obtained by using the QUAPI method for the decay rate Γ of a dissipative TLS driven by a high frequency ac-field vs. the Ohmic coupling parameter α. In contrast to the undriven case (dotted line), the high frequency rate is largely *independent* of the parameters of the environment and of the driving frequency, depending only on the driving strength. The dissipative parameters are $k_{\rm B}T = 5\hbar\Delta_0$, and $\omega_{\rm c} = 10\Delta_0$. Moreover, the solid squares indicate results for a generic ac-field with $\hat{\varepsilon} = 30\Delta_0$, $\Omega = 7.5\Delta_0$ while the hollow circles refer to parameters such that CDT occurs in the absence of dissipation, i.e., $\hat{\varepsilon} = 30\Delta_0$, $\Omega = 5.44\Delta_0$. In this parameter regime the decay rate Γ is analytically well approximated by the high-frequency NIBA rate $\Gamma_{\rm H}$ (not shown).

$(k_0^+(0) - k_0^-(0))/2$ rates does not hold anymore true. The destruction of detailed balance by a strong periodic field may be characterized by an effective energy bias, i.e.,

$$\hbar\varepsilon_{\rm eff} = k_{\rm B}T \ln(\Gamma_{\rm f}/\Gamma_{\rm b})\,. \tag{354}$$

In the limit of vanishing field $\hat{\varepsilon} \to 0$, this apparent bias $\varepsilon_{\rm eff}$ coincides with the static bias ε_0.

(vi) Eq. (349) yields information on both the transient and the long-time dynamics of the TLS. Hence, it can be used to investigate the modification of the quantum coherent motion of the isolated TLS by thermal and external driving forces [225,226,238]. Here we restrict ourselves to the case of a symmetric TLS, i.e., $\varepsilon_0 = 0$, and of Ohmic dissipation (294), and study the poles of (349) resulting from the equation $\lambda + k_0^+(\lambda;\hat{\varepsilon}) = 0$ in the high-frequency regime $\Omega \gg 2\pi\alpha k_{\rm B}T/\hbar, \Delta_0$. We refer to [226] for a discussion of the influence of a phononic bath where $J(\omega) \propto \omega^3$. For our purposes it is convenient to express the kernels $k_0^+(\lambda;\hat{\varepsilon})$ in terms of the static one

$\mathscr{K}(\lambda) := \lim_{\varepsilon \to 0} k_0^+(\lambda;\hat{\varepsilon})$ as

$$k_0^+(\lambda;\hat{\varepsilon}) = \sum_{n=-\infty}^{\infty} J_n^2(\hat{\varepsilon}/\Omega)\mathscr{K}(\lambda + in\Omega)\,, \tag{355}$$

where, when $\alpha < 1$ [34,32],

$$\mathscr{K}(\lambda) = \frac{\Delta_e}{\pi}\left(\frac{\hbar\beta\Delta_e}{2\pi}\right)^{1-2\alpha} \frac{\Sigma(\lambda)}{\alpha + \hbar\beta\lambda/2\pi}\,, \tag{356}$$

$$\Sigma(\lambda) = \Gamma(1 + \alpha + \hbar\beta\lambda/2\pi)/\Gamma(1 - \alpha + \hbar\beta\lambda/2\pi)\,. \tag{357}$$

In Eq. (356) above, $\Gamma(z)$ denotes the Gamma function, and Δ_e is the bath-renormalized tunneling splitting when $\alpha < 1$, cf. Eq. (310). Here we made the high cutoff approximation $\omega_c\tau \gg 1$, $\hbar\omega_c \gg k_B T$ in the correlation functions $Q'(\tau)$ and $Q''(\tau)$ given in Eq. (295). The above expression (356) is valid for any value $\alpha < 1$ of the coupling constant α. Using Eq. (356), the pole equation predicts for the static case with $\alpha \leq \frac{1}{2}$ a destruction of quantum coherence by bath-induced incoherent transitions above a transition temperature $T^*(\alpha)$ [32,34]. For $\alpha \geq \frac{1}{2}$ the dynamics is incoherent down to $T = 0$. For weak Ohmic damping $\alpha \ll 1$ one obtains from Eq. (357) that $\Sigma(\lambda) \simeq 1$. Hence, the pole equation becomes just a quadratic equation in λ and the transition temperature is determined by the condition of the solutions being real and degenerate [32,34]. Such a situation is strongly modified if the additional influence of an ac-field is considered. Taking into account the high-frequency condition $\Omega \gg 2\pi\alpha k_B T/\hbar, \Delta_0$, up to the order $O((2\pi\alpha k_B T/\hbar\Omega)^4)$, $O((\Delta_0/\Omega)^4)$, and for $\alpha \ll 1$, one finds [238]

$$k_0^+(\lambda;\hat{\varepsilon}) = \mathscr{K}(\lambda)\left[J_0^2(\hat{\varepsilon}/\Omega) + \left(\frac{\alpha + \hbar\beta\lambda/2\pi}{\hbar\beta\Omega/2\pi}\right)^2 \sum_{n\neq 0} \frac{J_n^2(\hat{\varepsilon}/\Omega)}{n^2}\right]. \tag{358}$$

This equation is very useful to understand the role of driving fields on the tunneling dynamics. Its two parts act in fact in preserving or suppressing quantum coherence, respectively. When the first contribution dominates, the effect of a fast field essentially results in renormalizing Δ_0 as

$$\Delta_0 \to \Delta_{\text{eff}} = \Delta_0 J_0(\hat{\varepsilon}/\Omega)\,, \tag{359}$$

in accordance with the results for the undamped TLS, cf. Eq. (99). In turn, the effective tunneling matrix element Δ_e in Eq. (310) is renormalized as $\Delta_e \to \Delta_{\text{eff},e} = \Delta_e |J_0(\hat{\varepsilon}/\Omega)|^{1/1-\alpha}$, $\alpha < 1$. Hence, from static considerations, one finds the transition temperature $T^*_{\text{eff}}(\alpha) \simeq \hbar\Delta_{\text{eff},e}/\pi\alpha k_B$ when $\alpha \ll 1$. Because $T^*_{\text{eff}}(\alpha) \leq T^*(\alpha)$, the effect of asymmetry driving results in an overall reduction of quantum coherence [225,238]. Near the zeros of $J_0(\hat{\varepsilon}/\Omega)$ quantum coherence is strongly suppressed and the particle tunnels incoherently with the rate $\Gamma_H = \Gamma_0(2\pi\alpha/\hbar\beta\Omega)^2 \sum_{n\neq 0} J_n^2(\hat{\varepsilon}/\Omega)/n^2$ down to $T = 0$.

We finally remark that, in contrast to the Ohmic case, for a phononic bath with $J(\omega) \propto \omega^3$, the decay rate decreases proportional to J_0^2 when $J_0(\hat{\varepsilon}/\Omega) \simeq 0$; at the same time the driving-renormalized tunneling frequency decreases still linearly with J_0 [226]. Hence, only (damped) quantum coherence survives near the zeroes of J_0.

(vii) Eq. (349) gives also information on the effects of dissipation on the coherent destruction of tunneling (CDT) in a symmetric TLS induced by a fast ac-field, cf. Section 3.2.2

[24,67–72,191,192]. The condition $J_0(\hat{\varepsilon}/\Omega) = 0$ was found to be the necessary, but not sufficient [67], criterion for CDT in the case of a driven TLS in the absence of dissipation [24,67–72]. In the presence of (weak) Ohmic dissipation, it can be deduced from the discussion in (iv) that, because $\Gamma_{\rm H} < \Gamma_0 \ll \Omega$, suppression of tunneling may be stabilized over several periods of the driving force in accordance with previous findings [191,192]. The same phenomenon is found to happen for a super-Ohmic phonon bath [226].

12.1.2. Quantum coherence for weak dissipation and low temperatures

At low temperatures, weak dissipation and nonzero static bias, the NIBA breaks down because inter-blip correlations contribute to linear order in the spectral density $J(\omega)$. Hence, in this regime the tunneling dynamics needs to be investigated using approximation schemes different from the NIBA.

12.1.2.1. High-frequency regime. Using the weak coupling expressions (312), the transient driven dynamics in the high-frequency regime $\Omega \gg \Gamma_{\rm H}, \Delta, \varepsilon_0$ described by $P_{\rm H}(t)$ has been investigated in Refs. [222,245]. Here, as in Eq. (349) above, $P_{\rm H}(t)$ denotes the quantum expectation value of σ_z averaged over the fast driving field, and $\Gamma_{\rm H}$ is the high frequency relaxation rate, cf. Eq. (364) below. In this high-frequency regime the Laplace transform of $P_{\rm H}(t)$ formally obeys the same equation as Eq. (349), so that again the resulting dynamics is conveniently solved by Laplace transformation. We can identify two different parameter regimes.

(i) Within the regime $\Omega \gg \hat{\varepsilon}$, the *undamped* driven system is characterized by three bias frequencies, $\varepsilon_1 = \varepsilon_0; \varepsilon_2 = \varepsilon_0 + \Omega; \varepsilon_3 = \varepsilon_0 - \Omega$, and by three tunneling frequencies ν_1, ν_2, and ν_3. The square of these frequencies are the solutions of a cubic equation in ν^2, namely, $\nu^6 - a_4\nu^4 + a_2\nu^2 - a_0 = 0$. The coefficients are

$$\begin{aligned} a_0 &= \varepsilon_1^2\varepsilon_2^2\varepsilon_3^2 + [\Delta_1^2\varepsilon_2^2\varepsilon_3^2 + \Delta_2^2\varepsilon_1^2\varepsilon_3^2 + \Delta_3^2\varepsilon_1^2\varepsilon_2^2]\,, \\ a_2 &= [\Delta_1^2(\varepsilon_2^2 + \varepsilon_3^2) + \varepsilon_2^2\varepsilon_3^2] + [\Delta_2^2(\varepsilon_1^2 + \varepsilon_3^2) + \varepsilon_1^2\varepsilon_3^2] + [\Delta_3^2(\varepsilon_1^2 + \varepsilon_2^2) + \varepsilon_1^2\varepsilon_2^2]\,, \\ a_4 &= [\varepsilon_1^2 + \Delta_1^2] + [\varepsilon_2^2 + \Delta_2^2] + [\varepsilon_3^2 + \Delta_3^2]\,, \end{aligned} \tag{360}$$

with the modified tunneling matrix elements reading

$$\Delta_1^2 = (1 - \hat{\varepsilon}^2/2\Omega^2)\Delta_0^2, \qquad \Delta_2^2 = \Delta_3^2 = (\hat{\varepsilon}^2/2\Omega^2)\Delta_0^2\,. \tag{361}$$

The *undamped* and driven system thus exhibits coherent oscillations,

$$P_{\rm H}^{(0)}(t) = p_0 + \textstyle\sum_j p_j \cos(\nu_j t) \tag{362}$$

with the amplitudes p_1, p_2, p_3 defined in a cyclic way. One obtains,

$$p_1 = \frac{(\nu_1^2 - \varepsilon_1^2)(\nu_1^2 - \varepsilon_2^2)(\nu_1^2 - \varepsilon_3^2)}{\nu_1^2(\nu_1^2 - \nu_2^2)(\nu_1^2 - \nu_3^2)}, \qquad p_0 = \prod_{j=1}^{3} \frac{\varepsilon_j^2}{\nu_j^2}\,, \tag{363}$$

with the sum rule $\sum_{j=0}^{3} p_j = 1$ being obeyed.

On the other hand, as a result of the bath influence, the poles of the Laplace transform of $P_{\rm H}^{(0)}(t)$ are shifted from the imaginary axis into the negative-real halfplane, and there appears an additional

pole at the origin. The residuum of this pole (denoted by $P_{\mathrm{H,ns}}$) represents the equilibrium population reached at long times. The dynamics is described by the expression[9] [222]

$$P_{\mathrm{H}}(t) = \sum_{j=1}^{3} p_j \cos(\nu_j t)\, \mathrm{e}^{-\Gamma_j t} + (p_0 - P_{\mathrm{H,ns}})\, \mathrm{e}^{-\Gamma_{\mathrm{H}} t} + P_{\mathrm{H,ns}}\,, \tag{364}$$

where the four damping rates $\Gamma_j, j = 1, 2, 3$, and Γ_{H} depend explicitly on the characteristics of the bath, and on the driving parameters Ω and $\hat{\varepsilon}$ [222]. Hence, in this parameter regime, $P_{\mathrm{H}}(t)$ still displays damped coherent oscillations as in the undriven case. Though, due to the driving, three main oscillation frequencies ν_j as well as corresponding damping rates Γ_j come into play.

(ii) When $\hat{\varepsilon} \geq \Omega$ the parameter regime is met where CDT may occur. This effect has been investigated in Ref. [245] using a generalized Bloch equation formalism applied to a super-Ohmic bath where $J(\omega) \propto \omega^3$, cf. Eq. (238). There, it is argued that, at high temperatures, the effect of the driving field is simply to renormalize the bare tunneling frequency Δ_0 as $\Delta_0 \to \Delta_0 J_0(\hat{\varepsilon}/\Omega)$. Hence, the localization transition occurs again near the zeros of the zeroth-order Bessel function $J_0(\hat{\varepsilon}/\Omega)$. As in the NIBA case, because the transition rate vanishes faster than the tunneling frequency, this implies that in the symmetric case, $\varepsilon_0 = 0$, there will be a slow coherent oscillation near the localization transition, in agreement with [226]. On the other hand, for the biased case one expects pure exponential decay in the vicinity of the transition.

12.1.2.2. Adiabatic frequency regime. For weak dissipation, low temperatures and in the adiabatic regime $\hbar\Omega \ll E(t)$, $|\hbar\dot{\theta}(t)| \ll E(t)$, where $\theta(t) = -\operatorname{arccot}(\varepsilon(t)/\Delta_0)$, the tunneling dynamics can be investigated with the help of the adiabatic approach discussed in Section 11.5 [263,264]. Here, $E(t) = \hbar(\Delta_0^2 + \varepsilon^2(t))^{1/2}$ is the adiabatic level splitting of the TLS Hamiltonian $H_{\mathrm{TLS}}(t)$ in Eq. (320). In this case, in contrast to the adiabatic regime discussed within the NIBA, cf. Eq. (347), the relevant dynamical variable is the difference $N(t)$ between occupation numbers in the lower and upper adiabatic states of $H_{\mathrm{TLS}}(t)$, cf. Eq. (71) for the zero driving case, and not the tunneling quantity $P(t)$. Neglecting the adiabatic term $-\mathrm{i}\hbar R(t)(\mathrm{d}R^{-1}/\mathrm{d}t)$ in Eq. (324), one then finds that, at *long times*, the dynamics of $N(t)$ is governed by a rate equation which is formally similar to Eq. (343) with Eq. (347), i.e.,

$$\dot{N}(t) = -\Gamma(t)[N(t) - N_{\mathrm{ad,ns}}(t)]\,, \tag{365}$$

where the adiabatic equilibrium distribution of the TLS is given by $N_{\mathrm{ad,ns}}(t) = \tanh(E(t)/2k_{\mathrm{B}}T)$, and where second-order perturbation theory in the bath-TLS coupling leads to the rate expression

$$\Gamma(t) = (\hbar\Delta_0/E(t))J(E(t)/\hbar)\coth(E(t)/2k_{\mathrm{B}}T)\,, \tag{366}$$

with $J(\omega)$ being the environmental spectral density, cf. Eq. (238). A formal solution for $N(t)$ is obtained in terms of quadratures as

$$N(t) = \int_{-\infty}^{t} \mathrm{d}t' \exp\left(-\int_{t'}^{t} \mathrm{d}t''\Gamma(t'')\right)\Gamma(t')N_{\mathrm{ad,ns}}(t')\,. \tag{367}$$

[9] We disregard real-valued shifts of the oscillation frequencies ν_j, as well as shifts of the amplitudes p_j caused by coupling to the environment, as they are of secondary interest here.

The position expectation value $P(t)$ can now be evaluated from the relation, cf. Eq. (70) for the static case,

$$P(t) = \cos[\theta(t)]N(t) + \sin[\theta(t)]M(t)\,, \tag{368}$$

with $M(t) := \mathrm{Tr}\{\rho_{\mathrm{E}}(t)\sigma_x\}$, $N(t) := \mathrm{Tr}\{\rho_{\mathrm{E}}(t)\sigma_x\}$, and $\rho_E(t)$ being the reduced density matrix evolving in the adiabatic basis. Observing that asymptotically $M(t \to \infty) \approx 0$, the asymptotic behaviour of $P(t)$ may be evaluated from Eq. (367) together with the relation $P(t) = (\hbar\varepsilon(t)/E(t))N(t)$.

We refer to [263,264] for an application of these results to the investigation of the nonlinear acoustic response in vibrating-reed experiments on dielectric glasses at low temperatures [265]. In this case, in fact, the dissipative mechanism mainly originates from the interaction between thermal phonons and TLS-like low-energy excitations arising from the disordered glassy structure [266,267]. A weak coupling approach in the TLS–phonon interaction is generally correct to treat the low-temperature dynamics. Thus, Eq. (367) with Eq. (366) given in terms of the phononic spectral density $J(\omega) \propto \omega^3$ yields the formal solution of the dynamics for insulating glasses driven by low-frequency strain fields, being the case for the vibrating-reed experiments [265]. In contrast, when vibrating-reed experiments in metallic glasses are considered [265], the interaction of the TLS with electrons cannot be described within a perturbative treatment. In this case the NIBA equation (343) within the adiabatic limit (347) properly describes the dynamics [268].

12.1.3. Driving-induced coherence: The case $\alpha = 1/2$

In the limit of a large cutoff ω_{c}, where the approximation (296) for the Ohmic kernels holds, the equation for $P(t)$ for $\alpha = \frac{1}{2}$ is given by Eq. (298). Let us consider only asymmetry driving as in the Hamiltonian of Eq. (325). From Eq. (298), the harmonics $p_m(\Omega, \hat{\varepsilon})$ of $P(t)$ are given by the expression [221]

$$p_m(\Omega, \hat{\varepsilon}) = \frac{\Gamma_0}{\Gamma_0 - \mathrm{i}m\Omega} \frac{2\omega_{\mathrm{c}}}{\pi} h_m(-\mathrm{i}m\Omega, \Gamma_0) \tag{369}$$

with

$$\begin{aligned} h_{2k}(\lambda, \Gamma_0) &= \int_0^\infty \mathrm{d}\tau\, \mathrm{e}^{-\lambda\tau - \Gamma_0\tau/2 - Q'(\tau)} A_{2k}^-(\tau)\,, \\ h_{2k+1}(\lambda, \Gamma_0) &= \int_0^\infty \mathrm{d}\tau\, \mathrm{e}^{-\lambda\tau - \Gamma_0\tau/2 - Q'(\tau)} A_{2k+1}^-(\tau)\,, \end{aligned} \tag{370}$$

where the coefficients $A_k^-(\tau)$ have been defined in Eq. (334). Here, $\Gamma_0 = \pi\Delta_0^2/2\omega_{\mathrm{c}}$. In Fig. 15 the fundamental spectral amplitude $\eta_1(\Omega, \hat{\varepsilon}) = 4\pi|p_1(\Omega, \hat{\varepsilon})/\hat{\varepsilon}|^2$ is plotted vs. frequency for different temperatures. As the temperature is decreased, resonances are found at submultiples $\Omega = \varepsilon_0/n$ $(n = 1, 2, \ldots)$ of the static bias. Correspondingly, the dynamics is intrinsically non-Markovian. As the temperature is increased, the coherence is increasingly lost, note the behavior of the dot-dashed and dashed lines in Fig. 15.

12.1.4. Quantum stochastic resonance

The phenomenon of stochastic resonance constitutes a cooperative effect of noise and periodic driving in bistable systems, resulting in an increase of the response to the applied periodic signal for

some optimal value of the noise strength. Since its discovery in 1981 [269], this intriguing phenomenon has been the object of many investigations in classical contexts [270–272]. Classically, the maximal enhancement in the output signal is assumed when the thermal hopping frequency is near the frequency of the modulation. Hence, the term *resonance*. Here, we shall focus on the deep quantum regime, where tunneling is the only channel for barrier crossing and one can treat the bistable system within the two-level system approximation discussed in this section. As we shall see, qualitative new features occur as compared to the classical case [232–234]. As the temperature is increased, the investigation of quantum stochastic resonance (QSR) requires to go beyond the two-level system approximation discussed in this section. QSR in the regime where both quantum tunneling and thermal hopping over the barrier contribute to the escape mechanism has been investigated in [235] by use of a semiclassical analysis. Recently, this regime has been investigated numerically in [203] via the QUAPI method discussed in Section 10.2.

The relevant theoretical quantity describing the dissipative dynamics under the external perturbation is the expectation value $P(t) = \langle \sigma_z \rangle_t$. On the other hand, the quantity of experimental interest for Quantum Stochastic Resonance (QSR) is the time-averaged power spectrum

$$\bar{S}(\omega) = \int_{-\infty}^{+\infty} \mathrm{d}\tau \mathrm{e}^{\mathrm{i}\omega\tau} \bar{C}(\tau)\,, \tag{371}$$

defined as the Fourier transform of the time-averaged, asymptotic (i.e., $t_0 \to -\infty$) symmetrized correlation function $\bar{C}(\tau)$ where

$$\bar{C}(\tau) = \frac{\Omega}{2\pi} \int_0^{2\pi/\Omega} \mathrm{d}t \frac{1}{2} \langle \sigma_z(t+\tau)\sigma_z(t) + \sigma_z(t)\sigma_z(t+\tau) \rangle. \tag{372}$$

The combined influence of dissipative and driving forces render extremely difficult an evaluation of the correlation function $\bar{C}(\tau)$ (and hence of the power spectrum) at short times. Matters simplify for times t, τ large compared to the time scale of the transient dynamics, when $P(t)$ acquires the periodicity of the external perturbation, cf. Eq. (328). Correspondingly, $\bar{C}(\tau)$ and its related power spectrum in the asymptotic regime read

$$\lim_{\tau \to \infty} \bar{C}(\tau) = C^{(\mathrm{as})}(\tau) = \sum_{m=-\infty}^{\infty} |p_m(\Omega, \hat{\varepsilon})|^2 \mathrm{e}^{-\mathrm{i}m\Omega\tau} \tag{373}$$

and

$$S^{(\mathrm{as})}(\omega) = 2\pi \sum_{m=-\infty}^{\infty} |p_m(\Omega, \hat{\varepsilon})|^2 \delta(\omega - m\Omega)\,. \tag{374}$$

Hence, the amplitudes $|p_m|$, as given in Eq. (330), of the super-harmonics of $P^{(\mathrm{as})}(t)$ determine the weights of the δ-spikes of the power spectrum in the asymptotic state. In order to investigate QSR [232–234] we shall examine the scaled power amplitude η_m in the mth frequency component of $S_{\mathrm{as}}(\omega)$ [273]

$$\eta_m(\Omega, \hat{\varepsilon}) = 4\pi |p_m(\Omega, \hat{\varepsilon})/\hbar\hat{\varepsilon}|^2\,. \tag{375}$$

The quantitative study of QSR requires thus to solve the asymptotic dynamics of the nonlinearly driven dissipative bistable system. Here, we shall discuss some characteristics of QSR as they emerge from the study of the dynamics of a TLS in an Ohmic bath, cf. Eq. (294), and under ac-modulation of the bias energy as in Eq. (325). We shall focus on the low temperature regime and high cutoff limit $\hbar\omega_c \gg k_B T, \Delta_0$, where the approximation (296) for the Ohmic bath correlation function holds. The main features of QSR for Ohmic friction can be summarized as follows:

(i) In contrast to classical [270–272] and semiclassical [235] studies of stochastic resonance, where the spectral amplification η_1 is maximal for a symmetric system, QSR in the deep quantum regime and high cutoff limit can arise only in the presence of a static asymmetry when the Ohmic strength α is less than one [232]. In particular, the static asymmetry should always be larger than the applied driving strength, cf. Fig. 23 [233,234]. Qualitatively, one needs some incoherence for QSR to occur.

As the friction strength α is increased above one, and/or for sufficiently large temperatures such that either the TLS approximation and/or the low-temperature approximation (296) for the Ohmic kernels breaks down QSR can occur also in the absence of a static asymmetry [235,203], cf. also Fig. 34 below.

(ii) In the investigation of QSR, the interplay between an incoherent dynamics induced by the environmental stochastic forces and a coherent dynamics induced either by quantum interference effects, or because of driving, is crucial. In particular, QSR arises only when *incoherent* processes dominate over coherent ones [233,234]. For example, QSR cannot be observed for moderate-to-high driving fields in the temperature regime dominated by driving-induced coherence, see Figs. 15 and 23. In Fig. 23 the power amplitude $\eta_1(\Omega, \hat{\varepsilon})$ is plotted as a function of the *temperature* for different driving strengths $\hat{\varepsilon}$ for the case $\alpha = \frac{1}{2}$ (frequencies are in units of $\Gamma_0 = \pi\Delta_0^2/2\omega_c$,

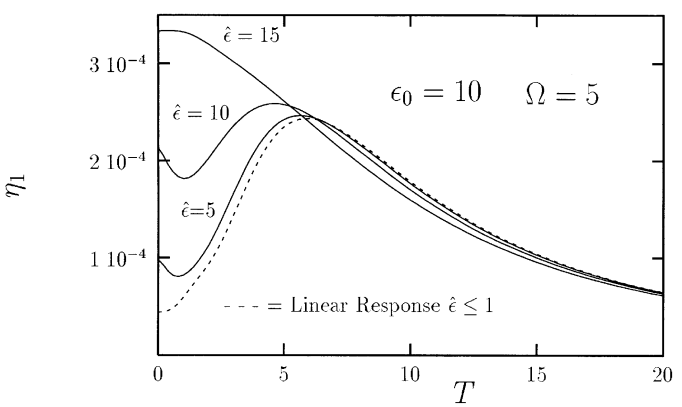

Fig. 23. Quantum stochastic resonance (QSR) in the deep quantum regime. The power amplitude $\eta_1(\Omega, \hat{\varepsilon})$ is plotted as a function of the temperature for different driving strengths $\hat{\varepsilon}$ for the case $\alpha = \frac{1}{2}$ of Ohmic dissipation. Frequencies are in units of $\Gamma_0 = \pi\Delta_0^2/\omega_c$, temperatures in units of $\hbar\Gamma_0/k_B$. For highly nonlinear driving fields $\hat{\varepsilon} > \varepsilon_0$, the power amplitude decreases monotonically as the temperature increases (uppermost curve). As the driving strength $\hat{\varepsilon}$ is decreased, a shallow minimum followed by a maximum appears when the static asymmetry ε_0 equals, or slightly overcomes, both the external frequency Ω *and* strength $\hat{\varepsilon}$ (intermediate curves). For even smaller external amplitudes, the nonlinear QSR can be studied within the linear response theory (dashed curve).

temperatures in units of $\hbar\Gamma_0/k_B$). For highly nonlinear driving fields $\hat{\varepsilon} > \varepsilon_0$ the power amplitude decreases monotonically as the temperature increases (uppermost curve). As the driving strength $\hat{\varepsilon}$ is decreased, a shallow minimum followed by a maximum appears when the static asymmetry ε_0 equals or slightly overcomes both the external frequency Ω *and* strength $\hat{\varepsilon}$ (intermediate curves). For even smaller external amplitudes, the nonlinear QSR can be studied within the linear response theory (dashed curve). In the linear region the shallow minimum is washed out, and only the principal maximum survives. It is now interesting to observe that, because for the undriven case the TLS dynamics for $\alpha = \frac{1}{2}$ is *always incoherent* down to $T = 0$, the principal maximum arises at the temperature T at which the relaxation process towards thermal equilibrium is maximal. On the other hand, the minimum in η_1 appears in the temperature region where *driving-induced* coherent processes are of importance, cf. Fig. 15. This means that the power amplitude η_1 plotted *versus frequency* shows resonances when $\Omega \approx \varepsilon_0/n$ ($n = 1, 2, \ldots$). As the temperature is increased, this coherence is increasingly lost.

(iii) QSR can be well understood within a linear response analysis in an intermediate-to-low-frequency regime.

Within linear response, only the harmonics $0, \pm 1$ of $P^{(as)}(t)$ in Eq. (373) are different from zero, $p_0 = P_{st}$ being just the thermal equilibrium value in the absence of driving, and $p_{\pm 1} = \hat{\varepsilon}\tilde{\chi}(\pm\Omega)$ being related to the linear susceptibility $\tilde{\chi}(\Omega)$ by Kubo's formula. With increasing strength $\hat{\varepsilon}$ linear response theory fails, and higher harmonics become important.

Let us consider the regime $\hbar\Omega \ll 2\pi\alpha k_B T$ and $k_B T > \hbar\Delta_0$, and/or $\alpha > 1$, and/or $\varepsilon_0 \gg \Delta_0$, where incoherent transitions dominate the dynamics and NIBA applies. The susceptibility is then explicitly obtained in the form, cf. Eq. (342),

$$\tilde{\chi}(\Omega) = \frac{1}{4k_B T}\frac{1}{\cosh^2(\hbar\varepsilon_0/2k_B T)}\frac{1}{1 - i\Omega\Gamma_0^{-1}}\,. \tag{376}$$

Here, the Ohmic static rate Γ_0, cf. Eq. (309),

$$\Gamma_0 = \frac{\Delta_0^2}{2\omega_c}\left(\frac{\hbar\beta\omega_c}{2\pi}\right)^{1-2\alpha}\frac{|\Gamma(\alpha + i\hbar\beta\varepsilon_0/2\pi)|^2}{\Gamma(2\alpha)}\cosh(\hbar\beta\varepsilon_0/2)\,, \tag{377}$$

can be regarded as the sum of the (static) backward Γ_b and forward Γ_f rates out of the metastable states. The factor $1/\cosh^2(\hbar\varepsilon_0/2k_B T)$ expresses that the two rates are related by the detailed balance condition $\Gamma_f = e^{\hbar\beta\varepsilon_0}\Gamma_b$. It is now interesting to note that the *same* formal expression for the incoherent susceptibility (and hence for η_1) holds true – in leading order – for the classical case, with Γ_0 being the sum of the forward and backward Arrhenius rates in the asymmetric bistable system [272]. Hence, in classical SR the maximum arises due to a competition between the thermal Arrhenius dependence of the rates and the algebraic factor $(k_B T)^{-1}$ that enters the linear susceptibility. For low driving frequencies the maximum amplification is then obtained at the temperature T such that the thermal hopping time scale approximately equals the driving period $\mathscr{T} = 2\pi/\Omega$ [272]. On the other hand, quantum rates possess a rather weak temperature dependence as compared to the Arrhenius rate. The crucial role is now taken over by the Arrhenius-like exponential factor $1/\cosh^2(\hbar\varepsilon_0/2k_B T)$, where in the two-state picture $\hbar\varepsilon_0$ is of the order of the bias between the well minima. Hence, whenever $\hbar\varepsilon_0 \ll k_B T$ the energy levels are essentially equally occupied and no response to the external signal occurs. The maximum arises near the temperature obeying $k_B T \simeq \hbar\varepsilon_0$ over a wide frequency range.

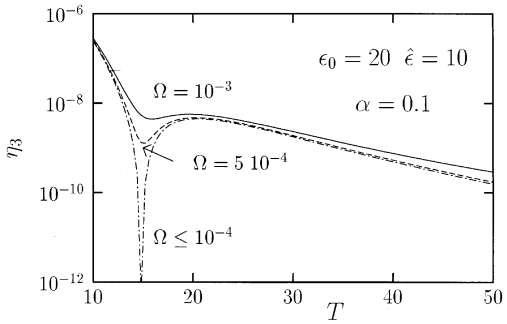

Fig. 24. Noise-induced suppression (NIS) of higher harmonics. The third power amplitude η_3 when plotted versus temperature reveals a striking characteristic: As the driving frequency is decreased, a noise-induced suppression (NIS) occurs in correspondence of the QSR maximum in the fundamental harmonic. Frequencies are in units of the bath-renormalized tunneling splitting Δ_e, cf. Eq. (310), temperatures in units of $\hbar\Delta_e/k_B$.

Similar qualitative results are obtained also in the parameter region of low temperatures $k_B T \leq \hbar\Delta_0$ and weak coupling $\alpha \ll 1$ where underdamped quantum coherence occurs and NIBA breaks down [233,234].

(iv) Even if QSR can be well understood within a linear response theory, novel interesting effects arise in the regime of *nonlinear* QSR, when higher order harmonics become resolvable. In particular, quantum noise can substantially *enhance*, but also *suppress*, the nonlinear response. Fig. 24 depicts the behavior of the third power amplitude η_3 versus temperature. It reveals a striking effect: As the driving frequency is decreased, a noise-induced suppression (NIS) of higher harmonics occurs in correspondence of the stochastic maximum in the fundamental harmonic η_1. To understand the results shown in Fig. 24 it is convenient to rewrite $p_m(\Omega)$ as the sum of a quasistatic (frequency-independent) contribution

$$p_m^{(qs)} = \frac{1}{2\pi}\int_0^{2\pi} dx \tanh\left[\hbar\beta(\varepsilon_0 + \hat{\varepsilon}\cos x)/2\right]\cos(mx)\,, \tag{378}$$

and a retarded one $p_m^{(ret)}(\Omega)$. The latter becomes negligible when $\Omega \to 0$. For the parameters in Fig. 24 this amounts to $\Omega \leq 10^{-4}\Delta_0$. A numerical evaluation shows that the NIS is most pronounced when the retarded contribution becomes negligible, so that $p_m(\Omega) \simeq p_m^{(qs)}$.

The same reasoning holds true in the parameter regime of low-driving frequencies, low temperatures and weak coupling to the bath where adiabatic quantum coherence occurs [233,234].

Hence, the discussion of this subsection makes clear that quantum noise does not necessarily represent a nuisance but rather can be a useful tool when used within the interplay of nonlinearity, driving and (quantum) noise.

12.2. Pulse-shaped periodic driving

Given the results of the previous subsections, we have all the necessary tools to discuss the case of pulse-shaped periodic driving of the form

$$\varepsilon(t) = \varepsilon_0 + \hat{\varepsilon}\eta(t)\cos(\Omega t), \qquad \eta(t + \mathscr{T}_p) = \eta(t)\,, \tag{379}$$

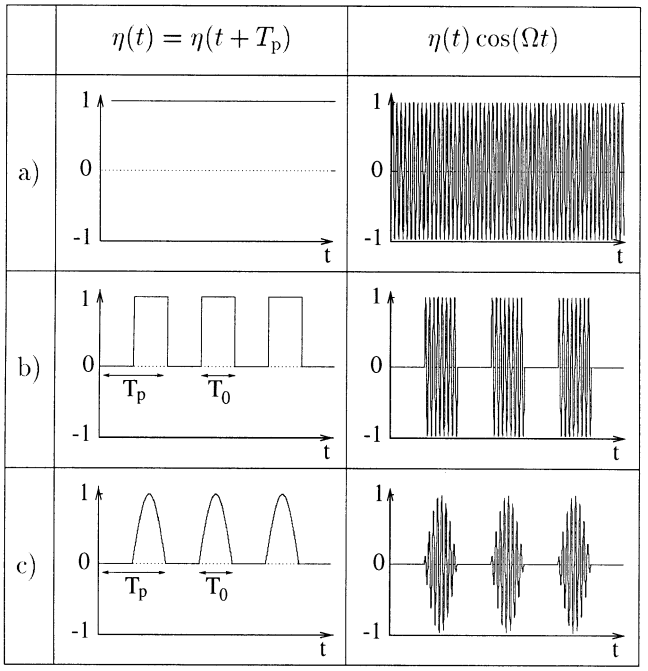

Fig. 25. Different periodic driving signals can be used to control tunneling: (a) monochromatic driving; (b) and (c) pulse-shaped polychromatic driving of period $\mathscr{T}_p$. The latter are obtained by modulating a monochromatic signal by a pulse function of pulse duration $\mathscr{T}_0$.

and $\Delta(t) = \Delta_0$. The quantity $\eta(t)$ is a "pulse" function of period $\mathscr{T}_p = 2\pi/\Omega_p \geq \mathscr{T} = 2\pi/\Omega$ that modulates the monochromatic part, $\cos(\Omega t)$, of the signal. Depending on the particular shape of the 'pulse' function $\eta(t)$, different experimental realizations may be mimicked, as shown in Fig. 25.

Because Eqs. (343) and (350) are restricted only by the assumption of a separation of time scales, in the parameter regime $\tau_K^{-1} \gg \Omega, \Omega_p, \Gamma_{H,\eta}$, with $\Gamma_{H,\eta}$ the appropriate time-averaged relaxation rate, the resulting dynamics is Markovian. The dynamics can then be approximated by Eq. (343). An additional approximation to Eq. (343) can be discussed in the parameter regime $\Omega \gg \Gamma_{H,\eta} \gg \Omega_p$. That is, we assume that the pulse-shape function $\eta(t)$ is a slowly varying function on the time scale set by the transient dynamics, while, on the contrary, the monochromatic part $\cos(\Omega t)$ is fastly changing. Although the oscillatory long-time dynamics will assume the periodicity of the slow pulse shape function $\eta(t)$, see Eq. (328), the dynamics within a pulse period $\mathscr{T}_p$ is also determined by the fast monochromatic signal. Hence, due to the assumption $\Omega \gg \Gamma_{H,\eta}$, a good approximation to Eq. (343) can be obtained by performing the average $\langle P_M(t)\rangle_{\mathscr{T}}$ of $P_M(t)$ over the fast oscillating field.

The evaluation of the time-averaged kernels in turn is readily accomplished by noting that this average has only to be carried out on the field dependent contributions $\cos[\zeta(t,t')]$ and $\sin[\zeta(t,t')]$.

The average over the period $\mathscr{T} = 2\pi/\Omega$ yields [231,246]

$$\begin{aligned}
\langle \cos[\zeta(t,t')] \rangle_{\mathscr{T}} &= J_0\left(\frac{2\hat{\varepsilon}\eta(t)}{\Omega}\sin\left(\frac{\Omega(t-t')}{2}\right)\right)\cos[\varepsilon_0(t-t')]\,, \\
\langle \sin[\zeta(t,t')] \rangle_{\mathscr{T}} &= J_0\left(\frac{2\hat{\varepsilon}\eta(t)}{\Omega}\sin\left(\frac{\Omega(t-t')}{2}\right)\right)\sin[\varepsilon_0(t-t')]\,.
\end{aligned} \tag{380}$$

The smooth, slowly oscillating function $\langle P_{\mathrm{M}}(t) \rangle_{\mathscr{T}}$ therefore satisfies the rate equation (343) with relaxation rate given by

$$\Gamma_{\mathrm{M},\eta}(t) = \int_0^\infty \mathrm{d}\tau\, h^{(+)}(\tau) J_0\left(\frac{2\hat{\varepsilon}\eta(t)}{\Omega}\sin\left(\frac{\Omega\tau}{2}\right)\right)\cos(\varepsilon_0\tau)\,. \tag{381}$$

The nonstationary asymptotic quantity is $P_{\mathrm{ns},\eta}(t) = \rho_{\mathrm{M},\eta}(t)/\Gamma_{\mathrm{M},\eta}(t)$, where

$$\rho_{\mathrm{M},\eta}(t) = \int_0^\infty \mathrm{d}\tau\, h^{(-)}(\tau) J_0\left(\frac{2\hat{\varepsilon}\eta(t)}{\Omega}\sin\left(\frac{\Omega\tau}{2}\right)\right)\sin(\varepsilon_0\tau)\,, \tag{382}$$

with $h^{(\pm)}$ defined in Eq. (308). Note that when $\eta(t) = 1$ the high-frequency approximation (350) is recovered. This is in agreement with the physical intuition saying that a monochromatic signal can be thought to be a pulse-shaped signal with an infinite pulse period $\mathscr{T}_{\mathrm{p}}$. The asymptotic oscillatory dynamics for the case of Ohmic friction and pulse-shaped driving of the type (b) in Fig. 25 is shown in Fig. 26. For comparison, the prediction of the rate equation (343) with Eqs. (344) and (346) is also depicted. In addition, we show the prediction of Eq. (343) where the approximated equations (381) and (382), obtained in the Markovian limit of low Ω_{p} and high Ω, are used. This latter Markov $-+-$ high Ω approximation describes the TLS oscillations between the two bounding values $P_{\mathrm{st}} := P_{\mathrm{ns},\eta=0}$ and $P_{\mathrm{H,ns}} := P_{\mathrm{ns},\eta=1}$. These bounds are indicated by the arrows in Fig. 26. The low Ω_{p}-high Ω approximation scheme clearly misses the fine structure due to the monochromatic driving. The possibility to use this effect to control long-range electron-transfer reactions have been proposed in [230].

12.3. Dynamics under ac-modulation of the coupling energy

In this section our focus is on the effect of ac-modulation of the coupling energy of the TLS. We shall assume for the driven TLS the form

$$H_{\mathrm{TLS}}(t) = -\tfrac{1}{2}\hbar[\Delta_0 \exp(\delta\cos\Omega_\delta t)\sigma_x + \varepsilon_0\sigma_z]\,. \tag{383}$$

This time dependence of the coupling parameter could arise for example from an ac-modulation of the barrier height or width of the underlying double-well potential. For example, for a particle of mass m moving in a double-well potential with barrier height E_{B}, vibrational frequency ω_0 at the bottom of each well, and tunneling distance d, the bare tunneling splitting Δ_0 in WKB approximation is given by $\Delta_0 = \omega_0 \exp[-d(2mE_{\mathrm{B}}/\hbar)^{1/2}]$. This kind of driving could be realized in a superconducting loop with two Josephson junctions [208]. It is important to observe that, while the effect of

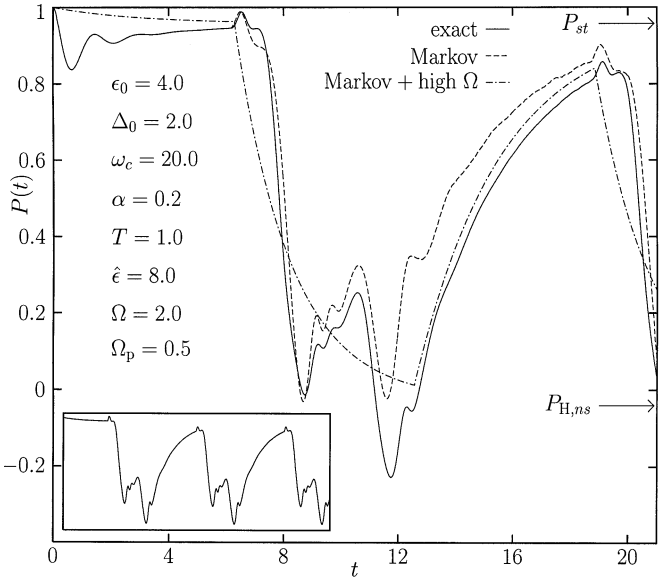

Fig. 26. Dynamics of the population difference $P(t)$ induced by a periodic pulse of the form in Fig. 25b. A low-frequency periodic square pulse of period $\mathscr{T}_\mathrm{p} = 2\pi/\Omega_\mathrm{p}$ and pulse duration $\mathscr{T}_0 = \mathscr{T}_\mathrm{p}/2$ is multiplied by a monochromatic signal of intermediate frequency Ω. The oscillatory dynamics within the exact NIBA (solide line) is depicted in the inset where $P(t)$ is plotted for longer times. The predictions of the exact NIBA are compared with two Markovian approximations, namely the Markovian approximation in Eq. (343) with Eqs. (344) and (346) (dashed curve), or with Eqs. (381) and (382) (dot–dashed curve) being valid for slow pulses with internal high-frequency oscillations. The latter Markov – + – high Ω approximation describes the population oscillations between the two bounds P_st and $P_\mathrm{H,ns}$, as indicated by the arrows. Frequencies are in units of $\delta = \Delta_0/2$, temperatures in units of $\hbar\delta/k_\mathrm{B}$.

asymmetry modulation is additive, a barrier modulation results in a *multiplicative* (exponential) modification of the coupling parameter. In the following, we shall refer to the situation of pure asymmetry modulation as "case I", to that of pure barrier modulation as "case II", respectively.

Due to the generality of the master equation within the NIBA (300), and following the lines of the analysis of the previous sections, it is straightforward to investigate the dynamics under the driving in Eq. (383). The obtained results are as follows [238]:

(i) As for the case I of bias modulation, the asymptotic dynamics is periodic and an equation for the harmonics of $P^{(\mathrm{as})}(t)$ is given by Eq. (330), where for the driving of Eq. (383) the functions $k_m^{\pm}$ are explicitly given by

$$k_m^-(\lambda,\delta) = (-1)^m \Delta_0^2 \int_0^\infty \mathrm{d}\tau\, \mathrm{e}^{-\lambda\tau - Q'(\tau)} \mathrm{e}^{-\mathrm{i}m\Omega_\delta\tau/2} \sin[Q''(\tau)] \sin(\varepsilon_0\tau) I_m\left(2\delta\cos\frac{\Omega_\delta\tau}{2}\right),$$

$$k_m^+(\lambda,\delta) = (-1)^m \Delta_0^2 \int_0^\infty \mathrm{d}\tau\, \mathrm{e}^{-\lambda\tau - Q'(\tau)} \mathrm{e}^{-\mathrm{i}m\Omega_\delta\tau/2} \cos[Q''(\tau)] \cos(\varepsilon_0\tau) I_m\left(2\delta\cos\frac{\Omega_\delta\tau}{2}\right), \tag{384}$$

where $I_m(z)$ denotes the modified Bessel function of order m.

(ii) As shown in Section 12.1 above, for a *symmetric* TLS, spatial symmetry properties of the kernels $k_m^{\pm}(\lambda)$ imply that all the Fourier components of $P^{(\mathrm{as})}(t)$ with *even* index vanish for case I, cf. Eq. (333) and the discussion below. In contrast, here we find that *all* super-harmonics vanish identically for ac-modulation of the coupling energy.

(iii) Some interesting new features of case II driving can be found in the high frequency regime $\Omega_\delta \gg \Gamma_\delta := k_0^+(0,\delta)$, where the high-frequency approximation (349) holds. As shown for case I, a fast field suppresses the periodic long times oscillations, and the TLS approaches incoherently the steady value $p_0 = k_0^-(0,\delta)/k_0^+(0,\delta)$ with relaxation rate $k_0^+(0,\delta) := \Gamma_\delta$.

Let us consider the case of Ohmic dissipation (294). In contrast to case I, where the effect of a fast asymmetry modulation is an overall reduction of the incoherent tunneling rate (whenever $\alpha < \frac{1}{2}$), the tunneling rate Γ_δ is now always *increased* (due to $I_0(z) \geq 1$).

Furthermore, the modification of the quantum coherent motion by thermal and driving forces results from an investigation of the zeros of $\lambda + k_0^+(\lambda;\delta) = 0$. In the high-frequency regime $\Omega_\delta \gg 2\pi\alpha k_{\mathrm{B}}T/\hbar$, Δ_0, and for $\alpha \ll 1$, one obtains

$$k_0^+(\lambda;\delta) = \mathscr{K}(\lambda)\left[I_0^2(\delta) + \left(\frac{\alpha + \hbar\beta\lambda/2\pi}{\hbar\beta\Omega_\delta/2\pi}\right)^2 \sum_{n\neq 0} \frac{I_n^2(\delta)}{n^2}\right], \tag{385}$$

where the static kernel $\mathscr{K}(\lambda)$ is defined in Eq. (356), and where the high cutoff limit is considered. Because $I_0(\delta) \geq 1$, the first contribution in the r.h.s. of Eq. (385) always dominates over the second one. Therefore, CDT *never* occurs for case II. In other words, the driving field modulation of the coupling energy essentially results in a renormalization of the bare tunneling splitting Δ_0 as

$$\Delta_0 \to \Delta_{\mathrm{eff},\delta} = \Delta_0 I_0(\delta) \geq \Delta_0 \,. \tag{386}$$

Equivalently, $\Delta_\delta = \Delta_{\mathrm{e}} I_0(\delta)^{1/1-\alpha}$, and Δ_{e} is the bath-renormalized tunneling splitting for $\alpha < 1$, cf. Eq. (310). Hence, when $\alpha \ll 1$, the transition temperature from coherent to incoherent tunneling is given by $T_\delta^*(\alpha) \simeq \hbar\Delta_\delta/\pi\alpha k_{\mathrm{B}}$. With $T_\delta^*(\alpha) \geq T_0(\alpha)$, quantum coherence is thus always enhanced in case II.

12.4. Dichotomous driving

Up to now we considered the effects of a deterministic external driving on the TLS dynamics. Here, we shall consider the case where the driving constitutes an external discrete two-state stochastic process (dichotomous process). In contrast to equilibrium noise produced by the harmonic (Gaussian) bath in the spin–boson model, such a noise must be considered as a source of nonequilibrium noise. This situation arises, for example, in proteins, where the transfer of electrons between different sites may be influenced not only by thermal phonons, but also by large-amplitude local excitations [239–241]. If one considers the simplest case of a dichotomous Markovian process (DMP), this can simulate, for example, the hopping of a relevant molecular group or ion between two equivalent positions. Let us thus consider the noisy TLS

$$H_{\mathrm{TLS}}(t) = -\tfrac{1}{2}\hbar[\Delta_0\sigma_x + (\varepsilon_0 + \hat{\varepsilon}\eta(t))\sigma_z] \,, \tag{387}$$

where $\eta(t) = \pm 1$ is a stationary DMP with zero mean $\langle\eta(t)\rangle_\eta = 0$ and exponentially decaying autocorrelation function

$$\langle\eta(t)\eta(t')\rangle_\eta = \exp[-\nu|t-t'|] \,. \tag{388}$$

Here, $\langle\ \rangle_\eta$ denotes the average over the stochastic process. It should be distinguished from the thermal statistical average denoted by $\langle\ \rangle$ in the previous sections. We shall derive the NIBA equations for the TLS dynamics averaged over the discrete two-state stochastic process. Generally, this is a nontrivial problem. It can be done exactly, however, for the case of a DMP. For a more detailed discussion we refer to Refs. [239,240]. The case of a dichotomously fluctuating tunneling matrix element has instead been treated in Refs. [241,242].

Within the NIBA, the dynamics of the driven and dissipative TLS is described by the equations of motion (300) for the quantum expectation value $P(t) = \langle\sigma_z\rangle_t$ of the position. To average Eq. (300) one has to evaluate the correlator $\langle S(t,t')P(t')\rangle_\eta$, where $S(t,t') = \exp[-\mathrm{i}\hat{\varepsilon}\int_{t'}^{t}\mathrm{d}t''\eta(t'')]$. As follows from a theorem due to Bourret et al. [274] one finds that

$$\langle S(t,t')P(t')\rangle_\eta = S_0(t-t')\langle P(t')\rangle_\eta + S_1(t-t')\langle\eta(t')P(t')\rangle_\eta\,, \tag{389}$$

where $S_0(t-t') = \langle S(t,t')\rangle_\eta$, and $S_1(t-t') = \langle\eta(t')S(t,t')\rangle_\eta$. In the same way one has

$$\langle\eta(t)S(t,t')P(t')\rangle_\eta = S_1(t-t')\langle P(t')\rangle_\eta + S_2(t-t')\langle\eta(t')P(t')\rangle_\eta\,, \tag{390}$$

where $S_2(t-t') = \langle\eta(t)\eta(t')S(t,t')\rangle_\eta$. The next step consists in the evaluation of the averaged functions S_0, S_1, S_2. This can be done with the help of a theorem due to Shapiro and Loginov [275], namely,

$$\frac{\mathrm{d}}{\mathrm{d}t}\langle\eta(t)R(t)\rangle_\eta = -v\langle\eta(t)R(t)\rangle_\eta + \left\langle\eta(t)\frac{\mathrm{d}R(t)}{\mathrm{d}t}\right\rangle_\eta \tag{391}$$

holds for any retarded functional $R(t)$. Applying this theorem to the correlator $\langle\eta(t)S(t,t')\rangle_\eta$, one obtains a closed set of differential equations for $S_0(t-t')$ and $S_1(t-t')$. The solution of these equations yields

$$S_0(\tau) = \exp\left(-\frac{v\tau}{2}\right)\left[\cosh\left(\frac{\bar{v}\tau}{2}\right) + \frac{v}{\bar{v}}\sinh\left(\frac{\bar{v}\tau}{2}\right)\right], \tag{392}$$

where $\bar{v} = \sqrt{v^2 - 4\hat{\varepsilon}^2}$. In the same way one obtains

$$\begin{aligned} S_1(\tau) &= -\frac{\mathrm{i}2\hat{\varepsilon}}{\bar{v}}\exp\left(-\frac{v\tau}{2}\right)\sinh\left(\frac{\bar{v}\tau}{2}\right), \\ S_2(\tau) &= \exp\left(-\frac{v\tau}{2}\right)\left[\cosh\left(\frac{\bar{v}\tau}{2}\right) - \frac{v}{\bar{v}}\sinh\left(\frac{\bar{v}\tau}{2}\right)\right]. \end{aligned} \tag{393}$$

Finally, by applying again the theorem (391) to the correlator $\langle\eta(t)P(t)\rangle_\eta$ one obtains an exact set of coupled equations for $\langle P(t)\rangle_\eta$ and $\langle\eta(t)P(t)\rangle_\eta$, i.e.,

$$\begin{aligned} \frac{\mathrm{d}}{\mathrm{d}t}\langle P(t)\rangle_\eta = &-\int_0^t \mathrm{d}\tau[S_0(\tau)h^{(+)}(\tau)\cos(\varepsilon_0\tau)\langle P(t-\tau)\rangle_\eta \\ &-\mathrm{i}S_1(\tau)h^{(+)}(\tau)\sin(\varepsilon_0\tau)\langle\eta(t-\tau)P(t-\tau)\rangle_\eta + S_0(\tau)h^{(-)}(\tau)\sin(\varepsilon_0\tau)] \end{aligned} \tag{394}$$

and

$$\frac{\mathrm{d}}{\mathrm{d}t}\langle\eta(t)P(t)\rangle_\eta = -\nu\langle\eta(t)P(t)\rangle_\eta - \int_0^t \mathrm{d}\tau[S_2(\tau)h^{(+)}(\tau)\cos(\varepsilon_0\tau)\langle\eta(t-\tau)P(t-\tau)\rangle_\eta$$
$$- \mathrm{i}S_1(\tau)h^{(+)}(\tau)\sin(\varepsilon_0\tau)\langle P(t-\tau)\rangle_\eta + \mathrm{i}S_1(\tau)h^{(-)}(\tau)\cos(\varepsilon_0\tau)]\,. \tag{395}$$

The initial conditions are $\langle P(0)\rangle_\eta = 1$, and $\langle\eta(0)P(0)\rangle_\eta = 0$. These equations should be considered as the generalization of the NIBA to the case of dichotomous driving. They account for the effects of the discrete two-state stochastic process exactly. The above equations are still rather complicated. In the case of a TLS with zero bias, $\varepsilon_0 = 0$, they simplify because the two coupled equations separate into two independent equations. In particular, the one for the expectation value $\langle P(t)\rangle_\eta$ reads

$$\frac{\mathrm{d}}{\mathrm{d}t}\langle P(t)\rangle_\eta = -\int_0^t \mathrm{d}\tau\, S_0(\tau)h^{(+)}(\tau)\langle P(t-\tau)\rangle_\eta\,. \tag{396}$$

Eq. (396) can be solved by Laplace transformation. The resulting dynamics can be coherent or incoherent, depending on the interplay between quantum interference effects, dissipation and driving. In particular, in the incoherent regime the resulting decaying rate Γ_{DMP} has the form

$$\Gamma_{\mathrm{DMP}} = \frac{1}{2}\left[\left(1 - \frac{\nu}{\bar{\nu}}\right)\hat{h}^{(+)}\left(\frac{\nu+\bar{\nu}}{2}\right) + \left(1 + \frac{\nu}{\bar{\nu}}\right)\hat{h}^{(+)}\left(\frac{\nu-\bar{\nu}}{2}\right)\right], \tag{397}$$

where $\hat{h}^{(+)}(\lambda)$ is the Laplace transform of the function $h^{(+)}(t)$. The predictions of Eq. (396) with Eq. (397) for the case of long-range electron transfer reactions have been worked out in Ref. [241]. Finally, the combined effects of a symmetric DMP and of an additional, externally applied dc–ac field have been investigated recently in [276].

12.5. The dissipative Landau–Zener–Stückelberg problem

In this section we investigate the influence of dissipation on the Landau–Zener–Stückelberg problem discussed in Section 3.5 [247–250,277]. In this context, one considers the time-dependent variation of the energy levels of a dissipative quantum system. This situation is encountered frequently ranging from the case of the solar neutrino puzzle [278], to the physics of nuclear magnetic resonance [279]. It turns out to be of relevance also in the context of macroscopic quantum tunneling in a rf SQUID [248], when the external flux is changed at a constant rate.

Quantitatively, the problem is described by the time-dependent spin–boson Hamiltonian (270), with TLS Hamiltonian

$$H_{\mathrm{LZS}}(t) = -\tfrac{1}{2}\hbar(\Delta_0\sigma_x + vt\sigma_z)\,, \tag{398}$$

where $\hbar\Delta_0$ is the energy gap between the two levels, cf. Eq. (114). We then ask for the probability $P_{\mathrm{LZS}} := (1 - \langle\sigma_z\rangle_{t\to\infty})/2$ of finding the system in the excited state in the far future, cf. Fig. 3.

In the absence of dissipation the exact result $P_{\mathrm{LZS}} = \mathrm{e}^{-2\pi\gamma}$ in (123) holds, where γ is the dimensionless parameter $\gamma = \Delta_0^2/(2|v|)$ and, as shown in Fig. 3, $\tau_{\mathrm{LZS}} = \Delta_0/|v|$ is interpreted as the

time spent in the crossover region. With coupling to the environment, two other time scales $\tau_c = 1/\omega_c$ and $\tau_v = \omega_c/|v|$ come into play. Because ω_c is the highest frequency of the environment, cf. Eq. (238), τ_c defines the reaction-time of the bath to an external perturbation.

In the fast-passage limit $\gamma \ll 1$, and with $\omega_c \ll \sqrt{|v|}$, the system remains only a small time in the cross-over region as compared to both the tunneling period and the bath reaction time. That is, the undamped result is not modified by dissipation [248,249]. One obtains to first order in γ the result

$$P_{\mathrm{LZS}} = 1 - 2\pi\gamma\,. \tag{399}$$

In the slow passage limit $\gamma \gg 1$ the situation becomes more complex. Here, we consider the case of very weak dissipation. To tackle the problem, it is convenient to perform the adiabatic transformation (322) which leads to the effective Hamiltonian appearing in the time-evolution operator, cf. Eq. (324),

$$H_{\mathrm{eff}} = -\tfrac{1}{2}E(t)\sigma_z + H_{\mathrm{B}} - (\hbar v t/E(t))X\sigma_z + (\hbar\Delta_0/E(t))X\sigma_x + (\hbar^3 v\Delta_0/E^2(t))\sigma_y\,, \tag{400}$$

where $\pm E(t) = \pm\hbar\sqrt{v^2t^2 + \Delta_0^2}$ define the corresponding adiabatic energies, cf. Fig. 3. In the limit $\gamma \to \infty$, i.e., $|v| \to 0$, the adiabatic term $(\hbar^3 v\Delta_0/E^2(t))\sigma_y$ vanishes. Note that, of course, the bath contribution $\propto \sigma_x$ remains finite. In fact, the problem becomes time-independent and the rotation (322) simply transforms the original Hamiltonian as $\sigma_x \to \sigma_z$ and $\sigma_z \to -\sigma_x$. This transformation has been first applied to the Landau–Zener–Stückelberg problem in Refs. [248,249]. Though, the authors there identify both of the off-diagonal terms in the Hamiltonian (400) as adiabatic contributions, and in turn make a first-order expansion in both the true adiabatic contribution $\propto \sigma_y$, and the bath-induced contribution $\propto \sigma_x$. The bath-induced contribution $\propto \sigma_z$, however, has been considered to all orders. This neither constitutes an adiabatic approximation nor a weak coupling expansion in the interaction with the bath. Thus, this procedure seems awkward to us; see also in [277], where in the adiabatic passage limit $\gamma \gg 1$ and in the limit of weak coupling with the bath, a first-order expansion both in the adiabatic term and in the bath interaction is done. One then obtains $P_{\mathrm{LZS}} = P_0 + \Delta P$, where P_0 is the Landau–Zener–Stückelberg probability in the absence of dissipation, while ΔP gives the first-order correction due to the environment. It reads [277]

$$\Delta P = \frac{1}{\hbar^2}\int_{-\infty}^{+\infty} \mathrm{d}t_1 \int_{-\infty}^{+\infty} \mathrm{d}t_2 \mathrm{e}^{\mathrm{i}\eta(t_2,t_1)/\hbar} K(t_2 - t_1)\frac{\hbar^2\Delta_0^2}{E(t_2)E(t_1)}\,, \tag{401}$$

where $K(t)$ is the force–force correlation of the bath in Eq. (229), and $\eta(t_2, t_1) = \int_{t_1}^{t_2} \mathrm{d}t\, E(t)$. This equation, though, is still too complicated to be handled without approximations. In the low-temperature regime $\hbar\beta\Delta_0 \gg 1$ one obtains

$$\Delta P \approx 2\alpha\left(\pi \mathrm{e}^{-4\pi\gamma} + \gamma\frac{\mathrm{e}^{-\hbar\beta\Delta_0/2}}{\hbar\beta\Delta_0/2}\right), \tag{402}$$

while in the high-temperature regime $\hbar\beta\Delta_0 \ll 1$, but still $\hbar\beta\omega_c \gg 1$, one finds

$$\Delta P \approx 2\alpha\left(\pi \mathrm{e}^{-4\pi\gamma} + \gamma\frac{1}{\hbar\beta\Delta_0/2}\right). \tag{403}$$

Though approximate, the results (402) and (403) show that the interaction with the bath modifies the non-dissipative result even at $T = 0$. Moreover, the transition probability *increases* monotonically as the temperature grows. This is in contrast with the results in [248,249] where no influence of the bath was found at $T = 0$, and with those in [250] where even a *reduction* of the transition probability was predicted.

13. The driven dissipative periodic tight-binding system

In this section we consider the effect of dissipation on the driven infinite tight-binding (TB) model introduced in Section 4. The dissipative TB system can serve as an idealized model for the diffusion of a quantum particle on a surface of a single-crystal, or among interstitials inside a crystal [280]. It can also be invoked to investigate quantum effects in the current–voltage characteristic of a small Josephson junction [281] or of superlattices driven by strong dc- and ac-fields [18–22,92]. Finally, this multistate system can be related to the Luttinger liquid model [282,283] for the conductance between two one-dimensional quantum wires connected by a weak link via a formally exact mapping [284].

The dissipative multistate system in the absence of time-dependent driving has been the object of intense research in the past years [285–290]. In contrast, in Section 4 we investigated localization effects in dc–ac-driven TB lattices in the absence of thermal noise. Here, we extend the analysis by investigating the combined effects of dissipation and driving on the tunneling dynamics. As a starting model we consider the one-dimensional infinite tight-binding lattice described by the Hamiltonian $H(t) = H_{\mathrm{TB}} + H_{\mathrm{ext}}(t) + H_{\mathrm{SB}} + H_{\mathrm{B}}$, cf. Eq. (222). The first term H_{TB} is the Hamiltonian of the bare multistate system, cf. Eq. (130), i.e.,

$$H_{\mathrm{TB}} = -\frac{\hbar\Delta_0}{2}\sum_n \left(|n\rangle\langle n+1| + |n+1\rangle\langle n|\right), \tag{404}$$

where $|n\rangle$ denotes a (Wannier) state localized at the nth site, while $2\hbar\Delta_0$ is the width of the single energy band. The influence of the driving force is described by Eq. (131), i.e.,

$$H_{\mathrm{ext}}(t) = -q\hbar[\varepsilon_0 + \hat{\varepsilon}\cos(\Omega t)]/d, \quad q = d\sum_n n|n\rangle\langle n|, \tag{405}$$

where the operator q measures the position of the particle on the lattice. Finally, the Hamiltonian term $H_{\mathrm{SB}} + H_{\mathrm{B}}$ describes the influence of an environmental bath of harmonic oscillators as given by Eq. (224).

Suppose that the particle has been prepared at time $t_0 = 0$ at the origin, with the bath having a thermal distribution at temperature T. Then, the dynamical quantity of interest is the probability $P_n(t)$ for finding the particle at site n at time $t > 0$. In turn, the knowledge of $P_n(t)$ enables the evaluation of all the transport quantities of interest in the problem. For example, the nonlinear mobility $\mu(\varepsilon_0, \hat{\varepsilon})$ reads

$$\mu(\varepsilon_0, \hat{\varepsilon}) = \lim_{t\to\infty} \frac{d}{\hbar\varepsilon_0}\frac{\Omega}{2\pi}\int_t^{t+2\pi/\Omega} \mathrm{d}t'\, \dot{P}(t'), \tag{406}$$

and the nonlinear diffusion coefficient $D(\varepsilon_0, \hat{\varepsilon})$ is given by

$$D(\varepsilon_0,\hat{\varepsilon}) = \lim_{t\to\infty} \frac{\Omega}{4\pi}\int_t^{t+2\pi/\Omega} \mathrm{d}t'\, \dot{S}(t')\,, \tag{407}$$

where the position's expectation value $P(t) := \langle q\rangle_t$, as well as the variance $S(t) := \langle q^2\rangle_t - \langle q\rangle_t^2$, are defined in Eq. (132).

The path-integral evaluation of the velocity $v(t) = \dot{P}(t)$ in the presence of ac–dc fields has been addressed in Ref. [291], to the lowest perturbative order Δ_0^2 in the tunneling matrix element, under the assumption that the particle tunnels incoherently from site to site. As demonstrated in Ref. [292] for the case of a dc-field, and in [293] in the presence of a time-dependent field, in this case the resulting dynamics is identical to that of a nearest-neighbor hopping model in which the occupation probabilities obey rate equations. These equations can be thought as the generalization of the NIBA Markovian equation (343) to the case of a tight-binding lattice. More generally, by abandoning the Markovian assumption, the NIBA set of coupled equations for a driven tight-binding lattice reads [294]

$$\begin{aligned}\dot{P}_n(t) = &\int_0^t \mathrm{d}t'[W_{\mathrm{f}}(t,t')P_{n-1}(t') + W_{\mathrm{b}}(t,t')P_{n+1}(t')]\\ &- \int_0^t \mathrm{d}t'(W_{\mathrm{f}}(t,t') + W_{\mathrm{b}}(t,t'))P_n(t')\,,\end{aligned} \tag{408}$$

where the backward $W_{\mathrm{b}}(t,t')$ and forward $W_{\mathrm{f}}(t,t')$ kernels can be expressed in terms of the NIBA kernels $K^{(\pm)}(t,t')$ in Eq. (303) by using the relations $K^{(+)}(t,t') = W_{\mathrm{f}}(t,t') + W_{\mathrm{b}}(t,t')$ and $K^{(-)}(t,t') = W_{\mathrm{f}}(t,t') - W_{\mathrm{b}}(t,t')$. In the Markovian limit, one obtains from Eq. (408) the coupled set of equations [293]

$$\dot{P}_n(t) = \Gamma_{\mathrm{f}}(t)P_{n-1}(t) + \Gamma_{\mathrm{b}}(t)P_{n+1}(t) - (\Gamma_{\mathrm{f}}(t) + \Gamma_{\mathrm{b}}(t))P_n(t)\,, \tag{409}$$

where the backward Γ_{b} and forward Γ_{f} tunneling rates can be expressed in terms of the NIBA Markovian kernels $\Gamma_{\mathrm{M}}(t)$ and $\rho_{\mathrm{M}}(t)$ in Eqs. (344) and (346) using the relations $\Gamma_{\mathrm{M}}(t) = \Gamma_{\mathrm{f}}(t) + \Gamma_{\mathrm{b}}(t)$ and $\rho_{\mathrm{M}}(t) = \Gamma_{\mathrm{f}}(t) - \Gamma_{\mathrm{b}}(t)$.

The general solution of Eq. (409) can be obtained in the form

$$P_n(t) = \exp[-(F(t) + B(t))](F(t)/B(t))^{-n/2} I_n(2\sqrt{F(t)B(t)})\,, \tag{410}$$

with

$$B(t) = \int_0^t \mathrm{d}t'\,\Gamma_{\mathrm{b}}(t'), \qquad F(t) = \int_0^t \mathrm{d}t'\,\Gamma_{\mathrm{f}}(t')\,, \tag{411}$$

and $I_n(z)$ is the modified Bessel function of order n. This in turn leads to the result

$$P(t) = d[F(t) - B(t)]\,, \qquad S(t) = d^2[F(t) + B(t)]\,. \tag{412}$$

In the dc-limit $\hat{\varepsilon} \equiv 0$ one recovers the known relations $P(t) = d\rho_0 t$ and $S(t) = d^2\gamma_0 t$, where $\Gamma_0 = \Gamma_M|_{\hat{\varepsilon}=0}$ and $\rho_0 = \rho_M|_{\hat{\varepsilon}=0}$, cf. Eqs. (306) and (307). Hence, the particle diffuses *linearly* in time with nonlinear dc-mobility $\mu_0(\varepsilon_0) = d^2\rho_0(\varepsilon_0)/\hbar\varepsilon_0$ and dc-diffusion coefficient $D_0(\varepsilon_0) = d^2\Gamma_0(\varepsilon_0)/2$. Turning next to the explicit expression for the nonlinear mobility $\mu(\varepsilon_0, \hat{\varepsilon})$ and the nonlinear diffusion coefficient $D(\varepsilon_0, \hat{\varepsilon})$, one finds [293]

$$\mu(\varepsilon_0, \hat{\varepsilon}) = \frac{d^2\Delta_0^2}{\hbar\varepsilon_0}\int_0^\infty \mathrm{d}\tau\, J_0\left(\frac{\hat{\varepsilon}}{\Omega}\sin\left(\frac{\Omega\tau}{2}\right)\right)h^{(-)}(\tau)\sin(\varepsilon_0\tau)\,, \tag{413}$$

$$D(\varepsilon_0, \hat{\varepsilon}) = \frac{d^2}{2}\Delta_0^2\int_0^\infty \mathrm{d}\tau\, J_0\left(\frac{\hat{\varepsilon}}{\Omega}\sin\left(\frac{\Omega\tau}{2}\right)\right)h^{(+)}(\tau)\cos(\varepsilon_0\tau)\,, \tag{414}$$

with $h^{(\pm)}(\tau)$ defined in Eq. (308). Hence, the nonlinear diffusion has the same form as the incoherent tunneling rate of a two-state system driven by a fast ac-field, cf. Eq. (351).

Thus far, our NIBA results have been general. For quantitative calculations we restrict ourselves to the important case of Ohmic dissipation (294). In our reported calculations we have used a high-frequency cutoff $\omega_c = 20\Delta_0$.

The mean square deviation $S(t)$ vs. time is depicted by the curves in Fig. 27. The average slope of the curves in Fig. 27 is well approximated by twice the diffusion coefficient $D(\varepsilon_0, \hat{\varepsilon})$ in Eq. (414). For generic values of ε_0, $\hat{\varepsilon}$ and Ω, the ac-controlled diffusion is reduced as compared to the undriven case ($\varepsilon_0 = \hat{\varepsilon} = 0$). Though, near resonances $\varepsilon_0 = n\Omega$, the diffusion can be enhanced. For values of $\hat{\varepsilon}$ and Ω such that $J_0(\hat{\varepsilon}/\Omega) \simeq 0$, i.e., $\hat{\varepsilon}/\Omega \simeq 2.4$, see the dot–dashed curves in Fig. 27, the diffusion becomes very slow, especially for zero dc-bias ε_0 and high driving frequencies Ω. This choice for $\hat{\varepsilon}/\Omega$ corresponds to the condition for dynamic localization (DL) found for nondissipative TB systems, cf. Section 4. This behavior can also be inferred by inspecting Fig. 21 where the high-frequency rate $\Gamma_H = 2D(\varepsilon_0, \hat{\varepsilon})/d^2$ is plotted versus the dc-bias ε_0.

In Fig. 28a the dimensionless current $I(\varepsilon_0, \hat{\varepsilon}; \alpha)/ed\Delta_0$, where $I = e(\hbar\varepsilon_0/d)\mu$, with e denoting the elementary electron charge, is plotted vs. the dissipative strength α for different driving frequencies Ω. Two striking effects occur for weak damping and strong damping, respectively: (i) A *negative current* at weak dissipation is observed. Moreover, for fixed $\hat{\varepsilon}$ and Ω the amplitude of the negative current is *maximal* for a characteristic value $\alpha = \alpha^*$ of the Ohmic strength. (ii) For stronger dissipation the current becomes independent of the ac-frequency and of dissipation on a wide range. As the frequency is increased further, the linear response regime $\hat{\varepsilon}/\Omega \ll 1$ is approached and the current moves towards its dc-limit, full-line in Fig. 28a. In Fig. 28b, $I(\varepsilon_0, \hat{\varepsilon}; \alpha)/ed\Delta_0$ is plotted vs. the applied dc-voltage ε_0 for different values of the applied ac-voltage $\hat{\varepsilon}$. A negative current vs. static bias ε_0, i.e., a "negative conductance" is observed for small dc-bias.

To explain the results of Figs. 27 and 28 it is convenient to expand $J_0((\hat{\varepsilon}/\Omega)\sin(\Omega\tau/2))$ in Fourier series, yielding

$$\mathscr{R}(\varepsilon_0, \hat{\varepsilon}; \alpha) = J_0^2\left(\frac{\hat{\varepsilon}}{\Omega}\right)\mathscr{R}_0(\varepsilon_0; \alpha) + \sum_{n=-\infty, n\neq 0}^{\infty} J_n^2\left(\frac{\hat{\varepsilon}}{\Omega}\right)\mathscr{R}_0(\varepsilon_0 + n\Omega; \alpha)\,, \tag{415}$$

where $\mathscr{R}_0(\varepsilon_0; \alpha) := \mathscr{R}(\varepsilon_0, \hat{\varepsilon} = 0; \alpha)$, and $\mathscr{R} = I$ or D. Thus, the ac-voltage produces new channels for dc-current flow or dc-diffusion due to photon emission ($n < 0$) and absorption ($n > 0$), each

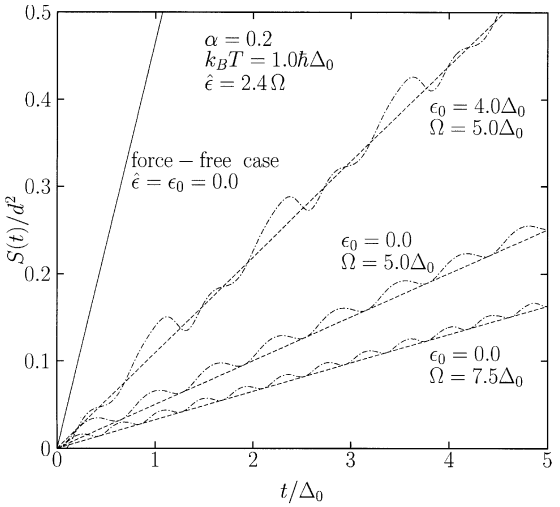

Fig. 27. Diffusion in the driven and dissipative tight-binding system. The dimensionless variance $S(t)/d^2 = (\langle q^2\rangle_t - \langle q\rangle_t^2)/d^2$ vs. time (full straight line and dot–dashed curves) can be reduced or enhanced as compared to the force-free case. It assumes its minimal values for zero dc-bias, high ac-frequencies Ω and when $\hat{\varepsilon} \simeq 2.4\Omega$. The dashed straight lines depict the curve $2D(\varepsilon_0,\hat{\varepsilon})t$, where D is the diffusion constant in Eq. (414). Ohmic dissipation is considered.

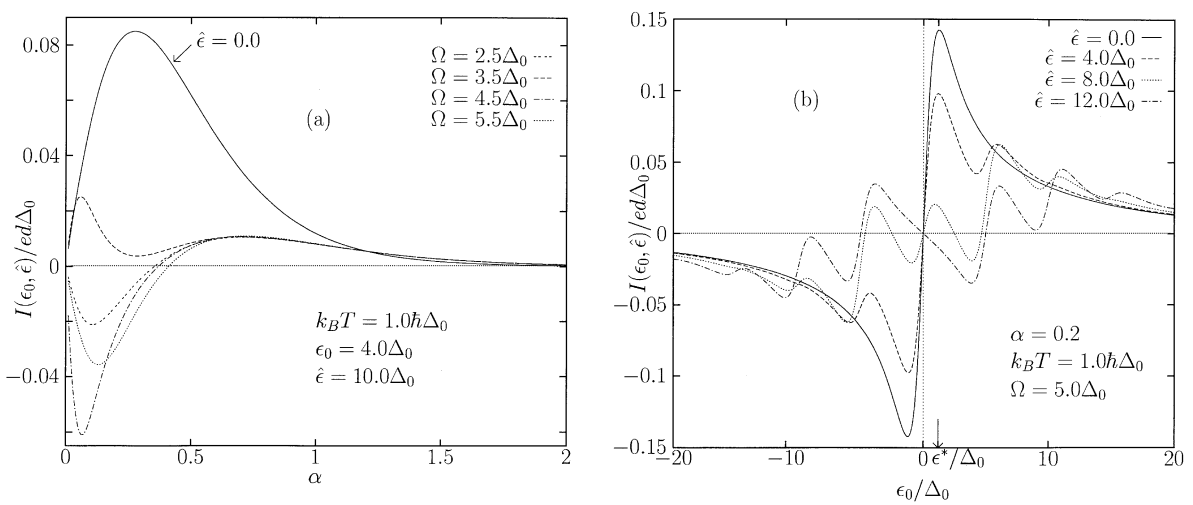

Fig. 28. Dimensionless average current $I/ed\Delta_0$ in the driven and dissipative tight-binding system. $I/ed\Delta_0$ is plotted vs. the dissipative Ohmic coupling strength α (panel (a)) and vs. the dc-bias ε_0 (panel (b)). For weak dissipation a negative current occurs which is maximal for a nonzero value of α. For stronger dissipation the current becomes independent of both the ac-frequency Ω and of the dissipative strength α on a wide range.

weighted by the factor $J_n^2(\hat{\varepsilon}/\Omega)$. With $\mathscr{R}$ being the current I, we note that Eq. (415) formally coincides with the driven tunneling current of Tien–Gordon theory [15] in Eq. (155): The result for the corresponding dc-tunneling current is here substituted by the dissipation renormalized static current, resulting from Eq. (413) with $\hat{\varepsilon} = 0$.

Let us discuss the time-averaged current further. The current inversion in Fig. 28 is due to the competition between the channels with $n \geq 0$, each of which always gives a positive contribution to the total current, and higher-order channels with $n < 0$ which may give a negative contribution. In fact, with the help of the blocking effect, i.e., $J_0(\hat{\varepsilon}/\Omega) \simeq 0$ of the $n = 0$ channel, it can be more favorable in current gain (in absolute value) to emit n photons than to absorb n of them, even if the weight $J_n^2(\hat{\varepsilon}/\Omega)$ of the sidebands is the *same*. For example, for the dot–dashed curve in Fig. 28a the main contribution to the current is found to come from the first negative channel ($n = -1$) (not shown). Correspondingly, the maximal negative inversion occurs for $\alpha = \alpha^* \neq 0$ such that $|I_0(\varepsilon_0 - \Omega; \alpha)|$ is maximal as a function of α, cf. Fig. 28a. For fixed $\hat{\varepsilon}$, $I(\varepsilon_0, \hat{\varepsilon}; \alpha)$ vs. ε_0 may have several minima $\varepsilon_{\min}^{(n)}$ determined by the condition

$$\varepsilon_{\min}^{(n)} + \varepsilon^* = n\Omega\,, \tag{416}$$

where ε^* is the maximum of the dc-current I_0 vs. the dc-bias, see Fig. 28b. Note that the positions of these minima do not depend on the strength $\hat{\varepsilon}$ of the ac-field. The ac-field strength determines instead the weight of the different channels. For the parameters chosen in Fig. 28b, the maximal negative current occurs when $\hat{\varepsilon}$ is chosen such that the first channel dominates, i.e., $J_n^2(\hat{\varepsilon}/\Omega) \simeq 0, n \neq 1$. A similar reasoning applies to explain the behaviour of the variance in Fig. 27.

Finally, we observe that the structure in Eq. (415) is *universal*, i.e., it does not depend on the specifics of the thermal bath. Dissipation determines instead the shape of the dc-current I_0, and of the dc-diffusion D_0. Hence, as long as the dc-current vs. the dc-bias presents the physical characteristics of being antisymmetric, i.e., positive (negative) for $\varepsilon_0 > 0$ ($\varepsilon_0 < 0$) with a maximum at $\varepsilon_0 = \varepsilon^*$, a current reversal is possible even for a dissipative mechanism which is different from the Ohmic one. In the same spirit, in the investigated temperature regime $k_B T \ll \hbar\omega_c$, the nonlinear diffusion will be strongly reduced in the parameter regime of dynamic localization.

Indeed, a similar behavior for the current vs. the dc-bias in semiconductor superlattices at room temperature has been theoretically described in [16–18,92] within a phenomenological approach based on a classical Boltzman equation with a single collision time ansatz; and in [98] within the framework of a bias modulated Bardeen Hamiltonian for N quantum wells. Recently, such time-averaged negative currents vs. the dc-bias have been experimentally observed in semiconductor superlattices [20,21].

Note, however, the fact that the dc-current $I_0 \to 0$ as the dc-strength $\varepsilon_0 \to \infty$ is solely a peculiarity of the single band approximation used for the Hamiltonian H_{TB} in Eq. (404). Such an approximation in fact breaks down whenever the externally applied dc- and ac-field strength ε_0 and $\hat{\varepsilon}$, as well as the driving frequency Ω, become comparable with the interband level spacing. The effect of higher bands on the dc-voltage characteristics in dc-ac driven superlattices has recently been discussed in [295] within the framework of the Bardeen Hamiltonian. There, the characteristic saw-tooth profile of the average current vs. dc-bias due to the formation of high-field domains is also discussed.

Finally, we observe that an absolute negative conductance has recently been predicted also for a dissipative TB particle under the combined effect of a dc- and of a dichotomous field [294]. Again, this effect is found to be largely independent of the specifics of the shape of the dc-current I_0 vs. dc-bias.

14. Dissipative tunneling in a driven double-well potential

In Section 6 the nondissipative tunneling motion of a particle moving in a driven double well, cf. Eqs. (172) and (173), has been discussed, while in Sections 11 and 12 we investigated the driven and dissipative dynamics restricting our attention only to the lowest doublet of the potential, i.e., in the two-level-system (TLS) approximation. Here we shall investigate the dissipative motion within the full double-well dynamics.

14.1. The driven double–doublet system

The first new feature arising in the full double-well potential (DW), as compared to the TLS, is the possibility of vibrational relaxation (i.e., intradoublet transitions) in addition to left-to-right tunneling (i.e., interdoublet transition). The competition between intra- and interwell relaxation rates for the undriven DW has been discussed analytically in [296,297] and [298].

When an external ac-field is applied, the possibility of controlling tunneling by pumping population from the lower to the upper tunneling pairs occurs. Very recently, a calculation in this direction has been initiated in [299,300], where the authors restrict themselves to the case of a DW when only the two lowest energy doublets are thermally accessible. In [299,300], the polaron transformation [259] usually applied to investigate the two-level system [257,158] is extended to the double–doublet system (DDS) problem. A second-order perturbative calculation in the Franck–Condon renormalized tunneling doublets is then carried out. As suggested in [299,300], because the upper doublet is at least one order of magnitude larger than the lower one, even a small increase of the upper doublet's population can lead to a significative increase in population transfer between the localized states of the underlying double-well potential.

Some of the most intriguing results for an external field which is resonant with the interdoublet spacing can be summarized as follows:

(i) The asymptotic upper doublet population $p_{\mathrm{up}}(\infty)$ is naturally increased by an external resonant field as compared to the nondriven case.

(ii) As long as the vibrational relaxation rate is larger than the interdoublet tunneling rates, the upper and lower doublet populations will reach their asymptotic values on a shorter time scale as compared to the left–right scale. The overall left–right rate constant is then the sum of the individual doublet left–right rate constants, each weighted by the corresponding steady-state doublet population. Because the asymptotic upper doublet population $p_{\mathrm{up}}(\infty)$ is increased by an external field as compared to the nondriven case, the external field serves to pump population in the upper doublet, from where it can be more effectively transferred to the right well by left–right tunneling transitions.

(iii) When, on the contrary, vibrational relaxation occurs on a much longer time scale as compared to interdoublet tunneling, the two doublets are effectively decoupled in the absence of an external field.

In the presence of an external resonant field, the up–down population would oscillate indefinitely at the gap frequency if the left–right rate processes were absent. Dissipation qualitatively changes the characteristics of the left (right) population, which reaches asymptotically the steady value $\frac{1}{2}$. The evolution of the left (right) population towards the steady-state value $\frac{1}{2}$ may be underdamped or extremely overdamped depending on the choice of the parameters.

14.2. Coherent tunneling and dissipation

Here, we shall apply the Floquet–Markov–Born approach of Section 9 to investigate numerically the effects of dissipation on driven tunneling in the DW. For the numerical calculations the dimensionless variables and parameters are given by $D = E_B/\hbar\omega_0$, $\bar{T} = k_B T/\hbar\omega_0$, $\bar{\gamma} = \gamma/\omega_0$, $\bar{\Omega} = \Omega/\omega_0$, $\bar{S} = Sx_0/\hbar\omega_0$, where $x_0 = \sqrt{\hbar/m\omega_0}$, see also Eqs. (174) and (175), and γ is the damping coefficient which enters in the Ohmic spectral density Eq. (235). In the following we omit the overbars. The driven double-well potential $V_1(q,t)$ introduced in Eq. (226) then reads

$$V_1(q,t) = -\frac{q^2}{4} + \frac{q^4}{64D} + Sq\cos(\Omega t)\,, \tag{417}$$

where D is the dimensionless barrier height.

We report on the predictions on the tunneling dynamics of the driven double-well resulting from the simple RWA in Eq. (251), and from its improved version, see discussion above Eq. (251). The latter form will have to be used when investigating the coherent destruction of tunneling induced by the monochromatic field, where quasidegeneracies in the quasienergy spectrum occur. A thermal bath with a spectral density $J(\omega)$ of the Ohmic–Drude form as in Eq. (236) has been chosen.

Using the results of Refs. [191,192], the slow dynamics generated by the simplest RWA equation (251) is depicted in Fig. 29 in a stroboscopic manner. In Fig. 29a we show the time evolution of the correlation function $P(t_n) = \mathrm{Tr}\{\rho(t_n)\rho(t_0)\}/\mathrm{Tr}\{\rho(t_0)^2\}$, where $\rho(t_0)$ is the reduced density matrix at the initial time, and $t_n = n\mathscr{T}$. A pure coherent state centered at one of the classical attractors in the right well is chosen as the initial state. The chosen parameters are $D = 6$, $\gamma = 10^{-5}$, $T = 0$, $S = 0.08485$, and $\Omega = 0.9$, so that the driving frequency Ω is close to the fundamental first resonance. Note that for these values of the damping and barrier height the condition $\Delta_0 \gg \gamma$ for the validity of the Markov–Born approximation, with Δ_0 of the order of the lowest tunneling doublet, is not satisfied. Though, the results still qualitatively reproduce the correct dynamics. There is a slow decaying oscillation of $P(t_n)$ between 0 and 1, which corresponds to the familiar tunneling, and superimposed there is a fast oscillation of smaller amplitude due to a participation of additional, higher lying quasienergy states. The broadening of the energy levels due to the incoherent transitions induced by the reservoir can be read from the Fourier transform $\tilde{P}(\omega)$ of $P(t_n)$, which is depicted in Fig. 29b. The spatially resolved states $P(q,t_n) = \langle q|\rho(t_n)|q\rangle$ after 20 (graph 1), 40 (graph 2), 8910 (graph 3) and 5×10^4 (graph 4) driving periods $\mathscr{T}$ of the ac-driving, respectively, as well as for $t \to \infty$ are presented in Fig. 29c. While the slow oscillations $[(1,2) \to 3]$ correspond to a flow of probability between the two potential wells, the fast oscillations are associated with transport within the wells. The stationary state, thick line in Fig. 29c, in turn, does bear the signature of the classical dynamics. Fig. 29d depicts a phase space representation of this state in terms of the Husimi function [167]. A comparison with the corresponding stationary states of the deterministic classical systems (sharp peaks in Fig. 29d) demonstrates that the occurrence of two pairs of maxima coincides with the bifurcation of the classical stationary distribution into two separate point attractors (in a stroboscopic picture) in each well.

Fig. 30a and b are dedicated to the inspection of the influence of dissipation on the coherent suppression of tunneling. Because we have to investigate the dynamics in the vicinity of the manifold where a crossing of quasienergies occurs, one cannot use the simplified RWA master

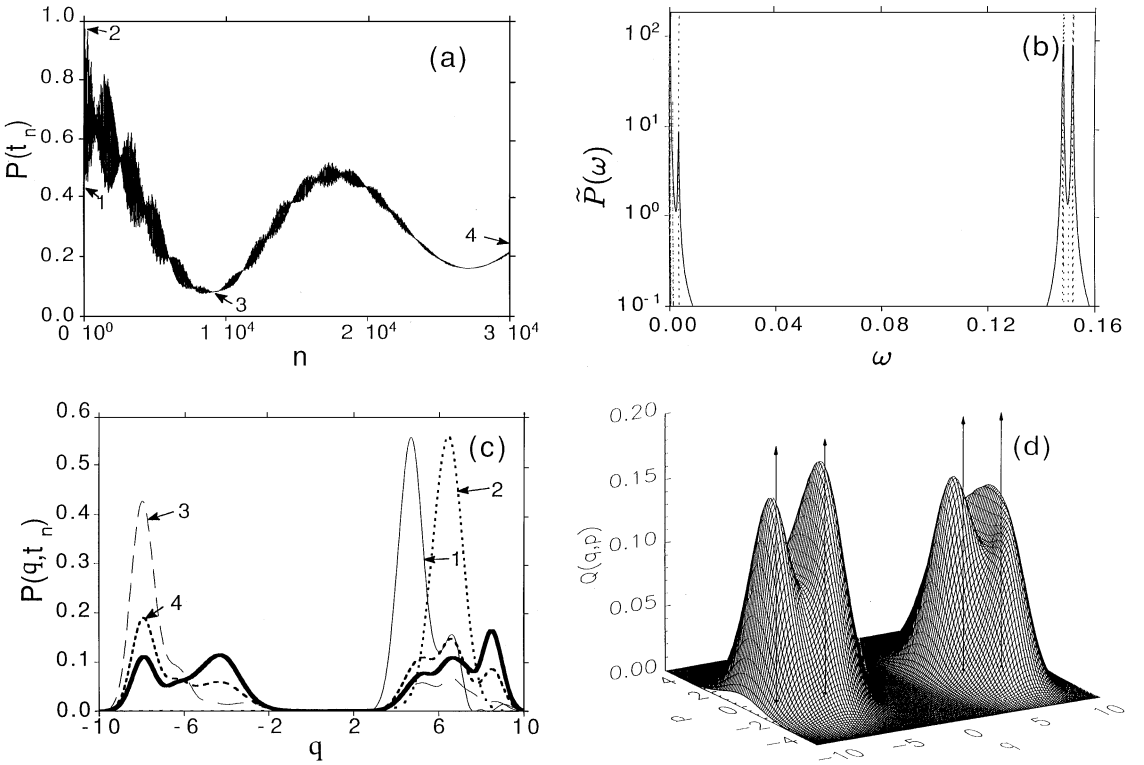

Fig. 29. Tunneling in the ac-driven double well with Ohmic dissipation. The scaled parameters are $D = 6$, $\Omega = 0.9$, $S = 0.08485$, $\gamma = 10^{-5}$, and $T = 0$. (a) Time evolution of the autocorrelation function $P(t_n)$, $t_n = 2\pi n/\Omega$, over the first 10^4 time steps, starting from a state centered in one of the wells; (b) a section of the Fourier transform of (a) (dashed: the same function for the undamped case); (c) spatially resolved states at times t_n (graph 1) $n = 20$, 2) $n = 40$, 3) $n = 8910$, 4) $n = 5 \times 10^4$ and stationary state (thick curve); (d) Husimi distribution of the stationary state, compared with the corresponding classical distribution (sharp peaks).

equation in Eq. (251). Fig. 30a depicts the time evolution of the correlation function $P(t_n)$ for parameters of the double well slightly offset from the localization manifold for $\gamma = 10^{-6}$, $D = 2$ and various values of the temperature T. $P(t_n)$ is evaluated in the improved master equation beyond RWA, where only terms with $k \neq k'$ have been dropped. At low temperatures, $P(t_n)$ exhibits a slowly decaying coherent oscillation with a very long period, due to the small detuning from the quasi-energy crossing. The fast decay of superimposed oscillations reflecting the admixture of higher order quasienergy states is shown in Fig. 30b. Asymptotically, the distribution among the wells (in this stroboscopic picture) is completely thermalized. Upon increasing temperature, the decay time of the coherent oscillations first decreases until this oscillation is suppressed from the beginning (not shown). After going through a minimum, however, the decay time τ_d of $P(t_n)$, defined by $P(t_n) \simeq \exp(-n/\tau_d)$, *increases* again, until it reaches a resonance-like maximum at an optimal temperature T^*, see Fig. 30b. This maximum occurs at a temperature T^* such that the time scale of the incoherent processes induced by the reservoir *stabilizes* the localization of the wave packet in one of the two wells.

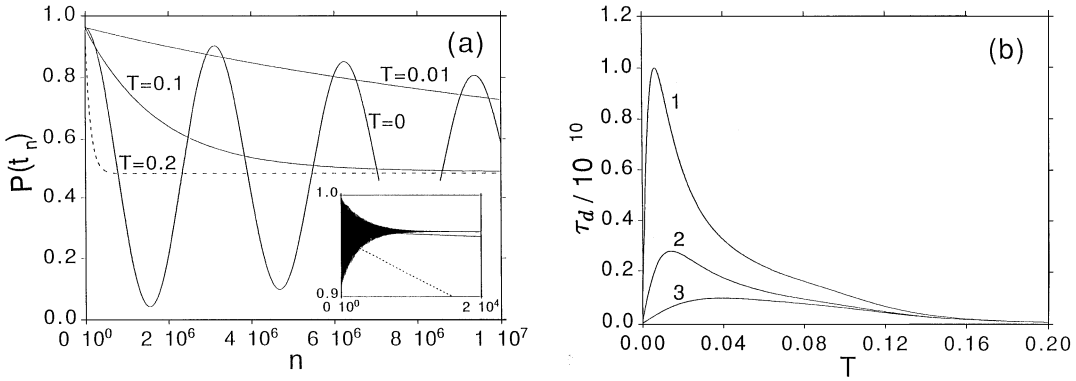

Fig. 30. Coherent suppression of tunneling in the presence of Ohmic dissipation. (a) Time evolution of the autocorrelation function $P(t_n)$ over the first 10^7 time steps. The scaled parameters being $D = 2$, $\Omega = 0.01$, $S = 3.171 \times 10^{-3}$ and $\gamma = 10^{-6}$. Inset: The first 2×10^4 time steps on an enlarged time scale; temperature dependence of the decay time τ_d (defined by $P(t_n) \simeq \exp(-n/\tau_d)$) for three values of the detuning $\Delta\Omega = \Omega - \Omega_{loc}(S)$ from the localization manifold. Graph (1) $\Delta\Omega = -1.4 \times 10^{-7}$, (2) $\Delta\Omega = 5 \times 10^{-7}$ at $S = 3.1712 \times 10^{-3}$, (3) $\Delta\Omega = 1.4 \times 10^{-6}$ at $S = 3.1715 \times 10^{-3}$. The other parameters are as in (a).

14.3. Dynamical hysteresis and quantum stochastic resonance

The QUAPI method discussed in Section 10 is applied to investigate the dynamics in a driven double-well potential

$$V_1(q,t) = -\frac{q^2}{4} + \frac{q^4}{64D} - Sq\cos(\Omega t)\,, \tag{418}$$

in the presence of Ohmic dissipation, cf. Eq. (237) [203,204]. In parametric form, i.e., in a panel of $\langle q \rangle_t$ vs. $F(t) = -S\cos(\Omega t)$, one then observes at asymptotic times a hysteresis loop, cf. Fig. 31, where the area $\mathscr{A}$ comprised by the hysteresis curve is conveniently characterized by

$$\mathscr{A} = \oint \langle q \rangle_t \, \mathrm{d}F(t) = S\Omega \int_0^{2\pi/\Omega} \mathrm{d}t \langle q \rangle_t \sin(\Omega t)\,. \tag{419}$$

The area $\mathscr{A}$ of the hysteresis curve is investigated in Fig. 32. The driving strength is assumed to be so strong that after the time interval τ_{bi} one of the two potential minima disappears and the potential exhibits only one global minimum. This driven bistable device can then be thought as a quantum switch. Moreover, in the investigated temperature regime both quantum and classical fluctuations contribute to the particle's dynamics. In Fig. 32 the area $\mathscr{A}$ is plotted vs. driving frequency for different temperatures. For low driving frequencies the hysteresis area is very small, because the particle has enough time to tunnel from one metastable minimum to the global minimum induced by the driving force. Enhancing the frequency the area becomes larger. For even higher frequencies, though, the particle cannot follow anymore the details of the potential modulation and it feels an effective static barrier. In this latter case the area is reduced again, and the particle is on average situated in the potential barrier region. From this discussion it is clear that the maximal area occurs at some intermediate driving frequency. Similar as for the case of

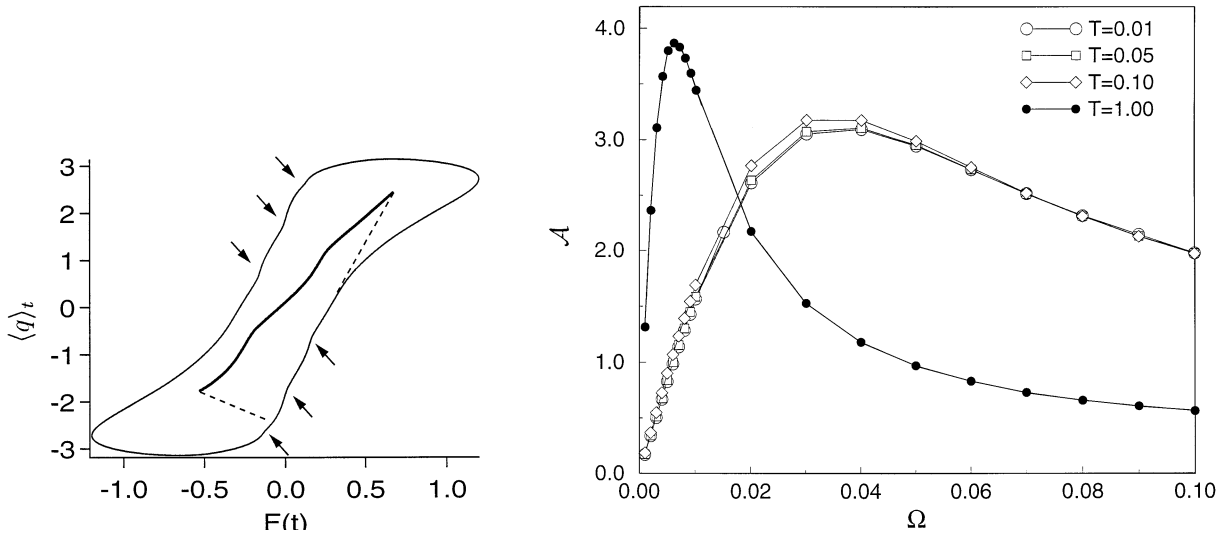

Fig. 31. Quantum hysteresis. The position expectation value $\langle q \rangle_t$ computed parametrically as a function of an external force $F(t) = -S\cos(\Omega t)$ exhibits a hysteresis loop. As a signature of quantum dynamics, steps in the quantum hysteresis loop, as indicated by the arrows, occur. Inset: enlarged part of the hysteresis loop where steps can be observed. Parameters in scaled units are $D = 1.5$, $S = 1.2$, $\Omega = 10^{-4}$, $\gamma = 0.005$, $T = 0.1$.

Fig. 32. The area $\mathscr{A}$ of the hysteresis loop for a driven and dissipative double well. The area $\mathscr{A}$ is shown vs. driving frequency Ω for dimensionless parameters $\gamma = 1.0$, $D = 1$ and $S = 0.8$ at different temperatures. A maximum occurs at finite frequencies which, at low temperatures, is independent of temperature.

classical hysteresis, it can be argued that the maximum occurs for the optimal frequency $\Omega_{\max}$ such that half the time interval $\tau_{bi} \propto 1/\Omega_{\max}$ during which the system is bistable balances the decay time τ_d to cross the barrier due to incoherent tunneling [203]. This matching condition is confirmed by Fig. 32 which shows that at low temperatures the area is only weakly temperature dependent, in agreement with semiclassical results on the decay time τ_d [33]. For higher temperatures, the optimal matching frequency $\Omega_{\max}$ is shifted to lower values. This is surprising since it implies a decrease of the relaxation rate with increasing temperatures.

An intriguing feature is shown in Fig. 31, where the quantum hysteresis loop exhibits *steps* [204]. The same feature has recently been observed experimentally in high-spin molecular magnets [306]. However, it should be remembered that the two physical systems are rather different. To understand better the origin of these steps, the transient time-dependent response $\langle q \rangle_t$ is plotted vs. time in Fig. 33. The system has been prepared in a steady state with a strong tilt to the left, and subsequently has been let slowly evolve towards a positive tilt. Steps similar to those in the hysteresis loop occur. In correspondence to these steps, the energy spectrum computed parametrically as a function of a static control force (i.e., $\Omega = 0$) exhibits avoided level crossing. There, tunneling is enhanced, and a step occurs. The first step for negative tilt is characteristic for thermally assisted resonant tunneling. In agreement with such avoided level crossing features, a multiresonance structure of the relaxation rate plotted vs. a static force is observed [204].

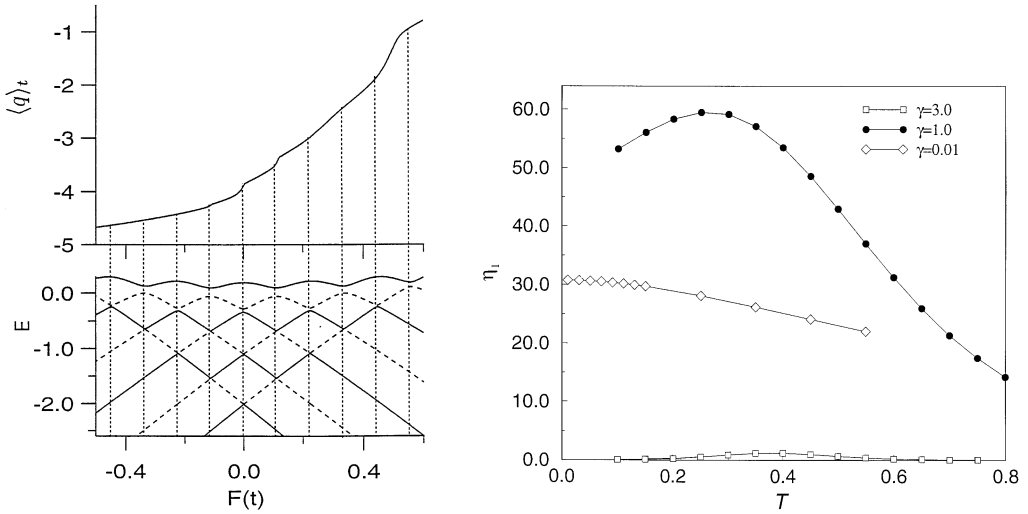

Fig. 33. Avoided level crossing dynamics for a quantum switch. Upper panel: Position expectation value $\langle q\rangle_t$ vs. $F(t) = -S\cos(\Omega t)$. Characteristic steps are observed. The chosen parameters in scaled units are $D = 2.5$, $S = 0.7$, $\Omega = 10^{-4}$, $\gamma = 0.001$, $T = 0.1$. Lower panel: The first adiabatic energy levels (alternatingly dashed and solid lines) computed parametrically as a function of a *static* control force. The steps in $\langle q\rangle_t$ occur in correspondence with avoided level crossings.

Fig. 34. Quantum stochastic resonance (QSR) for a strongly driven double well. The spectral amplification η_1 is plotted vs. temperature at $\Omega = 0.015$, $S = 0.4$ and $D = 1$, for various Ohmic friction strengths γ. The occurrence of the maximum at finite temperatures indicates QSR. As the damping strength γ is decreased the maximum disappears, i.e., QSR vanishes when quantum coherent processes start to dominate over incoherent ones.

Finally, upon noting that $\langle q\rangle_{t\to\infty} = \sum_m p_m(\Omega, S)\mathrm{e}^{-\mathrm{i}m\Omega t}$, the spectral amplification

$$\eta_1 = 4\pi|p_1(S,\Omega)/S|^2\,, \tag{420}$$

describes quantum stochastic resonance (QSR), cf. Section 12.1.4. The temperature dependence of η_1 is shown in Fig. 34 for different damping strengths. A maximum at finite temperatures indicates QSR. It should be observed that for the parameters chosen in the figure the unperturbed double well potential has only one tunneling doublet below the barrier. Nevertheless, due to the very high driving strength considered, and the relatively high-temperature regime at which the maximum occurs, the two-level system approximation discussed in Section 11 is now no longer valid.

15. Conclusions

With this long review we have attempted to present a "tour of horizon" of the physics that is governed by driven quantum tunneling events. With the present day availability of strong radiation sources such as e.g. free-electron laser systems yielding strong and coherent electric driving fields, together with the advances in micro- and nano-technology, the challenges involving *driven*

quantum transport have moved into the limelight of present day scientific activities. In doing so, several novel interpretative concepts as well as new analytic and computational tools have been put forward. These tools, such as the Floquet approach, the (t, t')-formalism or the computational quasiadiabatic propagator method, to name only a few, are intrinsically nonperturbative in nature. Thus, they are ideally suited to describe non-linear novel driven tunneling phenomena beyond conventional perturbation schemes.

In the foregoing sections we hopefully have conveyed several novel features that characterize quantum tunneling as it arises as the result from an interplay involving *nonlinearity*, *time-dependent forcing* and *dissipation*. As shown repeatedly, the application of suitably tailored strong driving forces allows one to selectively control, a priori, quantum tunneling-dominated processes such as population transfer, energy transfer, tunneling probabilities, reaction rates, diffusion coefficients, or current–voltage characteristics.

The material in the first seven sections solely deals with driven tunneling in *absence* of dissipative, environmental influences. The remaining parts account for the modifications that are acquired when frictional quantum effects additionally perturb the driven tunneling dynamics. Although the main scope of this review has been on the theoretical development we have interfaced the presentation with experimental corroboration and/or applications to the best of our knowledge. In doing so, the authors share the hope that both *theory* and even more *experiment* will become invigorated by readers of this present review.

Certain topics involving driven tunneling have remained untouched. To a large extent the authors focused – although not exclusively – on tunneling problems for which the underlying quantum states are localized, implying bounded transport quantities. In the case of a pure ac-drive, these quantum states can be described in terms of a pure *point spectrum* for corresponding quasienergies and corresponding square integrable Floquet modes, respectively. In contrast, driven tunneling in periodic structures, cf. Sections 4 and 13, involve extended (scattering) states that belong to an absolute *continuous spectrum*, which in turn rule unbounded transport quantities. A field-induced barrier transparency in a periodically driven potential barrier has been recently discussed in [301]. In situations where extended quantum states determine the physics, such as in ionization, dissociation, decay of resonances, ac-driven quantum decay, etc., it is often necessary to rotate the coordinates of the Hamiltonian into the complex plane (complex scaling) [302,303]. Characteristic applications are ac-induced dissociation from a nonlinear quantum well [304] or ac-driven quantum decay out of a metastable well [305]. In both of these cases the quantum dynamics becomes governed by complex-valued quasienergies.

The field of driven tunneling is presently enjoying widespread interest among the communities of both physics and chemistry. Without doubt, we shall experience still many novel effects that are predominantly ruled by driven quantum tunneling; nevertheless, we share the confident belief that this survey, although not complete, captures a good snapshot of the present state of the art of a very dynamic research area.

Note added in proof

After submission of this review several contributions to a timely topic, namely the *spontaneous dc-current generation* in the presence of external, *unbiased* time-dependent fields have appeared.

For example, this effect has been predicted in ac-driven semiconductor superlattices when a symmetry breaking mechanism due to repulsive electron–electron interaction occurs [307]. Likewise, a new class of discrete *Brownian rectifiers* occurs when considering the dissipative motion of a tightbinding particle in the presence of unbiased, asymmetric forcing, such as e.g. in the presence of harmonic mixing signals of the form $\hat{\varepsilon}_1 \cos(\Omega t) + \hat{\varepsilon}_2 \cos(\Omega t + \varphi)$ [308], or in the presence of an asymmetric dichotomic Markov field [309]. Directed, quantum noise induced current is generated also in *quantum ratchets*, i.e., in periodic structures that lack reflection symmetry. In this context, the induced current in a continuous ratchet potential has been investigated in [310], and for a discrete model in [311].

Acknowledgements

M. Grifoni and P. Hänggi greatly acknowledge the support of the Deutsche Forschungsgemeinschaft via the Schwerpunktprogramm "Zeitabhängige Phänomene und Methoden in Quantensystemen der Physik und Chemie" (HA 1517/14-2). We also thank L. Hartmann for preparing some figures for this review. Moreover, we thank L. Hartmann, M. Holthaus, N. Makri, M. Thorwart, R. Utermann, M. Wagner and M. Winterstetter for providing original figures relating to their works. In the course of writing this review we enjoyed numerous insightful discussions with friends and colleagues around the world, in particular, among others, with R. Aguado, R. Coalson, Y. Dakhnovskii, T. Dittrich, M. Holthaus, I. Goychuk, F. Grossmann, J. M. Gomez-Llorente, L. Hartmann, G. Ingold, P. Jung, H.-J. Korsch, S. Kohler, N. Makri, N. Moiseyev, P. Neu, P. Pechukas, U. Peskin, G. Platero, P. Reimann, M. Sassetti, J. Shao, J. Stockburger, M. Thorwart, D. Tannor, R. Utermann, M. Wagner, M. Winterstetter and U. Weiss.

References

[1] N.L. Manakov, V.D. Ovsiannikov, L.P. Rapoport, Phys. Rep. 141 (1986) 319.
[2] S.-I. Chu, Adv. Chem. Phys. 73 (1986) 739.
[3] F.H. Faisal, Theory of Multiphoton Processes, Plenum, New York, 1987.
[4] G. Casati, L. Molinari, Prog. Theor. Phys. Suppl. 98 (1989) 287; G. Casati, B.V. Chirikov, D.L. Shepelyansky, I. Guaneri, Phys. Rep. 154 (1987) 77.
[5] A.G. Fainshtein, N.L. Manakov, V.D. Ovsiannikov, L.P. Rapoport, Phys. Rep. 210 (1992) 111.
[6] M. Kleber, Phys. Rep. 236 (1994) 331.
[7] W. Domcke, P. Hänggi, D. Tannor (Eds.), Dynamics of driven quantum systems, Chem. Phys. 217 (1997) 117–416 (special issue).
[8] H.R. Reiss, Phys. Rev. Lett. 25 (1970) 1149.
[9] M. Gavrila, J.Z. Kaminski, Phys. Rev. Lett. 52 (1984) 614; Q. Su, J.H. Eberly, Phys. Rev. A 44 (1991) 5997; F. Bensch, H.J. Korsch, N. Moiseyev, Phys. Rev. A 43 (1991) 5145; H. Wiedemann, J. Mostowski, F. Haake, Phys. Rev. A 49 (1994) 1171; M. Gavrila, in: M. Gavrila (Ed.), Atoms in Intense Laser Fields, Academic Press, New York, 1992, pp. 435–510.
[10] For reviews see: G. Casati, I. Guarneri, D.L. Shepelyansky, IEEE J. Quant. Elect. 24 (1988) 1420; R. Shakeshaft, J. Opt. Soc. Am. B4 (1987) 705; R. Shakeshaft, Comments At. Mol. Phys. 28 (1992) 179; Laser Phys. 3(2) (1993); A.M. Prokhorov (Ed.), Atoms, Ions and Molecules in a Strong Laser Field (Special issue).
[11] D.J. Tannor, S.A. Rice, Adv. Chem. Phys. 70 (1988) 441.
[12] P. Brumer, M. Shapiro, Ann. Rev. Phys. Chem. 43 (1992) 257.

[13] D.J. Tannor in: A.D. Bardrak (Ed.), Molecules and Laser Fields, Marcel Dekker, 1993, pp. 403–446.
[14] A.H. Dayem, R.J. Martin, Phys. Rev. Lett. 8 (1962) 246.
[15] P.K. Tien, J.P. Gordon, Phys. Rev. 129 (1963) 647.
[16] V.V. Pavlovich, E.M. Epshtein, Sov. Phys. Semicond. 10 (1976) 1196.
[17] A.A. Ignatov, Yu. A. Romanov, Trans. USSR Higher School (Ser. Phys.) 25 (1982) 81.
[18] F.G. Bass, A.P. Teterov, Phys. Rep. 140 (1986) 237.
[19] B.J. Keay, S.J. Allen Jr., J. Galán, J.P. Kaminski, J.L. Campman, A.C. Gossard, U. Bhattacharya, M.J.W. Rodwell, Phys. Rev. Lett. 75 (1995) 4098.
[20] B.J. Keay, S. Zeuner, S.J. Allen Jr., K.D. Maranowski, A.C. Gossard, U. Bhattacharya, M.J.W. Rodwell, Phys. Rev. Lett. 75 (1995) 4102.
[21] S. Zeuner, B.J. Keay, S.J. Allen, K.D. Maranowski, A.C. Gossard, U. Bhattacharya, M.J.W. Rodwell, Phys. Rev. B 53 (1996) R1717; A. Wacker, A.-P. Jauho, S. Zeuner, S.J. Allen, Phys. Rev. B 56 (1997) 13268.
[22] K. Unterrainer, B.J. Keay, M.C. Wanke, S.J. Allen, D. Leonard, G. Medeiros-Ribeiro, U. Bhattacharya, M.J.W. Rodwell, Phys. Rev. Lett. 76 (1996) 2973.
[23] F. Hund, Z. Physik 43 (1927) 805.
[24] F. Grossmann, T. Dittrich, P. Jung, P. Hänggi, Phys. Rev. Lett. 67 (1991) 516; for an extended discussion see also: P. Hänggi, Control of Tunneling, in: H.A. Cerdeira et al. (Ed.), Quantum Dynamics of Submicron Structures, Kluwer Acad. Publishers, Dordrecht, 1995, pp. 673–686.
[25] F. Grossmann, P. Jung, T. Dittrich, P. Hänggi, Z. Phys. B 84 (1991) 315.
[26] T. Dittrich, Physik in unserer Zeit 28, No. 6 (1997) 238.
[27] R. Bavli, H. Metiu, Phys. Rev. A 47 (1993) 3299.
[28] Y. Dakhnovskii, R. Bavli, Phys. Rev. B 48 (1993) 11020.
[29] Y. Dakhnovskii, H. Metiu, Phys. Rev. A 48 (1993) 2342.
[30] A.O. Caldeira, A.J. Leggett, Phys. Rev. Lett. 46 (1981) 211.
[31] A.O. Caldeira, A.J. Leggett, Ann. Phys. (N.Y.) 149 (1983) 374; erratum, Ann. Phys. (N.Y.) 153 (1994) 445.
[32] A.J. Leggett, S. Chakravarty, A.T. Dorsey, M.P.A. Fisher, A. Garg, W. Zwerger, Rev. Mod. Phys. 59 (1987) 1; erratum, Rev. Mod. Phys. 67 (1995) 725.
[33] P. Hänggi, P. Talkner, M. Borkovec, Rev. Mod. Phys. 62 (1990) 251.
[34] U. Weiss, Quantum Dissipative Systems, World Scientific, Singapore, 1993.
[35] V.A. Benderskii, D.A. Makarov, Ch.A. Wright, Chemical Dynamics at Low Temperatures, Adv. Chem. Phys., vol. 88, 1994, pp. 1–385.
[36] G. Floquet, Ann. de l'Ecole Norm. Sup. 12 (1883) 47; E.L. Ince, Ordinary Differential Equations, Dover, New York, 1956; W. Magnus, S. Winkler, Hill's Equation, Dover, New York, 1979.
[37] J.H. Shirley, Phys. Rev. 138 (1965) 979.
[38] Ya.B. Zeldovitch, Sov. Phys. JETP 24 (1967) 1006 [Zh. Eksp. Teor. Fiz. 51 (1966) 1492].
[39] V.I. Ritus, Sov. Phys. JETP 24 (1967) 1041 [Zh. Eksp. Teor. Fiz. 51 (1996) 1544].
[40] H. Sambe, Phys. Rev. A 7 (1973) 2203.
[41] Y. Aharonov, J. Anandan, Phys. Rev. A 38 (1987) 5957.
[42] A.G. Fainshtein, N.L. Manakov, L.P. Rapoport, J. Phys. B 11 (1978) 2561.
[43] J. von Neumann, E. Wigner, Physik. Z. 30 (1929) 467.
[44] Ya.B. Zeldovitch, Usp. Fiz. Nauk. 110 (1973) 139.
[45] M.V. Kuzmin, V.N. Saznov, Sov. Phys. JETP 52 (1981) 889; [Zh. Eksp. Teor. Fiz. 79 (1980) 1759].
[46] T.-S. Ho, S.-I. Chu, Chem. Phys. Lett. 141 (1987) 315.
[47] J.E. Avron, J.S. Howland, B. Simon, Commun. Math. Phys. 128 (1990) 497.
[48] D.W. Hone, R. Ketzmerick, W. Kohn, Phys. Rev. A 56 (1997) 4045.
[49] D. Farelly, J.A. Milligan, Phys. Rev. E 47 (1993) R2225.
[50] H.R. Jauslin, J.L. Lebowitz, Chaos 1 (1991) 114.
[51] J. Bellisard, in: S. Albeverio, Ph. Blanchard (Eds.), Trends in the Eighties, World Scientific, Singapore, 1985.
[52] P.M. Blekher, H.R. Jauslin, J.L. Lebowitz, J. Stat. Phys. 68 (1992) 271.
[53] C.R. de Oliveira, Europhys. Lett. 31 (1995) 63.
[54] M.D. Feit, J.A. Fleck Jr., A. Steiger, J. Comput. Phys. 47 (1982) 412.

[55] R. Kosloff, D.J. Kosloff, J. Comput. Phys. 63 (1986) 363.
[56] R. Kosloff, J. Phys. Chem. 92 (1988) 2087.
[57] J. Howland, Math. Ann. 207 (1974) 315.
[58] U. Peskin, N. Moiseyev, J. Chem. Phys. 99 (1993) 4590; P. Pfeifer, R.D. Levine, J. Chem. Phys. 79 (1983) 5512; N. Moiseyev, Comments At. Mol. Phys. 31 (1995) 87.
[59] W. Gordon, Z. Phys. 40 (1926) 117.
[60] D.M. Volkov, Z. Phys. 94 (1935) 250.
[61] K. Husimi, Progr. Theor. Phys. 9 (1953) 381; see also in: F.H. Kerner, Can. J. Phys. 36 (1958) 371.
[62] A.M. Perelomov, V.S. Popov, Teor. Mat. Fiz. 1 (1970) 275; V.S. Popov, A.M. Perelomov, Sov. Phys. JETP 30 (1970) 910 [Zh. Eksp. Teor. Fiz. 57 (1969) 1684].
[63] C. Zerbe, P. Hänggi, Phys. Rev. E 52 (1995) 1533.
[64] D.R. Dion, J.O Hirschfelder, Adv. Chem. Phys. 35 (1976) 265; P.K. Aravind, J.O. Hirschfelder, J. Phys. Chem. 88 (1984) 4788.
[65] I.I. Rabi, Phys. Rev. 51 (1937) 652; see also the preceding work in that issue: J. Schwinger, Phys. Rev. 51 (1937) 648.
[66] F. Bloch, A. Siegert, Phys. Rev. 57 (1940) 522.
[67] F. Grossmann, P. Hänggi, Europhys. Lett. 18 (1992) 571.
[68] J.M. Gomez-Llorente, J. Plata, Phys. Rev. A 45 (1992) R6958; erratum Phys. Rev. E 49 (1994) 3547.
[69] L. Wang, J. Shao, Phys. Rev. A 49 (1994) R637.
[70] H. Cheng, M.L. Ge, J. Shao, Phys. Lett. A 191 (1994) 1.
[71] X.-G. Zhao, Phys. Lett. A 193 (1994) 5.
[72] Y. Kayanuma, Phys. Rev. A 50 (1994) 843.
[73] Y. Kayanuma, Phys. Rev. A 55 (1997) 2495.
[74] Y. Dakhnovskii, R. Bavli, Phys. Rev. B 48 (1993) 11010.
[75] H. Wang, X.-G. Zhao, J. Phys.: Condens. Matter 7 (1995) L89; H. Wang, X.-G. Zhao, Phys. Lett. A 217 (1996) 225.
[76] C. Cohen-Tannoudji, J. Dupont-Roc, G. Grynberg, Atom Photon Interactions, Wiley, New York, 1992.
[77] J. Plata, J.M. Gomez-Llorente, Phys. Rev. A 48 (1993) 782.
[78] D.E. Makarov, Phys. Rev. E 48 (1993) R4164.
[79] P. Neu, R.J. Silbey, Phys. Rev. A 54 (1996) 5323.
[80] R. Graham, M. Höhnerbach, Z. Phys. B 57 (1984) 233.
[81] J. Shao, P. Hänggi, Phys. Rev. A 56 (1997) R4397.
[82] L.D. Landau, Phys. Z. Sowjetunion 1 (1932) 89.
[83] C. Zener, Proc. R. Soc. London, Ser. A 137 (1932) 696.
[84] E.G.C. Stückelberg, Helv. Phys. Acta 5 (1932) 369.
[85] Y. Kayanuma, J. Phys. Soc. Jap. 53 (1984) 108.
[86] R.P. Feynman, Phys. Rev. 84 (1951) 108.
[87] D.J. Tannor, Nature 369 (1994) 445.
[88] R. Kosloff, A.D. Hammerich, D.J. Tannor, Phys. Rev. Lett. 69 (1992) 2172.
[89] R. Graham, M. Schlautmann, P. Zoller, Phys. Rev. A 45 (1996) R19.
[90] M. Ben Dahan, E. Peik, J. Reichel, Y. Castin, C. Salomon, Phys. Rev. Lett. 76 (1996) 4508; S.R. Wilkinson, C.F. Bharucha, K.W. Madison, Q. Niu, M.G. Raizen, Phys. Rev. Lett. 76 (1996) 4512.
[91] C. Waschke, H. Roskos, R. Schwedler, K. Leo, H. Kurz, K. Köhler, Phys. Rev. Lett. 70 (1993) 3319.
[92] A.A. Ignatov, Yu.A. Romanov, Phys. Status Solidi (b) 73 (1976) 327; A.A. Ignatov, K.F. Renk, E.P. Dodin, Phys. Rev. Lett. 13 (1993) 1996; A.A. Ignatov, E. Schomburg, J. Grenzer, K.F. Renk, E.P. Dodin, Z. Phys. B 98 (1995) 187.
[93] M. Holthaus, Z. Phys. B 89 (1992) 251.
[94] M. Holthaus, Phys. Rev. Lett. 69 (1992) 1596.
[95] M. Holthaus, G.H. Ristow, D.W. Hone, Phys. Rev. Lett. 75 (1995) 3914.
[96] M. Holthaus, G.H. Ristow, D.W. Hone, Europhys. Lett. 32 (1995) 241.
[97] M. Holthaus, D.W. Hone, Phil. Mag. B 74 (1996) 105.
[98] G. Platero, R. Aguado, Appl. Phys. Lett. 70 (1997) 3546.

[99] F.H.M. Faisal, J.Z. Kamiński, Phys. Rev. A 54 (1996) R1769; Phys. Rev. A 56 (1997) 748.
[100] F. Bloch, Z. Phys. 52 (1928) 555.
[101] G.H. Wannier, Phys. Rev. 117 (1960) 432; Rev. Mod. Phys. 34 (1962) 645.
[102] J.E. Avron, Ann. Phys. (N.Y.) 143 (1982) 33.
[103] H. Fukuyama, R.A. Bari, H.C. Fogedby, Phys. Rev. B 8 (1973) 5579.
[104] C. Zener, Proc. Roy. Soc. A 145 (1934) 523.
[105] D.H. Dunlap, V.M. Kenkre, Phys. Rev. B 34 (1986) 3625; Phys. Lett. A 127 (1988) 438; Phys. Rev. B 37 (1988) 6622.
[106] W.V. Houston, Phys. Rev. 57 (1940) 184.
[107] I. Zak, Phys. Rev. Lett. 71 (1993) 2623.
[108] H. Yamada, K. Ikeda, M. Goda, Phys. Lett. A 182 (1993) 77.
[109] S. Raghavan, V.M. Kenkre, D.H. Dunlap, A.R. Bishop, M.I. Salkola, Phys. Rev. A 54 (1996) R1781.
[110] X.-G. Zhao, Phys. Lett. A 155 (1991) 299.
[111] N. Hong Shon, H.N. Nazareno, J. Phys.: Condens. Matter 4 (1992) L611.
[112] J. Rotvig, A.-P. Jauho, H. Smith, Phys. Rev. Lett. 74 (1995) 1831.
[113] K. Drese, M. Holthaus, J. Phys.: Condens. Matter 8 (1996) 1193.
[114] E.M. Zanardi, J.M. Gomez-Llorente, Chem. Phys. 217 (1997) 221.
[115] F.H.M. Faisal, R. Genieser, Phys. Lett. A 141 (1989) 297.
[116] J.R. Tucker, M.J. Feldman, Rev. Mod. Phys. 57 (1985) 1055.
[117] J.R. Tucker, M.F. Miella, Appl. Phys. Lett. 33 (1978) 611.
[118] L.P. Kouwenhoven, S. Jauhar, K. McCormick, D. Dixon, P.L. McEuen, Yu.V. Nazarov, N.C. van der Vaart, C.T. Foxon, Phys. Rev. B 50 (1994) R2019; L.P. Kouwenhoven, Science 268 (1995) 1440; T.H. Oosterkamp, L.P. Kouwenhoven, A.E.A. Koolen, N.C. van der Vaart, C.J.P.M. Harmans, Phys. Rev. Lett. 78 (1997) 1536.
[119] R.H. Blick, R.J. Haug, D.W. van der Weide, K. von Klitzing, K. Eberl, Appl. Phys. Lett. 67 (1995) 3924.
[120] S. Verghese, R.A. Wyss, Th. Schlaepper, A. Foerster, M.J. Rooks, Q. Hu, Phys. Rev. B 52 (1995) 14834.
[121] R.A. Wyss, C.C. Eugster, J.A. del Alamo, Q. Hu, Appl. Phys. Lett. 63 (1993) 1522.
[122] H. Drexler, J.S. Scott, S.J. Allen, K.L. Campman, A.C. Gossard, Appl. Phys. Lett. 67 (1995) R2816.
[123] D.D. Coon, H.C. Liu, J. Appl. Phys. 58 (1985) 2230; H.C. Liu, Appl. Phys. Lett. 52 (1988) 453.
[124] V.I. Mel'nikov, Phys. Rev. A 45 (1992) 5474.
[125] D. Sokolovski, Phys. Rev. B 37 (1988) 4201; D. Sokolovski, J. Phys. C 21 (1988) 639.
[126] N.S. Wingreen, Appl. Phys. Lett. 56 (1990) 253.
[127] A.P. Jauho, Phys. Rev. B 41 (1990) 12327.
[128] W. Cai, T.F. Zheng, P. Hu, M. Lax, K. Shum, R.R. Alfano, Phys. Rev. Lett. 65 (1990) 104.
[129] A.P. Jauho, N.S. Wingreen, Y. Meir, Phys. Rev. B 50 (1994) 5528.
[130] C. Bruder, H. Schoeller, Phys. Rev. Lett. 72 (1994) 1076; Ph. Brune, C. Bruder, H. Schoeller, Phys. Rev. B 56 (1997) 4730.
[131] J. Iñarrea, G. Platero, C. Tejedor, Phys. Rev. B 50 (1994) 4581.
[132] R. Aguado, J. Iñarrea, G. Platero, Phys. Rev. B 53 (1996) 10030.
[133] M. Wagner, Phys. Rev. B 49 (1994) 16544.
[134] M. Wagner, Phys. Rev. A 51 (1995) 798.
[135] Y. Dakhnovskii, R. Bavli, H. Metiu, Phys. Rev. B 53 (1996) 4567.
[136] S. Feng, Q. Hu, Phys. Rev. B 48 (1993) 5354.
[137] K. Yakubo, S. Feng, Q. Hu, Phys. Rev. B 54 (1996) 7987.
[138] R. Aguado, G. Platero, Phys. Rev. B 55 (1997) 12860.
[139] W.A. Lin, L. Reichl, Phys. Rev. A 37 (1988) 3972.
[140] H.P. Breuer, M. Holthaus, Ann. Phys. (N.Y.) 245 (1991) 249.
[141] B. Birnir, B. Galdrikian, R. Grauer, M. Sherwin, Phys. Rev. B 47 (1993) 6795.
[142] M. Wagner, Phys. Rev. Lett. 76 (1996) 4010.
[143] H.A. Kramers, Quantum Mechanics, North-Holland, Amsterdam 1956; W.C. Henneberger, Phys. Rev. Lett. 21 (1968) 838; see also W. Pauli, M. Fierz, Nuovo Cimento 15 (1938) 167.

[144] M. Büttiker, R. Landauer, Phys. Rev. Lett. 49 (1992) 1740.
[145] W.S. Truscott, Phys. Rev. Lett. 70 (1993) 1900.
[146] J.M. Gomez-Llorente, J. Plata, Phys. Rev. E 49 (1994) 2759.
[147] P. Goetsch, R. Graham, Ann. Physik 1 (1992) 662.
[148] J.-Y. Shin, Phys. Rev. E 54 (1996) 289.
[149] T. Seidemann, M.Yu. Ivanov, P.B. Corkum, Phys. Lett. 75 (1995) 2819.
[150] H. Sekiya, Y. Nagashima, T. Tsuji, Y. Nishimura, A. Mori, H. Takeshita, J. Phys. Chem. 95 (1991) 10311; S. Takada, H. Nakamura, J. Chem. Phys. 102 (1995) 3977.
[151] P. Kraminski, M. Ploszajczak, R. Avieu, Europhys. Lett. 26 (1994) 1.
[152] R. Bavli, H. Metiu, Phys. Rev. Lett. 69 (1992) 1986.
[153] M. Holthaus, Phys. Rev. Lett. 69 (1992) 1596.
[154] D.F. Escande, Phys. Rep. 121 (1985) 165.
[155] L. Reichl, The Transition to Chaos, Springer, New York, 1992.
[156] M.J. Davis, E.J. Heller, J. Chem. Phys. 75 (1986) 246.
[157] O. Bohigas, S. Tomsovic, D. Ullmo, Phys. Rev. Lett. 64 (1990) 1479.
[158] O. Bohigas, S. Tomsovic, D. Ullmo, Phys. Rep. 223 (1993) 43.
[159] S. Tomsovic, D. Ullmo, Phys. Rev. E 50 (1994) 145.
[160] S.C. Creagh, N. Whelan, Phys. Rev. Lett. 77 (1996) 4975.
[161] V. Averbuckh, N. Moiseyev, B. Mirbach, H.J. Korsch, Z. Phys. D 35 (1995) 247.
[162] H. Wiescher, H.J. Korsch, J. Phys. A 30 (1997) 1763.
[163] B.S. Helmkamp, D.A. Browne, Phys. Rev. E 49 (1994) 1831.
[164] W.A. Lin, L.E. Ballentine, Phys. Rev. Lett. 65 (1990) 2927.
[165] W.A. Lin, L.E. Ballentine, Phys. Rev. A 45 (1992) 3637.
[166] J. Plata, J.M. Gomez-Llorente, J. Phys. A 25 (1992) L303.
[167] K. Husimi, Proc. Phys. Math. Soc. Japan 22 (1940) 264.
[168] M. Hillery, R.F. O'Connell, M.O. Scully, E.P. Wigner, Phys. Rep. 106 (1984) 121.
[169] R. Utermann, T. Dittrich, P. Hänggi, Phys. Rev. E 49 (1994) 273.
[170] P. Hänggi, R. Utermann, T. Dittrich, Physica B 194–196 (1994) 1013.
[171] H.G. Roskos, M.C. Nuss, J. Shah, K. Leo, D.A.B. Miller, A.M. Fox, S. Schmitt-Rink, K. Köhler, Phys. Rev. Lett. 68 (1992) 2216.
[172] N. Dagli, G. Snider, J. Waldman, E. Hu, J. Appl. Phys. 69 (1991) 1047.
[173] M.Yu. Ivanov, P.B. Corkum, Phys. Rev. A 48 (1993) 580; M. Iganov, P.B. Corkum, P. Dietrich, Laser Phys. 3 (1939) 375.
[174] A. Levinson, M. Segev, G. Almogy, A. Yariv, Phys. Rev. A 49 (1994) R661.
[175] P.C.E. Stamp, E.M. Chudnovsky, B. Barbara, Int. J. Mod. Phys. B 6 (1992) 1355; S. Miyashito, K. Saito, H. De Raedt, Phys. Rev. Lett. 80 (1998) 1525.
[176] L. Gunther, B. Barabara (Eds.), Quantum Tunneling of Magnetization QTM'94, NATO ASI Series, Series E: Applied Sciences, vol. 301, Kluwer Academic Press, Dordrecht, 1995.
[177] J.L. van Hemmen, A. Süto, J. Phys.: Condens. Matter 9 (1997) 3089.
[178] J.L. van Hemmen, H. Hey, W.F. Wreszinski, J. Phys. A 30 (1997) 6371.
[179] J.L. van Hemmen, A. Süto, Physica B 141 (1986) 37.
[180] V.B. Magalinskij, Sov. Phys. JETP 9 (1959) 1942.
[181] I.R. Senitzky, Phys. Rev. 119 (1960) 670.
[182] G.W. Ford, M. Kac, P. Mazur, J. Math. Phys. 6 (1965) 504.
[183] P. Ullersma, Physica (Utrecht) 32 (1966) 27, 56, 74, 90.
[184] G.W. Ford, M. Kac, J. Stat. Phys. 46 (1987) 803.
[185] P. Hänggi, in: L. Schimansky-Geier, T. Pöschel (Eds.), Stochastic Dynamics, Lecture Notes in Physics, vol. 484, Springer, Berlin, 1997, pp. 15–22.
[186] R.P. Feynman, F.L. Vernon, Ann. Phys. (N.Y.) 24 (1963) 118.
[187] H. Grabert, P. Schramm, G.L. Ingold, Phys. Rep. 168 (1988) 115.
[188] U. Weiss, H. Grabert, P. Hänggi, P. Riseborough, Phys. Rev. B 35 (1987) 9535.
[189] R. Blümel, A. Buchleitner, R. Graham, L. Sirko, U. Smilansky, H. Walther, Phys. Rev. A 44 (1991) 4521.

[190] S. Kohler, T. Dittrich, P. Hänggi, Phys. Rev. E 55 (1997) 300.
[191] T. Dittrich, B. Oelschlägel, P. Hänggi, Europhys. Lett. 22 (1993) 5.
[192] B. Oelschlägel, T. Dittrich, P. Hänggi, Acta Physica Polonica B 24 (1993) 845.
[193] F. Haake, in: G. Höhler (Ed.), Quantum Statistics in Optics and Solid-State Physics, Springer Tracts in Modern Physics, vol. 66, Springer, Berlin, 1973.
[194] R. Alicki, K. Lendi, in: W. Beigböck (Ed.), Quantum Dynamical Semigroups and Applications, Lecture Notes in Physics, vol. 286, Springer, Berlin, 1987.
[195] W.H. Louisell, Quantum Statistical Properties of Radiation, Wiley, New York, 1973.
[196] N. Makri, J. Math. Phys. 36 (1995) 2430.
[197] N. Makri, D. Makarov, J. Chem. Phys. 102 (1995) 4600.
[198] N. Makri, D. Makarov, J. Chem. Phys. 102 (1995) 4611.
[199] D.O. Harris, G.G. Engerholm, W.D. Gwinn, J. Chem. Phys. 43 (1965) 1515.
[200] D.E. Makarov, N. Makri, Phys. Rev. B 52 (1995) 2257.
[201] N. Makri, J. Chem. Phys. 106 (1997) 2286.
[202] N. Makri, L. Wei, Phys. Rev. E 55 (1997) 2475.
[203] M. Thorwart, P. Jung, Phys. Rev. Lett. 78 (1997) 2503.
[204] M. Thorwart, P. Reimann, P. Jung, R.F. Fox, Phys. Lett. A 239 (1998) 233; Special Issue of Chemical Physics In Memory of Prof. V.J. Mel'nikov, in press.
[205] H. Wipf, D. Steinbinder, K. Neumaier, P. Gutsmiedl, A. Nagerl, A.J. Dianoux, Europhys. Lett. 4 (1987) 1379.
[206] D.M. Eigler, E.K. Schweitzer, Nature 344 (1990) 524.
[207] A.A. Louis, J.P. Sethna, Phys. Rev. Lett. 74 (1995) 1363.
[208] S. Han, J. Lapointe, J.E. Lukens, Phys. Rev. Lett. 66 (1991) 810.
[209] B. Golding, N.M. Zimmerman, S.N. Coppersmith, Phys. Rev. Lett. 68 (1992) 998.
[210] K. Chun, N.O. Birge, Phys. Rev. B 48 (1993) 11500.
[211] R.A. Marcus, J. Chem. Phys. 24 (1956) 966; J. Chem. Phys. 43 (1965) 679.
[212] V.G. Levich, R.R. Dogonadze, Dokl. Acad. Nauk SSSR 124 (1959) 123 [Proc. Acad. Sci. Phys. Chem. Sect. 124 (1959) 9].
[213] A.V. Ovchinnikov, M.Ya. Ovchinnikova, Zh. Eksp. Teor. Fiz. 56 (1969) 1278 [Sov. Phys. JETP 29 (1969) 688].
[214] L.D. Zusman, Chem. Phys. 49 (1980) 295.
[215] A. Garg, J.N. Onuchic, V. Ambegaokar, J. Chem. Phys. 83 (1985) 4491.
[216] I. Rips, J. Jortner, J. Chem. Phys. 87 (1987) 2090.
[217] G.L. Closs, J.R. Miller, Science 240 (1988) 440; Electron transfer, Special Issue Chem. Phys. 176 (1993).
[218] R.P. Bell, The Tunnel Effect in Chemistry, Chapman & Hall, London, 1980.
[219] E.D. German, A.M. Kuznetov, R.R. Doganadze, J. Chem. Soc. Faraday Trans. 2 76 (1980) 1128.
[220] S. Chakravarty, Phys. Rev. Lett. 49 (1982) 681; A.J. Bray, M.A. Moore, Phys. Rev. Lett 49 (1982) 1546.
[221] M. Grifoni, M. Sassetti, J. Stockburger, U. Weiss, Phys. Rev. E 48 (1993) 3497.
[222] M. Grifoni, M. Sassetti, U. Weiss, Phys. Rev. E 53 (1996) R2033.
[223] M. Morillo, R.I. Cukier, J. Chem. Phys. 98 (1993) 4548.
[224] R.I. Cukier, M. Morillo, Chem. Phys. 183 (1994) 375.
[225] Yu. Dakhnovskii, Phys. Rev. B 49 (1994) 4649.
[226] Yu. Dakhnovskii, Ann. Phys. 230 (1994) 145.
[227] Yu. Dakhnovskii, J. Chem. Phys. 100 (1994) 6492.
[228] Yu. Dakhnovskii, R.D. Coalson, J. Chem. Phys. 103 (1995) 2908.
[229] M. Grifoni, M. Sassetti, P. Hänggi, U. Weiss, Phys. Rev. E 52 (1995) 3596.
[230] D.G. Evans, R.D. Coalson, Yu. Dakhnovskii, Phys. Rev. Lett. 75 (1995) 3649.
[231] D.G. Evans, R.D. Coalson, Yu. Dakhnovskii, J. Chem. Phys. 104 (1996) 2287.
[232] R. Löfstedt, S.N. Coppersmith, Phys. Rev. Lett. 72 (1994) 1947; Phys. Rev. E 49 (1994) 4821.
[233] M. Grifoni, P. Hänggi, Phys. Rev. Lett. 76 (1996) 1611.
[234] M. Grifoni, P. Hänggi, Phys. Rev. E 54 (1996) 1390.
[235] M. Grifoni, L. Hartmann, S. Berchtold, P. Hänggi, Phys. Rev. E 53 (1996) 5890; erratum Phys. Rev. E 56 (1997) 6213.
[236] I.A. Goychuk, E.G. Petrov, V. May, Chem. Phys. Lett. 353 (1996) 428.

[237] M. Morillo, R.I. Cukier, Phys. Rev. B 54 (1996) 1362.
[238] M. Grifoni, Phys. Rev. E 54 (1996) R3086.
[239] I.A. Goychuk, E.G. Petrov, V. May, J. Chem. Phys. 103 (1995) 4937.
[240] I.A. Goychuk, E.G. Petrov, V. May, Phys. Rev. E 51 (1995) 2982.
[241] I.A. Goychuk, E.G. Petrov, V. May, Phys. Rev. E 52 (1995) 2392.
[242] E.G. Petrov, I.A. Goychuk, V. May, Phys. Rev. E 54 (1996) R4500; J.A. Goychuk, E.G. Petrov, V. May, J. Chem. Phys. 106 (1997) 4522.
[243] M. Grifoni, M. Winterstetter, U. Weiss, Phys. Rev. E 56 (1997) 334.
[244] M. Winterstetter, U. Weiss, Chem. Phys. 217 (1997) 155.
[245] P. Neu, J. Rau, Phys. Rev. E 55 (1997) 2195.
[246] M. Grifoni, L. Hartmann, P. Hänggi, Chem. Phys. 217 (1997) 167; Chem. Phys. 232 (1998) 371 (erratum).
[247] Y. Kayanuma, Phys. Rev. Lett. 58 (1987) 1943.
[248] P. Ao, J. Rammer, Phys. Rev. Lett. 62 (1989) 3004.
[249] P. Ao, J. Rammer, Phys. Rev. B 43 (1991) 5397.
[250] Y. Gefen, E. Ben-Jacob, A.O. Caldeira, Phys. Rev. B 36 (1987) 2770.
[251] P. Chvosta, Physica A 166 (1990) 361.
[252] R. Egger, U. Weiss, Z. Phys. B 89 (1992) 97.
[253] T.A. Costi, C. Kieffer, Phys. Rev. Lett. 76 (1996) 1683.
[254] R. Egger, H. Grabert, U. Weiss, Phys. Rev. E 55 (1997) 3809.
[255] M. Sassetti, U. Weiss, Phys. Rev. A 41 (1990) 5383.
[256] C.H. Mak, R. Egger, Phys. Rev. E 49 (1994) 1997.
[257] C. Aslangul, N. Pottier, D. Saint-James, Phys. Lett. A 110 (1985) 249.
[258] C. Aslangul, N. Pottier, D. Saint-James, J. Phys. (Paris) 47 (1986) 1657.
[259] T. Holstein, Ann. Phys. (N.Y.) 8 (1959) 343.
[260] A. Würger, Phys. Rev. Lett. 78 (1997) 1759.
[261] U. Weiss, M. Wollensak, Phys. Rev. Lett. 62 (1989) 1663; R. Görlich, M. Sassetti, U. Weiss, Europhys. Lett. 10 (1989) 507.
[262] P. Jung, P. Hänggi, Europhys. Lett. 8 (1989) 505; P. Hänggi, P. Jung, C. Zerbe, F. Moss, J. Stat. Phys. 70 (1993) 25.
[263] D.A. Parshin, Z. Phys. B 91 (1993) 367.
[264] J. Stockburger, M. Grifoni, M. Sassetti, Phys. Rev. B 51 (1995) 2835.
[265] P. Esquinazi, R. König, F. Pobell, Z. Phys. B 87 (1992) 305.
[266] P.W. Anderson, B.I. Halperin, C.M. Varma, Philos. Mag. B 25 (1972) 1.
[267] W.A. Phillips, J. Low Temp. Phys. 7 (1972) 351.
[268] J. Stockburger, M. Grifoni, M. Sassetti, U. Weiss, Z. Phys. B 94 (1994) 447.
[269] R. Benzi, A. Sutera, A. Vulpiani, J. Phys. A 14 (1981) L453.
[270] For reviews see: P. Jung, Phys. Rep. 234 (1993) 175; F. Moss, D. Pierson, D. O'Gorman, Int. J. Bifurcation Chaos 4 (1994) 1383.
[271] See, for example, in: F. Moss et al. (Eds.), Proc. Nato Workshop on SR in Physics and Biology, J. Stat. Phys. 70 (1993) 1.
[272] For a comprehensive review see: L. Gammaitoni, P. Hänggi, P. Jung, F. Marchesoni, Rev. Mod. Phys. 70 (1998) 223.
[273] P. Jung, P. Hänggi, Europhys. Lett. 8 (1989) 505; P. Jung, P. Hänggi, Phys. Rev. A 44 (1991) 8032.
[274] R.C. Bourret, U. Frisch, A. Pouquet, Physica 65 (1973) 303.
[275] V.E. Shapiro, V.M. Loginov, Physica A 91 (1978) 563.
[276] I.A. Goychuk, E.G. Petrov, V. May, Phys. Rev. E 56 (1997) 1421.
[277] J. Allinger, Diploma Thesis, Univ. of Stuttgart (1990).
[278] H.A. Bethe, Phys. Rev. Lett. 56 (1986) 1305.
[279] C.P. Slichter, Principles of Magnetic Resonance, Springer, Berlin, 1978.
[280] C.P. Flynn, A.M. Stoneham, Phys. Rev. B 1 (1970) 3936.
[281] G. Schön, A. Zaikin, Phys. Rep. 198 (1990) 237.
[282] C.L. Kane, M.P.A. Fisher, Phys. Rev. Lett. 68 (1992) 1220.

[283] For a review, see M. Sassetti, in: B. Kramer (Ed.), Quantum Transport in Semiconductor Submicron Structures, Kluwer Acad. Publishers, Dordrecht, 1996.
[284] M. Sassetti, H. Schomerus, U. Weiss, Phys. Rev. B 53 (1996) R2914.
[285] A. Schmid, Phys. Rev. Lett. 51 (1983) 1506.
[286] F. Guinea, V. Hakim, A. Muramatsu, Phys. Rev. Lett. 54 (1985) 263.
[287] M.P.A. Fisher, W. Zwerger, Phys. Rev. B 32 (1985) 6190.
[288] U. Eckern, F. Pelzer, Europhys. Lett. 3 (1987) 131.
[289] U. Weiss, M. Wollensak, Phys. Rev. B 37 (1988) 2729.
[290] U. Weiss, M. Sassetti, T. Negele, M. Wollensak, Z. Phys. B 84 (1991) 471.
[291] M. Sassetti, U. Weiss, B. Kramer, Solid State Commun. 97 (1996) 605.
[292] U. Weiss, H. Grabert, Phys. Lett. A 108 (1985) 63.
[293] L. Hartmann, M. Grifoni, P. Hänggi, Europhys. Lett. 38 (1997) 497.
[294] I.A. Goychuk, E.G. Petrov, V. May, Phys. Lett. A 238 (1998) 59.
[295] R. Aguado, G. Platero, Phys. Stat. Sol. 164 (1997) 235.
[296] P.E. Parris, R. Silbey, J. Chem. Phys. 83 (1985) 5619.
[297] D.R. Reichmann, R. Silbey, J. Phys. Chem. 99 (1995) 2777.
[298] H. Dekker, Physica A 175 (1991) 485; 178 (1991) 220; 178 (1991) 289; 179 (1991) 81; erratum 210 (1994) 507.
[299] M. Morillo, C. Denk, R.I. Cukier, Chem. Phys. 212 (1996) 157.
[300] R.I. Cukier, C. Denk, M. Morillo, Chem. Phys. 217 (1997) 179.
[301] I. Vorobeichik, R. Lefebvre, N. Moiseyev, Europhys. Lett. 41 (1998) 111.
[302] W.P. Reinhardt, Annu. Rev. Phys. Chem. 33 (1982) 223.
[303] Y.K. Ho, Phys. Rep. 99 (1983) 1.
[304] N. Moiseyev, H.J. Korsch, Phys. Rev. A 41 (1990) 498.
[305] F. Grossmann, P. Hänggi, Europhys. Lett. 18 (1992) 1; F. Grossmann, P. Hänggi, Chem. Phys. 170 (1993) 295.
[306] J. Friedman, M.P. Sarachik, J. Tejada, R. Ziolo, Phys. Rev. Lett. 76 (1996) 3830; L. Thomas, F. Lionti, R. Ballon, D. Gatteschi, R. Sessoli, B. Barbara, Nature 383 (1996) 145; E.M. Chudnovsky, Science 274 (1996) 938; C. Sangregorio, T. Ohm, C. Paulsen, R. Sessoli, D. Gatteschi, Phys. Rev. Lett. 78 (1997) 4645.
[307] K.N. Alekseev, E.H. Cannon, J.C. McKinney, F.V. Kusmartsev, D.K. Campbell, Phys. Rev. Lett. 80 (1998) 2669.
[308] I. Goychuk, P. Hänggi, Europhys. Lett. 43 (1998), in press.
[309] I. Goychuk, M. Grifoni, P. Hänggi, Phys. Rev. Lett. 81 (1998) 649.
[310] P. Reimann, M. Grifoni, P. Hänggi, Phys. Rev. Lett. 79 (1997) 10.
[311] S. Yukawa, M. Kikuchi, G. Tatara, H. Matsukawa, J. Phys. Soc. Japan 66 (1997) 2953.